UNIVERSIDADE FEDERAL DE SÃO CARLOS - UFSCar
CENTRO DE CIÊNCIAS EXATAS E DE TECNOLOGIA - CCET
PROGRAMA DE PÓS-GRADUAÇÃO EM ENGENHARIA QUÍMICA

NONLINEAR CONSTRAINED OPTIMIZATION WITH FLEXIBLE TOLERANCE METHOD: IMPROVEMENT AND APPLICATION IN SYSTEMS SYNTHESIS OF MASS INTEGRATION

Alice Medeiros de Lima

UFSCar - São Carlos - Brasil
2015

UNIVERSIDADE FEDERAL DE SÃO CARLOS - UFSCar
CENTRO DE CIÊNCIAS EXATAS E DE TECNOLOGIA - CCET
PROGRAMA DE PÓS-GRADUAÇÃO EM ENGENHARIA QUÍMICA

NONLINEAR CONSTRAINED OPTIMIZATION WITH FLEXIBLE TOLERANCE METHOD: IMPROVEMENT AND APPLICATION IN SYSTEMS SYNTHESIS OF MASS INTEGRATION

Alice Medeiros de Lima

A thesis submited to Postgraduate Program in Chemical Engineering [Programa de Pós-Graduação em Engenharia Química] of Federal University of São Carlos in partial fullfilment of the requirements for Doctors's Degree in Chemical Engineering.

Adviser: Dr. Wu Hong Kwong

Co-adviser: Dr. Antonio José Gonçalves da Cruz

UFSCar - São Carlos - Brasil
2015

Ficha catalográfica elaborada pelo DePT da Biblioteca Comunitária/UFSCar

L732nc

Lima, Alice Medeiros de.
Nonlinear constrained optimization with flexible tolerance method : improvement and application in systems synthesis of mass integration / Alice Medeiros de Lima. -- São Carlos : UFSCar, 2015.
182 f.

Tese (Doutorado) -- Universidade Federal de São Carlos, 2015.

1. Engenharia química. 2. Otimização não-linear com restrições. 3. Método das tolerâncias flexíveis. 4. Hibridização. 5. Integração mássica. 6. Biorrefinarias. I. Título.

CDD: 660 (20ª)

MEMBROS DA BANCA EXAMINADORA DA DEFESA DE TESE DE ALICE MEDEIROS DE LIMA APRESENTADA AO PROGRAMA DE PÓS-GRADUAÇÃO EM ENGENHARIA QUÍMICA DA UNIVERSIDADE FEDERAL DE SÃO CARLOS, EM 13 DE MARÇO DE 2015.

BANCA EXAMINADORA:

Wu Hong Kwong
Orientador, UFSCar

Antonio José Gonçalves da Cruz
Coorientador, UFSCar

André Ribeiro Lins de Albuquerque
PENTAGRO

Samuel Conceição de Oliveira
UNESP

Antonio Carlos Luperni Horta
UFSCar

To my family

Acknowledgements

To God, my source of strength and hope.

I would like to thank my advisor, Dr. Wu Hong Kwong, and my co-advisor, Dr. Antonio José Gonçalves da Cruz, for guiding and supporting me during the development of this work.

To CAPES (Coordenação de Aperfeiçoamento de Pessoal de Nível Superior) and CNPq (Conselho Nacional de Desenvolvimento Científico e Tecnológico) for financial support.

A special thanks to my family. Words cannot express how grateful I am to my mother, and father for all of the sacrifices that you've made on my behalf. Your prayer for me was what sustained me thus far. I would also like to thank my sister Anete, who supported me and incentive me to strive towards my goal. I thank to my friends for being by my side and always giving me reasons to cheer. At the end I would like express appreciation to my beloved husband Anderson who spent sleepless nights with and was always my support in the moments when there was no one to answer my queries.

'My dear, here we must run as fast as we can, just to stay in place. And if you wish to go anywhere you must run twice as fast as that.'

Lewis Carroll, Alice in Wonderland

Abstract

Nonlinear Constrained Optimization With Flexible Tolerance Method: Improvement And Application In Systems Synthesis Of Mass Integration

This work is focused in constrained nonlinear optimization using the Flexible Tolerance Method (FTM) and in applying in systems synthesis of mass integration. Mass integration is a technique that allows an overall understanding of the mass flow within the process, and employs such knowledge in identification of performance improvements and optimization of the generation and mapping of species throughout the process. The mass integration is based on the fundamental principles of chemical engineering combined with system analysis using graphical and optimization tools. In this context, the direct method of optimization was used as the basis for improvements in order to make possible the application in process synthesis problems, especially mass integration.

The Flexible Tolerance Method is a direct method of optimization that present some advantages as simplicity, the ability to lead with equality and inequality constraints without employ derivative calculus. The method uses two searches to satisfy feasibility constraint. The external search is a variation of the Nelder-Mead method (or the Flexible Polyhedron method or FPM). This one seeks to minimizes the objective function. The internal search minimizes the value of the positive function for all equality and/or inequality constraints of the problem. This internal search can be performed by any unconstrained nonlinear optimization method. In this work, the Flexible Tolerance Method was hybridized with different unconstrained methods to perform the inner search: the BFGS (Broyden, Fletcher, Goldfarb and Shanno Method) and the modified Powell. The stochastic PSO method was also employed to perform the initialization and generation of the feasible start point to sequential application of the determination method

(FTM and modifications). Others modifications tested were the scaling of variables, the use of Nelder-Mead adaptive parameters and the addition of a barrier.

The algorithms proposed in this work were applied to a benchmark of constrained nonlinear problems that comprises real world optimization problems. The best codes obtained were the Modified Flexible Tolerance Method Scaled (MFTMS) and the hybrid FTMS-PSO (the Flexible Tolerance Method with scaling of variables hybridized with PSO (Particle Swarm Optimization)). These best codes were applied with success in the solution of mass integration problems.

The results found in this work demonstrate the capacity of simple and direct methods in deals with complex optimization problems, as the mass integration problems. Additionally an inedited problem of mass integration proposed in this work, the mass integration of 1G, 2G and 3G sugarcane biorefinery was successful solved with the methods proposed in this work (MFTMS and FTMS-PSO). The first generation (1G) includes the ethanol production using the sugarcane juice and production of vapor and electricity throughout cogeneration. The second generation (2G) includes the ethanol production using the lignocellulosic biomass feedstock via the biochemical route. The third generation (3G) includes the algae use for production of biofuels (ethanol and biodiesel). The findings of this study case provide an indication of an economically viable way of achieving substantial advances in terms of water consumption and pollution reduction.

Keywords: Constrained Optimization, Flexible Tolerance Method, Hybridization, Mass Integration, Sugarcane Biorefinery

Resumo

Otimização Não-Linear com Restrições Utilizando o Método das Tolerâncias Flexíveis: Melhoria e Aplicação em Síntese de Sistemas de Integração Mássica

Este trabalho visa a otimização não-linear restrita usando o Método das Tolerâncias Flexíveis (FTM) e na aplicação do mesmo na síntese de sistemas de integração mássica. A integração mássica é uma técnica que permite a compreensão global do fluxo de massa dentro do processo, e emprega tais conhecimentos na identificação de melhorias de desempenho e otimização da geração e mapeamento de espécies ao longo do processo. A integração de massa baseia-se nos princípios fundamentais da engenharia química combinada com a análise do sistema usando ferramentas gráficas e de otimização. Neste contexto, o método direto de otimização foi usado como base para melhorias a fim de tornar possível sua aplicação em problemas de síntese de processo, especialmente a integração de massa.

O Método das Tolerância Flexíveis é um método direto de otimização que apresenta algumas vantagens como simplicidade e a capacidade de lidar com igualdade e desigualdade sem empregar o cálculo de derivadas. O método utiliza duas buscas para satisfazer a restrição de viabilidade. A busca externa é uma variação do método de Nelder-Mead (ou o método Poliedro Flexível ou FPM) que minimiza a função objetivo. A busca interna minimiza o valor da função formada pelas restrições de igualdade e/ou desigualdade do problema. Esta busca interna pode ser realizada por qualquer método de otimização não linear irrestrita. Neste trabalho, o método das tolerâncias flexíveis foi hibridizado com diferentes métodos irrestritos para realizar a busca interna: BFGS (Método de Broyden, Fletcher, Goldfarb and Shanno) e Powell modificado. O método estocástico do Enxame de Partículas (PSO) também foi empregado para efetuar a inicialização e geração do ponto de partida viável para sequencial aplicação do método de-

terminístico (FTM e modificações). Outras modificações testadas foram o escalonamento de variáveis, a utilização de parâmetros adaptativos Nelder-Mead e a adição de uma barreira.

Os algoritmos propostos neste trabalho foram aplicados a um conjunto de problemas não-lineares restritos que compreende problemas de otimização reais. Os códigos que apresentaram melhor desempenho foram o Método Modificado das Tolerâncias Flexíveis com variáveis escalonadas (MFTMS) e o híbrido FTMS-PSO (o Método das Tolerância Flexíveis com escalonamento de variáveis e hibridizado com PSO). Estes melhores códigos foram aplicados com sucesso na solução de problemas de integração em massa.

Os resultados encontrados neste trabalho demonstram a capacidade de métodos simples e diretos em lidar com problemas de otimização complexos, como os problemas de integração mássica. Além disso, um problema inédito de integração mássica proposto neste trabalho, a integração mássica de uma biorefinaria de cana-de-açúcar incluindo 1G, 2G e 3G, foi resolvido com êxito com os métodos propostos neste trabalho (MFTMS e FTMS-PSO). A primeira geração (1G) inclui a produção de etanol utilizando o caldo da cana-de-açúcar e produção de vapor e eletricidade pela cogeração. A segunda geração (2G) utiliza a biomassa lignocelulósica para produção de etanol pela rota bioquímica. A terceira geração (3G) inclui a utilização de algas para produção de biocombustíveis (etanol e biodiesel). Os resultados deste estudo de caso fornecem uma indicação de uma forma economicamente viável de conseguir avanços substanciais em termos de consumo de água e redução da poluição.

Palavras-chave: Otimização Não-Linear Com Restrições, Método das Tolerâncias Flexíveis, Hibridização, Integração Mássica, Biorefinaria de cana-de-açúcar

Contents

List of Figures

List of Tables

Abbreviations

AOC	Annualized Operational Cost
BPE	Boiling Point Elevation
BFGS	Broyden, Fletcher, Goldfarb and Shanno Method
CCS	Carbon dioxide Capture and Storage
CDM	Clean Development Mechanism
CEPCI	Chemical Engineering Plant Cost Index
CID	Composition Interval Diagram
FTM	Flexible Tolerance Method
FPM	Flexible Polyhedron Method
FTMA	Flexible Tolerance Method with adaptive parameters
FTMAS	Flexible Tolerance Method with adaptive parameters and scaling
FTMS	Flexible Tolerance Method with scaling
FTMS-BFGS	Flexible Tolerance Method with scaling and hybridized with BFGS Method
FTMS-PSO	Flexible Tolerance Method with scaling and hybridized with PSO
FTMS-Powell	Flexible Tolerance Method with scaling and hybridized with Modified Powell Method
FCI	Fixed Capital Investment
GHG	Greenhouse Gas
IPCC	Intergorvernmental Panel on Climate Change
MFTMS	Modified Flexible Tolerance Method with scaling and barrier
MEN	Mass Exchanger Network

MSA	Mass Separating Agent
NTP	Normal Temperature and Pressure
PSO	Particle Swarm Optimization
SQP	Sequential Quadratic Programming
TAC	Total Annualized Cost
TEL	Table of Exchangeable Loads
WCI	Working Capital Investment

Symbology

A	Evaporator area
b_j	Linear coefficient of equilibrium line of the j^{th} MSA
C_j	Cost
C_r	Cost of fresh source
C_1	Cognition learning rate
C_2	Social learning rate
δ_{k-1}	Residual mass of target specie entering interval k^{th}
δ_k	Residual mass of target specie leaving interval k^{th}
δ_0	Residual mass of target specie entering the first interval
d	Search direction
ε_i	Tolerance
ε_i	Minimum allowed composition difference for the j^{th} MSA
e_i	ith unit vector
f	Objective function
$\Phi_{(k)}$	Flexible tolerance criteria
F_r	Flowrate of fresh source
g	Inequality constraints
G_i	Mass flow of rich stream i^{th}
G_j	Flowrate of sink
GEN	Number of generations

h	Equality constraints
H	Hessian matrix
k	Dessin coefficient
L_j^C	Upper bound on available flowrate of the j^{th} MSA
L_j	Mass flow of the j_{th} MSA
m	Number of equality constraints
m_j	Slope of equilibrium line for the j^{th} MSA
N_{int}	Number of composition intervals
N_{sp}	Number of MSA of the processo
N_R	Number of rich streams
N_{sinks}	Number of process sinks
$N_{sources}$	Number of process sources
N_{fresh}	Number of fresh sources
N_{Int}	Number of interceptors
N	Population size
N_{eval}	Number of objective function evaluations
N_{it}	Number of iterations
p	Number of inequality constraints
P	Penalty function
P_n	Outlet pressure of each effect of evaporation
P_0	Inlet pressure
P_f	Outlet pressure
$P(\mathbf{x})$	Penalty function
r	Positive penalty parameter
r_{th}	Fresh source
$T(\mathbf{x})$	Positive functional
T_s	Temperature of heating steam in the calandria
$T_{s,n}$	Heating steam temperature feed in the effect n
$T_{0,n}$	Feed temperature of vinasse in the effect n

t	Size of the initial polyhedron
τ	Small positive scalar
t_{proc}	Processing time (seconds)
U	Overall heat transfer coefficient
υ	Slack variable of GRG method
Υ	Penalty parameter
$x_{brix,out}$	Brix in outlet
x_j^S	Available composition of key component at j^{th} of MSA
x_j^t	Target composition of of key component at j^{th} of MSA
$x_j^{out,max}$	Maximum feasible composition of outlet of the lean stream
x_r	Composition of fresh source
$\mathbf{x}_i^{(k)}$	ith vertex of the polyhedron in $\Re^n$
$\mathbf{x}_{cent}^{(k)}$	The vertex corresponding to the centroid
y	Composition of key component in any waste stream
y_{k-1}	Top composition of the lines defined in interval k^{th}
y_i	Composition of process sources
$W_{i,k}^R$	Quantity of mass that pass from rich stream i^{th} through interval k^{th}
W_i	Mass flowrate of process sources
ω	Inertia weight
z_j^{in}	Entering composition of sink
z_j^{min}	Minimum allowed composition at unity j.
z_j^{max}	Maximum allowed composition at unity j.

CHAPTER 1

Introduction

Process integration is an important tool for chemical industry due to the great benefits derived from the application of this technique, such as reduced capital investment and energy use, improving environmental performance, among others. According to the International Energy Agency, process integration is:

> "Systematic and general methods for designing integrated production systems, ranging from individual processes to total sites, with special emphasis on the efficient use of energy and reducing environmental effects."

Many advances have been made in process integration, however there is much yet to be developed. One of the challenges in the field is to find solutions to problems of integrating networks in a robust and efficient manner. One of the difficulties is to implement an optimization method capable of dealing with the great complexity of this type of problem (nonlinearities, convexities, discontinuities). As the problems of integration processes become more complex, the optimization methods based on the gradient are unable to deal with the constraints, discontinuities and inflection, because the information of the gradient, if any, also becomes more complex and difficult be obtained.

The flexible tolerance method is a direct search deterministic optimization method, easy to implement and to use (Himmelblau, 1972). However, its applicability and performance in process synthesis problems, and specifically in integration processes has not yet been analyzed. The purpose of this work fits into this scenario.

1.1 Objective

The objective of this work is the application of a simple method of optimization with direct search, the flexible tolerance method (FTM) with changes/improvements in mass integration systems synthesis.

The specific objectives are:

- To analyze the performance of the flexible tolerance method in problems of systems synthesis of mass integration;
- To identify the bottlenecks of the proposed method to solve problems of systems synthesis of mass integration;
- To assess enhancements for the optimization algorithm;
- To obtain an optimization method based on the flexible tolerance method able to deal with problems of systems synthesis of mass integration;
- To perform the case study of mass integration in a sugarcane biorefinery using the developed algorithm.

1.2 Thesis organization

Chapter 2 provides a brief review of optimization methods used for solving nonlinear problems, and in particular, it provides details on the flexible tolerance method, the focus of this work. This chapter also presents the most important concepts of mass integration, as the formulation types most commonly used for solving process synthesis problems in this scope. A brief literature review shows the applications of the flexible tolerance method, and the main formulations and methods/algorithms for solving mass integration problems.

Chapters 3-6, which present the development and the results of this thesis. In each chapter, it will be found: (a) a brief introduction in which is shown the purpose of the chapter; (b) the development; and (c) the conclusion, where the main findings are highlighted.

Chapter 3 presents the implementation of the Flexible Tolerance Method (FTM) in some classical problems of mass integration proposed in the literature and compares its performance with two other methods: SQP (Sequential Quadratic Programming) and GRG (Generalized Reduced Gradient). In this chapter, it is performed a preliminary analysis of the effectiveness of FTM by using classical problems of mass integration systems synthesis, in order to detect the bottlenecks that can interfere in the application of such simple method in more complex problems, such as the synthesis of chemical processes.

From the difficulties encountered by the flexible tolerance method for solving mass integration problems, Chapter 4 shows the proposed changes in order to improve the performance

of the original method. Such changes include the scheduling of variables through the transformation of variables and hybridization with different deterministic unrestricted optimization methods (BFGS, Powell) to perform the internal search of the flexible tolerance method and non-deterministic ones (PSO) to perform the initialization. At this point, a set of optimization problems with constraints generally employed for optimization algorithms performance analysis was used.

From the results found in Chapter 4, other modifications of the Flexible Tolerance Method are proposed in Chapter 5: the use of adaptive parameters in Flexible Polyhedron Method or Nelder-Mead Method that performs the internal search in the original algorithm, and the imposition of a barrier during the optimization process for the variables that go beyond the imposed limits. The performance of the method with modifications is tested for the same set of problems from Chapter 4, and the best algorithms found is then used to solve mass integration problems.

The algorithm of the flexible tolerance method modified (MFTMS) in Chapter 5 and the hybrid method obtained in Chapter 4 (FTMS-PSO) were used for solving a new problem of mass integration proposed in this paper. It is the mass integration of a sugarcane biorefinery, considering as target sources: (i) water, (ii) vinasse and (iii) carbon dioxide. It is performed the assessment of water reuse, vinasse concentration and carbon dioxide reuse through some ways (algae, capture and production of sodium bicarbonate).

Finally, Chapter 7 presents the conclusions and final remarks of this study and suggestions for future works.

CHAPTER 2

Theoretical Foundations and Literature Review

2.1 Theoretical Foundations

2.1.1 Nonlinear Optimization

The nonlinear constrained optimization problem can be represented as follows:

$$\text{Minimize:} \quad f(\mathbf{x}) \quad \mathbf{x} \in \Re^n \tag{2.1}$$

$$\text{Subject to:} \quad h_i(\mathbf{x}) = 0 \quad i = 1, ..., m \tag{2.2}$$

$$g_i(\mathbf{x}) \geq 0 \quad i = m+1, ..., p \tag{2.3}$$

where $f(\mathbf{x})$ is the objective function, $h_i(\mathbf{x})$ is the equality constraints and $g_i(\mathbf{x})$ is the constraints of inequality.

The optimization methods can be broadly divided into deterministic and stochastic methods. In deterministic methods, every step can be predicted by knowing the starting point, i.e., it always presents the same answer if beginning from the same starting point. However, for the stochastic methods, several choices are made based on random numbers, drawn at the time of code execution. Since, at every code execution, all the numbers will be different, a random method does not perform the same sequence of operations in two successive runs. Starting from the same starting point, each code execution will follow their own path and possibly lead to a different final answer (Silva, 2009).

2.1.1.1 Deterministics Methods

The deterministic methods that may or may not be based on the gradient, have as advantage a low number of objective function assessments, making the convergence faster. However, they have difficulties in escaping from optimum locals.

Among the methods based on gradient, it can be highlighted SQP and GRG.

Sequential Quadratic Programming (SQP) basically consists of the sequential approach of the non-linear programming problem as a quadratic programming problem. Since it is based on gradients, there is a need to calculate the derivatives of the objective function and constraints. Such derivatives can be estimated numerically, but convergence may not be good. The best option is the analytical determination of such derivatives. Unlike other methods, which try to convert the problem into a sequence of unconstrained optimization subproblems, the SQP tries to solve the optimization problem iteratively, where the solution in each step is obtained by solving an approximation of the nonlinear problem where the objective $f(\mathbf{x})$ is replaced by a quadratic approximation and nonlinear constraints $h_i(\mathbf{x})$ and $g_i(\mathbf{x})$) are replaced by linear approximations. The SQP method, at every iteration, solves the following problem of quadratic programming, Teles (2010):

$$\text{Minimize:} \quad \nabla^T f(x^k)d + \frac{1}{2}d^T H(x^k, \lambda^k, \mu^k) \tag{2.4}$$

$$\text{Subject to:} \quad h(x^k) + \nabla^T h(x^k)d = 0 \tag{2.5}$$

$$g(x^k) + \nabla^T g(x^k)d \geq 0 \tag{2.6}$$

where H is a positive definite approximation of the Hessian matrix of the Lagrangian function, which can be updated by any method of variable metric (DFP - David Fletcher, Powell, BFGS, etc.). Further details of such method can be found in Edgar et al. (2001).

The Generalized Reduced Gradient method (GRG) is an extension of Wolfe algorithm (Himmelblau, 1972) to accommodate the objective and nonlinear constraint functions. Essentially, the method employs linear or linearized constraints, and converts the gradient into that new base. The problem solved by the GRG is as the following Himmelblau (1972):

$$\text{Minimize:} \quad f(\mathbf{x}) \quad \mathbf{x} \in \Re^n \tag{2.7}$$

$$\text{Subject to:} \quad h_i(\mathbf{x}) = 0 \quad i = 1, ..., m \tag{2.8}$$

$$L_j \leq x_j \leq U_j \quad j = 1, ..., n \tag{2.9}$$

$$h_i(\mathbf{x}) = g_i(\mathbf{x}) - \upsilon_i^2 \quad i = m+1, ..., p \tag{2.10}$$

$$-\infty \leq \upsilon_i^2 \leq \infty \tag{2.11}$$

where inequality constraints are included by subtracting a break variable, υ, transforming

it into a constraint of equality. A detailed description of method can be found in Himmelblau (1972) and Edgar et al. (2001).

The methods that are not based on gradient perform the search directly, and the search directions are determined from successive assessments of the objective function. As a general rule, the optimization methods that use the gradient and the second derivatives converge faster than the direct search methods. However, in practice, the gradient-based methods present two major difficulties in their implementation: (i) for problems with many variables, providing analytical derivatives of the functions may become very laborious or even impossible in some cases; and (ii) despite the possibility of replacing the analytical derivatives for their numerical approximations, the error introduced by such procedure in the vicinity of the ends may be an obstacle. On the other hand, the direct search methods do not require regularity and / or continuity of objective functions and / or constraints, or the existence of its derivatives. Another important point is that the time spent in the problem preparation for solution with methods that require the derivatives of the functions is much greater than the time spent in preparation of the problem for solution with a method of direct search (Himmelblau, 1972).

Among the direct constrained optimization methods, the ones based on penalty functions must be highlighted. In the literature, there are many methods belonging to this family. Essentially, all of such methods transform a restricted nonlinear programming problem into an unrestricted problem or into a sequence of unconstrained problems. It may be mentioned the following methods: MINIMAL, SUMT, among others.

Weisman MINIMAL method combined three different techniques: direct search of Hooke and Jeeves, the random search and the concept of penalty function. The formed penalty function is given by eq. (2.12), where $\delta_i = (1 - U_i)$ is zero when the constraint is satisfied, and it is one when it is not satisfied. The equality constraints are included when rewriting them as inequality constraints by adding a tolerance (ε_i), as shown in eq. (2.13).

$$P(\mathbf{x}, r) = f(\mathbf{x}) + \sum_{i=1}^{p} \delta_i r_i g_i^2(\mathbf{x}) \tag{2.12}$$

$$g_i(\mathbf{x}) = |h_i(\mathbf{x})| - \varepsilon_i \leq 0 \tag{2.13}$$

The SUMT original method (Sequential Unconstrained Minimization Technique) has been extended to accommodate constraints of equalities by Fiacco and McCormick. The basic idea of such method is to repeatedly solve a sequence of unconstrained problems whose solutions in the limit approach the minimum of the unrestricted non-linear programming problem. Thus, the problem described by eq. (2.1) - (2.3), can be transformed into a sequence of unconstrained problems defined by the function P as shown in eq. (2.14).

$$P(\mathbf{x}^{(k)}, r^{(k)}) = f(\mathbf{x}^{(k)}) + (r^{(k)})^{-\frac{1}{2}} \sum_{i=1}^{m} h_i^2(\mathbf{x}^{(k)}) + r^{(k)} \sum_{i=m+1}^{p} \frac{1}{g_i(\mathbf{x}^{(k)})} \tag{2.14}$$

where r is a positive and monotonically decreasing weighting factor. There are other possibilities for formulating the P function, and further details of such method can be found in Himmelblau (1972).

2.1.1.2 Flexible Tolerance Method

Another direct search method is the flexible tolerance method (FTM) proposed by Paviani and Himmelblau (1969). The algorithm of flexible tolerance enhances the value of the objective function by using the information provided by feasible points, as well as some non-feasible points, called near-feasible points. Near-feasibility gradually becomes narrower as the search goes to the solution of the problem, to the extent where only feasible $\mathbf{x}$ vectors of eq. (2.1) - (2.3) are accepted. As a result of this basic strategy, the optimization problem, eq. (2.1) - (2.3) can be rewritten as follows, eq. (2.15) and (2.16):

$$\text{Minimize:} \quad f(\mathbf{x}) \quad \mathbf{x} \in \Re^n \tag{2.15}$$

$$\text{Subject to:} \quad \Phi_{(k)} - T(\mathbf{x}) \geq 0 \tag{2.16}$$

where $\Phi_{(k)}$ is the flexible tolerance criteria for viability at stage k of the search, and $T(\mathbf{x})$ is a positive function for all equality and/or inequality constraints of the problem, used as a degree measurement of the restriction violation extension.

FTM uses two searches to satisfy feasibility constraint. The external search is a variation of the Nelder-Mead method (or the Flexible Polyhedron method or FPM), shown in Figure 2.1. This one seeks to minimizes the objective function $f(\mathbf{x})$. When a new vertex is found during the search, its viability is assessed. If the vertex (and thus all the polyhedron) is close to the viability, the search continues the procedure in Figure 2.1. If the external search selects a non-feasible vertex, an internal search is performed to convert it into a near-feasible vertex.

The internal search minimizes the value of $T(\mathbf{x})$. The search starts at a non-feasible vertex found by the external search and it is applied the Nelder-Mead method (FPM) to perform a search in the search space of constraints until the found vector satisfies the conditions of feasibility (or near-feasibility). Once found, the FTM continues with the external search. It should be emphasized that the use of Nelder-Mead method is not limited to performing the internal search on FTM, thus, any other multi-variable technique may be used.

The method of Nelder and Mead minimizes a function of n independent variables using $(n+1)$ vertices of a flexible polyhedron. The procedure of finding a vertex in which the objective function has a better value involves four operations: reflection, expansion, contration and reduction; and a possible outcomes for a function with $n = 2$ is showed in Figure 2.2. In problems with large number of variables the polyhedron can assume the form indicated in Figure 2.3.

Such method, FTM, was chosen for the optimization of problems of mass integration system

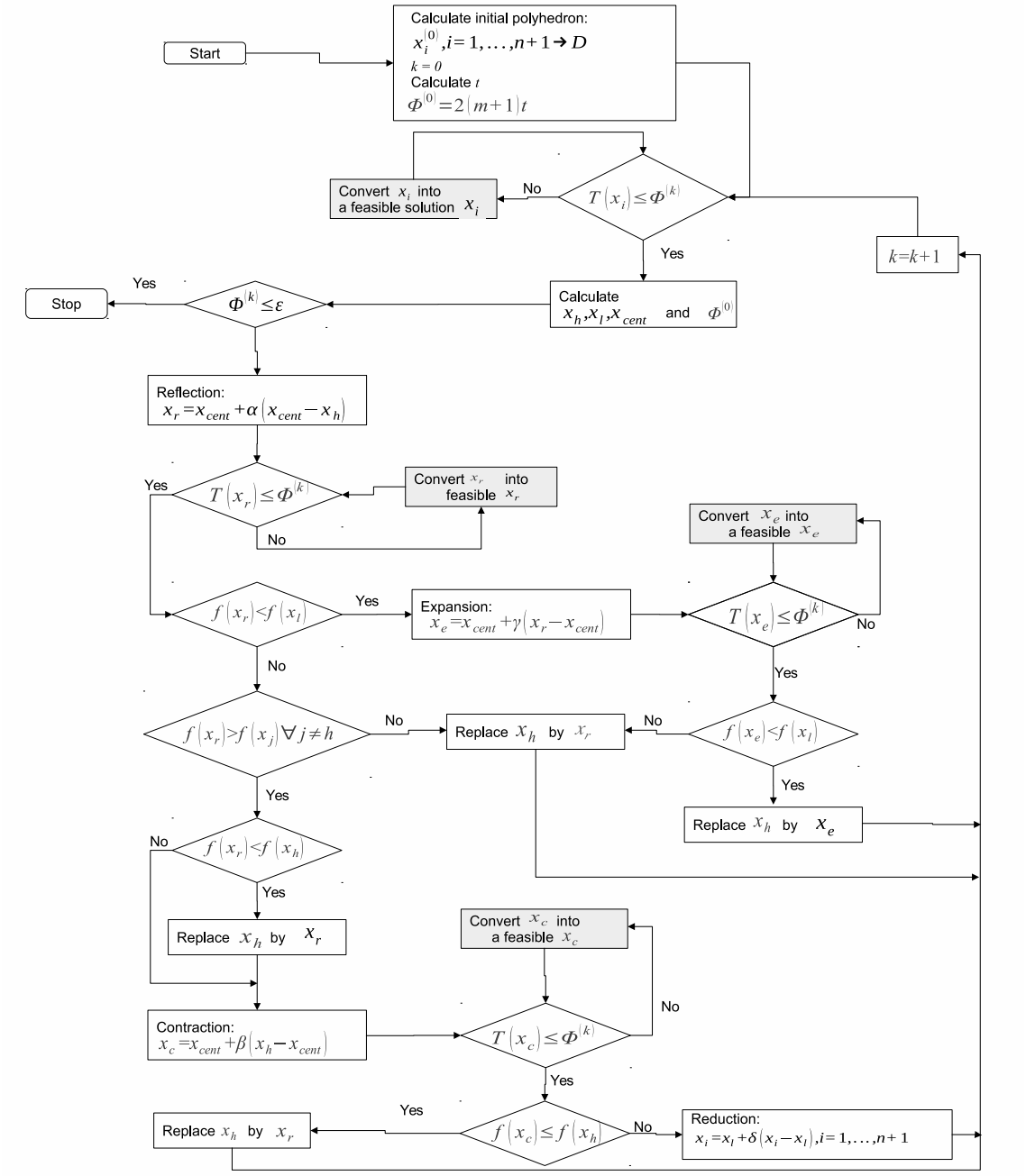

Figure 2.1: FTM algorithm flowchart for performing the outer search that minimizes the objective function $f(\mathbf{x})$. All vectors $\mathbf{x}$ are assumed to represent $x^{(k)}$, unless noted otherwise. Adapted and modified from (Naish, 2004).

synthesis in this work. Among the motivations that led to this choice, it may be mentioned: (i) as integration problems become more complex, optimization methods based on gradient become unable to deal with a large number of constraints, discontinuities and inflections, and the gradient information becomes increasingly difficult and complex to be obtained; (ii) it is a simple method, easy to be implemented and used; and (iii) it was not found in the literature, studies that report the use of FTM in process integration problems.

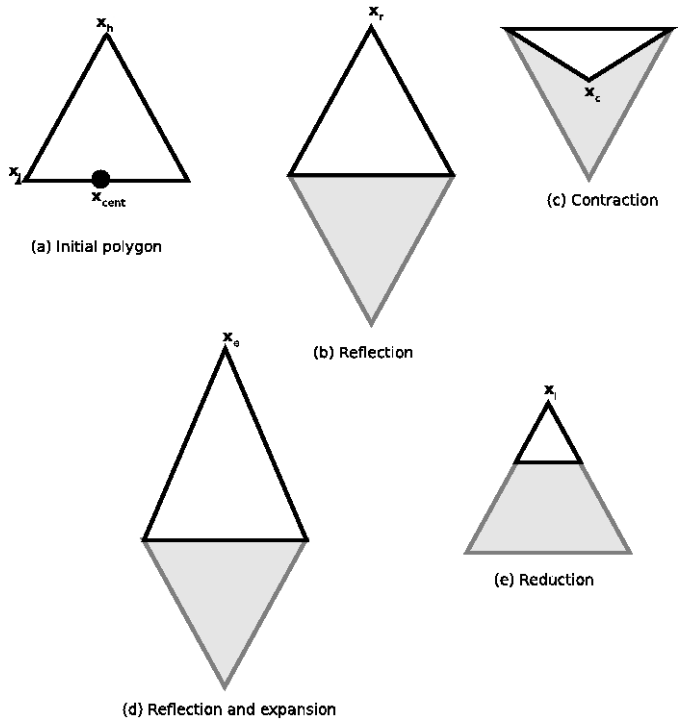

Figure 2.2: Possible outcomes for an interation of the Nelder-Mead Method (FPM) for $n = 2$, where $\mathbf{x}_{cent}$ is the centroid, $\mathbf{x}_l$ the smallest value of objective function, $\mathbf{x}_h$ the highest value of objective function, $\mathbf{x}_r$ the value of objective function obtained after reflection, $\mathbf{x}_c$ the value of objective function obtained after contraction, $\mathbf{x}_e$ the value of objective function obtained after expansion. Adapted and modified from (Naish, 2004).

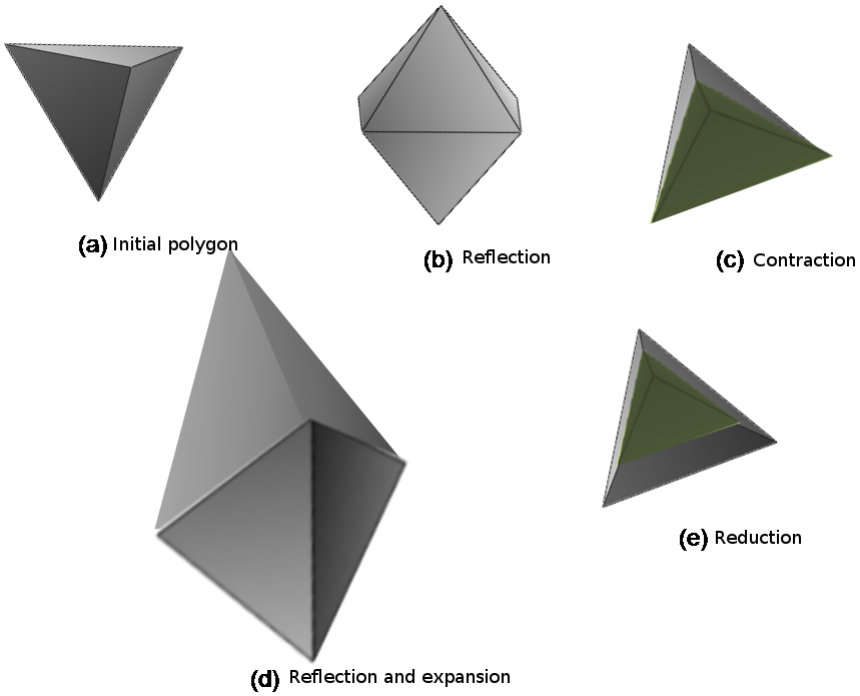

Figure 2.3: Possible outcomes for an interation of the Nelder-Mead Method (FPM) for $n = 3$.

2.1.1.3 Non-deterministics Methods

Stochastic methods have been a strong trend in recent years. Since the 1950s, through analogies with nature, it was created several non-deterministic algorithms in an attempt to simulate biological phenomena. Such algorithms, called Natural Optimization Methods, have some aspects in common. The most striking one is its random character, in an attempt to simulate the chance that seems to govern distinct processes in nature, from the evolution of species to the social behavior of animals. Furthermore, such methods have the advantages of easy implementation, robustness and they require no continuity in the problem definition.

The main methods are Simulated Annealing, Particle Swarm Optimization, Ant Colony Optimization techniques and Genetic Algorithms (Nelles, 2001).

Simulated Annealing (SA) has its origin in the analogy between the physical process of cooling a molten metal and the optimization problem. The objective function in this metaheuristics corresponds to the system energy level, which in both situations, physical or simulated, is desired to be minimized. The temperature of the physical system has no equivalent in the optimization problem. It will only be a control parameter. In the iterative process, if only configurations that lead to a reduction in energy are accepted, there will be a rapid convergence of an elevated temperature to a temperature equal to zero ($T = 0$), which physically means a quenching or a metastable solution from a mathematical point of view, Soeiro et al. (2010).

Optimization by Ant Colony has as basic idea the use of a mechanism known as positive reinforcement, based on the analogy with the behavior of certain species of ants that place a chemical called pheromone in the paths they make, enabling the strengthening of the most used paths, which are possibly the best. A virtual pheromone is used to keep the good solutions in computer memory. There is also the concept of negative reinforcement, implemented by analogy of the evaporation process that the pheromone suffers in nature. The combination of positive reinforcement (pheromone deposit) with the negative one (evaporation), allows one to avoid, in most cases, a premature convergence of the algorithm for solutions, possibly not bad, but perhaps far from optimal. Cooperative behavior is another important concept: ant colony algorithms use the simultaneous exploration of different solutions through different ants. The best ants influence the exploitation of others, through the strategies employed to update the pheromone in paths, Becceneri et al. (2010).

Particle Swarm method was proposed by Kennedy and Eberhart (1995) and explores the analogy with the social behavior of animals as swarms, shoals or flocks of birds. In those, each individual in the group makes its own decisions, but always somewhat based on the group leader's experience. Mathematically, each individual of the group is considered a point of the space search. The speed of that individual is the search direction to be used in the point candidate for the solution. The search direction in an iteration is determined by weighing the experience of that solution and the best solution already found by the group (metaphorically, the leading solution), Silva (2009).

Genetic algorithms are a particular class of evolutionary algorithms that uses techniques inspired by evolutionary biology such as inheritance, mutation, natural selection and recombination (or crossing over). In its implementation, a population of abstract representations of solutions is selected in search of better solutions. Evolution usually starts from a set of solutions randomly created and it is carried through generations. In every generation, the adaptation of each solution in the population is assessed, some individuals are selected for the next generation, and recombined or mutated to form a new population. The new population is then used as input for the next iteration of the algorithm, Mitchell (1998).

2.1.2 Process Integration

Process integration began with energy integration, when Linnhoff and colleagues published "Guide for Optimal Use of Energy in Process Industries" in 1982, where the concept of process integration was presented. The methods developed for energy analysis of processes are based on thermodynamics (Pinch Analysis) or on optimization techniques (mathematical programming). Pinch analysis is a method based on the second law of thermodynamics[1] , in which the concept was expanded to the management of energy use in a whole plant. The method is about the optimal structure of heat exchangers between process streams, as well as the optimal use of utilities. Pinch analysis uses graphical tools and does not require much computational performance, it is easy to apply, the reason why it is one of the most used methods.

Parallel to the development of Pinch analysis method, another approach based on mathematical programming has been proposed. The methods from mathematical programming can be divided into two classes: sequential and simultaneous. Sequential methods generate partially optimized networks that meet one of the criteria: (i) minimal use of utilities, (ii) minimum investment or (iii) minimum number of heat exchangers. In the simultaneous method, an existing superstructure is strictly optimized using the MINLP (Mixed Integer Nonlinear Programming). Currently, the two techniques (Pinch and Mathematical programming) are complementary. While Pinch analysis serves as a conceptual tool, mathematical programming serves as a tool for the automatic design of networks of heat exchangers.

Many approaches have been made to solve energy integration problems such as the use of hybrid methods, deterministic methods and non-deterministic methods for the generation of optimal network of heat exchangers. With the improvement of resolution methods and with the application of information technology (IT), computer tools have been developed and are able to provide fast and accurate (when possible) solutions with a friendly interface. Some of the main software developed for energy integration are: (i) SPRINT[2]: energy recovery systems design for individual processes in a plant; ii) STAR[3]: design of utilities in plants and cogeneration systems;

[1] Second law of thermodynamics establishes the conditions in which the thermodynamic transformations may occur.

[2] SPRINT - Process Integration Software - `http://www.ceas.manchester.ac.uk/research/centres/centreforprocessintegration/software/packages/sprint/`

[3] STAR - Process Integration Software - `http://www.ceas.manchester.ac.uk/research/centres/`

iii) WORK[1]: design of processes at low temperatures; iv) SuperTarget®[2]: energy integration in new and retrofit projects; among others.

Mass integration is a methodology that allows an overall understanding of the mass flow within the process, and employs such knowledge in identification of performance improvements and optimization of the generation and mapping of species throughout the process. It began in 1989 with the work by El-Halwagi and Manousiouthakis, "Synthesis of mass exchanger network", in which it was proposed a procedure in two stages El-Halwagi and Manousiouthakis (1989). Initially, it is performed a thermodynamically driven process to identify "pinch points" that limit the extension of the mass exchange between the rich and lean process streams. Then, the design of those preliminary networks is enhanced until reaching the final configuration of the MEN (Mass Exchange Network) satisfying the desired exchange at minimum cost.

Despite the analogy between mass transfer and energy transfer, a direct and simple extension of the synthesis of heat exchanger network for the synthesis of mass exchange networks is not possible due to differences in transport mechanisms and balancing criteria. Furthermore, MEN synthesis is a more general problem and larger than the synthesis problem of heat exchanger networks.

One developed software based on the mass integration concept is WATER[3], specific to water systems design in process industries. Based on the identification of opportunities for reuse, regeneration and recycling, it is possible to obtain the minimum water consumption. WATER software includes: minimization of water use, multiple sources of water, automatic design of water reuse networks, water regeneration and calculation of pipe costs and effluent treatment.

Recently a new category of process integration was proposed, property integration. Property integration is a holistic approach for allocating and handling chains and process units, which is based on the monitoring, adaptation, assigning and combination of functions along the process El-Halwagi (2006). Property integration can be used in material reuse problems, which are governed by the properties or features of a certain stream and not by their chemical constitution (as mass integration). For example: the emission of pollutants is dependent on its properties (volatility, solubility, etc.); environmental regulations involves limits on the properties (pH, color, toxicity, etc.), among several others.

In general, there are two basic alternatives for dealing with the problems of process integration. The first alternative is independent on the structure, called targeting, and it is based on the particular task resolution in a sequence of stages. At each stage a "design target" can be identified and used in subsequent stages. Those objectives (or targets) are determined before the detailed design and without commitment to the final system configuration. The main ad-

centreforprocessintegration/software/packages/star/

[1]WORK - Process Integration Software - http://www.ceas.manchester.ac.uk/research/centres/centreforprocessintegration/software/packages/work/

[2]KBC - SuperTarget®- http://www.kbcat.com/Software-Solutions/SuperTarget/

[3]WATER - http://www.ceas.manchester.ac.uk/research/centres/centreforprocessintegration/software/packages/water/

vantages of such alternative are: (i) within each stage of the extent of the problem is reduced to a manageable size, which avoids combinatorial problems; and (ii) it provides valuable information about the characteristics and system performance. The second approach is dependent on the structure and it is applied for the generation and selection of alternatives, which involves the development of frameworks[1] . The mathematical formulation in this type of approach does not involve mixed-integer linear programming (MINLP). Although the latter is more robust than the former (targeting), its success is heavily dependent on three challenging factors: (i) the representation of the system must include all possible alternatives; (i) non-linearities in the mathematical formulation mean that having a global solution in the optimization programs can sometimes be an elusive goal; and (iii) the task of synthesis is formulated as a MINLP, thus, entries, preferences, judgments and perceptions of the engineer are set aside, and they must be included as part of the problem formulation, which can be a quite tedious slow tasks.

This work deals exclusively with mass integration problem solving by using the flexible tolerance method and its modifications; the main concepts and methods used in this approach are described next.

2.1.3 Mass integration

Among the important advantages for the processes, mass integration enables: minimal consumption of utilities (solvents, water, etc.), minimal discharge of effluents, minimal use of new utilities (fresh), minimal production of undesirable byproducts and maximum production of the desired product. According to El-Halwagi and Manousiouthakis (1989) the mass integration is based on the fundamental principles of chemical engineering combined with system analysis using graphical and optimization tools. The first step to be taken when using mass integration techniques is the development of a full representation of mass allocation of the entire system from the point of view of the involved species, as shown in Figure 2.4.

For each designated species, there are sources (streams that carry the species) and sinks (units that can accept the species). Sinks include reactors, heaters, coolers, treatment plants, waste discharges, etc. Streams leaving the sinks (exhausted streams) become sources. Thus, sinks are also sources of the designed species. Each sink can be manipulated through design and/or operational changes to change the flow and composition for specific conditions of each sink. Generally, the sources are prepared so they can be used in sinks, which have constraints as to the concentration of the species through segregation and separation. Some concepts relating to the strategies used in mass integration are described next El-Halwagi (1997):

Segregation It prevents the mixture of streams. In many cases, segregating streams with waste at the source makes those streams environmentally acceptable and reduces the total cost of treatment. Furthermore, the segregation of streams with different compositions avoid

[1] The frameworks can include graphics of the process, representation by state tree and representation by superstructures.

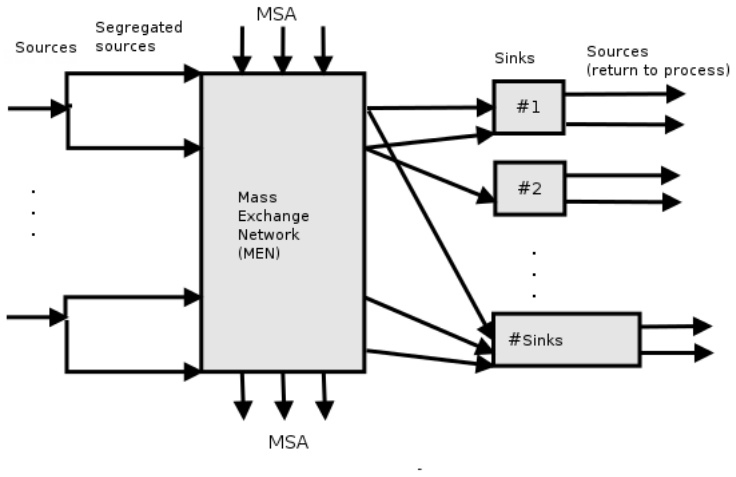

Figure 2.4: Representation of mass allocation in a system.

unnecessary dilution of streams. That reduces the cost of removing certain species of a more concentrated stream. Such strategy also allows streams at concentration levels that can be directly recycled at the process units.

Recycling It refers to the use of a source in a process unit (a sink). Each sink has a number of constraints in the characteristics (e.g. flow and composition) in the feeding that it can process. If the source meets those constraints, it can be recycled directly at the sink. However, if the source violates those constraints, segregation, mixture and / or interception can be used for the preparation of the stream for recycling.

Interception It indicates the use of a single operation of separation to adjust the composition of the streams, in order to make it acceptable to the sinks. Those separations can include the use of mass separating agents (MSA) and/or energy separation agents (ESA). A systematic technique is required to search the plurality of separation agents and separation technologies to find the optimal separation system. The synthesis of a physical separation induced by an MSA is called mass exchange network synthesis (MEN). The interception network using reactive MSA is called reactive mass exchange network (REAMEN). The mass exchange network synthesis technique can count on other separation systems such as membrane separation, separation networks induced by heat and sequence of distillation columns.

Sink manipulation It involves the design and operational changes that alter the flow or composition of a certain stream entering or leaving the process unit. Such changes include: changes in the temperature/pressure, a unit replacement, catalyst modification, replacement of the raw material, reaction path changes, changes in the reaction system and replacement of the solvent.

Methods employed for the synthesis of mass exchange networks are briefly described next.

2.1.3.1 Methods based in Algorithms Procedures

The group of methods based on algorithmic procedures is largely based on the Bottleneck Technology or Pinch Technology. Some methods still use the concepts of Pinch Technology and of heuristics rules. Next, it is presented the Pinch method and the algebraic method based on Pinch technology, as described by El-Halwagi (2006).

2.1.3.1.1 Pinch Method

Pinch method (or graphical method) has two stages: targeting and design. In the targeting step, problem data is used to thermodynamically predict optimal performance. Then, the network is designed in order to achieve the objectives.

The first method based on Pinch technology was presented by El-Halwagi and Manousiouthakis (1989). Pinch diagram is constructed by plotting the transferred mass versus its composition for all rich and lean streams. Each stream is represented by an arrow whose ends matches its input composition and its beginning represents its output composition. The slope of the arrow corresponds to the flow of the stream. Combining all rich streams into a single profile through the diagonal overlap rule, the composition curve for the rich stream is determined. Similarly, it is determined the composition curve of the lean stream. When the curve corresponding to the rich streams touch the lean stream curve, it characterizes the pinch point. Pinch point is the critical point from where the transfer between the streams becomes impracticable.

The lean stream composite curve may move down and up, which implies different decisions on mass transfer. If the lean stream composite curve is moved up, so that there is no horizontal overlap with the rich stream composite curve, there is no mass integration between the rich streams composite curve and MSA process. Such configuration is shown in Figure 2.5, in which x_j^S is the available composition of the key component in jth MSA, x_j^t is the objctive composition of the key component in j^{th} MSA, m_j is the slope of the equilibrium line for j^{th} MSA, b_j is the linear coefficient of the j^{th} MSA equilibrium line, ε_i is the minimum difference of composition allowed for the j^{th} MSA, and y is the composition of the key component of any residue streams. As the composite curve of lean streams moves down, so that there is some horizontal overlap, some mass integration may be performed, as shown in Figure 2.6. The optimal situation occurs when the composite curve of lean streams touches the composite curve of rich streams at a point (point Pinch of mass transfer), as shown in Figure 2.7. In this case, the mass integration is maximal, and has a minimum consumption of external MSA.

To achieve the objectives of maximum integration and minimum use of external MSA, it is necessary to follow three rules for the design El-Halwagi (2006):

- No mass must be transferred through Pinch.
- No excess of capacity must be removed from MSA below Pinch.

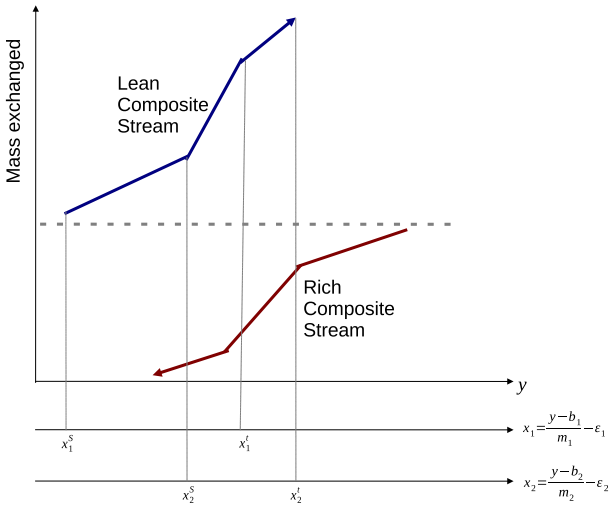

Figure 2.5: Pinch diagram without integration between the composite curve of the rich streams and process MSA. Adapted from El-Halwagi (2006).

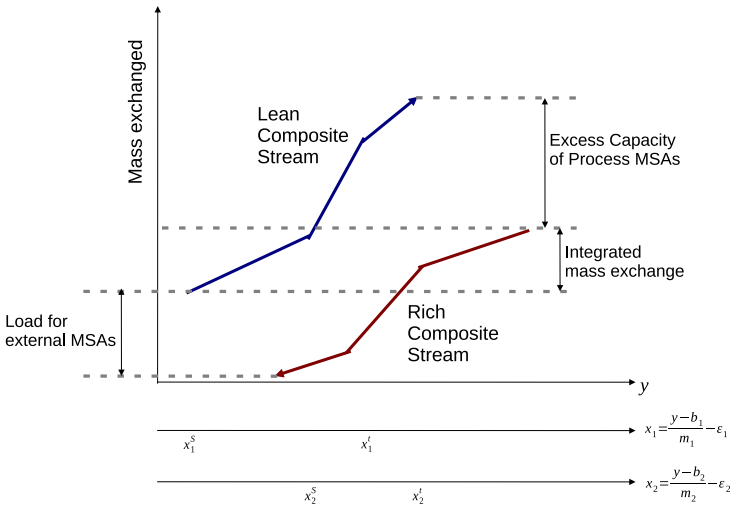

Figure 2.6: Pinch diagram with partial integration between the composite curve of the rich streams and process MSA. Adapted from El-Halwagi (2006).

- No external MSA must be used above pinch.

Pinch methodology informs the potential for integration that the streams have, however does not contribute much to identify which network will achieve this goal, thus this method will not be used in this work. Further construction details Pinch diagram and its applications can be found at El-Halwagi (2006) and El-Halwagi (1997).

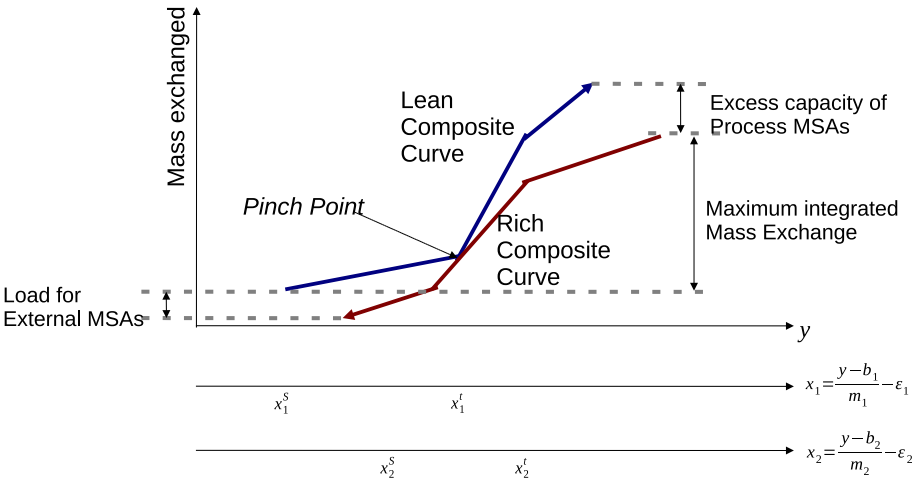

Figure 2.7: Pinch diagram with maximum integration between the composite curve of the rich streams and process MSA. Adapted from El-Halwagi (2006).

2.1.3.1.2 Algebraic Method

The algebraic technique produces the same results from the Pinch method. It is an effective method to deal with major problems, when they can be manipulated using spreadsheets and calculators. In addition, this technique can be integrated with other design tools including simulators. Afterwards, it is presented a brief summary of this method, further details can be found in El-Halwagi and Manousiouthakis (1989), El-Halwagi (2006) and El-Halwagi (1997).

Initially Composition Interval Diagram (CID) is build to evaluate the thermodynamic feasibility of mass transfer. In the diagram, a number, $N_{sp}+1$, of composition axes are generated. First, the axis of composition, y, is set for rich streams (they do not need to be at scale). Each rich stream is represented by a vertical arrow, whose beginning corresponds to the available composition and whose end corresponds to the objective composition. The calculation of the objective composition of every MSA is performed using eq. (2.17), in which $x_j^{out,max}$ is the maximum output feasible composition in the lean stream, y_i^{in} is the composition of the key component in the rich stream i^{th}, m_j is the equilibrium line slope for the j^{th} MSA, b_j is the linear coefficient of the j^{th} MSA equilibrium line, and ε_j is the minimum difference of composition allowed for the j^{th} MSA. Similarly to rich streams, each MSA of the process (or lean stream) is represented versus its composition axis with vertical arrows going from the available composition to the objective composition.

$$x_j^{out,max} = \frac{y_i^{in} - b_j}{m_j} - \varepsilon_j \tag{2.17}$$

Then, the horizontal lines are drawn at the beginning and end of the arrows, the distance between two horizontal lines is the composition interval. The number of intervals is related to the number of streams of the process through eq (2.18):

$$N_{int} \leq 2(N_R + N_{sp}) - 1 \tag{2.18}$$

where: N_{int} is the number composition intervals, N_{sp} is the number of the process MSA and N_R is the number of rich streams.

Figure 2.8 shows the schematic representation of a CID. The mass transfer is thermodynamically feasible (and possible) from rich streams to MSA within the same interval. It is also possible to transfer rich stream mass to a lean stream that is in a lower interval.

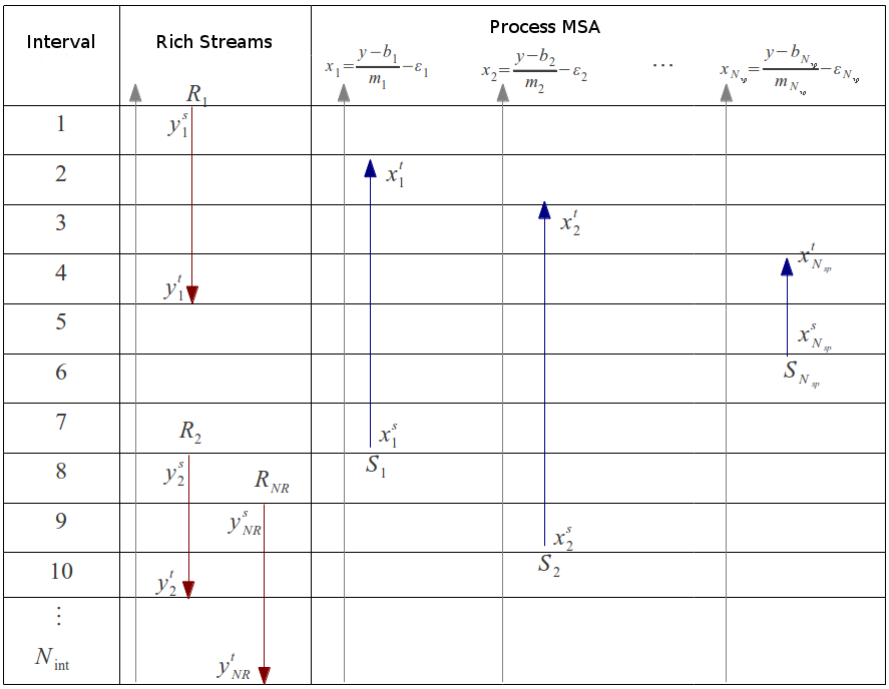

Figure 2.8: Composition interval diagram. Adapted from El-Halwagi (2006).

The determination of the amount of transferable mass between the lean and rich streams in each interval is achieved through the construction of the Table of Exchangeable Loads (TEL). The quantity of mass ($W_{i,k}^R$) passing from the rich stream i^{th} through the k^{th} interval is calculated according to eq. (2.19).

$$W_{i,k}^R = G_i(y_{k-1} - y_k) \tag{2.19}$$

where y_{k-1} and y_k are the corresponding compositions of the top and the base of the lines defined in the interval k^{th}, G_i is the mass flow of the rich stream i^{th}. Similarly, the maximum load

that can be received by the j^{th} stream of MSA of the process within the interval k is determined by eq. (2.20):

$$W_{j,k}^{S} = L_{j}^{C}(x_{j,k-1} - x_{j,k}) \tag{2.20}$$

The total load of rich streams within the k^{th} interval is calculated by summing the individual loads for each rich stream passing through the interval (eq. 2.21):

$$W_{k}^{R} = \sum_{\text{i passing through interval } k} W_{i,k}^{R} \tag{2.21}$$

Similarly, the total loads in lean streams within the k^{th} interval is given by eq. (2.22):

$$W_{k}^{S} = \sum_{\text{j passing through interval } k} W_{j,k}^{R} \tag{2.22}$$

The next step is to make the mass exchange between the rich and lean streams, which performed by making up a mass balance (eq. 2.23) in each interval (Figure 2.9).

$$W_{k}^{R} + \delta_{k-1} - W_{k}^{S} = \delta_{k} \tag{2.23}$$

where δ_{k-1} and δ_{k} are the residual masses of the objective species entering and leaving interval k^{th}, and the residual mass entering the first interval δ_{0} is zero.

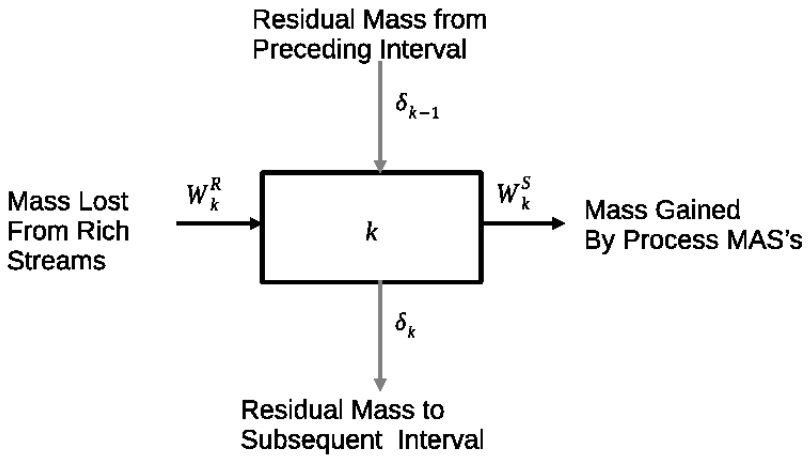

Figure 2.9: Mass balance by component around composition interval. Adapted from El-Halwagi (2006).

The thermodynamic feasibility is guaranteed when all δ_{k} are positive. Thus, a negative δ_{k} indicates that the capacity of the lean streams of the process at this level is greater than the load of rich streams. The most negative value of δ_{k} corresponds to excess capacity of the MSA of the process in removing the objective species. This excess in capacity can be reduced

by decreasing the mass flow rate and/or the output composition of one or more of the MSA. After the removal of excess of MSA capacity, it can be constructed a revised CID in which the streams and compositions have been adjusted. Thus, a revised cascade diagram may be generated, and the interval at which the residual mass is zero corresponds to the pinch point. Next, an overall mass balance for the network must be performed. The residual mass leaving the lowest composition interval of the revised cascade diagram must be removed by an external MSA.

2.1.3.2 Methods based in Mathematical Programming

It will be described some formulations used for mass integration within mathematical programming methods.

2.1.3.2.1 LP Formulation

Linear programming problem may or may not involve the generation of a superstructure. Such type of formulation involves a smaller number of possible superstructures. Then, it will be described the formulation that does not involve the generation of a superstructure. LP programming examples with superstructures can be found in Savelski and Bagajewicz (2000).

The resolution by the transshipment model is a formulation that does not depend on the superstructure. The synthesis of MEN is done based on composition intervals. The disadvantage of this method is that MEN may not be fully determined only through its use. This method is an extension of the algebraic mathematical programming method described above. Initially, as the algebraic method, the composition interval diagram (CID) is developed, then the table of exchangeable loads (TEL). A transshipment model allows the finding of a minimum cost of MSA, minimum flow of MSA, and the lean stream, which may be used to remove the keystone species from a rich stream in a certain concentration interval. The optimization problem can be described by mathematical modeling shown next, with the aim to minimize the cost of MSA,(eq. 2.24 - 2.30).

$$\min \sum_{j=1}^{N_s} C_j L_j \tag{2.24}$$

in which C_j is the cost (\$/kg MSA) and L_j is the mass flowrate of j_{th} MSA.

Subject to:

- Mass balance in each composition interval k (Figura 2.9):

$$\delta_k - \delta_{k-1} + \sum_{\text{j pass through interval k}} L_j W_{j,k}^S = W_k^R \quad k \in \{1,2,...,N_{int}\} \tag{2.25}$$

- MSA availability:

$$L_j \leq L_j^c \quad j \in \{1,2,...,N_S\} \tag{2.26}$$

in which L_j^c is the upper limit of mass flowrate available of j_{th} MSA.

- No residual mass entering or leaving the cascate:

$$\delta_0 = 0 \tag{2.27}$$

$$\delta_{N_{int}} = 0 \tag{2.28}$$

- Non negativity constraints:

$$\delta_k \geq 0 \quad k \in \{1,2,...,N_{int-1}\} \tag{2.29}$$

$$L_j \geq 0 \quad j \in \{1,2,...,N_S\} \tag{2.30}$$

This transshipment model is a linear program whose solution determines the minimum cost of MSA, the optimal flow rate of each MSA, the residual mass exchange and the location of the pinch (corresponding to residual flow zero). Further details of this model can be found in El-Halwagi (2006) and El-Halwagi (1997).

2.1.3.2.2 NLP Formulation

This type of formulation allows the identification of the minimum cost (or mass flow) of fresh streams, the best allocation of the process sources to the sinks, and residual disposal. The representation of this problem is shown in Figure 2.10. The nonlinearities are due, mainly, to the fact that the constraints from the mass balance of the components are bilinear in relation to flow and concentration, and to process model equations (when used), which are generally nonlinear (e.g. Kremser equation in the modeling of a absorber).

The problem may be expressed as follows for a given process:

- A net of sinks (units): $Sinks = \{j = 1,2,...,N_{sinks}\}$. Each sink requires feeding at a given mass flow, G_j, and composition, z_j^{in}, that satisfies the constraint:

$$z_j^{min} \leq z_j^{in} \leq z_j^{max} \quad j \in \{1,2,...,N_{sinks}\} \tag{2.31}$$

in which z_j^{min} and z_j^{max} are the minimum and maximum allowed composition at unity j.

- A net of process sources: $Sources = \{i = 1,2,...,N_{sources}\}$ that can be recycled/reused in the process sinks. Each source have a mass flowrate, W_i, and a composition, y_i.

- A net of fresh sources (or news): $Fresh = \{r = 1,2,...,N_{fresh}\}$ that can be bought to supplement the use of the process sources in the sink process. The cost of fresh source

r_{th} is represented by C_r (\$/kg), its composition by x_r and the flowrate by F_r.

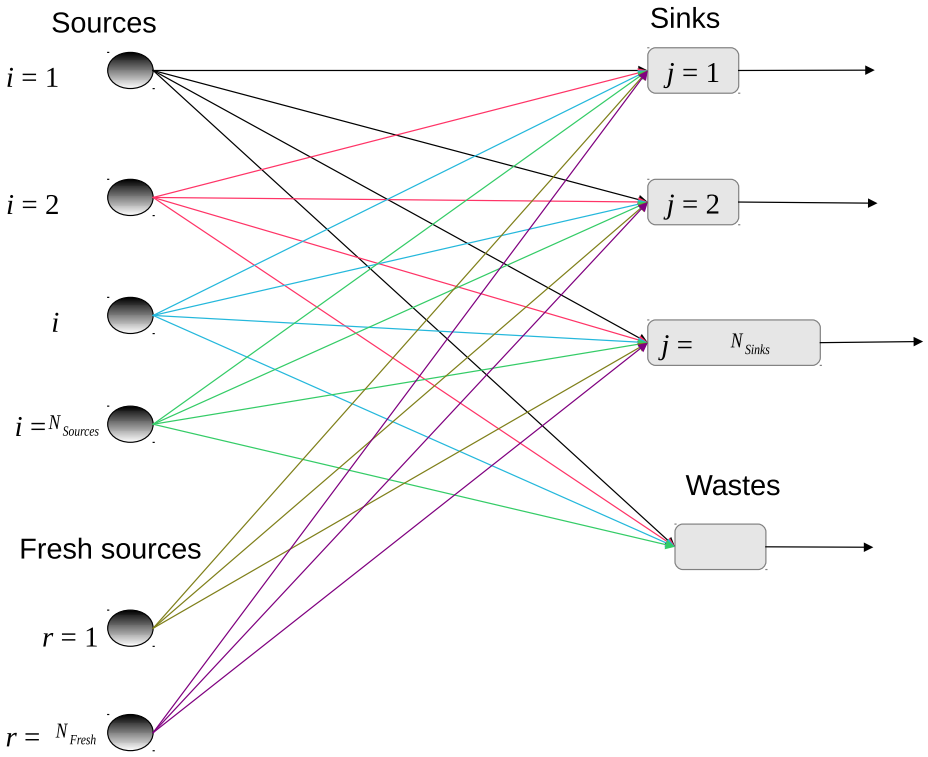

Figure 2.10: Superstructure used in NLP formulation representing the source-sink alocation. Adapted from El-Halwagi (2006).

The optimization problem formulation is given by eq. 2.32 - 2.40.

The objective function may be the minimization of the cost of fresh sources (eq. 2.32) or minimization of mass flow of fresh sources (eq. 2.33).

$$\text{Minimize} \sum_{r=1}^{r=N_{fresh}} C_r F_r \tag{2.32}$$

$$\text{Minimize} \sum_{r=1}^{r=N_{fresh}} F_r \tag{2.33}$$

The constraints of such modeling are:

- Each source, i, is divided into N_{sinks} fractions that can be allocated in several sinks (Figure 2.11). The flow of each fraction is $w_{i,j}$; and one of these fractions is directed to the

waste[1] ($w_{i,waste}$). Similarly, each fresh source is divided into N_{sinks} that are allocated to the various sinks ($f_{r,j}$).

Therefore, the constraint corresponding to the division of the process sources is:

$$W_i = \sum_{j=1}^{N_{sinks}} w_{i,j} + w_{i,waste} \quad i \in \{1,2,...,N_{sources}\} \tag{2.34}$$

Thus, a similar constraint corresponding to the division of fresh sources:

$$F_r = \sum_{j=1}^{N_{sinks}} f_{r,j} \quad r \in \{1,2,...,N_{fresh}\} \tag{2.35}$$

$$Wastes = \sum_{i=1}^{N_{sources}} w_{i,waste} \tag{2.36}$$

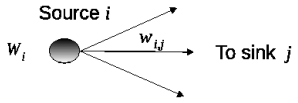

Figure 2.11: Sources division. Adapted from El-Halwagi (2006).

- Then, it is analyzed the opportunities of mixing these fractions and their allocation to the sinks (Figure 2.12). The constraints relating to the mixture into the sink j^{th} are described by eq. 2.37 - 2.38:

$$G_j = \sum_{i=1}^{N_{sources}} w_{i,j} + \sum_{r=1}^{N_{sources}} f_{r,j} \quad j \in \{1,2,...,N_{sinks}\} \tag{2.37}$$

$$G_j.z_j^{in} = \sum_{i=1}^{N_{sources}} w_{i,j}.y_i + \sum_{r=1}^{N_{sources}} f_{r,j}.x_r \quad j \in \{1,2,...,N_{sinks}\} \tag{2.38}$$

- To ensure non-negativity in the fresh streams and in the fractions of the sources allocated to the sinks, the constraints of eq. 2.39 and 2.40 are added:

$$f_{r,j} \geq 0 \quad r = 1,2,...,N_{fresh} \quad \text{e} \quad j \in \{1,2,...,N_{sinks}\} \tag{2.39}$$

$$w_{i,j} \geq 0 \quad i = 1,2,...,N_{sources} \quad \text{e} \quad j \in \{1,2,...,N_{sinks}\} \tag{2.40}$$

This same formulation can be used in the case of multiple components. In this model, it can

[1]This stream can be sent to waste treatment plant, or it can be a non-recycling material stream in the original waste sink

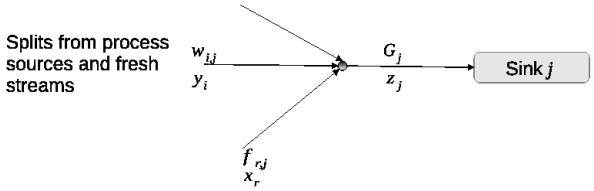

Figure 2.12: Mixture of the fractions of process sources and fresh, and sinks alocation. Adapted from El-Halwagi (2006).

still be included constraints related to the process model, the cost of pipes, etc. Further details can be found in El-Halwagi (2006) and El-Halwagi (1997).

2.1.3.2.3 MINLP Formulation

The MINLP formulation is more general, a superstructure layout is shown in Figure 2.13. Each source is divided into unknown flows fractions (to be optimized). Such fractions are allocated on the mass exchange network (MEN). Intercepted streams are allocated into the sinks. The flow rate of each stream allocated must also be optimized. Unallocated streams are fed to the waste sink.

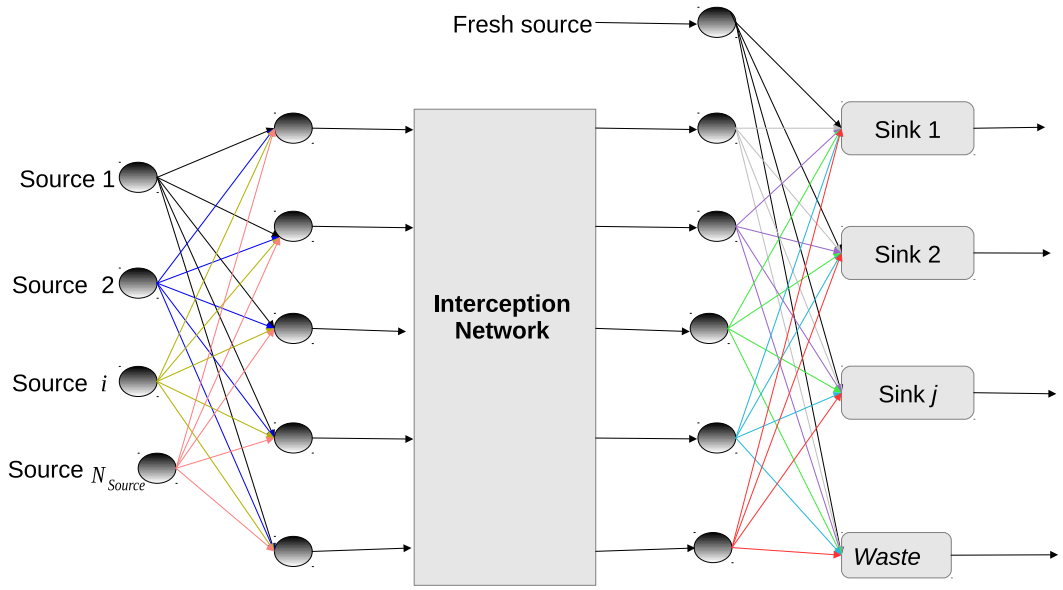

Figure 2.13: Superstructure representation referring to MINLP programming. Adapted from El-Halwagi (2006).

In the optimization of a superstructure of the source-interceptor-sink type, the given process is described by the process sources, fresh sources, sinks and interceptors. The first three have already been described in the NLP formulation. An interception unit (e.g. a separator) uses MSA to remove the species of the process sources. In a given process, the interception units are defined as:

- A set of interception units: $Interceptors = \{k = 1, 2, ..., N_{Int}\}$ that can be used to remove keystone species from the process sources.

The purpose of this formulation is to minimize the costs of fresh sources, of interception and waste treatment equipment. Thus, the objective function can be formulated by eq. 2.41,

$$\text{Minimize} \quad TAC = C_{Fr} \sum_{j=1}^{N_{sinks}} Fr_j + \sum_{k=1}^{N_{int}} C_{Int_k}.E_k + C_{waste}.Wastes \tag{2.41}$$

where:
TAC is the total annual cost
C_{Fr} is the cost of fresh source
Fr_j is the amount of fresh source fed to the sink j^{th} per year
C_{Int_k} is the total annual cost of the equipment used in interception k
E_k is the binary integer variable having the value 1 or 0 depending on whether the unit k is used or not, respectively
C_{waste} is the total annual cost of treating waste
$Wastes$ is the total annual flow sent to waste treatment.

The constraints of this formulation are:

- Division of the sources for all interception units:

$$F_i = \sum_{k=1}^{N_{Int}} w_{i,k} \quad \forall \quad i \in \{1, ..., N_{sources}\} \tag{2.42}$$

  where F_i is the flow rate of the i^{th} source.

- Mixture of sources before the interception units:

$$W_k = \sum_{i=1}^{N_{sources}} w_{i,k} \quad \forall \quad k \in \{1, ..., N_{Int}\} \tag{2.43}$$

- Mass balance per component for the mixture before the interception units:

$$W_k.Y_k^{in} = \sum_{i=1}^{N_{sources}} w_{i,k}.y_i^{in} \quad \forall \quad k \in \{1, ..., N_{Int}\} \tag{2.44}$$

- Performance function of the interception unit k^{th}:

$$y_k^{out} = f_k(Y_k^{in}, W_k, D_k, P_k) \quad \forall \quad k \in \{1, ..., N_{Int}\} \tag{2.45}$$

  where D_k and P_k are design and operation variables of unit k.

- Division of sources after the interception units:

$$W_k = \sum_{j=1}^{N_{sinks}} g_{k,j} \quad \forall \quad k \in \{1, ..., N_{Int}\} \tag{2.46}$$

  where $g_{k,j}$ is the flow of interception unit k for sink j.

- Mixture for the sink j_{th}:

$$G_j = F_j + \sum_{j=1}^{N_{sinks}} g_{k,j} \quad \forall \quad k \in \{1, ..., N_{Int}\} \tag{2.47}$$

- Considering the fresh source, the mass balance per component around the mixing point of the fresh feeding for sinks:

$$G_j.z_j^{in} \geq F_j.y_{fresh} + \sum_{k=1}^{N_{Int}} g_{k,j}.y_k^{out} \quad \forall \quad j \in \{1, ..., N_{sinks}\} \tag{2.48}$$

$$z_j^{min} \leq z_j^{in} \leq z_j^{max} \quad \forall \quad j \in \{1, ..., N_{sinks}\} \tag{2.49}$$

- The remaining unused mass follows for the waste treatment before its disposal:

$$Wastes = \sum_{k=1}^{N_{Int}} g_{k,j=waste} \tag{2.50}$$

- The non-negativity constraints of each fraction of: the sources allocated to the sinks and to the interception units, the fresh flows fed to sinks and the total waste:

$$g_{k,j} \geq 0 \quad \forall \quad j \in \{1, ..., N_{sinks}\} \quad e \quad k \in \{1, ..., N_{Int}\} \tag{2.51}$$

$$w_{i,k} \geq 0 \quad \forall \quad i \in \{1, ..., N_{sources}\} \quad e \quad k \in \{1, ..., N_{Int}\} \tag{2.52}$$

$$F_j \geq 0 \quad \forall \quad j \in \{1, ..., N_{sinks}\} \tag{2.53}$$

$$Wastes \geq 0 \tag{2.54}$$

Additionally, the performance equations of each interception unit (or the mathematical model of each of these units) and waste treatment unit, must be included and related to the objective function. Further details on this formulation can be found at Gabriel and El-Halwagi (2005).

2.1.3.2.4 Reformulation of MINLP in LP

Due to the non-convexity of the objective function and the large number of bilinear constraints, the global solution of MINLP cannot be guaranteed in commercial software (Gabriel and El-Halwagi, 2005). In order to address such problem, Gabriel and El-Halwagi (2005) proposed the reformulation of MINLP in an LP problem. The adopted simplifications were:

- No mixture of sources is allowed before the interception; the mixture is used primarily after interception and prior to the entry into the sinks. This assumption of source separation (a) prevents loss of the driving force as a result of the mixture and (b) prevents contamination of the stream due to the introduction of a pollutant from one into another stream. The disadvantage of this assumption is that it can be reached a larger number of interception equipment.
- Each interception unit is discretized in the number of interceptors with a given removal efficiency. Figure 2.14 shows the discretization scheme. Each source is split into several substreams which are allocated in discretized interceptor (represented by u). As removal efficiency (α_u) is fixed for each discretized interceptor (u) it is possible to determine the cost of interception (C_u) outside the optimization formulation, becoming a pre-synthesis task. Thus, with a given source and the removal efficiency, detailed simulation and calculation of costs are performed before synthesis, which eliminates a significant source of non-convexity and improves computational efficiency.

The objective function of the reformulated problem is given by eq. 2.55:

$$\text{Minimize} \quad TAC = C_{Fr} \sum_{j=1}^{N_{sinks}} Fr_j + \sum_{u=1}^{NU} C_u.\alpha_u.w_u.y_u^{in} + C_{waste}.Wastes \tag{2.55}$$

where y_u^{in} is the input composition of interceptor u and w_u is th flow in interceptor u.

The constraints are:

- Division of the sources for the interception equipment:

$$F_i = \sum_{u \in U_i} w_u \quad i = 1,2,...,N_{Fontes} \tag{2.56}$$

- Pollutant removal (or keystone species) from interceptor u_{th}:

$$y_u^{out} = (1-\alpha_u).y_u^{in} \quad u = 1,2,...,NU \tag{2.57}$$

- Separation of sources after the interception equipment:

$$w_u = \sum_{j=1}^{N_{Sinks}} g_{u,j} + g_{u,waste} \quad u = 1,2,...,NU \tag{2.58}$$

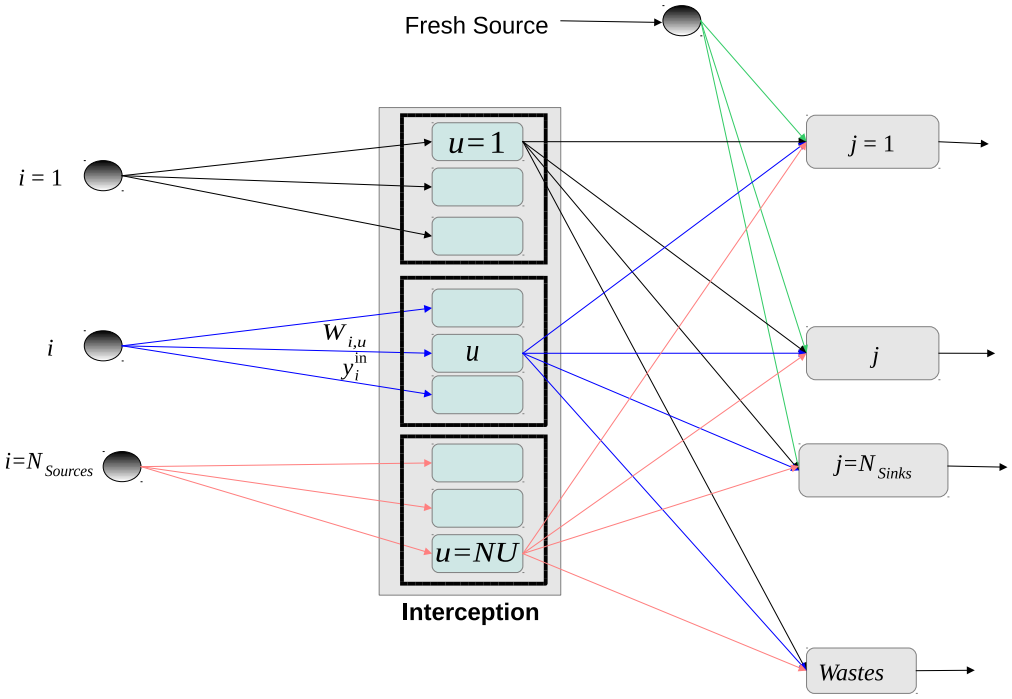

Figure 2.14: Superstructure representation refering to MINLP reformulation with interceptors discretization. Adapted from Gabriel and El-Halwagi (2005).

- Overall mass balance on the mixture feed point to the sink:

$$G_j = Fr_j + \sum_{u=1}^{NU} g_{u,j} \quad j = 1,2,...,N_{Sinks} \tag{2.59}$$

- Mass balance per component mixture feed point to the sink:

$$G_j.z_j^{in} = Fr_j.y_{Fr} + \sum_{u=1}^{NU} g_{u,j}.y_u^{out} \quad j = 1,2,...,N_{sinks} \tag{2.60}$$

$$z_j^{min} \leq z_j^{in} \leq z_j^{max} \quad \forall \quad j \in \{1,...,N_{sinks}\} \tag{2.61}$$

- The flow of the sources that were not used are fed to the waste treatment prior to disposal:

$$Wastes = \sum_{u=1}^{NU} g_{u,waste} \tag{2.62}$$

Non-negativity constraints must be included. The above formulation is LP and can be solved globally and efficiently to determine the minimum cost of fresh sources and interception units that satisfy the constraints of the process, the optimal allocation of sources to sinks, optimal selection of interception equipment and the optimal allocation of sources to interception units.

In some cases, the model process may be present in the above formulation, which can bring some nonlinearities and transform the problem into a NLP, which can also be solved efficiently.

Problems of synthesis of mass integration addressed in this work are based on the formulation LP, NLP and MINLP reformulated in LP/NLP. Thus, it is possible to obtain the solution of the problem of synthesis using an NLP optimization method as described in the previous section. In this thesis, the flexible tolerance method and its modifications will be used.

2.2 Literature Review

Despite the simple implementation and application, flexible tolerance method (FTM) is little used. Some of its applications (in the original formulation or with modifications) in the literature are described next.

Fenton et al. (1989) proposed a modification in FTM and apply the method in solution of NLP optimization problems. In the modification, the random search technique is used to complement the flexible tolerance method by generating a datafile which contains feasible solutions of the optimization problem in question. According to the authors, the modification proposed improved the efficiency and effectiveness of the flexible tolerance method.

Zhang and Ren (1989) applied FTM to multicomponent spectrophotometric analyses. It was found that FTM was an efficient procedure for optimization of multidimensional problems, especially in the presence of interactions between variables and when the problem was ill-conditioned.

Constantinescu (2000) used FTM to determine smooth and time-optimal path-constrained trajectories for robotic manipulators. The method was chosen for two reasons: the derivatives of the constraints and the cost function were not available; and the solution sought was expected to be on the boundary of the admissible region (in which case it is desirable to use information about points on both sides of the limiting surface in order to converge to the surface). The FTM proved to be efficient in solving the problem of trajectories with time optimality and smoothness.

Chen and Yin (2006) used the FTM to solve the optimization problems for determining hydrologic parameters in the root zone: water uptake rate, spatial root distribution, infiltration rate, and evaporation.

Shang et al. (2009) used FTM with an AGA (adaptive genetic algorithm) to solve nonlinear, multimodal and multi-constraint optimization problems. FTM, serving as one of the AGA operators, used a flexible tolerance criterion for near-feasible points to minimize the constraint violation of an objective function. Complex functions were evaluated, and the authors concluded that the hybrid method was suitable for resolution of real-world problems.

Omowunmi and Susu (2011) used FTM to estimate the kinetic parameters of an autocatalytic reaction involving the pyrolysis of neicosane. The method effectively minimized the sum of squares residuals between the experimental and predicted rates of reaction.

Among the various applications of the flexible tolerance method, there is no record in the literature of the use of the method for solving problems of synthesis of chemical process, especially mass integration. A major part of mass integration systems synthesis reported in the literature use commercial software for solving the optimization problem. El-Halwagi (2006) and El-Halwagi (1997) use LINGO whose solution for nonlinear systems is based on the Generalized Reduced Gradient algorithm (GRG). Faria (2004) used Optimization Toolbox of Matlab and GAMS in the reduction of raw water uptake and generation of effluents from a petroleum refinery through the reuse and/or recycle of streams sent to the effluent treatment station. Fontana (2002) also used GAMS software to solve a MINLP formulation for water recovery processes.

Tables 2.1 and 2.2 show some of the mass integration problems reported in the literature, indicating the type of formulation used, the problem and the software and/or algorithm used for solution.

As can be seen in Tables 2.1 and 2.2, most mass integration problems involves MINLP or NLP formulation, and the main software used is GAMS and LINGO. Within this perspective, this thesis aims to propose the synthesis solution of mass integration systems with a simple and direct optimization method, Flexible Tolerance Method and its modifications also proposed in this study.

Table 2.1: Survey of some recent work on mass integration.

Reference	Formulation	Problem	Software/Algorithm
Menon et al. (2001)	Transshipping model and MINLP	Synthetic Fuel plant. Presented by El-Halwagi and Manousiouthakis (1989), whose main objective is the conversion of a solid energy source, coal, in a form of energy easily used, such as liquid or gaseous fuels.	*Branch and Bound*
Fontana (2002)	MINLP	Water recovery in processes	GAMS (CONOPT e *Branch and Bound*)
El-Halwagi et al. (2003)	LP	Mass integration strategy development in conventional applications to support planetary housing systems	LINGO
Chen and Yin (2006)	MINLP and NLP	Strategy of mass exchange networks or heat exchange networks based on simulation, which involves uncertain temperatures, compositions and input flow rates.	GAMS (SBB, CONOPT)
Chen et al. (2007)	Algebric method and NLP	Methodology to calculate the minimum difference of composition for the minimization of total annual cost mass exchange network.	GAMS
Chew et al. (2009)	Approach based on games theory	Integration of water between plants of eco-industrial parks.	Games theory
Sujo-Nava et al. (2009)	Methodology based on heuristics development according to management demands .	Retrofit of a network acidic water in an oil refinery.	Heuristic
Gutterres et al. (2010)	NLP	Water reuse in tannery.	GAMS (solver MIMOS)
Nápoles-Rivera et al. (2010)	MINLP reformulated in MILP	Direct recycle strategy applied to a centralized treatment system (mass integration and properties)	–

Table 2.2: Survey of some recent work on mass integration (continuation).

Reference	Formulation	Problem	Software/Algorithm
Rubio-Castro et al. (2011)	MINLP reformulated into MILP	Integration of water in eco parks considering industrial streams with various pollutants.	GAMS (solver CPLEX)
Wagialla et al. (2012)	Pinch and MINLP	Prevention of in-plant pollution processes with multiple chains containing pollutants and properties environmentally undesirable.	LINGO
Wagialla (2012)	MILP and MINLP	Reduced total annual cost of a mass exchange network for applied to zinc recovery in a metal uncoating plant.	LINGO
Martinez-Hernandez et al. (2013)	Pinch analysis	Study case of a biorefinery producing bioethanol from wheat with arabinoxylan (AX) co-production using bioethanol for AX precipitation	-
Moncada et al. (2014)	Knowledge-based approach for the synthesis of chemicals	Analysis of the integration of first, second, and third generation biorefineries was based on two scenarios for two configurations of integrated biorefineries.	-
Hou et al. (2014)	New conceptual methodology for simultaneous integration of water and energy	Single- and multi-contaminant problems with fixed contaminant mass load.	Graphical aproach
Jiménez-Gutiérrez et al. (2014)	MINLP	Synthesis of water networks with a simultaneous integration of energy, mass and properties	GAMS

CHAPTER 3

Comparison and Application of Flexible Tolerance Method in Mass Integration

3.1 Introduction

This chapter is dedicated to apply and compare the performance of the Flexible Tolerance Method in mass integration problems. The case studies selected in this step are classic problems of mass integration involving networks synthesis, recycles, change in design and operation variables, and interaction between the process model and the synthesis of a network of mass exchangers.

The first case is a transshipment model, which is formulated as an LP problem. As described in the previous chapter, it was develop the composition interval diagram (CID), the table of exchangeable loads (TEL), then the mathematical model is optimized to minimize the cost of fresh streams. The second and third problem correspond to the NLP formulation, in which the superstructure generated do the allocation of the sources to sinks, corresponding to the direct recycle. The nonlinearities in these cases are due to the bilinear terms and the process model.

The preliminary analysis of FTM efficacy using these classical problems allows to detect bottlenecks that may interfere the application of this simple method in complex problems such as the mass integration problems.

3.2 Development

The development of this chapter is given below, in the article entitled *Comparative study and application of flexible tolerance method in synthesis and analysis of process with mass integra-*

tion, published in the *Journal of Chemistry and Chemical Engineering*[1], v. 7, p. 228 - 238, 2013.

[1]This publication is in Open Source, and can be freely accessed in: `http://www.davidpublishing.com/DownLoad/?id=12068`.

J. Chem. Chem. Eng. 7 (2013) 228-238

Comparative Study and Application of the Flexible Tolerance Method in Synthesis and Analysis of Processes with Mass Integration

Alice Medeiros de Lima*, Wu Hong Kwong and Antonio José Gonçalves da Cruz
Chemical Engineering Department, Federal University of São Carlos, São Paulo 13565-905, Brazil

Received: January 09, 2013 / Accepted: February 01, 2013 / Published: March 25, 2013.

Abstract: A direct search flexible tolerance method was used in the synthesis and analysis of processes with mass integration. The technique was compared with other gradient-based methods (GRG and LPQ) for resolution of a simple problem. Two large and complex problems involving synthesis and analysis of processes with mass integration were optimized using the proposed method. The results demonstrated the ability of this straightforward procedure to handle complicated problems involving mass integration.

Key words: Optimization, flexible tolerance method, mass integration.

1. Introduction

Process integration is an important tool used in the chemical industry. Application of this technique can provide benefits including reductions in investment capital and energy usage, and improved environmental performance, amongst others. However, despite considerable advances in recent years in the development of methodologies that are robust and effective in the search for solutions to process integration problems, numerous challenges remain. Work continues in the development and application of new optimization methods, such as hybrid approaches, multi-objective optimization and incorporation of the reaction synthesis step, as well as process simulation and the use of environmental impact indicators during integration problem formulation.

As integration problems become more complex, gradient-based optimization methods are unable to handle constraints, discontinuities and inflections, because gradient information also becomes more complex and very difficult to obtain.

FTM (flexible tolerance method) transforms objective, equality and inequality constraint functions (linear and/or nonlinear) in a problem of simple nonlinear optimization programming with the same solution after introduction of the concepts of tolerance criterion, restrictions violation and near-feasibility. FTM can improve the value of the objective function by using information provided by feasible points as well as certain non-feasible points called near-feasible points. The Nelder-Mead flexible polyhedron method was used in order to perform searching without restrictions. The procedure adopted has received little previous attention, and there are no reports in the literature concerning the use of FTM in process integration problems.

Zhang and Ren [1] applied FTM to multicomponent spectrophotometric analyses. It was found that FTM was an efficient procedure for optimization of multidimensional problems, especially in the presence of interactions between variables and when the problem was ill-conditioned.

*Corresponding author: Alice Medeiros de Lima, M.Sc., research fields: chemical engineering, simulation, modeling, and optimization of chemical processes. E-mail: alice.medeirosdelima@gmail.com.

Constantinescu [2] used FTM to determine smooth and time-optimal path-constrained trajectories for robotic manipulators. The method was chosen for two reasons: the derivatives of the constraints and the cost function were not available; and the solution sought was expected to be on the boundary of the admissible region (in which case it is desirable to use information about points on both sides of the limiting surface in order to converge to the surface). The FTM proved to be efficient in solving the problem of trajectories with time optimality and smoothness.

Shang et al. [3] used FTM with an AGA (adaptive genetic algorithm) to solve nonlinear, multimodal and multi-constraint optimization problems. FTM, serving as one of the AGA operators, used a flexible tolerance criterion for near-feasible points to minimize the constraint violation of an objective function. Complex functions were evaluated, and the authors concluded that the hybrid method was suitable for resolution of real-world problems.

Omowunmi and Susu [4] used FTM to estimate the kinetic parameters of an autocatalytic reaction involving the pyrolysis of neicosane. The method effectively minimized the sum of squares residuals between the experimental and predicted rates of reaction.

The objective of the present work was to compare the performance of FTM (direct method) with that of two indirect optimization methods, SQP (sequential quadratic programming) and GRG (generalized reduced gradient), and apply FTM in the synthesis and analysis of processes with mass integration.

2. Methodology

Three process integration problems were implemented in this work. One problem was a classic example of MEN (a mass exchange network), concerning wastewater cleaning, where an organic pollutant was required to be removed from two aqueous wastes. This problem was used to compare the performance of FTM with that of SQP and GRG in resolution of mass integration problems.

Two other problems involved the application of FTM in the resolution of problems of synthesis and analysis with mass integration. In the first problem, analysis was made of the effect of altering design and operating variables in the production of acetaldehyde by ethanol oxidation. In the second example, the interaction between the process model and the synthesis of a mass exchange network was analyzed for an ethyl chloride process.

2.1 Mass Integration

Mass integration is a systematic methodology that can provide a fundamental understanding of the global flow of mass within a process, enabling the identification of performance targets and optimization of the generation and routing of species throughout the process [5].

The objective in optimization of mass integration problems is minimization of the costs (C_{Fresh}) of the fresh resource (L_j), interception devices (C_{ID}) and waste treatment (C_{Waste}), and can be described as indicated in Eq. (1), where E_k is a binary integer that has the value of 1 or 0 depending on whether or not unit k is used.

$$Minimize: \sum_{j=1}^{N_{Fresh}} C_{Fresh}.L_j + \sum_{k=1}^{N_{ID}} C_{ID}.E_k + C_{Waste}.Waste \quad (1)$$

Restrictions in mass integration problems are related to thermodynamic feasibility, material balances, splitting of the sources to all the interception devices, splitting of the sources after the interception devices, pollutant removal in the interceptor, sink constraints and unused flows of sources sent to waste treatment. In some cases of process synthesis and analysis, it is necessary to incorporate a process model with the appropriate level of detail to keep track of the effect of process changes and embed them during the generation of mass integration strategies [5].

The thermodynamic feasibility of mass exchange can be determined using CID (a composition interval diagram). Mass exchange is thermodynamically (and

practically) feasible from rich streams to MSAs (mass separating agents) within the same interval, and from a rich stream to a lean stream that lies in an interval below it.

The exchangeable loads of the rich and lean streams in each interval are determined by construction of TEL (a table of exchangeable loads). The component material balance around each composition interval (i) is described by Eq. (2), where δ_i is the residual mass to the subsequent interval, δ_{i-1} is the residual mass from the preceding interval, W_i^S is the mass gained by the MSAs, and W_i^R is the mass lost from the rich streams.

$$\delta_i - \delta_{i-1} + \sum_{j\ through\ i} L_j W_{j,i}^S = W_i^R \quad (2)$$

Each source (fresh or from the process) can be split into fractions that are allocated to the various sinks (process units). This can be represented as shown in Fig. 1.

A complete mathematical formulation for a mass integration process can be found in Ref. [5].

2.2 FTM (Flexible Tolerance Method)

The general nonlinear programming problem can be stated as:

$$Minimize: f(X)\ X \in E^n \quad (3)$$

$$Subject\ to: h_i(X) = 0\ i = 1, \dots, m \quad (4)$$

$$g_i(X) \geq 0\ i = m+1, \dots, p\ ,$$

where, $f(X)$ is the objective function, and $h_i(X)$ and $g_i(X)$ are equality and inequality constraints, respectively, defined in the n-dimensional Euclidean space.

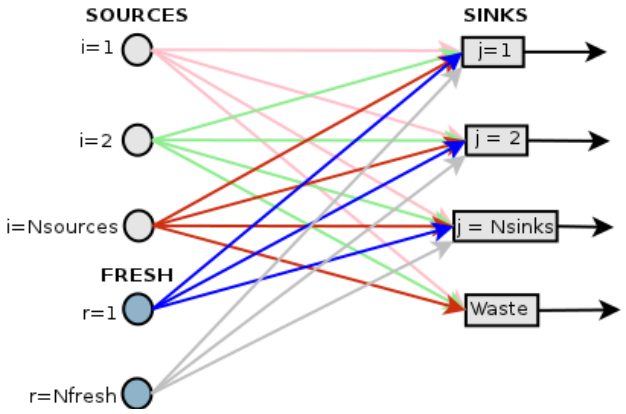

Fig. 1 Source-sink representation.

In many nonlinear programming methods, a considerable portion of the computation time is spent on satisfying rather rigorous feasibility requirements. FTM improves the value of the objective function by using information provided by feasible points, as well as certain non-feasible points termed near-feasible points [4]. On the other hand, FTM employs a tolerance criterion and an unconstrained nonlinear programming method for the constraint violation throughout the whole search, and thereby causes near-feasibility limits to be gradually more restrictive as the search proceeds toward the optimum solution, until at the limit only feasible *X* vectors in the model are accepted [3].

Because of this strategy, the constraints defined in Eq. (4) can be replaced by:

$$\Phi^{(k)} - T(X) \geq 0 \quad (5)$$

where, $T(X)$ is a positive functional of all the equality and/or inequality constraints, defined as shown in Eq. (6), where, $\mathcal{U}_i$ is the Heaviside operator, with $\mathcal{U}_i = 0$ for $g_i(X) \geq 0$, and $\mathcal{U}_i = 1$ for $g_i(X) < 0$.

$$T(X) = \left[\sum_{i=1}^{m} h_i^2(X) + \sum_{i=m+1}^{p} U_i g_i^2(X)\right]^{1/2} \quad (6)$$

$\Phi^{(k)}$ is the tolerance criterion for feasibility in the *k* th stage of the search. In this paper, the unconstrained search in the FTM was performed using the Nelder-Mead flexible polyhedron, so Φ can be described as:

$$\begin{cases} \Phi^{(k)} = min\left[\Phi^{(k-1)}, \theta^{(k)}\right] \\ \Phi^{(0)} = 2(m+1).t \\ \Phi^{(k)} = \frac{m+1}{r+1}\sum_{i=1}^{k+1}\left\|X_i^{(k)} - X_{r+2}^{(k)}\right\| \end{cases} \quad (7)$$

where, $\Phi^{(k-1)}$ is the value of the tolerance criterion in the $(k-1)$ th stage of the search, t is the size of the initial polyhedron, m is the number of equality constraints, r is the number of degrees of freedom of $f(X)$, and $r = (n - m)$, where n is the number of variables. $X_i^{(k)}$ is the i th vertex of the polyhedron in E^n, $X_{r+2}^{(k)}$ is the vertex corresponding to the centroid, and $\theta^{(k)}$ is the average distance from each $X_i^{(k)}$ to the centroid $X_{r+2}^{(k)}$ of the polyhedron in E^n. In each k th step of the search $\Phi^{(k)}$ is set equivalent to the

smallest value of $\Phi^{(k-1)}$ or $\theta^{(k)}$, the tolerance criterion $\Phi^{(k)}$ also collapses, and at the limit:

$$lim_{X \to X*} \Phi^{(k)} = 0 \quad (8)$$

$\Phi^{(k)}$ behaves as a positive decreasing function of X, although $\theta^{(k)}$ may increase or decrease during the progress of the search, and as the solution of the problem is approached, both $\theta^{(k)}$ and $\Phi^{(k)}$ become near to zero:

$$\Phi^{(0)} \geq \Phi^{(1)} \geq \cdots \geq \Phi^{(k)} \geq 0 \quad (9)$$

An important advantage of the FTM algorithm is that, at the beginning of the search, a large number of vertices are used to obtain information about $f(X)$, enhancing the possibility that an $X_i^{(k)}$will be found that leads to a local optimum that is better than any other local optimum.

In the Nelder-Mead method used for unconstrained searching, the procedure for finding a vertex in E^n at which $f(X)$ has a better value involves four operations:

Reflection: Reflect $X_h^{(k)}$ (X that gives the maximum value of $f(X)$ through the centroid by computing:

$$X_{n+3}^{(k)} = X_{n+2}^{(k)} + \alpha.\left(X_{n+2}^{(k)} - X_h^{(k)}\right) \quad (10)$$

where, $\alpha > 0$ is the reflection coefficient, and $X_{n+2}^{(k)}$ is the centroid computed by Eq. (11), in which index j designates each coordinate direction:

$$X_{n+2,j}^{(k)} = \frac{1}{n}\left[\left(\sum_{i=1}^{n+1} X_{ij}^{(k)}\right) - X_{hj}^{(k)}\right] \quad (11)$$

Expansion: If $f\left(X_{n+3}^{(k)}\right) \leq f\left(X_h^{(k)}\right)$, expand the vector $\left(X_{n+3}^{(k)} - X_{n+2}^{(k)}\right)$ by computing:

$$X_{n+4}^{(k)} = X_{n+2}^{(k)} + \gamma.\left(X_{n+3}^{(k)} - X_{n+2}^{(k)}\right) \quad (12)$$

where, $\gamma > 1$ is the expansion coefficient.

Contractions: If $f\left(X_{n+3}^{(k)}\right) > f\left(X_h^{(k)}\right)$ for all $i \neq h$, contract the vector $\left(X_h^{(k)} - X_{n+2}^{(k)}\right)$ by computing:

$$X_{n+5}^{(k)} = X_{n+2}^{(k)} + \beta.\left(X_h^{(k)} - X_{n+2}^{(k)}\right) \quad (13)$$

where, $0 < \beta < 1$ is the contraction coefficient.

Reduction: If $f\left(X_{n+3}^{(k)}\right) > f\left(X_h^{(k)}\right)$, reduce all the vectors $\left(X_i^{(k)} - X_l^{(k)}\right)$, where $X_l^{(k)}$ is the X that gives the minimum value of $f(X)$, and δ is the reduction coefficient (usually $\delta = 0.5$):

$$X_{n+4}^{(k)} = X_l^{(k)} + \delta.\left(X_i^{(k)} - X_l^{(k)}\right) \quad (14)$$

Under normal conditions, the values of $\alpha = 1.0$, $\beta = 0.5$, $\gamma = 2.0$ and $\delta = 0.5$ are recommended [4]. Further details on the implementation of FTM are described in Ref. [4].

2.3 Problem 1

This problem deals with an organic pollutant to be removed from two aqueous wastes [5]. The data for the rich streams (R1 and R*2*) are given in Table 1, and two process MSAs (L1 and L2) and two external MSAs (L3 and L4) are available, as shown in Table 2.

This simple case was used to compare three different optimization methods: (1) GRG [5], implemented in Lingo©; (2) SQP, implemented in this work using Matlab©; and (3) FTM, implemented in this work in FORTRAN.

As shown previously [5], the formulation of the problem can be expressed as:

Table 1 Data for the rich streams.

Stream	Flowrate, G_I (kg/s)	Supply composition of pollutant (mass Fraction), y_i^s	Target composition of pollutant (mass Fraction), y_i^t
R1	2.0	0.030	0.005
R2	3.0	0.010	0.001

Table 2 Data for the process and external MSAs.

Stream	Upper bound on flowrate, L_j^C (kg/s)	Supply composition of pollutant (mass fraction), x_j^s	Target composition of pollutant (mass fraction), x_j^t	Cost, C_j ($/kg MSA)
L1	17.0	0.007	0.009	0.00
L2	1.0	0.005	0.015	0.00
L3	∞	0.019	0.029	0.010
L4	∞	0.009	0.029	0.020

$$Minimize: x^* = C_3.L_3 + C_4.L_4 \quad (15)$$

The restrictions are formed by the material balance in each composition interval Eq. (2).

2.4 Problem 2

This example concerns yield targeting in acetaldehyde production by ethanol oxidation [6]. A diagram of the process is shown in Fig. 2, where some of the operational values are indicated. The objective was to maximize the overall process yield without adding new process equipment, although process modification and direct recycle could be used. Direct recycle was only allowed from the top of the third distillation column to the flash column. A detailed description can be found in Ref. [6], and the process model is summarized below. Ethanol is flashed and mixed with air, before being fed to the reactor where the reaction Eq. (16) occurs.

$$CH_3CH_2OH + {}^1/_2\, O_2 \rightarrow CH_3CHO + H_2O \quad (16)$$

Reactor:

$$Y_{reactor} = 0.33 - 4.2 \times 10^{-6} \times (T_{reactor} - 580)^2 \quad (17)$$

$$300 \leq T_{reactor}(K) \leq 860 \quad (18)$$

$$Y_{reactor} = \frac{A_{S5}}{E_{S3}} \quad (19)$$

$$E_{consumed} = \left(\frac{46}{44}\right) \times A_{S5} \quad (20)$$

In the above equations, $Y_{reactor}$ is the reactor yield, $T_{reactor}$ is the reactor temperature (K), A_{S5} is the acetaldehyde produced in the reactor, E_{S3} is the ethanol feed in the reactor, and $E_{consumed}$ is the ethanol consumed in the reactor related to acetaldehyde production, obtained using stoichiometry and molecular weights.

Flash column:

$$E_{S2} = a \times E_{S1} \quad (21)$$

$$a = 10.5122 - 0.0274 \times T_{flash} \quad (22)$$

$$380 \leq T_{flash}(K) \leq 384 \quad (23)$$

E_{S2} is the ethanol lost in the bottoms of the flash, E_{S1} is the ethanol feed in the flash, and T_{flash} is the flash temperature.

First distillation column:

$$A_{S14} = \tau \times A_{S9} \quad (24)$$

$$\tau = 0.14 \times Q_R + 0.89 \quad (25)$$

$$0.55 \leq Q_R(MW) \leq 0.76 \quad (26)$$

$A_{S14}$is the recovery of acetaldehyde as a top product,

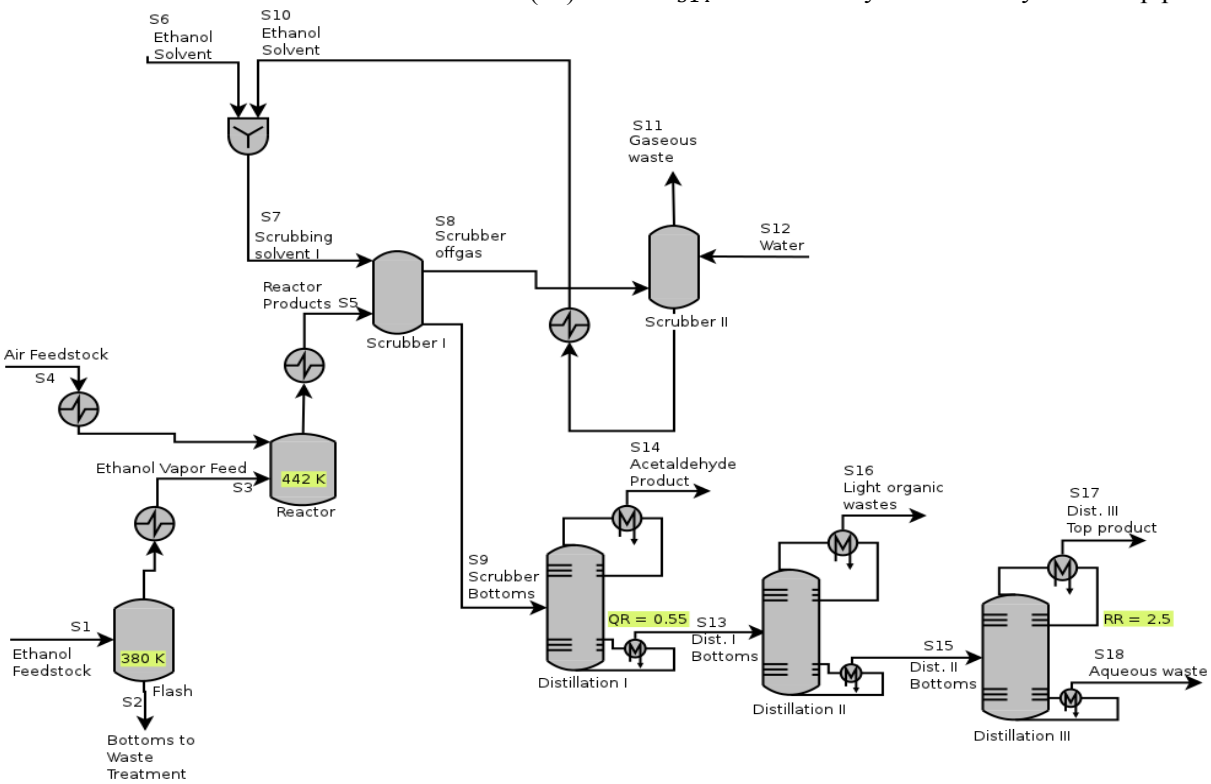

Fig. 2 Flowsheet of acetaldehyde production by ethanol oxidation (Problem 2, adapted from Ref. [6]).

A_{S9} is the acetaldehyde feed to the distillation, and Q_R is the reboiler heat duty.

Third distillation column:

$$E_{S17} = \varphi \times E_{S15} \quad (27)$$

$$\varphi = 0.653 \times e^{0.085 \times RR} \quad (28)$$

$$2.5 \leq RR \leq 5.0 \quad (29)$$

E_{S17} is the ethanol recovery in the top product, E_{S15} is the ethanol feed in the distillation, and RR is the reflux ratio.

Optimization formulation for this problem is described by Eq. (30), where Y_p is the overall process yield, defined as the ratio between acetaldehyde in the final product stream (S14) and fresh ethanol fed to the process as feedstock (S1).

$$Maximize: Y_p = \frac{A_{S14}}{E_{S1}} \quad (30)$$

The process model Eqs. (17-29) and the material balance for ethanol and acetaldehyde are the constraints of the problem. Detailed formulations can be found in Refs. [5, 6].

2.5 Problem 3

The objective of this problem was to determine the target for minimizing the total load of a toxic pollutant discharged into terminal plant wastewater, using segregation, mixing and recycle strategies. This case study (presented in Ref. [7]) concerns the production of ethyl chloride by catalytic reaction between ethanol and hydrochloric acid. A reaction byproduct is chloroethanol, a toxic pollutant whose discharge must be minimized. A block diagram of this process is shown in Fig. 3, where the values indicated refer to mass flows of gas (V) and liquid (L). The optimization problem in this process model includes source-sink representation to allow consideration of segregation, mixing, and direct recycle strategies, and the material balance of water and chloroethanol. The formulation is summarized below, and a detailed description can be found in Ref. [7].

Three liquid sources were considered for recycle: the reactor effluent (L6), and bottom liquids from scrubber I (L2) and scrubber II (L4). The recycle streams could be fed to three process sinks: the reactor (u = 1), scrubber I (u = 2), and scrubber II (u = 3).

A structural representation of the segregation, mixing, and direct recycle options is shown in Fig. 4, where z represents the chloroethanol concentration (in ppm), *Fu, out* and *Fu, in* represent the outlet and inlet flowrates associated with unit u and fiu represents

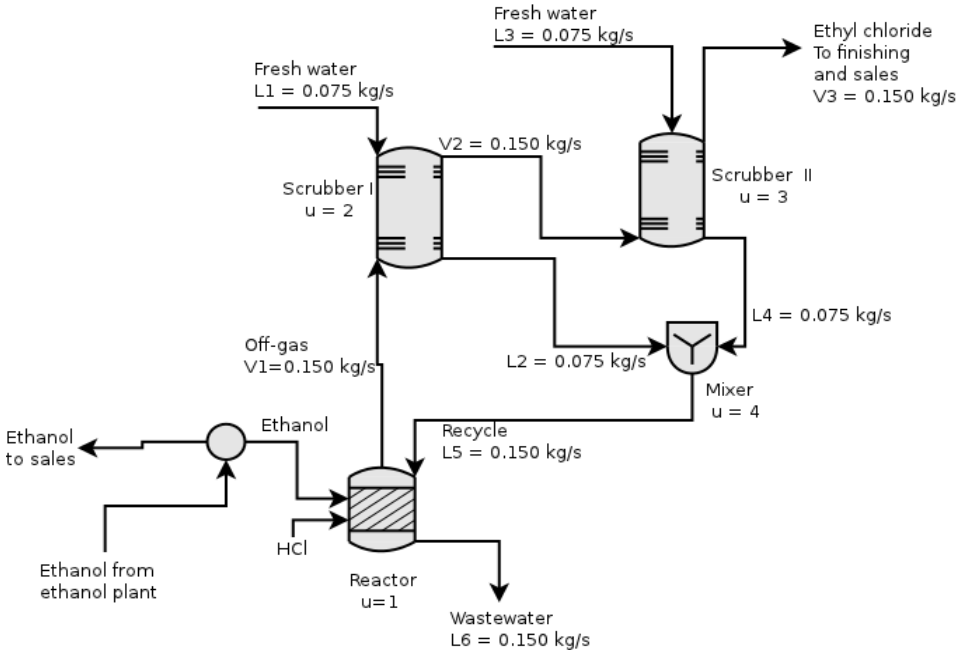

Fig. 3 Flowsheet for the production of ethyl chloride from ethanol and hydrochloric acid (Problem 3, adapted from Ref. [7]).

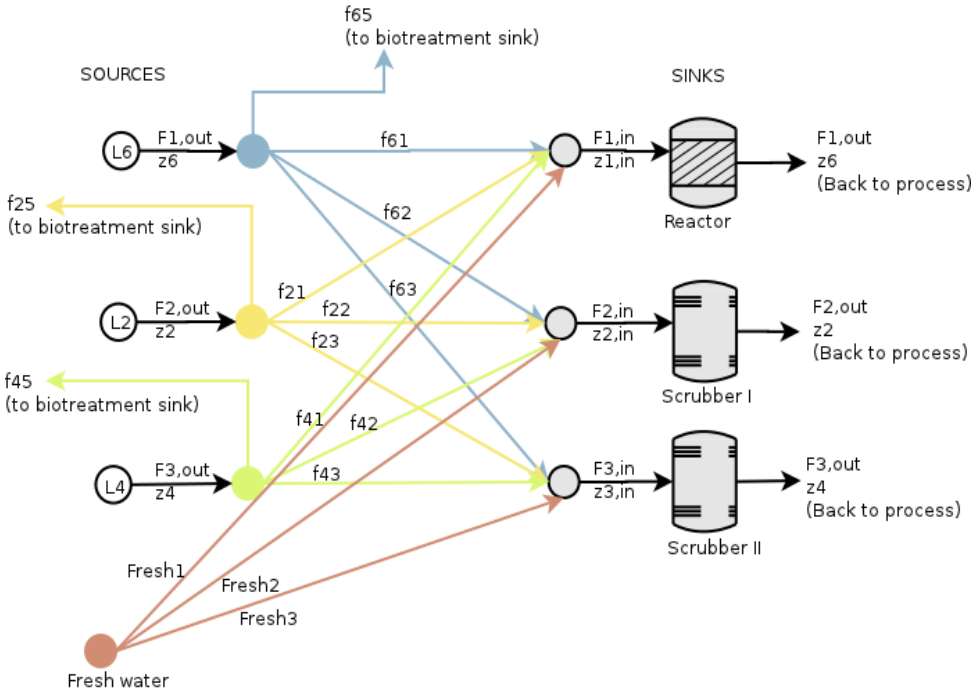

Fig. 4 Structural representation of segregation, mixing, and direct recycle options (Problem 3, adapted from Ref. [7]).

the flowrate of the streams passed from the source to the sink. The water and chloroethanol material balance around the sinks and sources to be split, shown in Fig. 4, gives the flowrates of the streams fed to the sinks. The restrictions to be considered for recycle are indicated in Eqs. (31) and (32).

Composition of aqueous feeds:

$$\begin{cases} z1,in \le 65 \text{ ppm} \\ z2,in \le 8 \text{ ppm} \\ z3,in = 0 \text{ ppm} \end{cases} \quad (31)$$

Flowrate of aqueous feeds:

$$\begin{cases} 0.090 \le F1,in \le 0.150 \\ 0.075 \le F2,in \le 0.090 \\ 0.075 \le F3,in \le 0.085 \end{cases} \quad (32)$$

In addition to the restrictions of mass balance, composition and flowrate limits, the process model needs to be considered. This is summarized below, and a more detailed formulation can be found in Ref. [7].

Reactor:

CE (the rate of chloroethanol) generation ($r_{CE,gen}$) by chlorination is given by:

$$r_{CE,gen} = 6.03 \times 10^{-6}\ kg/s \quad (33)$$

A fraction of the chloroethanol recycled to the reactor is reduced to ethyl chloride in a side reaction, and the rate of CE depletion ($r_{CE.red}$) is given by:

$$r_{CE,red} = 0.090 \times z1,in\ kg/s \quad (34)$$

The contents of CE in the gas and liquid phases of the reactor effluent are given by the equilibrium distribution coefficient:

$$y1/z6 = 5 \quad (35)$$

The mass balance around the reactor, including the reaction rate and the equilibrium distribution, is given by:

$$(V1 + z6 \times F1,in) \times y1 - F1,in \times z1,in - r_{CE,red} = r_{CE,gen} \quad (36)$$

Scrubbers:

Each scrubber contains two sieve plates and has an overall column efficiency of 65% (NTP = 1.3). The scrubbers can be modeled using the Kremser equation, with Henry's coefficient H = 0.1. The mass balances around scrubbers I and II are given by Eqs. (37) and (38), respectively. The column models for scrubbers I and II are described by Eqs. (39) and (40), respectively.

$$V1 \times (y1 - y2) = F2,in \times (z2 - z1,in) \quad (37)$$

$$V2 \times (y2 - y3) = F3,in \times (z4 - z3,in) \quad (38)$$

$$\left(\frac{F2,in}{V1}\right)^{NTP} - \frac{\left[\left(1 - H.{}^{V1}/_{F2,in}\right)(y1 - H.z2,in)\right]}{y2 - H.z2,in} - \frac{V1}{F2,in} = 0 \quad (39)$$

$$\left(\frac{F3,in}{V2}\right)^{NTP} - \frac{\left[\left(1 - H.{}^{V2}/_{F3,in}\right)(y2 - H.z3,in)\right]}{y2 - H.z2,in} - \frac{V2}{F3,in} = 0 \quad (40)$$

The objective function for this problem is indicated in Eq. (41). The optimization problem can be solved with the objective function, subject to the restrictions mentioned previously.

$$Minimize: x^* = f65 \times z6 + f25 \times z2 + f45 \times z4 \quad (41)$$

3. Results and Discussion

3.1 Problem 1

For the problem described previously in Section 2.3, the composition interval diagram is shown in Fig. 5, and the table of exchangeable loads is provided in Table 3 [5]. Table 4 shows the results for the three different methods used for optimization of the problem. FTM proved effective, since optimization was achieved with 10 variables, Ref. [7] equality constraints, and 12 inequality constraints. The optimum point found agreed with that obtained by the indirect methods (GRG and SQP). From the same starting point, FTM required a smaller number of function evaluations than the SQP method. Moreover, the use of FTM as a search technique did not require information of analytical derivatives, contributing to a shorter problem preparation time, compared to that required for the SQP method using the fmincon function in Matlab©. The Nelder-Mead parameters used in this problem were $\alpha = 1.0$, $\beta = 0.4$, $\gamma = 2.0$, and $\delta = 0.5$.

3.2 Problem 2

The problem described in Section 2.4 was solved here using FTM in FORTRAN, with results similar to those obtained earlier [6]. The main optimized values

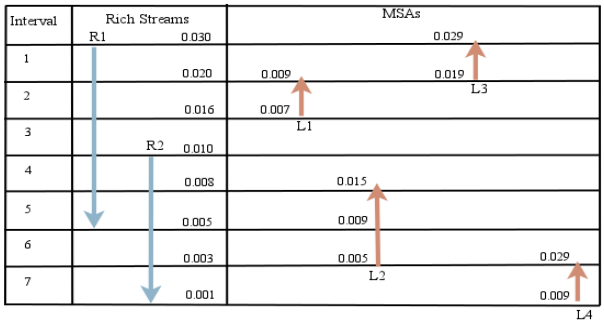

Fig. 5 Composition interval diagram for problem 1.

Table 3 Exchangeable loads for problem 1.

i	Load (kg/s)						
	R1	R2	R1+R2	L1	L2	L3	L4
1	0.020	-	0.020	-	-	0.010	-
2	0.008	-	0.008	0.002	-	-	-
3	0.012	-	0.012	-	-	-	-
4	0.004	0.006	0.010	-	-	-	-
5	0.006	0.009	0.015	-	0.006	-	-
6	-	0.006	0.006	-	0.004	-	-
7	-	0.006	0.006	-	-	-	0.020

Table 4 Optimization results for problem 1.

Variable	GRG (Lingo©) (El-Halwagi, 2006)	SQP (Matlab©)	FTM (FORTRAN)
x*	0.039	0.039	0.039
D1	0.020	0.020	0.0198
D2	0.000	0.000	0.000
D3	0.012	0.012	0.0118
D4	0.022	0.022	0.0218
D5	0.031	0.031	0.0308
D6	0.033	0.033	0.0328
L1	14.000	14.000	13.999
L2	1.000	1.000	0.999
L3	0.000	0.000	0.000
L4	1.950	1.950	1.949
Number of iterations		1	2
Number of objective function Evaluations		23	5

(operational conditions) are given in Table 5. A modified flowsheet is presented in Fig. 6.

The results obtained for this problem with 31 variables, 23 equality constraints and 36 inequality constraints demonstrated that FTM was effective in identifying the optimal point. Three iterations and 21 objective function evaluations were performed. The parameter values of the Nelder-Mead method used were $\alpha = 1.0$, $\beta = 0.4$, $\gamma = 2.0$ and $\delta = 0.5$.

3.3 Problem 3

The results obtained in this work using FTM are presented in Table 6. The optimal point differed from that reported previously [7]. Here, the total flow directed to biotreatment was 0.475 kg/s (1,710.0 kg/h), compared to the earlier value of 0.488 kg/s (1,756.8 kg/h). A difference of 46.8 kg/h represents an annual reduction of 409 t in the quantity of material

Table 5 Optimization results for problem 2.

Variables	Current Process	Optimized process [6]	Optimized process (this work)
Y_p	23.7%	95.5%	95.48%
$T_{reactor}$	442 K	580 K	580 K
T_{flash}	380 K	383.7 K	383.65 K
Q_R	0.55	0.76	0.766
RR	2.5	5.0	5.0
Ethanol recycled from the top of third distillation column to the flash column	-	199.367 t/year	199.367 t/year
Number of iterations			3
Number of objective function evaluations			21

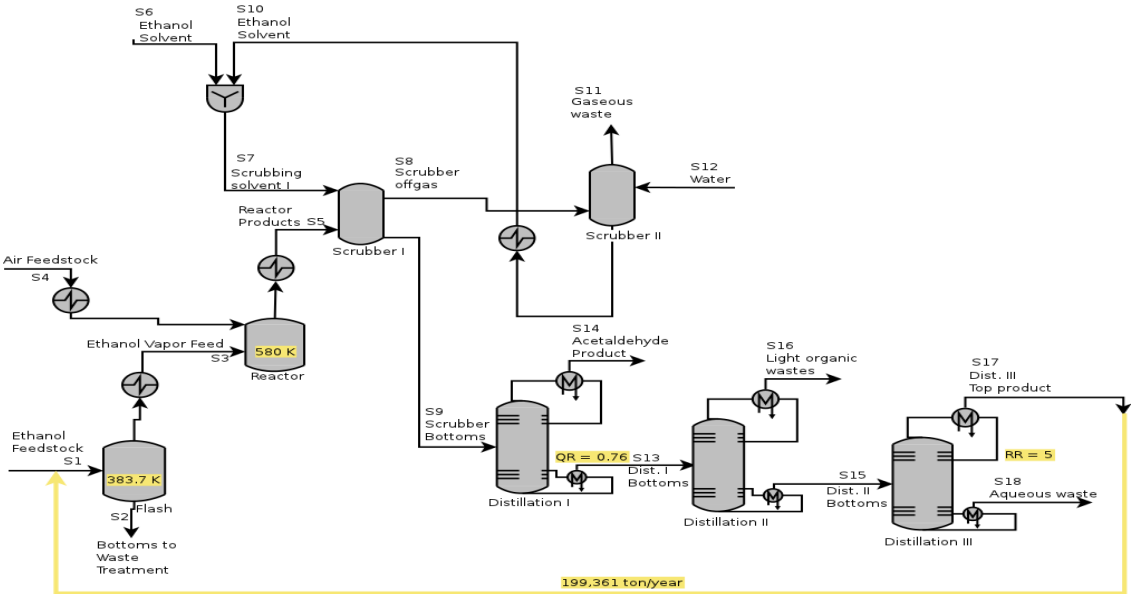

Fig. 6 Modified flowsheet of acetaldehyde production by ethanol oxidation (problem 2).

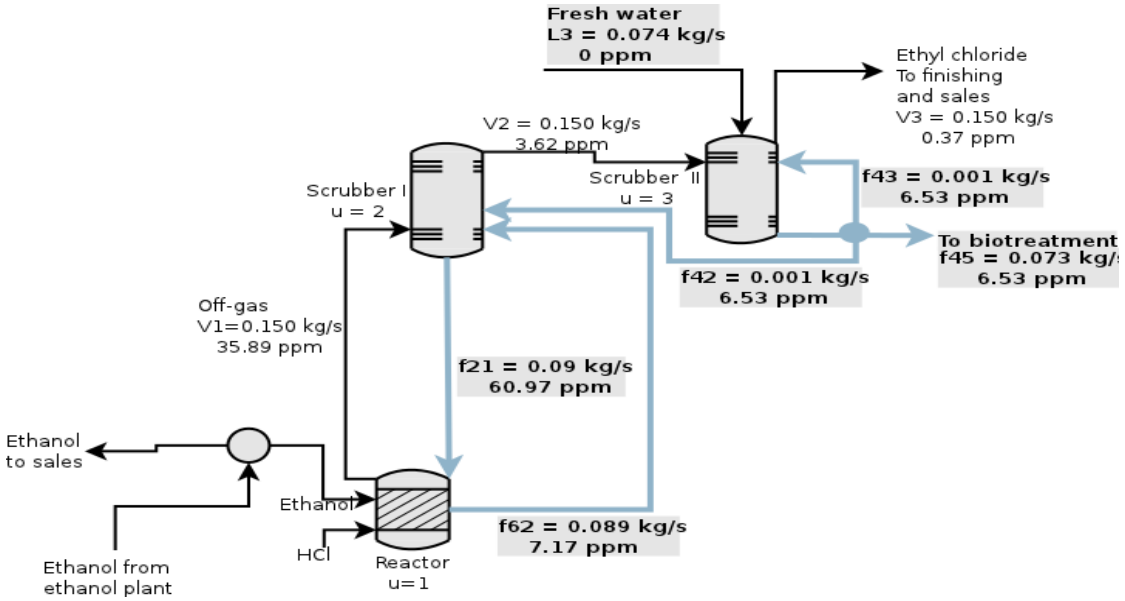

Fig. 7 Modified flowsheet of the production of ethyl chloride from ethanol and hydrochloric acid (problem 3).

Table 6 Optimization results for problem 3.

Variables	Current process	Optimized process [7]	Optimized process (this work)
x^*	1.500	0.488	0.475
f65	0.150	0.000	0.000
z6	10.0	7.178	7.179
f25	0.000	0.000	0.000
z2	49.5	60.968	60.976
f45	0.000	0.075	0.073
z4	9.0	6.508	6.531
F1, in	0.150	0.090	0.090
f21	0.075	0.090	0.090
f41	0.075	0.000	0.000
f61	0.000	0.000	0.000
Fresh1	0.000	0.000	0.000
F2, in	0.075	0.090	0.090
f22	0.000	0.000	0.000
f42	0.000	0.000	0.001
f62	0.000	0.090	0.089
Fresh2	0.075	0.000	0.000
F3, in	0.075	0.075	0.075
f23	0.000	0.000	0.000
f43	0.000	0.000	0.000
f63	0.000	0.000	0.000
Fresh3	0.075	0.075	0.074
z1, in	49.500	60.968	60.97
z2, in	0.000	7.178	7.179
z3, in	0.000	0.000	0.000
F1, out	0.150	0.090	0.090
F2, out	0.075	0.090	0.090
F3, out	0.075	0.075	0.075
y1	50.000	35.893	35.897
y2	5.000	3.619	3.620
y3	0.500	0.366	0.368
Number of iterations			1506
Number of objective function evaluations			2994

transferred to the biotreatment unit. The configuration of the plant is shown in Fig. 7. Significant differences, compared to the earlier work, were obtained for the recycles from the second scrubber to the first, and to itself. The two procedures gave similar results for the recycle from the reactor to the first scrubber, and for the feed of the effluent from the first scrubber to the reactor. The consumption of water obtained here was lower than in the earlier work, with a difference of 3.6 kg/h (equivalent to 31.5 t/year).

For this problem, the result of the FTM method was reached after 1,506 iterations and 2,994 evaluations of the objective function, with 30 variables, 19 equality constraints and 32 inequality constraints. The number of function evaluations was much higher, compared to problem 2 (21 evaluations), largely due to the nonlinearity present in this case. The Nelder-Mead parameter values of the method used in this problem were $\alpha = 1.0$, $\beta = 0.7$, $\gamma = 2.6$ and $\delta = 0.5$.

4. Conclusions

The flexible tolerance method was able to generate optimum values in the three cases studied. The performance of the technique was compared with other gradient-based methods (GRG and SPQ) for a simple case (problem 1), and was shown be efficient, requiring fewer objective function evaluations. For larger problems, the number of objective function evaluations increased substantially, but it was still possible to generate optimum values. An additional advantage was that the preparation time required for large problems was short, since derivatives of functions did not need to be informed. Some difficulties were noted when using the FTM method in problems involving mass integration. The initial values used for algorithm initialization did not always converge to the optimal solution; since these initial values were distant from the optimal region, the search became slow or convergence was not achieved. Another difficulty encountered was related to the parameter values of the Nelder-Mead method (for unconstrained searches). In all cases studied in this work, the recommended values did not provide the solution, so that a trial and error procedure was adopted until values were found for which FTM achieved convergence. Possible future FTM strategies include using the Nelder-Mead method with adaptive parameters, scaling optimization and hybridization

with the particle swarm method.

Acknowledgments

The authors thank CAPES (Brazil) for financial support.

References

[1] Zhang, P.; Ren, Y. Flexible Tolerance Simplex Method and Its Application to Multicomponent Spectrophotometric Determinations. *Anal. Chim. Acta.* **1989,** *222,* 323-333.

[2] Constantinescu, D. Smooth and Time-Optimal Trajectory Planning for Industrial Manipulators Along Specified Paths. *J. Rob. Syst*. **2000,** *17,* 223-249.

[3] Shang, W.; Zhao, S.; Shen, Y. A Flexible Tolerance Genetic Algorithm for Optimal Problems with Nonlinear Equality Constraints. *Adv. Eng. Inform.* **2009,** *23,* 253-264.

[4] Himmelblau, D. M. *Applied Nonlinear Programming;* McGraw-Hill: New York, 1972; p 498.

[5] El-Halwagi, M. M. *Process Integration;* Elsevier: San Diego, 2006; p 398.

[6] Al-Otaibi, M.; El-Halwagi, M. Targeting Techniques for Enhancing Process Yield. *Chem. Eng. Res. Des*. **2006,** *84,* 943-951.

[7] El-Halwagi, M. M. *Pollution Prevention Through Process Integration: Systematic Design Tools;* Academic Press: San Diego, 1997; p 318.

3.3 Conclusion

The FTM was able to find the optimal value for the classic mass integration problems proposed. In the first case presented, starting from the same initial values, the FTM conducted the search with a lower number of evaluations of the objective function than SQP, despite otherwise be expected since the SQP has more information (the value of the derivative of the objective function). The results found for the other two problems agree with the reported in literature.

This initial optimization study shows that the FTM is highly dependent of the initial conditions and the parameter values of the Nelder-Mead method used in the search without constraints. Moreover, nonlinear problems, as the third study case presented in the article, requires a large number of evaluations of the objective function, which makes the search a bit slow.

From the initial analysis of the applicability of FTM in solving optimization problems with mass integration, it was gathered information about the difficulties encountered by the method, and proposed strategies to improve the method. These strategies will be developed and discussed in the following chapters and involve : (i) hybridization with other optimization methods, (ii) scaling of the variables of the optimization problem, and (iii) use of adaptive parameters in the method of Nelder and Mead .

CHAPTER 4

Hybridization of Flexible Tolerance Method with different unconstrained optimization methods

4.1 Introduction

This chapter describes the use of different unconstrained methods to perform the inner search in the Flexible Tolerance Method. The methods used were Modified Powell, BFGS and PSO. It was used for the PSO (Particle Swarm Optimization) code the DEAP (Distributed Evolutionary Algorithms in Python), (Fortin et al., 2012). Powell and BFGS algorithms was from the SciPy library (Jones et al., 2001).

The codes obtained were tested in a set of 20 functions that describe real optimization problems. Thus, the results can be extended to mass integration optimization problems. The codes implemented are:

- **FTM**: Flexible Tolerance Method in its standard form
- **FTMS**: Flexible Tolerance Method with Scaled variables
- **FTMS-Powell**: Flexible Tolerance Method with Scaled variables and Modified Powell
- **FTMS-BFGS**: Flexible Tolerance Method with Scaled variables and BFGS
- **FTMS-PSO**: Flexible Tolerance Method with Scaled variables and PSO

4.2 Development

The Flexible Tolerance Method (FTM), which was the main method used in this work, is a deterministic method that does not use derivatives information to perform the search. Although

the FTM was first proposed in the 1960s (Paviani and Himmelblau, 1969), the method has been little explored and there are few applications reported in the literature.

In previous chapter and Lima et al. (2013) the FTM was used in the synthesis and analysis of processes with mass integration. The FTM was compared with two indirect optimization methods (GRG and SQP) and good results were obtained solving a classic case of mass integration. It was found that when the FTM was applied to solve engineering problems, the inner search became slow and difficult when the dimensions of the problem became larger. Another difficulty concerned variations involving the range of variables, which could make it hard for the FTM to achieve convergence. In order to try to resolve these issues, the present work proposes the transformation of variables by scaling, as well as hybridization with other methods. Selection of the methods used for hybridization with FTM was based on: (i) derivative-free use, (ii) ease of implementation and (iii) good performance reported in the literature.

4.2.1 Methodology

The general formulation of a nonlinear programming problem can be stated by eqs. (4.1) - (4.3) as follows:

$$\text{Minimize} \quad f(\mathbf{x}) \quad \mathbf{x} \in \Re^n \tag{4.1}$$

$$\text{Subject to:} \quad h_i(\mathbf{x}) = 0 \quad i = 1,...,m \tag{4.2}$$

$$g_i(\mathbf{x}) \geq 0 \quad i = m+1,...,p \tag{4.3}$$

where $f(\mathbf{x})$ is the objective function, $h_i(\mathbf{x})$ the equality constraints and $g_i(\mathbf{x})$ the inequality constraints.

The Flexible Tolerance Method (FTM) is a direct search method and was proposed by Paviani and Himmelblau (1969). The FTM algorithm improves the value of objective function using the information provided by feasible points, as well some non feasible points, called near-feasible points. The feasibility becomes more restrictive as the search moves towards the problem solution, until the limit where only the feasible vectors $\mathbf{x}$ of eq.s (4.1) - (4.3) are accepted. The result of this basic strategy, the optimization problem, eq.s (4.1) - (4.3), can be rewritten as indicated in eq.s (4.4) and (4.5):

$$\text{Minimize:} \quad f(\mathbf{x}) \quad \mathbf{x} \in \Re^n \tag{4.4}$$

$$\text{Subject to:} \quad \Phi^{(k)} - T(\mathbf{x}) \geq 0 \tag{4.5}$$

where $\Phi^{(k)}$ is the flexible tolerance criterion for feasibility in the k stage of the search, and $T(\mathbf{x})$ is the positive functional of all constraints of equality and/or inequality of the problem, used as a measure of the violation extent of constraints. The functional $T(\mathbf{x})$ is described by eq. (4.6),

where U is the Heaviside operator according to eq. (4.7).

$$T(\mathbf{x}) = [\sum_{i=1}^{m} h_i^2(\mathbf{x}) + \sum_{i=m+1}^{p} U_i g_i^2(\mathbf{x})]^{1/2} \tag{4.6}$$

$$U_i = \begin{cases} 0 & \text{for } g_i(\mathbf{x}) \geq 0, \\ 1 & \text{for } g_i(\mathbf{x}) < 0 \end{cases} \tag{4.7}$$

The tolerance criterion at the kth iteration is given by eq. (4.8), where m is the number of equality constraints, $r = (n-m)$ the number of degrees of freedom of $f(\mathbf{x})$, $\mathbf{x}_i^{(k)}$ the ith vertex of the polyhedron in $\Re^n$, $\mathbf{x}_{cent}^{(k)}$ the vertex corresponding to the centroid, t the size of the initial polyhedron and k the iteration index.

$$\Phi^{(k)} = \min\{\Phi^{(k-1)}, \frac{m+1}{r+1} \sum_{i=1}^{r+1} \|\mathbf{x}_i^{(k)} - \mathbf{x}_{cent}^{(k)}\|\} \tag{4.8}$$
$$\Phi^{(0)} = 2(m+1)t$$

The tolerance criterion $\Phi^{(k)}$ behaves as a positive decreasing function of $\mathbf{x}$, and the vector $\mathbf{x}^{(k)}$ is classified as follows:

- Feasible, if $T(\mathbf{x}^{(k)}) = 0$.
- Near-feasible, if $0 < T(\mathbf{x}^{(k)}) \leq \Phi^{(k)}$.
- Non-feasible, if $T(\mathbf{x}^{(k)}) > \Phi^{(k)}$.

The tolerance for near-feasible solutions is decreased until the limit when only feasible solutions are allowed, according to eq. (4.9), where $\mathbf{x}^*$ is the solution vector, within tolerance ε.

$$\lim_{\mathbf{x} \to \mathbf{x}^*} \Phi^{(k)} = 0 \tag{4.9}$$

The FTM performs an outer search that minimizes the objective function $f(\mathbf{x})$ and an inner search that minimizes the value of $T(\mathbf{x})$. The outer search (Figure 4.1) is a variation of the Nelder-Mead method, when a new vertice is founded during the search, its feasibility is evaluated. If the vertice is near of feasibility the search continues. If the outer search select a non feasible vertice, an inner search (indicated by gray boxes in Figure 4.1) is performed to convert this non-feasible vertice in a near-feasible or feasible vertice.

The inner search that minimizes the value of $T(\mathbf{x})$ can be performed using any multivariable search technique. According to proposed by Paviani and Himmelblau (1969) the inner search uses the Nelder-Mead Method (or Flexible Polyhedron Method, FPM), Algorithm 1.

The Nelder-Mead Method minimizes the function $T(\mathbf{x})$ of n independent variables using $n+1$ vertices of a flexible polyhedron in $\Re^n$. This standard formulation is designated as FTM.

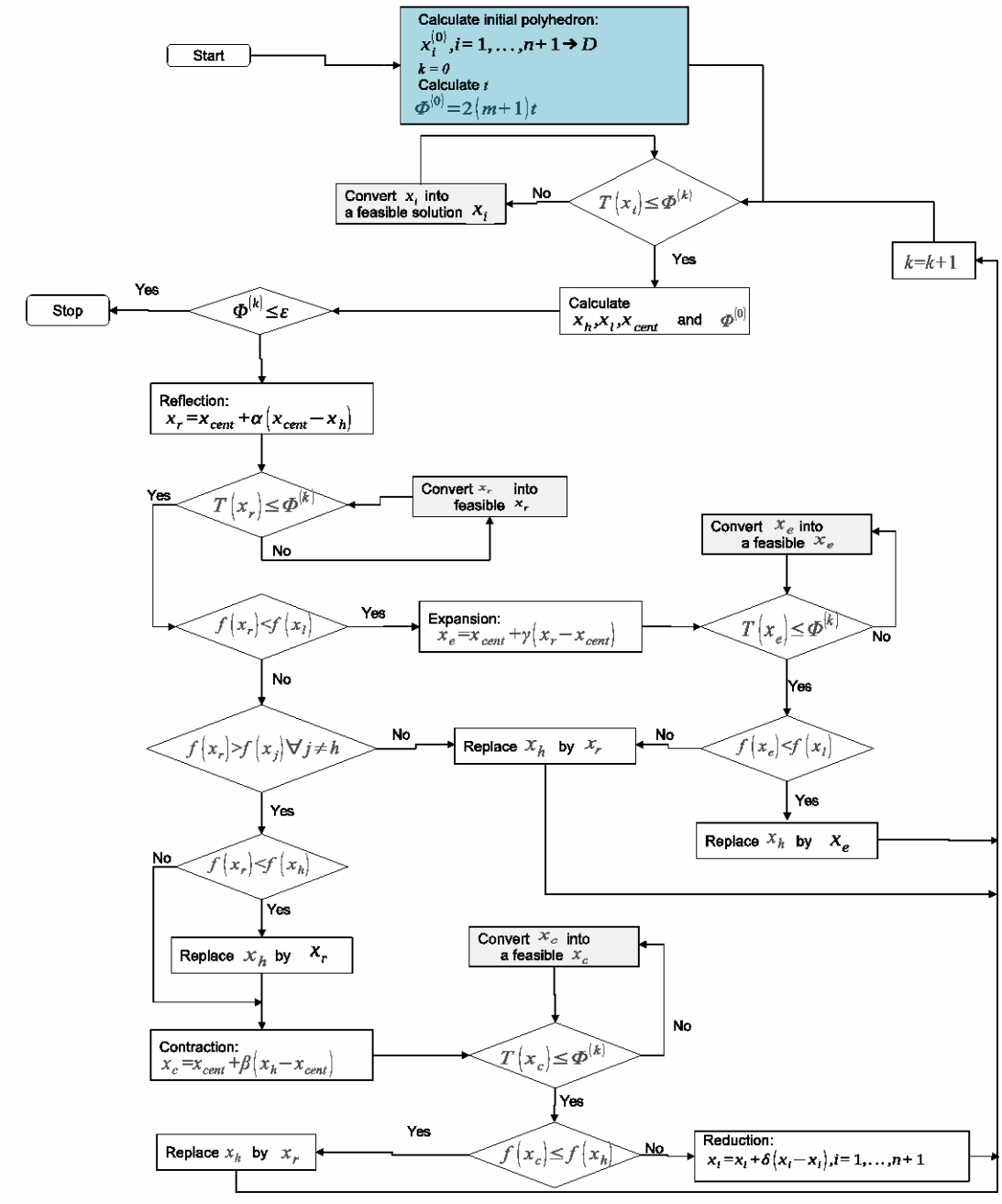

Figure 4.1: FTM algorithm flowchart for performing the outer search that minimizes the objective function $f(\mathbf{x})$. All vectors $\mathbf{x}$ are assumed to represent $x^{(k)}$, unless noted otherwise. Adapted and modified from Naish (2004). The gray boxes indicated the inner search that can be performed using different unconstrained minimization algorithms (in this work: Nelder-Mead, Powell and BFGS). The blue box indicate the initialization step that is replaced by PSO method in this work.

In addition to the standard FTM method and the FTM method with scaling of variables

Algorithm 1 Pseudocode of Nelder-Mead Method

Start: Calculate initial simplex: $\mathbf{x}_j^0$, $j = 1,...,n+1 \rightarrow \mathbf{D}$. Set $k = 0$
Step 1: Calculate $\mathbf{x}_h$, $\mathbf{x}_l$ and $\mathbf{x}_{cent}$
Step 2: Reflection: $\mathbf{x}_r = \mathbf{x}_{cent} + \alpha(\mathbf{x}_{cent} - \mathbf{x}_h)$
if $T(\mathbf{x}_r) < T(\mathbf{x}_l)$ **then**
  Step 3: Expansion: $\mathbf{x}_e = \mathbf{x}_{cent} + \gamma(\mathbf{x}_r - \mathbf{x}_{cent})$
  if $T(\mathbf{x}_e) > T(\mathbf{x}_l)$ **then**
    Step 6: Replace $\mathbf{x}_h$ by $\mathbf{x}_e$
  else
    Step 7: Replace $\mathbf{x}_h$ by $\mathbf{x}_r$
  end if
else
  if $T(\mathbf{x}_r) > T(\mathbf{x}_j) \forall j \neq h$ **then**

    if $T(\mathbf{x}_r) < T(\mathbf{x}_h)$ **then**
      Step 4: Replace $\mathbf{x}_h$ by $\mathbf{x}_r$
    end if
    Step 5: Contraction: $\mathbf{x}_c = \mathbf{x}_{cent} + \beta(\mathbf{x}_h - \mathbf{x}_{cent})$
  else
    Go to **Step 7**.
  end if
  if $T(\mathbf{x}_c) \leq T(\mathbf{x}_h)$ **then**
    Step 8: Replace $\mathbf{x}_h$ by $\mathbf{x}_c$
  else
    Step 9: Reduction: $\mathbf{x}_j = \mathbf{x}_l + \delta(\mathbf{x}_j - \mathbf{x}_l), j = 1,2,...,n+1$
  end if

  if $\sqrt{\frac{1}{n+1}\sum_{j=1}^{n+1}[T(\mathbf{x}_j) - T(\mathbf{x}_{cent})]^2} \leq \varepsilon$ **then**
    Stop.
  else
    $k = k+1$. Go to **Step 1**.
  end if
end if

(FTMS), additional variations used in this work employed other methods to perform the inner search. These methods were FTMS hybridized with the BFGS method (FTMS-BFGS), and FTMS hybridized with the Powell method (FTMS-Powell). FTMS was also hybridized with the PSO method (FTMS-PSO), where the PSO method was used to perform the initialization. These methods are described in the next section.

The codes used in this work were implemented in Python™and the optimization calculations were performed using Eclipse©IDE software, run under a Linux-like operating system installed on a 2 GHz Pentium (R) Dual-Core computer. The FTM parameters used were $\alpha = 1.0$, $\beta = 0.5$, $\gamma = 2.0$ and $\delta = 0.5$ as recommended previously, (Himmelblau, 1972). The tolerance adopted was $\varepsilon = 10^{-5}$, and the size of the initial polyhedron was $t = 0.4$.

The benchmark chosen for analysis of the performance of the optimization algorithms was the net of functions presented in CEC'06 (Liang et al., 2006), which cover a wide range of nonlinear constrained optimization problems, with real problems and some generated problems, and different constraint types (physical, time, geometric, etc.).

4.2.1.1 FTMS

The standard FTM using variable scaled is designated FTMS. The scaled variable (y_j) is defined according eq. (4.10), as reported by Gill et al. (1981), where U_j and L_j are the upper and lower bounds of variable (x_j). This transformation guarantees that $-1.0 \leq y_j \leq +1.0, \forall j$, regardless of value x_j within the interval $[U_j, L_j]$.

$$y_j = \frac{2x_j}{U_j - L_j} - \frac{L_j + U_j}{U_j - L_j} \tag{4.10}$$

4.2.1.2 FTMS-BFGS

The BFGS method employs the quasi-Newton procedure described by Broyden, Fletcher, Goldfarb, and Shanno (Nocedal and Wright, 1999). This method can use the gradient of the objective function. However, since the aim in this work was to use a derivative-free method, estimation was performed using first-differences. This employed the Scipy[1] library (Jones et al., 2001), especially the *scipy.optimize* package which provides several commonly used optimization algorithms.

The BFGS method with Scipy library was implemented based on Nocedal and Wright (1999), as shown in Algorithm 2. The jacobian of the objective function of the FTMS inner search ($T(\mathbf{x})$) was calculated using forward finite differences, as indicated in eq. (4.11), where τ is a small positive scalar, and e_i is the ith unit vector, for $i = 1, \ldots, n$.

$$\nabla T_k = \frac{\partial T}{\partial x_i} x \approx \frac{T(x + \tau e_i) - T(x)}{\tau} \tag{4.11}$$

[1] SciPy is a Python-based ecosystem of open-source software for mathematics, science and engineering.

Algorithm 2 Pseudocode of Broyden, Fletcher, Goldfarb, and Shanno (BFGS) Method

Given starting point $\mathbf{x}_0$, convergence tolerance $\varepsilon > 0$, inverse Hessian approximation H_0
$k = 0$
while $\|\nabla T_k\| > \varepsilon$ **do**
  Compute search direction: $p_k = -H_k \nabla T_k$
  Set $\mathbf{x}_{k+1} = \mathbf{x}_k + \alpha_k . p_k$, where α_k is computed from a line search procedure to satisfy the Wolfe conditions
  Define $\mathbf{s}_k = \mathbf{x}_{k+1} - \mathbf{x}_k$ and $\mathbf{y}_k = \nabla T_{k+1} - \nabla T_k$
  Compute $H_{k+1} = (I - \rho_k . \mathbf{s}_k . \mathbf{y}_k^T) H_k (I - \rho_k . \mathbf{y}_k . \mathbf{s}_k^T) + \rho_k . \mathbf{s}_k . \mathbf{y}_k^T$, where
  $\rho_k = \dfrac{1}{\mathbf{s}_k . \mathbf{y}_k^T}$
  $k = k + 1$
end while

The BFGS method was employed each time the FTMS called for minimization of the inner search ($T(\mathbf{x})$), indicated by the gray boxes in the algorithm flowchart of Figure 4.1.

4.2.1.3 FTMS-Powell

The method employed was a modification of Powell's method (Powell, 1964), which is a conjugate direction method that, is included in the *scipy.optimize* package from SciPy. It performs sequential one-dimensional minimizations along each vector of the directions set, which is updated at each iteration of the main minimization loop. The function need not be differentiable, and no derivatives are taken.

Powell's method was employed each time the FTMS called for minimization of the inner search ($T(\mathbf{x})$), indicated by the gray boxes in the algorithm flowchart of Figure 4.1.

4.2.1.4 FTMS-PSO

The PSO was hybridized with the FTMS method in a different way. In codes described previously (FTMS-BFGS and FTMS-Powell), the unconstrained optimization methods were used to perform the inner search. In the case of FTMS-PSO, the PSO method was used during the initialization of the FTMS, in order to find a feasible starting point. The PSO code in its standard form is available in the DEAP (Distributed Evolutionary Algorithms in Python) library that includes several evolutionary optimization algorithms in Python, (Fortin et al., 2012). The PSO from the DEAP library was the basis for building the PSO algorithm used in this work.

The PSO method employed here used the inertia weight (ω) calculated as indicated in eq. (4.12), (Hu and Eberhart, 2002). After some initial tests, the random term used for the inertia weight calculus was set between 0.1 and 1.2:

$$\omega = 0.5 + \frac{Rnd(0.1, 1.2)}{2} \tag{4.12}$$

The tuning of the other parameters of the PSO algorithm for all the problems solved were

Algorithm 3 Pseudocode of Powell's Modified Method

Given $s_k, k = 1,2,...,n \in \mathbf{P} \subseteq \Re^n$, a linearly independent set of vectors in $\mathbf{P}$
$\mathbf{p}_0$ is the starting point
Set $\mathbf{p}_0 = \mathbf{x}_i$, $i = 0$
for $k = 1,2,...n$ **do**
  Determine λ_k by minimizing $f(x_{k-1} + \lambda_k.s_k)$ defined by $x_k = x_{k-1} + \lambda_k.s_k$
end for
for $k = 1,2,...,n$ **do**
  $\Delta f_k = f(\mathbf{x}_k) - f(\mathbf{x}_{k-1})$
  Find index r, such that $\Delta f = |\Delta f_r| = max|\Delta f_r|$ is the magnitude of maximum decrease of f
  s_r is the direction of the maximum decrease about directions of the previous step
end for
repeat
  Set $i = i + 1$
  for $k = 1,2,...,n$ **do**
    $f_k = f(\mathbf{x}_k) - f(\mathbf{x}_{k-1})$
  end for
  Set $f_3 = f(2\mathbf{x}_n - \mathbf{x}_0)$, the function value in the new direction $2\mathbf{x}_n - \mathbf{x}_0$
  if $f_3 \geq f_0$ **or** $(f_0 - 2.f_n + f_3).(f_0 - f_n - \Delta f)^2 \geq \frac{1}{2}\Delta f(f_0 - f_s)^2$ **then**
    Use the old directions $s_1, s_2, ..., s_n$ for the next iteration and back to first step
  else
    Go to the next step
  end if
  Set $s_r = \mathbf{x}_n - \mathbf{x}_0$ with the sub index r obtained previously
  Define $s_r = \mathbf{x}_n - \mathbf{x}_0$, calculate λ_{min} minimizing $f(\mathbf{x}_n + \lambda_{min}.s_r)$, set $\mathbf{x}_i = \mathbf{x}_0 + \lambda.s_r$, as the starting point of the new iteration
until $|f(\mathbf{x}_{i+1})| < 10^{-10}$ **and** $\frac{\mathbf{x}_{i+1} - \mathbf{x}_i}{\mathbf{x}_i} < \varepsilon$

a cognition learning rate (C_1) of 2.0 and a social learning rate (C_2) of 2.0. The number of generations (GEN) was set at 100, and the population size (N) was set at 20, as suggested previously (Hu and Eberhart, 2002). The reason for a smaller population size and fewer number of generations was that this significantly decreased the computing time. Moreover, the objective of the PSO method was to find a feasible region that minimized the violation constraints before starting the FTMS, which would lead to the complete solution of the problem. The pseudocode indicated in Algorithm 4.

Algorithm 4 Pseudocode of the Particle Swarm Optimization (PSO) Method

Initialization: Generate random population (N) of particles (i) of positions and velocities in the search space D
repeat

for Each particle i **do**
Update the particle's best position ($f(pb_i)$)
if $f(x_i) < f(pb_i)$ **then**
$pb_i = x_i$
end if
Update the global best position ($f(gb)$)
if $f(pb_i) < f(gb_i)$ **then**
$gb = pb_i$
end if
end for
Update particle's velocity and position
for Each particle i **do**
for Each dimension d **do**
$v_i = \omega_i.v_i + C_1.Rnd().(pb_{i,d} - x_{i,d}) + C_2.Rnd().(gb_d - x_{i,d})$
$x_{i,d} = x_i + v_i$
end for
end for
$k = k + 1$
until $k <$ Number of generations (GEN)

For each particle generated, the penalty function $P(\mathbf{x})$, eq. (4.13), is evaluated, where Υ is the penalty parameter.

$$P(\mathbf{x}) = f(\mathbf{x}) + \Upsilon[T(\mathbf{x})] \tag{4.13}$$

The initialization with the PSO method described previously was performed until it find the best particle. The penalty parameter acts as indicated in Algorithm 5.

Algorithm 5 Pseudocode of FTMS-PSO

```
Initilization of PSO
Particles generated
Evaluation of P(x)
k = 1.0E − 6
if [T(x)] ≤ 10^−3 then
    The search continue with FTMS
else
    if ϒ < 10^−3 then
        ϒ = ϒ ∗ 10.0
    else
        ϒ = ϒ ∗ 2.0
    end if
end if
```

In this code, the initialization with the PSO method described previously was performed until the best particle was found, with the value of $T(\mathbf{x})$ (the constraint violation) being less than an arbitrary value (set at 10^{-3}).

When the best point satisfied this criterion, the FTMS was started as indicated previously without any modification. This code was perform 20 runs for each problem. The objective of using PSO hybridized with FTMS was to allow the optimization to explore different routes through the solution space and might help identify alternative solutions.

4.3 Results

A comparison of the performance of the optimization methods proposed in this work was conducted using a simple problem (a convex programming problem) with two variables, one equality constraint and one inequality constraint, as described in eq. (4.14), (Himmelblau, 1972). Figure 4.2 shows the objective function, the equality and inequality constraints and the optimum point.

$$\begin{aligned} \text{Minimize} \quad & f(\mathbf{x}) = (x_1-2)^2 + (x_2-1)^2 \\ \text{Subject to:} \quad & h_1(\mathbf{x}) = x_1 - 2x_2 + 1 = 0 \\ & g_1(\mathbf{x}) = -\frac{x_1^2}{4} - x_2^2 + 1 \geq 0 \end{aligned} \tag{4.14}$$

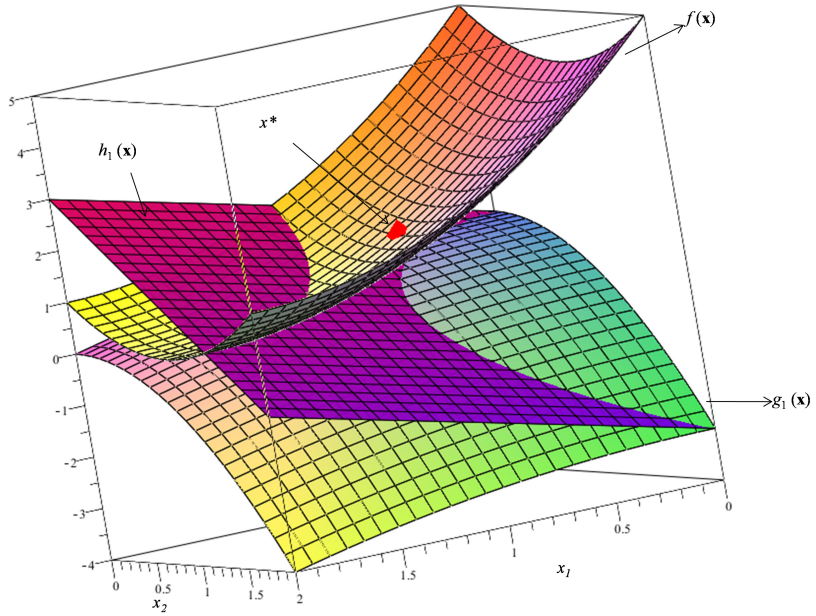

Figure 4.2: Objective function ($f(\mathbf{x})$), equality constraint ($h_1(\mathbf{x})$), inequality constraint ($g_1(\mathbf{x})$) and optimum point (x^*) for the test problem of eq. 4.14.

As can be observed in Table 4.1, the algorithms tested were able to find the optimum point for this simple problem. Comparing the number of objective function evaluations and iterations, the original FTM and the FTMS-BFGS methods presented the worst performance, with the largest values. The best performance were presented by the FTMS and FTMS-PSO methods. The FTMS showed the shortest processing time and the low numbers of iterations and objective function evaluations. For the FTMS-PSO method, the processing time was the longer, due to the time consumed by the initialization step with the PSO method, however presented the lower number of iterations and evaluations of objective function. The trajectories followed by each method (Figure 4.3) indicated that FTMS and FTMS-PSO had a more direct path than the other methods. FTMS-BFGS showed search path in which the objective function reached high values (distant from the optimum point, $f(\mathbf{x}) \simeq 7.165$), hence requiring a greater number of iterations and objective function evaluations in order to reach the optimal point.

Table 4.1: Results summary for the test problem described in eq. 4.14. N_{eval}: Number of objective function evaluations, N_{it}: Number of iterations, t_{proc}: Processing time (seconds).

	FTM	FTMS	FTMS-BFGS	FTMS-Powell	FTMS-PSO ‡
N_{eval}	50	28	45	29	22
N_{it}	18	12	24	15	9
t_{proc}	0.4913	0.0410	0.2565	0.3798	3.4341

‡ Best performance in 20 runs.

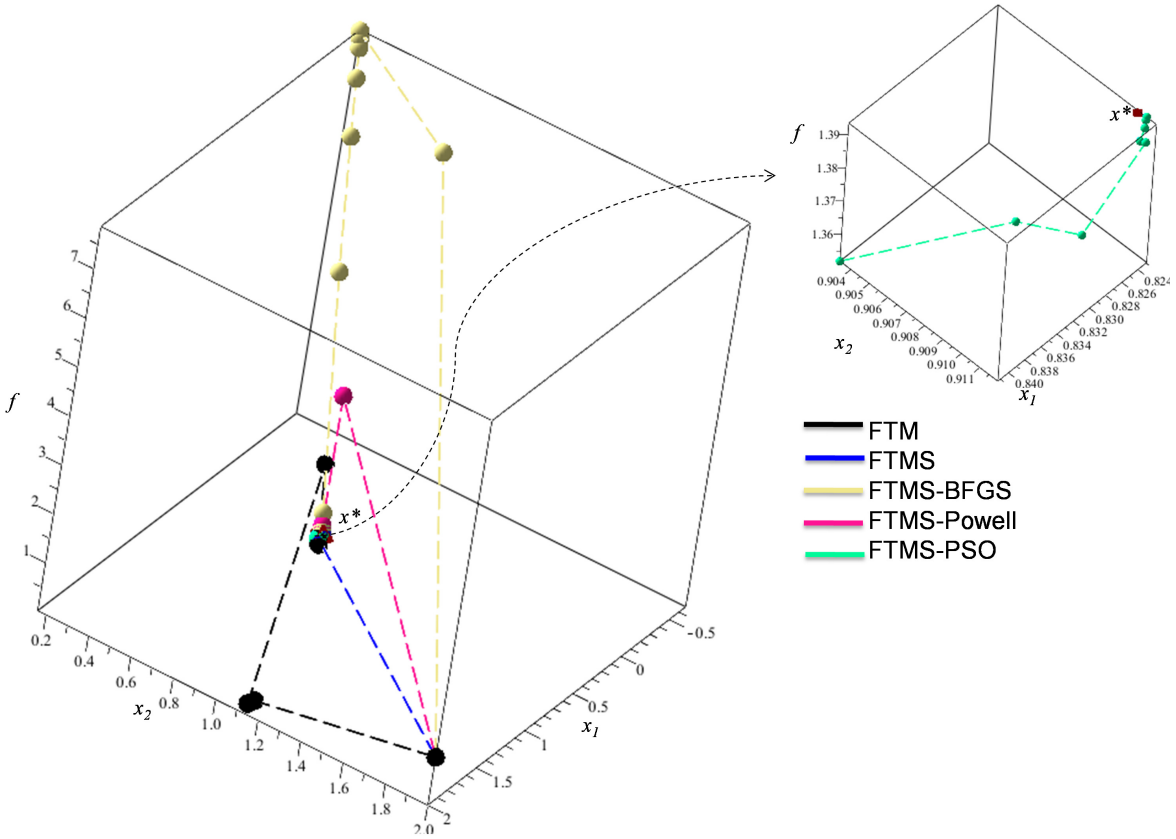

Figure 4.3: Trajectories from the nonfeasible initial vector obtained using the different optimization methods for test problem (eq. 4.14). The path followed by FTMS-PSO is showed separately due to the proximity of starting point from the optimal point.

Tables 4.2 and 4.3 show the number of variables, the type of objective function, the number of equality and inequality constraints, the upper and lower boundary constraints, and brief descriptions for the benchmark problems used in this work. The results were divided into two categories: (i) problems with small dimensions ($2 \leq n \leq 6$), and (ii) problems with larger dimensions ($n > 6$).

The results obtained after applying the optimization methods described previously (see Sect. 4.2.1) to the set of benchmark problems (from Liang et al., 2006) are described in Tables 4.4, 4.5, 4.6 and 4.7.

The success rates[1] of the methods were 85% for FTM, 100% for FTMS, 75% for FTMS-BFGS, 95% for FTMS-Powell and 85% for FTMS-PSO.

Table 4.4 and 4.5 show the optimum values found by the different optimization methods. For the first category of problems ($2 \leq n \leq 6$), it can be seen that FTMS-PSO and FTM presented the worst performance among the methods, with few problems solved. The best method was FTMS, which solved all the problems with good agreement. The other methods reached the

[1] In this work, the success rate is defined as the number of problems solved divided by the number of problems proposed for resolution (g01 to g20).

convergence for almost all the problem in this category ($2 \leq n \leq 6$), and were able to reach (or arrive close to) the known optima.

Table 4.2: Description of benchmark problems. Where: EC: equality constraints; IC: inequality constraints; ULBC: upper and lower bound constraints.

Function	n	Type	EC	IC	ULBC	Description
			Small problems			
g06	2	cubic	0	2	4	Problem with cubic objective function and quadratic constraints.
g08	2	nonlinear	0	2	4	Nonlinear problem with many local optima, the highest peaks are located along x axis. In the feasible region, the problem presents two maximum of almost equal fitness of value of 0.1.
g11	2	quadratic	1	0	4	Problem with quadratic objective function and quadratic constraint.
g12	3	quadratic	0	1	4	Problem with disjointed components, the feasible region of the search space consists of 9^3 disjointed spheres.
g15	3	quadratic	2	0	6	Nonlinear problem with nonlinear equality constraints.
g05	4	cubic	3	2	8	Problem with cubic objective function and nonlinear constraints.
g04	5	quadratic	0	6	10	Standard randomly generated test problem of non-convex quadratic objective function and constraints.
g13	5	nonlinear	3	0	10	Problem with nonlinear objective function and constraints.
g16	5	nonlinear	0	38	10	The objective function is the net profit of a hypothetical wood-pulp plant. The constraints include the usual material and energy balances as well as several empirical equations.
g17	6	nonlinear	4	0	12	Optimization of an electrical network.

Table 4.3: Description of benchmark problems. Where: EC: equality constraints; IC: inequality constraints; ULBC: upper and lower bound constraints.

Function	n	Type	EC	IC	ULBC	Description
			Larger problems			
g09	7	polynomial	0	4	14	Nonlinear problem with nonlinear constraints.
g10	8	linear	0	6	16	Heat exchanger design.
g18	9	quadratic	0	13	18	Maximization the area of a hexagon in which the maximum diameter was unity.
g07	10	quadratic	0	7	20	Problem with quadratic objective function and linear and nonlinear constraints.
g14	10	nonlinear	3	0	20	Problem of chemical equilibrium at constant temperature and pressure.
g01	13	quadratic	0	9	26	Standard randomly generated test problem of non-convex quadratic programming.
g19	15	nonlinear	0	5	30	Problem formulated by the Shell Development Company for the original Colville study.
g02	20	nonlinear	0	2	40	Nonlinear problem with global maximum unknown.
g03	20	polynomial	1	0	20	Problem with polynomial objective function and quadratic equality constraint.
g20	24	linear	14	6	48	Minimization of the cost of blending multicomponent mixtures.

Table 4.4: Optimum known and found by the algorithms for the benchmark problems.

Function	n	Optimum known	Optimum calculated					
			FTM	FTMS	FTMS-BFGS	FTMS-Powell	FTMS-PSO	
							Best	Worst
Small problems								
g06	2	-6,961.814	-6,962.275	-6,961.681	-6,959.518	-6,976.961	-6,961.814	-6,961.032
g08	2	0.100	0.096	0.096	0.096	0.096	0.096	0.094
g11	2	0.750	0.753	0.750	0.749	0.749	0.750	0.749
g12	3	-1.000	-0.859	-0.859	-0.840	-0.843	-0.859	-0.849
g15	3	961.715	961.716	961.715	961.715	961.715	961.716	961.715
g05	4	5,126.498	5,126.499	5,126.653	5,126.498	5,126.498	-	-
g04	5	-30,665.609	-	-32,217.421	-32,214.312	-32,196.566	-32,217.431	-32,217.431
g13	5	0.054	0.0546	0.054	0.438	0.054	0.054	0.439
g16	5	-1.905	-	-1.904	-	-	-	-
g17	6	8,853.540	-	8,853.649	-	8,853.540	-	-

Table 4.5: Optimum known and found by the algorithms for the benchmark problems.

Function	n	Optimum known	Optimum calculated					
			FTM	FTMS	FTMS-BFGS	FTMS-Powell	FTMS-PSO	
							Best	Worst
Larger problems								
g09	7	680.630	681.873	680.630	680.687	687.225	680.630	687.645
g10	8	7,049.331	-	7,050.925	-	9,623.854	7,049.308	7,095.352
g18	9	-0.866	-0.859	-0.866	-	-0.847	-0.866	-0.499
g07	10	24.306	24.083	24.120	78.069	14,865.964	24.331	21.900
g14	10	-47.765	-47.645	-47.443	-47.761	-47.761	-47.759	-47.549
g01	13	-15.000	-15.000	-15.000	-11.700	-11.700	-15.000	-11.074
g19	15	32.656 † 32.386✠	21.115	44.321	148.694	350.348	32.343	-0.477
g02	20	-0.804	-0.787	-0.793	-	-0.781	-0.379	-0.232
g03	20	1.000	0.986	0.997	1.000	0.881	-0.999	-0.776
g20	24	0.205† 0.057✠	0.0586	0.0577	0.0567	0.0576	0.0567	0.0583

† Optimum value reported by Liang et al. (2006).

✠ Optimum value reported by Himmelblau (1972).

Table 4.6: Number of objective function evaluations.

Function	n	FTM	FTMS	FTMS-BFGS	FTMS-Powell	FTMS-PSO	
						Best	Worst
Small problems							
g06	2	45	22	49	3554	21	22
g08	2	77	66	69	106	55	72
g11	2	75	185	244	266	76	271
g12	3	287	104	87	129	100	232
g15	3	154	176	195	268	107	202
g05	4	2931	36019	736	111	-	-
g04	5	1508	573	663	727	261	964
g13	5	130	242	315	279	208	243
g16	5	-	369	-	-	-	-
g17	5	-	10295	-	431	-	-
Larger problems							
g09	7	2401	862	748	1270	580	572
g10	8	-	734	-	1861	2035	763
g18	9	1704	784	-	823	655	737
g07	10	2504	2345	1209	972	2440	2423
g14	10	1492	1613	1515	1643	1328	850
g01	13	592	476	1752	3294	339	2769
g19	15	3109	2558	2289	2669	2231	1965
g02	20	2342	2320	-	2533	2623	2625
g03	20	2578	1962	2663	886	2427	2665
g20	24	1899	2200	3648	2746	2503	2478

Table 4.7: Number of iterations.

Function	n	FTM	FTMS	FTMS-BFGS	FTMS-Powell	FTMS-PSO	
						Best	Worst
Small problems							
g06	2	40	37	25	4	11	12
g08	2	40	37	36	58	30	37
g11	2	19	77	126	133	19	133
g12	3	137	31	48	53	31	107
g15	3	62	80	81	123	45	96
g05	4	739	1531	373	53	-	-
g04	5	586	329	352	396	112	518
g13	5	52	120	158	140	98	115
g16	5	174	146	-	-	-	-
g17	6	-	71	-	133	-	-
Larger problems							
g09	7	1614	558	418	729	364	359
g10	8	-	358	-	964	1203	356
g18	9	1025	445	-	428	388	433
g07	10	1765	1636	723	569	1722	1722
g14	10	860	924	1001	1023	786	460
g01	13	331	290	895	1639	194	1597
g19	15	2081	1892	1437	1703	1577	1289
g02	20	1413	1513	-	1911	1994	1994
g03	20	1640	1239	1640	422	1562	1718
g20	24	675	951	1808	1378	1075	1110

The agreement with known results for problem g12 was a little poor. This problem presents multiple disjointed regions and represents a challenge for any optimization method. The optima point showed by the methods proposed here for problem g12 stays at $f(\mathbf{x})^* = -0.85$, and the optimum known is $f(\mathbf{x})^* = -1.00$. Meanwhile, even using FTMS-PSO, that was run 20 times and thus the search started from different 20 initial points, the result converged to (or near to) the same point reported here.

The problems g05 and g17 have trigonometric functions in their equality constraints. This type of functions appeared to destabilize the swarm of particles, and the PSO was not able to reach feasible start points in both problems.

For the second category of problems ($n > 6$), FTMS-BFGS showed the worst performance, with three unsolved problems, and FTMS and FTMS-PSO presented the best performance. The FTMS, FTMS-Powell and FTMS-PSO methods were able to reach convergence, with the solutions found by FTMS and FTMS-PSO providing better fits to the known optima.

Problem g19 had a nonlinear objective function with 15 independent variables and 5 cubic constraints; the 15 variables also had lower bounds. The FTM, FTMS, FTMS-BFGS and FTMS-Powell converged very slowly to a local optimal solution. FTMS-PSO showed a good performance and converged more rapidly to the global optimum known in fewer number of iterations and objective function evaluations than the other methods. This problem clearly presents a large number of local optima, due the various local optimal points founded by the codes tested. This problem is a challenge for any direct method of optimization (since they are more prone to be stuck in a local optimum), and the hybridization of FTMS with PSO proved to be efficient to overcome this awkwardness.

Problem g16 presents a complex objective function with a large number of nonlinear constraints. For this problem, only the FMTS was able to found the solution. The other methods do not converged to a feasible solution. This same problem is reported in literature, (Himmelblau, 1972), and even indirect method (GRG) failed to solve it, probably due to difficulty of handle with first and second derivatives that is liable to human error, despite the large time required to problem preparation. It is important highlights that FTMS was able to solve this problem in few evaluations of objective function and iterations, moreover the preparation time was quite small.

The number of objective function evaluations and the number of iterations for each method are indicated in Tables 4.6 and 4.7, respectively.

Analysis of the first group of problems showed that for problems with the same number of variables, the number of evaluations could vary widely, probably due to the topology of the objective and constraint functions. Furthermore, even for a small number of variables, the number of objective function evaluations could reach high values, as in the case of problem g17 solved by FTMS. This problem (an electrical network optimization), which has a nonlinear objective function defined by parts and nonlinear equality constraints, was solved by FTMS after 10295 objective function evaluations and 71 iterations. For this same problem, the FTMS-Powell method reached the optimum after fewer objective functions evaluations (431) but with a larger number of iterations (133).

The FTMS, FTMS-Powell and FTMS-PSO methods presented the best performance for the second group of problems, which were all solved, with FTMS and FTMS-PSO providing better agreement with the known optima. The other methods (FTM and FTMS-BFGS) presented similar performance in terms of the numbers of iterations and objective function evaluations.

In the case of problem g20, which is complex and represents a challenge for any nonlinear programming method, the results found with the codes tested in this work were in agreement with those one reported elsewhere (Himmelblau, 1972).

FTMS-PSO showed a good performance compared with the other methods. This code can be useful when the optimization problem has an unknown starting point, or when the known starting point leads to an unfeasible solution. Numerical experiments also indicated improvements in the capacity of a direct method (as FTMS) escape from local optima when hybridized with PSO, that generate different starting points for the deterministic method of search.

4.4 Conclusions

This chapter proposes the use of the flexible tolerance method with scaling of variables and hybridization with different unconstrained methods (BFGS and modified Powell) to perform the inner search and with a stochastic method (PSO) to perform the initialization. The FTMS method proved be the most effective when applied to the benchmark problems.

The flexible tolerance method with scaling (FTMS) and hybridized with the stochastic method PSO, FTMS-PSO, presented some advantages applied to solution of the nonlinear optimization problems. The relative advantages of the methods (FTMS and PSO) could be employed, and the stochastic method PSO provided good initial points for the deterministic method FTMS and helped escape from local optima. This strategy was useful to corroborate the global optimum in nonlinear optimization problems, which the global optimum can not be guaranteed.

The flexible tolerance method with scaling (FTMS) was more efficient and computationally more economical than the original flexible tolerance method. Furthermore, the method required little tuning of parameters, and the same parameter configuration was able to solve all the problems in good agreement with the known solutions, with a few exceptions (such as the problem with disjointed regions). The FTMS employed the Nelder-Mead method to perform the inner search, as originally proposed by Paviani and Himmelblau (1969), and use scaled variables as proposed here. Hybridization with other methods (BFGS and Powell) did not result in any further enhancement of performance.

These codes (FTMS and FTMS-PSO) will be used in the next chapter to test other improvements and to apply in mass integration problems.

CHAPTER 5

The Modified Flexible Tolerance Method

5.1 Introduction

The objective of this chapter is to propose some modifications in the best codes founded in the previous chapter (FTMS and FTMS-PSO) and apply in mass integration problems.

Since no improvements were observed using the FTM hybridized with other methods to perform the unconstrained search, the focus of this chapter is to propose some alternatives in order to enhance the performance of the FTMS and FTMS-PSO.

Initially it was implemented adaptive parameters (reflexion, expansion, contraction and reduction) in the Nelder-Mead method. The methodology used was proposed previously by Gao and Han (2012), where the parameters are calculated in function of the number of variables of problem.

The improvement proposed was to add a barrier during the search process avoiding the polyhedron exceed the upper and lower limits of variables.

The codes used was the ones derivate from the standard flexible tolerance method (FTM), the scaled flexible tolerance method (FTMS) and the hybrid with PSO (FTMS-PSO) presented in the previous chapter, as follows:

- **FTMA**: flexible tolerance method (FTM) using adaptive parameters
- **FTMAS**: flexible tolerance method with scaling (FTMS) with adaptive parameters
- **MFTMS**: FTMS including the barrier modification
- **MFTMS-PSO**: MFTMS hybridized with PSO

5.2 Development

The codes were implemented in Python and the same benchmark of problems used in the previous chapter was employed.

The mass integration problems solved in this chapter comprises two of the problems presented in the Chapter 3 (the maximization the overall process yield and the minimization of the total load of a toxic pollutant discharged into terminal plant wastewater), and another problem reported in literature (Hortua, 2007), that deals with the production of phenol from cumene hydroperoxide.

The mass integration problems were reformulated using the explicit substitution method, in order to reduce the number of variables and the number of equality constraints. There are a large number of equality constraints in this type of problem, since many mass balances need be satisfied. Large number of equality constraints is a difficult issue for any optimization method, thus the use of strategies to reduce the computational effort spent in satisfying this type of constraint is a good rule of thumb.

5.2.1 Explicit Substitution Method

The explicit substitution method applied in resolution of an optimization problem of a scalar function f with n real variables with m equality constraints, consist in the explicit resolution of the system of m equations that define the constraints net, and obtaining a function that relates the n decision variables with each other, passing $(n-q)$ of them depend of the remaining q. Incorporating this function in objective function, the problem becomes a optimization problem with q variables, with the observation that any solution of this last problem consist in a part of problem solution, then is necessary couplet the solution using the function that relates the decision variables.

The optimization problem before defined by eqs. 5.1-5.3 with n variables, is now defined by eqs. 5.4-5.5 with q variables. In this new formulation the equality constraints h_i^* need to be reformulated considering the substitution of the $n-q$ variables. The functions obtained with the explicit resolution are embedded in optimization problem and are evaluated in each evaluation of objective function.

$$\text{Minimize:} \quad f(\mathbf{x}) \quad \mathbf{x} \in \Re^n \tag{5.1}$$

$$\text{Subject to:} \quad h_i(\mathbf{x}) = 0 \quad i = 1, ..., m \tag{5.2}$$

$$g_i(\mathbf{x}) \geq 0 \quad i = m+1, ..., p \tag{5.3}$$

$$\Downarrow$$

$$\text{Minimize:} \quad f(\mathbf{x}) \quad \mathbf{x} \in \Re^q \tag{5.4}$$

$$\text{Subject to:} \quad h_i^*(\mathbf{x}) = 0 \quad i = 1, ..., m \tag{5.5}$$

$$g_i(\mathbf{x}) \geq 0 \quad i = m+1, ..., p \tag{5.6}$$

This strategy was used to diminishing the number of variables to be evaluated in the optimization problem. Then, the polyhedron constructed during the search of optimum decreases and the algorithm becomes more efficient.

As reported in the previous chapter the flexible tolerance method with scaling of variables (FTMS) and hybridized with PSO (FTMS-PSO) was a powerful strategy to improve FTM performance. Thus, the FTMS and FTMS-PSO was employed in this work to try new modifications and possible improvements.

5.2.2 The Nelder-Mead Method

The Nelder-Mead method, also known as the flexible polyhedron method (FPM), is an unconstrained search method that was used in this work to perform the unconstrained searches in the FTM, as proposed by Himmelblau (1972). The FPM minimizes a function of n independent variables using $(n+1)$ vertices of a flexible polyhedron in $\Re^n$. The FPM starts with a set of $(n+1)$ vectors that represent the vertices of a regular simplex, described by matrix **D**, in which the columns represent the components of the vertices and the rows represent the coordinates (eq. 5.7).

$$\mathbf{D} = \begin{bmatrix} 0 & d_1 & d_2 & \cdots & d_2 \\ 0 & d_2 & d_1 & \cdots & d_2 \\ \vdots & \vdots & \ddots & \vdots & \\ 0 & d_2 & d_2 & \cdots & d_1 \end{bmatrix} \tag{5.7}$$

where d_1 and d_2 are described by eqs. 5.8 and 5.9, respectively, and t is the distance between two vertices.

$$d_1 = \frac{t}{n\sqrt{2}}(\sqrt{n+1} + n - 1) \tag{5.8}$$

$$d_2 = \frac{t}{n\sqrt{2}}(\sqrt{n+1}-1) \tag{5.9}$$

The flexibility of the polyhedron enables efficient searching and the avoidance of difficulties in the normal simplex procedure when the search encounters curving valleys or curving ridges in the search space. Improved objective function values are found by successively replacing the point with the highest value of $f(\mathbf{x})$ by better points, until the minimum $f(\mathbf{x})$. is found. A pseudocode of the Nelder-Mead Method or FPM is shown in Algorithm 1 (previous chapter).

5.2.3 Adaptive parameters of the Nelder-Mead method

In the standard implementation of the FPM or Nelder-Mead method, the parameters of reflection (α), expansion (γ), contraction (β), and reduction (δ) assume the values presented in eq. 5.10.

$$\begin{aligned} \alpha &= 1.0 \\ \gamma &= 2.0 \\ \beta &= 0.5 \\ \delta &= 0.5 \end{aligned} \tag{5.10}$$

It has been found previously that the FPM algorithm becomes inefficient in high dimensions ((Gao and Han, 2012); (Lima et al., 2013)). In order of trying to improve the performance of the FTM, the adaptive parameters suggested by Gao and Han (2012) were used in this work. According to the authors, these can reduce the chances of using reflection steps, while avoidance of rapid reduction in the simplex diameter should help to improve the performance of the FPM (and in this case also the FTM) for large dimensional problems. The coefficients are described in eq. 5.11.

$$\begin{aligned} \alpha &= 1.0 \\ \gamma &= 1.0 + \frac{2.0}{n} \\ \beta &= 0.75 - \frac{1.0}{2.0 \times n} \\ \delta &= 1.0 - \frac{1.0}{n} \end{aligned} \tag{5.11}$$

According to Gao and Han (2012), selection of $\gamma = 1.0 + \frac{2.0}{n}$ instead of $\gamma = 2.0$ can help to prevent the simplex experiencing distortion caused by expansion steps in high dimensions, $\beta = 0.75 - \frac{1.0}{2.0 \times n}$ instead of $\beta = 0.5$ can alleviate the reduction of the simplex diameter when n is large, and $\delta = 1.0 - \frac{1.0}{n}$ instead of $\delta = 0.5$ can prevent the simplex diameter from sharp

reduction when n is large.

5.2.4 Modified Flexible Tolerance Method proposed (MFTMS)

During the optimization process, the flexible tolerance method can found some vertices of polyhedron outside the limits of variables. This occur due to the steps of reflection, expansion, contraction and reduction not use the range of variable to perform their operations. Then, considering the scaled problem, the vertices sometimes exceed the upper bound (+1.0) or the lower bound (-1.0). This behavior cause the degeneration of the polyhedron and difficult the constraints minimization, since some vertices is outside the feasible search region. The proposed modification limit the variables that exceed the variation range in any of the optimization steps into the scaled interval, acting as a barrier, as indicated in eq. 5.12.

$$\begin{aligned} &\text{if} \quad x_i > 1.0 \quad \text{then} \quad x_i = 1.0 \quad \text{for} \quad i = 1,...,n \\ \text{if} \quad &x_i < -1.0 \quad \text{then} \quad x_i = -1.0 \quad \text{for} \quad i = 1,...,n \end{aligned} \tag{5.12}$$

The barrier acts as illustrated in Figure 5.1. In Figure 5.1 (a) is shown a possible polyhedron generated for a problem with $n = 3$ without scaling of variables. In (b) the variables were scaled ranged from $[-1.0, +1.0]$ as described in previous chapter for the code FTMS. In (c), some vertices of the scaled polyhedron reach values outside the defined search region $[-1.0, +1.0]$ in one of the algorithm steps (reflection, contraction, expansion, reduction), and can cause some difficulty to convergence. In (d), the barrier illustrated by the cube around the polyhedron is created each time the vertex found is outside the scaled range of the variables.

5.2.5 Hybridization of the Modified Flexible Tolerance Method proposed with PSO (MFTMS-PSO)

The method proposed in the previous section was hybridized with the PSO method. The same strategy reported in the previous chapter will be employed here. The PSO acts in the initialization of the search to find a net of values feasible, and then the MFTMS is applied to best particle.

5.2.6 Application in test problems

The codes proposed were applied using a set of functions from G-Suite from Liang et al. (2006), presented in the Congress of Evolutionary Computation in 2006, in order to evaluate what of the codes proposed here present the best performance and are suitable for solve mass integration

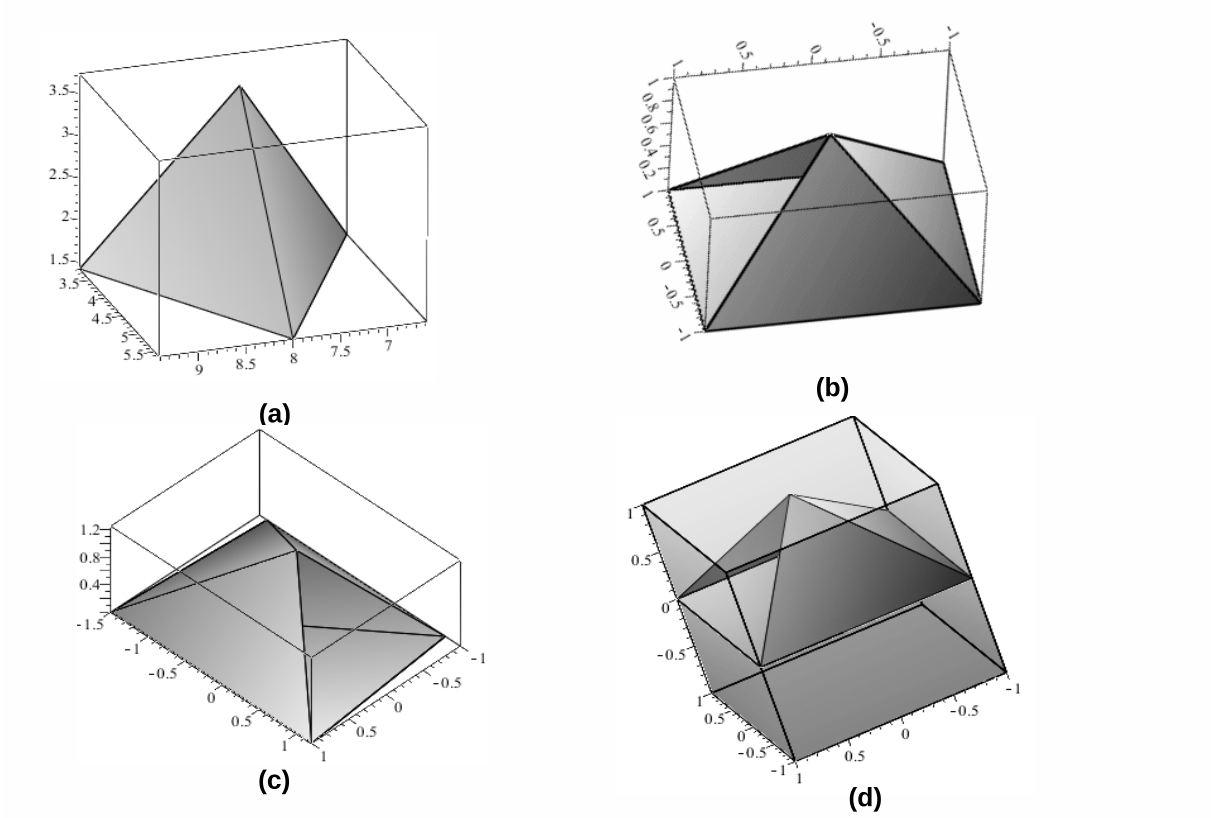

Figure 5.1: Possible outcomes for a polyhedron during the search by the Flexible Tolerance Method for $n = 3$ and the barrier proposed. (a) Initial polyhedron without scaling, (b) Scaled polyhedron, (c) Scaled polyhedron with some vertices outside the defined region and (d) the barrier illustrated by the cube around the polyhedron is created each time the vertex found is outside the scaled range of the variables.

problems. These set of functions, which cover a wide range of nonlinear constrained optimization problems, with real problems and some generated problems, and different constraint types (physical, time, geometric, etc.), have been used previously to validate optimization algorithms and compare their performance ((Deb and Srivastava, 2012); (Koziel and Michalewicz, 1999)). The functions are described in detail by Liang et al. (2006) and in Appendix A, and a brief problem description are reported in previous chapter.

The FTM/FTMS and modifications were implemented in Python™, and the optimization calculations were performed using Eclipse© IDE software, run under a Linux-like operating system installed on a 2 GHz Pentium (R) Dual-Core computer.

The performance of the FTM and the modified algorithms obtained in a previous chapter FTMS and FTMS-PSO was compared with the different codes proposed in this work:

- **FTMA**: The flexible tolerance method (FTM) using adaptive parameters of the Nelder-Mead method (FPM)

- **FTMAS**: The flexible tolerance method with scaling (FTMS) with adaptive FPM param-

eters

- **MFTMS**: The FTMS including the barrier modification
- **MFTMS-PSO**: The FTMS-PSO including the barrier modification. This code was run 20 times, and the best and worst results were reported.

The problems were grouped into two sets: (a) problems of small dimensions ($2 \leq n \leq 6$), and (b) larger problems ($n > 6$). In all cases it was adopted a tolerance of $\varepsilon = 10^{-5}$, and the size of the initial polyhedron was $t = 0.4$.

Based on the results found for the test problems of G Suite previously described, it was applied the best code to solve engineering problems, namely mass integration problems.

5.3 Results

In order to visualize the trajectory of the algorithms proposed in this work, a simple problem will be used for comparison. This same problem was used in a previous chapter. Figure 5.2 shows the objective function, the equality and inequality constraints and the optimum point.

$$\begin{aligned} \text{Minimize} \quad & f(\mathbf{x}) = (x_1 - 2)^2 + (x_2 - 1)^2 \\ \text{Subject to:} \quad & h_1(\mathbf{x}) = x_1 - 2x_2 + 1 = 0 \\ & g_1(\mathbf{x}) = -\frac{x_1^2}{4} - x_2^2 + 1 \geq 0 \end{aligned} \tag{5.13}$$

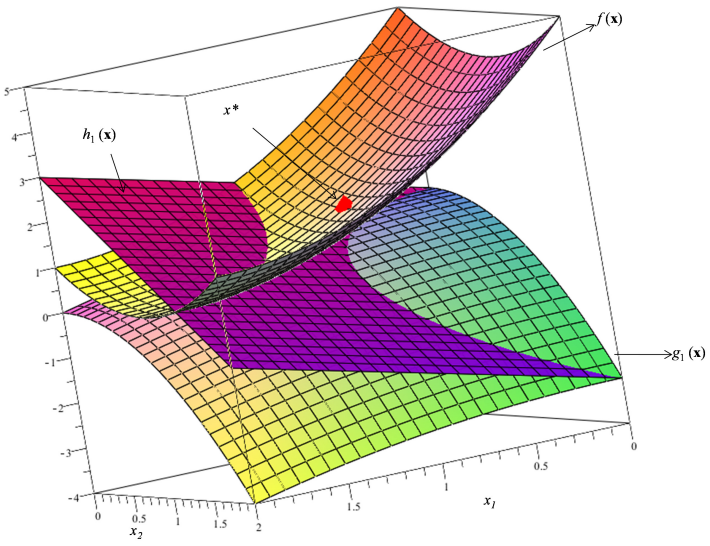

Figure 5.2: Objective function ($f(\mathbf{x})$), equality constraint ($h_1(\mathbf{x})$), inequality constraint ($g_1(\mathbf{x})$) and optimum point (x^*) for the test problem of eq. 5.13.

Table 5.1 shows the number of objective function evaluations, the number of iterations and the processing time (using the machine described previously) for the four optimization codes implemented in this work. The optimum value for this problem was $\mathbf{x}^* = [0.823 \quad 0.911]^T$ when the objective function assumed the value of $f(\mathbf{x})^* = 1.393$.

Table 5.1: Results summary for the test problem described in eq. 5.13. N_{eval}: Number of objective function evaluations, N_{it}: Number of iterations, t_{proc}: Processing time (seconds).

	FTMA	FTMAS	MFTMS	MFTMS-PSO ‡
N_{eval}	120	70	28	31
N_{it}	59	31	12	11
t_{proc}	0.116	0.259	0.065	4.29

‡ Best performance in 20 runs.

As can be observed in Table 5.1, the algorithms tested were able to find the optimum point for this simple problem. Comparing the number of objective function evaluations and iterations, the FTMA and the FTMAS methods presented the worst performance, with the largest values. The best performance were presented by the MFTMS and MFTMS-PSO methods. The MFTMS showed the shortest processing time and the low numbers of iterations and objective function evaluations. For the MFTMS-PSO method, the processing time was the longer, due to the time consumed by the initialization step with the PSO method, however presented the lower number of iterations and evaluations of objective function similar to MFTMS. The trajectories followed by each method (Figure 5.3) indicated that MFTMS had a more direct path than the other methods.

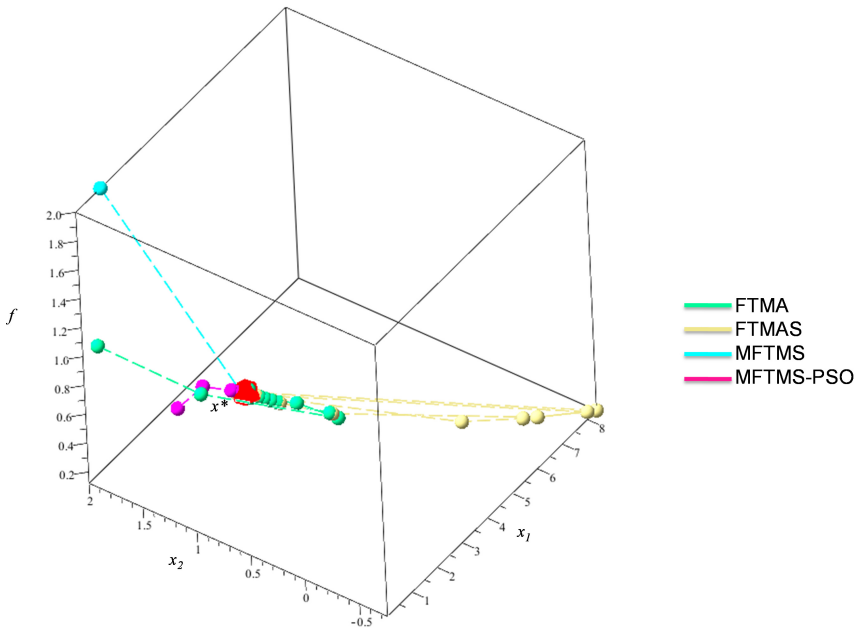

Figure 5.3: Trajectories from the nonfeasible initial vector obtained using the different optimization methods for test problem (eq. 5.13).

5.3.1 Problems of small dimensions ($2 \leq n \leq 6$)

Table 5.2 shows the objective function values for problems of small dimensions. The MFTMS and MFTMS-PSO codes showed the best performance in reaching the optimum. Table 5.3 summarizes the number of objective function evaluations required for FTMA, FTMAS, MFTMS and MFTMS-PSO for problems of small dimensions ($2 \leq n \leq 6$).

The adaptive parameter strategies (FTMA and FTMAS) showed poor performance compared to the other techniques (MFTMS and MFTMS-PSO), and required a significantly greater number of objective function evaluations in the cases where convergence was achieved. This was also noted by Gao and Han (2012) for problems with small dimensions. In almost all cases, convergence was not achieved using adaptive parameters.

FTMA was unable to reach the known optimum for the g08 function, despite the greater number of objective function evaluations compared to the other codes.

The feasible region of the search for problem g12 consisted of $9^3 = 729$ disjointed spheres. The ability of the methods to deal with multiple disjointed regions was poor, as can be observed from the objective function values found by MFTMS and MFTMS-PSO. This results agree with the ones reported previously.

The MFTMS and MFTMS-PSO showed similar performance to the codes without the barrier (FTMS and FTMS-PSO) reported previously.

The problem g05, that comprises difficult equality constraints, the MFTMS was able to reach the known optima in a smaller number of objective function evaluation and iterations (10658 [1013]) compared with the results reported by FTMS (36019 [1531]).

Solution of problem g16, that present complex objective function and a large number of nonlinear constraints, was difficult to be obtained even with indirect method, as GRG, that failed to solve it (Himmelblau, 1972). The MFTMS code reached convergence with a smaller number of objective function evaluations (284 [146]) when compared with the FTMS (369 [146]). The method hybridized with PSO, MFTMS-PSO, also achieved convergence (395 [225]) whereas FTMS-PSO did not converge.

Table 5.2: Objective function values for problems of small dimensions ($2 \leq n \leq 6$)

Function	n	Optimum known	Optimum calculated				
			FTMA	**FTMAS**	**MFTMS**	**MFTMS-PSO**	
						Best	Worst
g06	2	-6,961.814	-6,961.978	-6,961.769	-6,961.792	-	-
g08	2	0.100	0.029	0.096	0.096	0.096	0.096
g11	2	0.750	0.750	0.750	0.750	0.750	0.750
g12	2	-1.000	-	-	-0.853	-0.858	-0.857
g15	3	961.715	-	961.715	961.715	961.715	961. 715
g05	4	5,126.498	-	-	5,126.653	-	-
g04	5	-30,665.609	-32,217.433	-30,933.877	-32,217.431	-32,217.431	-32,217.431
g13	5	0.054	-	-	0.054	0.054	0.441
g16	5	-1.905	-	-	-1.905	-1.905	-1.897
g17	6	8,853.534	-	-	8853.548	-	-

Table 5.3: Number of objective function evaluation and iterations (in [ ]) for problems of small dimensions ($2 \leq n \leq 6$)

Function	n	**FTMA**	**FTMAS**	**MFTMS**	**MFTMS-PSO**	
					Best	Worst
g06	2	65 [19]	26 [14]	36 [15]	-	-
g08	2	159 [84]	131 [72]	66 [37]	46 [25]	71 [36]
g11	2	2971 [1569]	2967 [1553]	185 [77]	86 [21]	336 [171]
g12	2	-	-	171 [85]	99 [36]	100 [44]
g15	3	-	3123 [1553]	189 [89]	135 [63]	165 [76]
g05	4	-	-	10658 [1013]	-	-
g04	5	-	728 [586]	1317 [742]	352 [205]	468 [265]
g13	5	-	-	149 [60]	142 [64]	186 [83]
g16	5	-	-	284 [146]	395 [225]	386 [194]
g17	6	-	-	530 [235]	-	-

5.3.2 Larger problems ($n > 6$)

Table 5.4 summarizes the objective function values obtained for large problems, which showed a greater number of constraints than the preceding group. MFTMS and MFTMS-PSO achieved successful convergence, with MFTMS generally giving better results than MFTMS-PSO, and the use of adaptive coefficients did not improve the performance of FTMS or FTM.

The numbers of objective function evaluations for larger problems ($n > 6$) are illustrated in Table 5.5. The adaptive strategy was ineffective for use with this group of problems, since few convergences were achieved with FTMA and FTMAS. However, barrier proved to be a useful strategy, with the number of function evaluations required for MFTMS and MFTMS being similar to the ones reported previously.

The problem g19 as pointed out previously presents a large number of local optima. MFTMS-PSO presented a good performance reaching the known optima in similar number of objective function evaluations and iterations than FTMS-PSO.This problem represents a challenge for any direct method of optimization (since they are more prone to be stuck in a local optimum), and the hybridization of MFTMS with PSO also proved to be efficient to overcome this awkwardness.

Problem g20 is sufficiently complex to provide a challenge for any nonlinear programming algorithm. Despite this, MFTMS and MFTMS-PSO were able to converge to optima reported in literature (Himmelblau, 1972). MFTMS and MFTMS-PSO required a lesser number of objective function evaluations and iterations when compared with the corresponding codes without barrier.

Table 5.4: Objective function values for problems of large dimensions ($n > 6$).

Function	n	Optimum known	Optimum calculated				
			FTMA	**FTMAS**	**MFTMS**	**MFTMS-PSO**	
						Best	Worst
g09	7	680.630	680.630	687.348	680.630	680.633	680.630
g10	8	7,049.331	-	7,234.849	7,050.877	7,052.836	7,097.4266
g18	9	-0.866	-	-	-0.866	-0.866	-0.866
g07	10	24.306	-	26.526	25.304	24.156	24.089
g14	10	-47.765	-	-	-47.683	-47.767	-47.545
g01	13	-15.000	-	-	14.823	-14.774	-10.575
g19	15	32.656 [§] 32.386[‡]	-	-	44.3214	32.4915	2.2771
g02	20	-0.804	-	-	-0.791	-0.394	-0.307
g03	20	1.0000	0.996	-	0.998	0.995	0.971
g20	24	0.205[§] 0.057[‡]	-	-	0.0579	0.0575	0.0573

[§] Optimum value reported by Liang et al. (2006).
[‡] Optimum value reported by Himmelblau (1972).

Table 5.5: Number of objective function evaluations and iterations (in [ ]) for problems of large dimensions ($n > 6$).

Function	n	**FTMA**	**FTMAS**	**MFTMS**	**MFTMS-PSO**	
					Best	Worst
g09	7	1916 [1194]	2450 [1552]	862 [558]	701 [446]	2141 [1415]
g10	8	-	2878 [1787]	794 [372]	755 [374]	704 [292]
g18	9	-	-	599 [320]	573 [324]	835 [467]
g07	10	-	2515 [1722]	2419 [1722]	2398 [1679]	2356 [1679]
g14	10	-	-	345 [130]	3815 [1521]	415 [162]
g01	13	-	-	2411 [1762]	1237 [896]	1116 [789]
g19	15	-	-	1989 [1370]	2447 [1766]	2686 [1955]
g02	20	-	-	2324 [1488]	2020 [1662]	2526 [1911]
g03	20	2976 [1718]	-	2469 [1757]	2534 [1679]	2550 [1679]
g20	24	-	-	2052 [1304]	1888 [1004]	1930 [1113]

It has been reported previously that the use of adaptive parameters in the Nelder-Mead method can outperform the standard implementation for high dimensional problems (Gao and Han, 2012). Nonetheless, in the present case the combination of adaptive parameters with flexible tolerance did not prove to be efficient, although reasonable results were obtained in a few cases (such as g09).

This set of functions was evaluated in CEC2006 using different evolutionary algorithms as evolution strategies, evolutionary programming, differential evolution, particle swarm optimization and genetic algorithms (Liang and Suganthan, 2006). The advantage of MFTMS in comparison with the stochastic method is the possibility of prediction of all steps knowing the start point, that is, it always takes up the same response from the same starting point. Since using the MFTMS is unnecessary perform various runs and choice algorithm parameters that can change for a specific problem. Furthermore, the number of objective function evaluation was smaller that values reported (Liang and Suganthan, 2006), which was set in 5,000, 50,000 and 500,000 evaluations.

However, the use of stochastic method PSO together with MFTMS proved to be an efficient strategy in problems that present many local optima or even when the starting point used do not reach convergence. This hybrid method can also corroborate to find global optima in nonlinear constrained optimization, which the global optimum can not be guaranteed (Smith, 2005).

5.3.3 Mass integration problems

FTM was applied by Lima et al. (2013) and in Chapter 3 to solve mass integration problems. According to the authors the method presented some difficulties during the search process. Some of these difficulties were regarding to the unable capacity in reach the optimal process configuration from the current process situation, probably due the current process situation be a local optimal point. In this chapter three problems of mass integration was solved using the MFTMS code proposed in this chapter, and FTMS-PSO reported previously.

Mass integration problems are typically complex problems since the optimization needs consider a large number of equality constraints, and the variables generally has different range (as composition, temperature, pressure and others) of variation that difficult the search process in the viable space. The equality constraints are related with mass and energy balance, process equations and thermodynamic. The inequality constraints refer to environment issues (the pollutant level needs be less than a certain value), technical (temperature, pressure and/or flow rate cannot exceed determined value), and thermodynamic (positive values of driving force in transport process of mass and energy). Thus, solve this type of problem using a direct algorithm as FTM with or without modifications is a challenge. The capacity of FTM deal with this problem was previously investigated (Lima et al., 2013). Based on the results some modifications (previously discussed) were proposed and tested in the group of problems of G-Suite. The code that present best performance in this chapter was MFTMS. The hybridized method MFTMS-PSO presented similar performance to the FTMS-PSO, however FTMS-PSO fits better to the optimum known, thus this method will be used to solve mass integration problems.

Since this type of problems were difficult to solve using the direct optimization method FTM, in this chapter, the problems were reformulated using the explicit substitution method. This strategy was used to diminishing the number of variables to be evaluated in the MFTMS and FTMS-PSO. Then, the polyhedron constructed during the search of optimum decreases and the algorithm becomes more efficient.

5.3.3.1 Problem 1 - Maximize the overall process yield

This problem deals with yield targeting in acetaldehyde production by ethanol oxidation ((Al-Otaibi and El-Halwagi, 2006), (Lima et al., 2013)). The process flowsheet are shown in Figure 5.4. The objective was to maximize the overall process yield (Y_P) without adding new process equipment, although process modification and direct recycle. Direct recycle was only allowed from the top of the third distillation column to the flash column. This mass integration problem present a superstructure source-sink (nonlinear programming) with process model in its constraints. The original formulation presents 31 variables, 23 equality constraints and 36 inequality constraints. The complete problem formulation is described in Al-Otaibi and El-Halwagi (2006). After applying explicit substitution method 21 variables were made explicit, and the resulting problem present 9 variables, 2 equality constraints and 19 inequality constraints.

In the previous work (Lima et al., 2013) the FTM in its standard formulation demonstrated be able to found the optima (not starting the search from the current process point). However, using MFTMS the optimum point was reach starting the search at the current process configuration, despite the large number of objective function evaluations (2127) and 804 iterations.The optimum agree with the ones reported previously ((Al-Otaibi and El-Halwagi, 2006), (Lima et al., 2013)), however the operational parameters are different (see Figure 5.5 and Table 5.6).

The results found by FTMS-PSO showed a configuration that none ethanol is recycled to the flash, the process parameters are maintained and the increase in yield process is obtained

through manipulation of fresh ethanol fed to the flash (S1 stream).

These solutions obtained through direct optimization MFTMS method and the hybrid method FTMS-PSO may represent a local optimum.

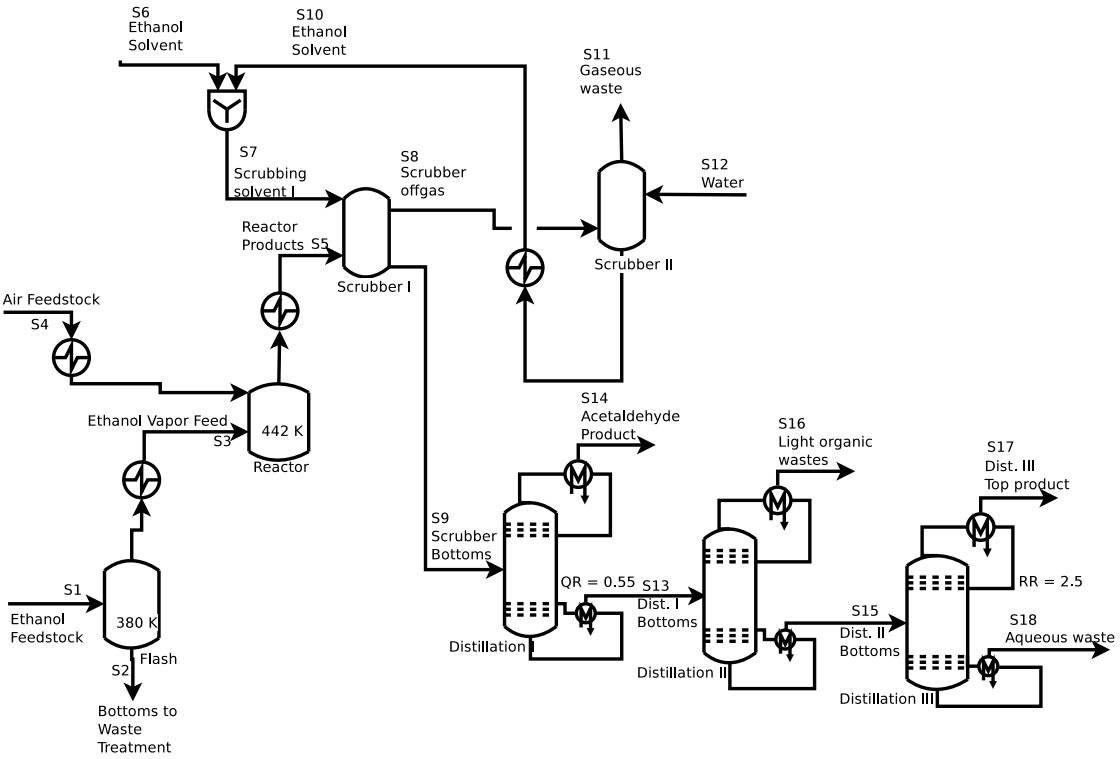

Figure 5.4: Flowsheet of acetaldehyde production by ethanol oxidation, Problem 1. From Lima et al., 2013.

The results founded by the different codes indicated that the yield process improvement can be achieve with different plant configurations. The optimized process flowsheet is shown in Figure 5.5, and the main optimized parameters are shown in Table 5.6.

Table 5.6: Main results for Problem 1. N_{it}: number of iterations, N_{eval}: number of objective function evaluations.

Variables	Current process	Optimized Process				
		Literature		MFTMS‡	FTMS-PSO	
		(Al-Otaibi and El-Halwagi, 2006)	† (Lima et al., 2013)		Best	Worst
Y_P (%)	23.70	95.50	95.48	95.50	95.50	95.50
$T_{reactor}$ (K)	442	580	580	531	442	442
T_{flash} (K)	380	383.7	383.65	383	380	380
Q_R	0.55	0.76	0.76	0.66	0.55	0.55
R_R	2.5	5.0	5.0	4.96	2.5	2.5
$Ethanol_{recycled}$ (ton/y)	0	199,367	199,367	6,533	-	-
N_{eval}	-	-	21	2127	141	2422
N_{it}	-	-	3	804	34	1315

† The search do not started from the current process.

‡ The search started from the current process.

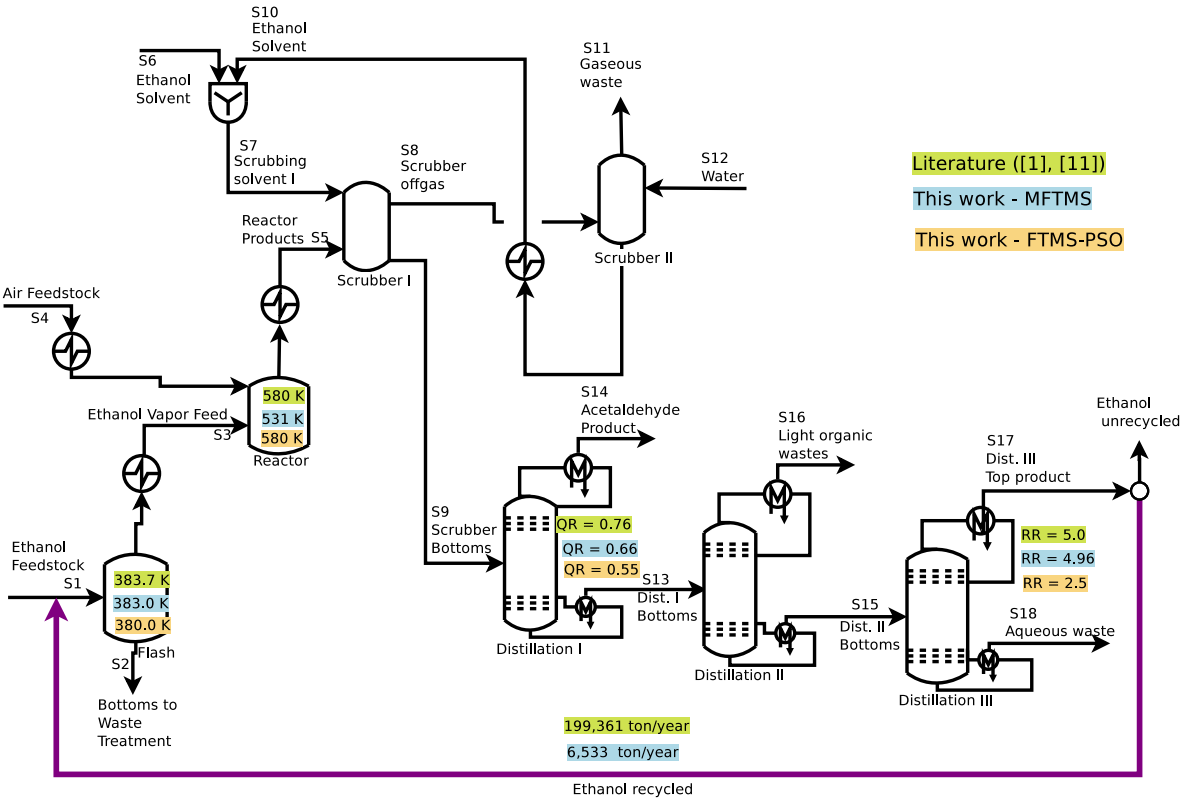

Figure 5.5: Optimized process flowsheet of acetaldehyde production by ethanol oxidation, Problem 1.

5.3.3.2 Problem 2 - Minimization of the total load of a toxic pollutant discharged into terminal plant wastewater

This problem deals with minimization of the total load of a toxic pollutant discharged into terminal plant wastewater, using segregation, mixing and recycle strategies. The process refers to the production of ethyl chloride by catalytic reaction between ethanol and hydrochloric acid El-Halwagi, 1997. The process diagram is indicated in Figure 5.6. The optimization problem in this process model includes source-sink representation (Figure 5.7) to allow consideration of segregation, mixing, and direct recycle strategies, and the material balance of water and chloroethanol. A detailed description of process can be found in El-Halwagi (1997).

The original problem formulation present 30 variables, 19 equality constraints and 32 inequality constraints. After explicit 16 variables, the problem has 14 variables, 3 equality constraints and 22 inequality constraints. The main parameters optimized are showed in Table 5.7.

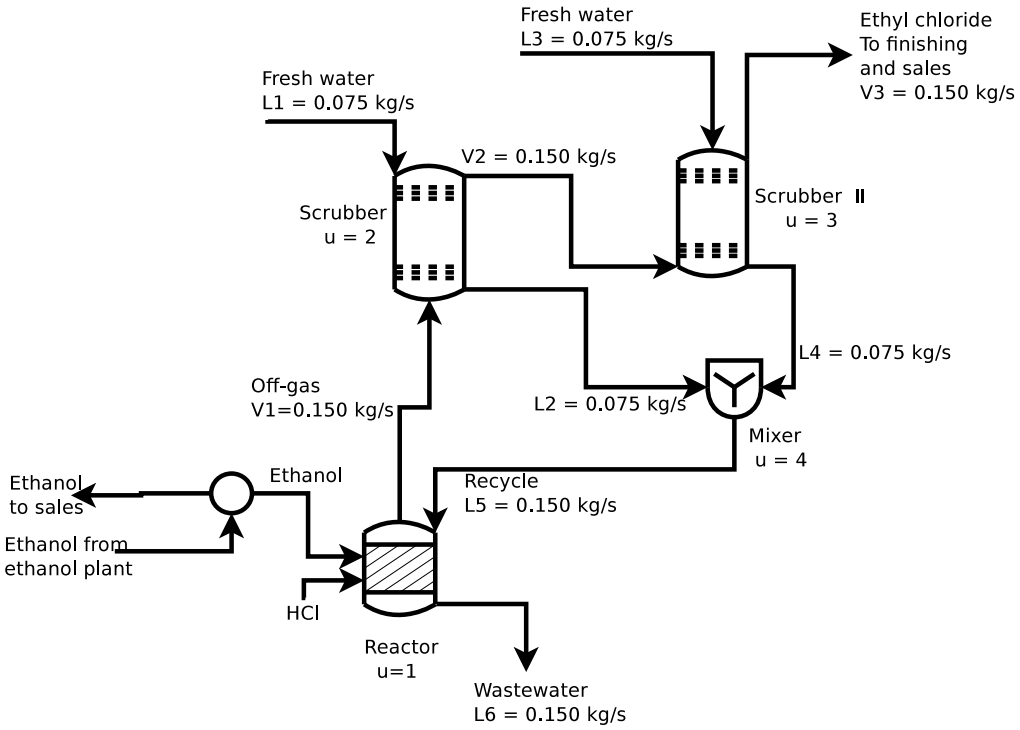

Figure 5.6: Flowsheet of the production of ethyl chloride, Problem 2. Adapted from Lima et al. (2013).

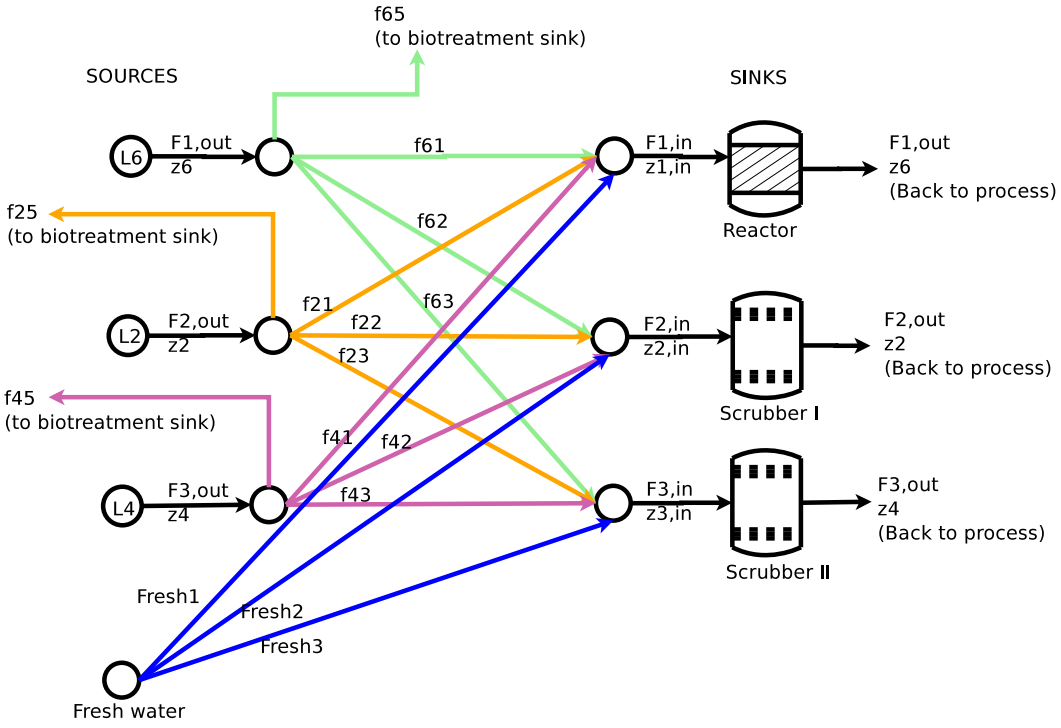

Figure 5.7: Source-sink representation of Problem 2. Adapted from Lima et al. (2013).

Table 5.7: Main results for Problem 2. N_{it}: number of iterations, N_{eval}: number of objective function evaluations.

Variables	Current process	Optimized Process				
		Literature		MFTMS‡	FTMS-PSO	
		(Al-Otaibi and El-Halwagi, 2006)	† (Lima et al., 2013)		Best	Worst
$Total_{load}$ (kg/s)	1.5	0.488	0.475	0.487	0.487	0.486
$L3$ (kg/s)	0.075	0.075	0.075	0.075	0.075	0.075
$f21$ (kg/s)	0.075	0.09	0.09	0.09	0.09	0.09
$f62$ (kg/s)	0.0	0.09	0.089	0.09	0.09	0.09
$f45$ (kg/s)	0.0	0.075	0.073	0.075	0.075	0.075
N_{eval}	-	-	2994	36371	11486	22717
N_{it}	-	-	1506	1506	842	1506

† The search do not started from the current process.

‡ The search started from the current process.

As mentioned for the Problem 1, the use of FTM in this case also was not able to reach the optimum from the current process situation as reported by Lima et al. (2013). Despite the large number of objective function evaluations, applying MFTMS and FTMS-PSO the optimum point was found and agree with the one reported (El-Halwagi, 1997), and leave to the configuration of optimized process shown in Figure 5.11, the main variables values are shown in Table 5.7. The results shown in this chapter differ from the results found in a previously work (Lima et al., 2013) for this problem using FTM without modifications (when the solution could be prone to a local optima).

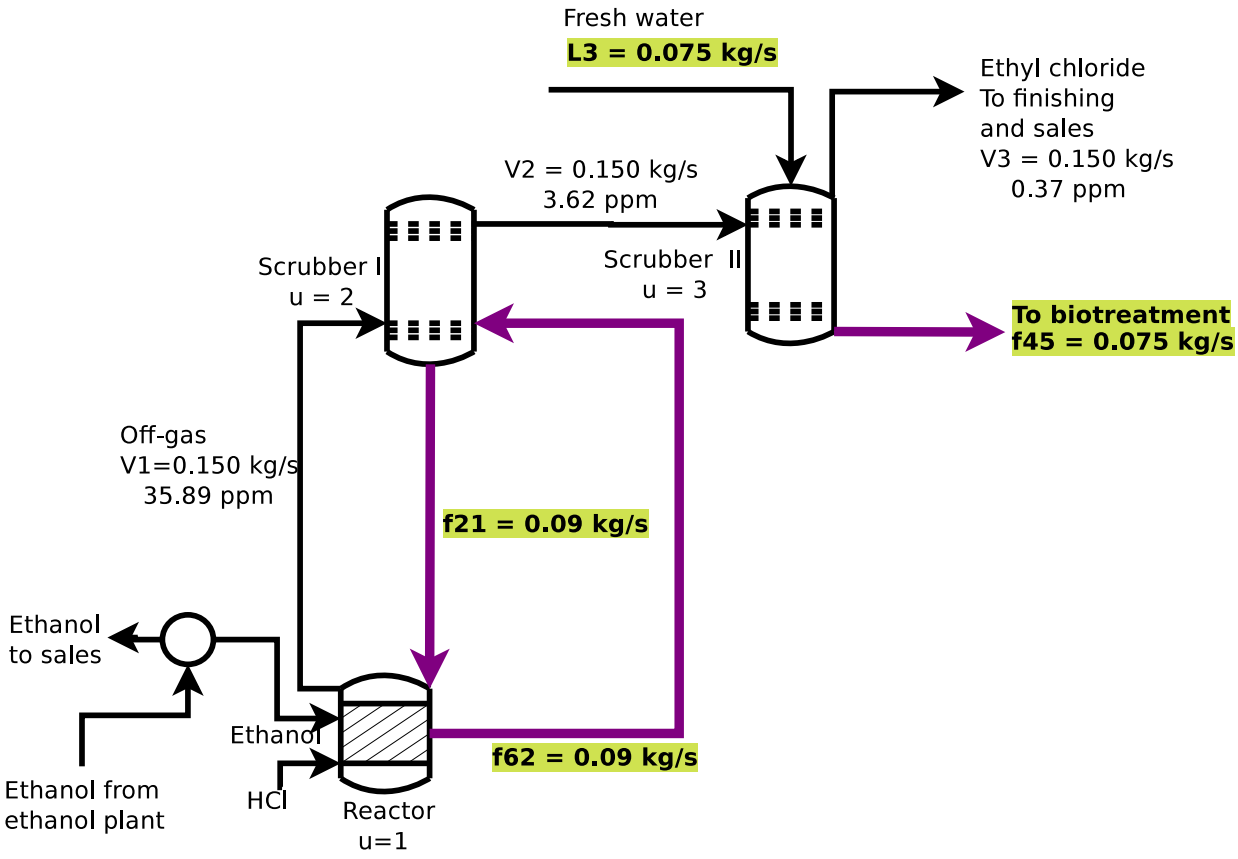

Figure 5.8: Optimized process flowsheet of the production of ethyl chloride, Problem 2.

5.3.3.3 Problem 3 - Production of phenol from cumene hydroperoxide

The objective of this problem is determining the targets for minimum consumption of freshwater, minimum wastewater discharge and minimum operational cost (including freshwater and piping cost). The complete process description can be found in Hortua (2007). The process flowsheet and the source-sink representation are shown in the Figures 5.6 and 5.10, respectively.

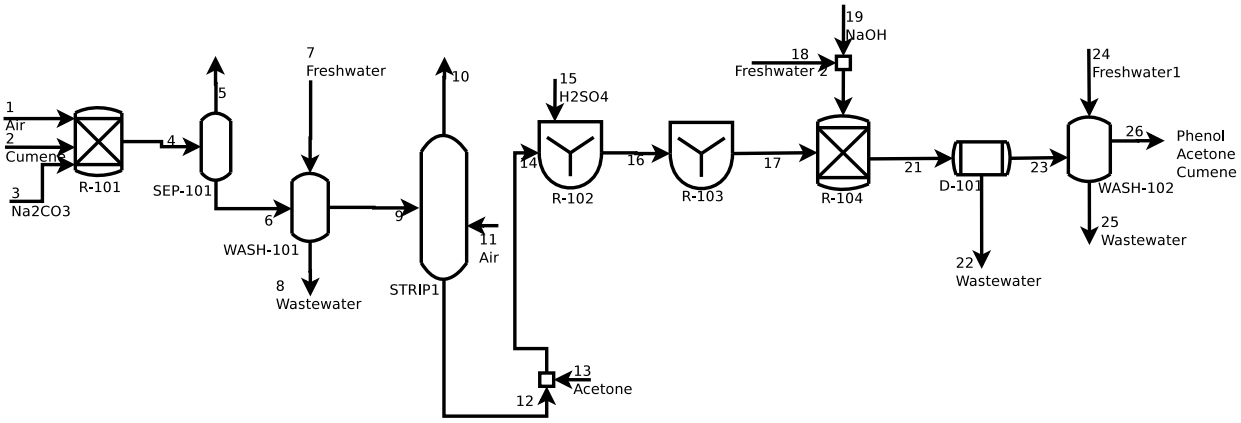

Figure 5.9: Flowsheet of the production of phenol from cumene hydroperoxide, Problem 3. Adapted from Hortua (2007).

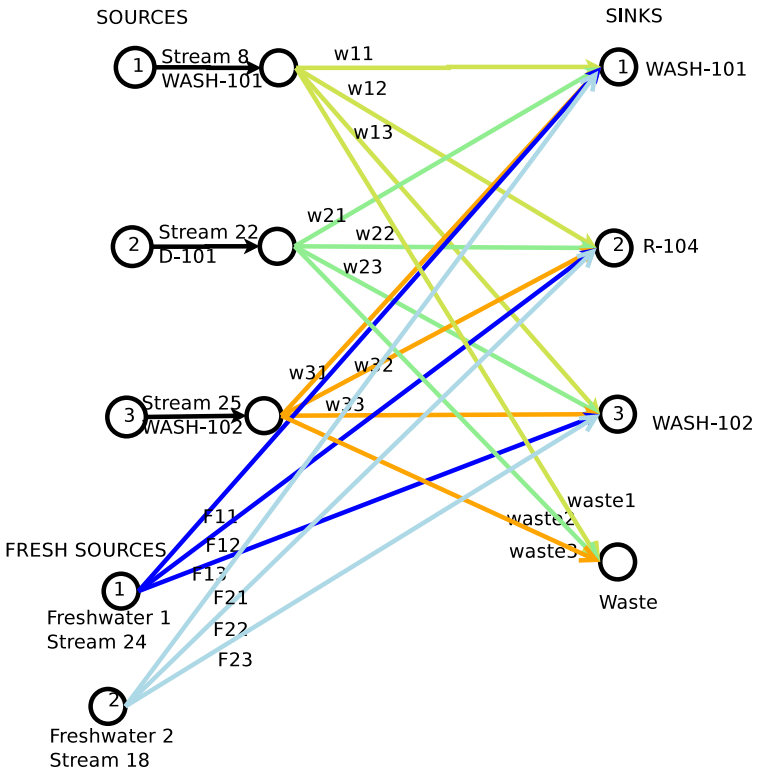

Figure 5.10: Source-sink representation of Problem 3.

Table 5.8: Main results for Problem 3. N_{it}: number of iterations, N_{eval}: number of objective function evaluations.

Variables	Current process	Optimized Process			
		Literature (Hortua, 2007)	MFTMS‡	FTMS-PSO	
				Best	Worst
$Total_{cost}$ ($/y)	-	41,815.89	41,815.9	41,815.9	41,815.7
$Freshwater_{consumption}$ (lb/h)	6,890.0	4,595.0	4,595.0	4,595.0	4,595.0
$Waste_{discharge}$ (lb/h)	15,263.5	6,969.28	6,969.28	6,969.28	6,969.28
N_{eval}	-	-	329	443	2991
N_{it}	-	-	150	222	990

‡ The search started from the current process.

The original problem formulation has 27 variables, 14 equality constraints and 30 inequality constraints. After explicit 13 variables, the problem has 14 variables, 1 equality constraint and 19 inequality constraints. From the current process configuration, the MFTMS and FTMS-PSO reach the optimum configuration considering mass integration issues (Table 5.8). The total cost found was 41815.91 $/year, with the minimum consumption of freshwater of 4595.0 lb/hr and a minimum target for waste discharge of 6969.32 lb/h, this values agree with the reported by Hortua (2007). The process flowsheet optimized with the recycle is shown in Figure 5.11.

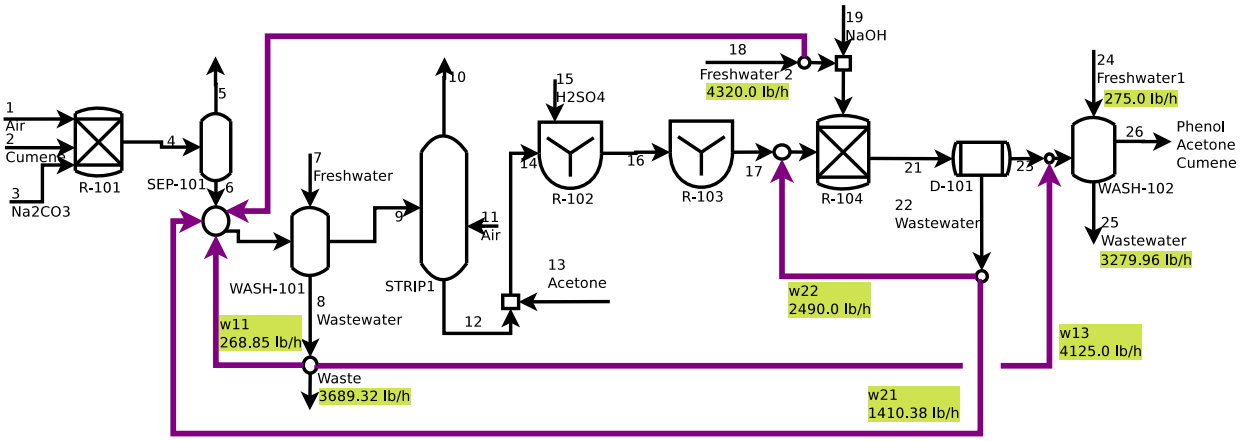

Figure 5.11: Optimized process flowsheet of the production of phenol from cumene hydroperoxide, Problem 3.

5.4 Conclusions

This chapter proposes the use of adaptive parameters in the flexible tolerance method (FTMA) and in the FTMS previously reported (FTMAS). An improvement to the FTMS was also proposed, the inclusion of a barrier to avoid the escape of polyhedron of the search region bounded by the upper and lower limits of the variables.

The numerical results demonstrated that MFTMS outperformed the standard FTMS for all the test functions investigated. Use of the Nelder-Mead algorithm with adaptive parameters was not an efficient strategy, although reasonable convergences could be achieved in some cases, notably for small dimensional problems.

The hybridization of the MFTMS with PSO (MFTMS-PSO) during initialization do not brought advantages in comparison with the FTMS-PSO previously reported.

The barrier strategy applied in the MFTMS also proved to be efficient, mainly in the mass integration problems. Since a good range of variables are known in most real cases, this strategy prevents the flexible polyhedron from experiencing serious deformation during the minimization procedure. The success rate of MFTMS was 100%, while MFTMS-PSO achieved 85%,

FTMAS 40%, and FTMA 30%. This demonstrates the improvement achieved using barrier in FTMS. The same strategy could be used in other optimization methods where the different amplitudes of variables make it hard to converge to an optimum.

The application of MFTMS in problems of mass integration was efficient to reach the optimum. Since from the current process situation, that often it is a local optimum, the code was able to found the global optimum, that is, the optimal process configuration with integration mass issues satisfied.

This class of problems was also solved with FTMS-PSO, however the results obtained with the runs performed in this chapter induce the MFTMS to be stuck in a region of local optima, as observed in Problem 1. The other two problems, the FTMS-PSO presented better performance, due ability to find the optimal configuration in a reasonable number of iterations and objective function evaluations.

The results found in this chapter brings an important conclusion because complex problems (as mass integration), usually solved with indirect methods, could be solved with a simple direct method improved, the MFTMS, and with an hybrid method, FTMS-PSO. Thus, problems that usually requires a large preparation time, with derivatives calculus, can be easily and quickly solved without gradient calculations.

For the solution of mass integration problems, the MFTMS and FTMS-PSO showed good performance. The MFTMS was able to find the optimum configuration of plant reported in literature in two of the three cases studied, starting the search in the current process configuration. The FMTS-PSO also could find the optima in this two cases.

Due the goods results obtained using MFTMS and FTMS-PSO optimization codes in mass integration problems, these codes will be used in the next chapter to solve an inedited problem of mass integration, that include an sugarcane biorefinery integration that comprises 1G, 2G and 3G.

CHAPTER 6

Mass Integration of 1G, 2G and 3G Sugarcane Biorefinery

6.1 Introduction

Biorefinery is a facility that integrates biomass conversion processes and equipment to produce fuels, power, heat, and value-added chemicals from biomass. Inside this concept the sugarcane factories in Brazil are actually biorefineries, since sugar, ethanol and energy are produced. Due environmental, economical issues and demand increase many efforts are employed in researches in the sugarcane production chain to improve the efficiency, reduce environmental impact and water consumption, produce other products and include celullosic material in the process.

The objective of this chapter is apply the Modified Flexible Tolerance Method (MFTMS) and Hybrid Flexible Tolerance Scaled Method (FTMS-PSO), described in the previous chapters, together with mass integration methodology in a sugarcane biorefinery. The targets are water captation reduction, vinasse volume reduction and CO_2 recovery. These targets agree with the initiatives as Clean Development Mechanism (CDM) defined in the Kyoto Protocol.

6.2 Methodology

The process adopted in this study case was proposed by Furlan et al. (2012) and Furlan et al. (2013). The authors used EMSO software (Environment for Modeling, Simulation and Optimization) to perform the simulations. The first generation (1G) plant simulated includes cleaning, milling, physical and chemical treatment, concentration, fermentation, distillation and cogeneration. The second generation (2G) plant includes pretreated using the weak acid pre-treatment, enzymatic hydrolysis and fermentation of the resulting sugars. The Figure 6.1 shows the process flowsheet of the sugarcane biorefinery.

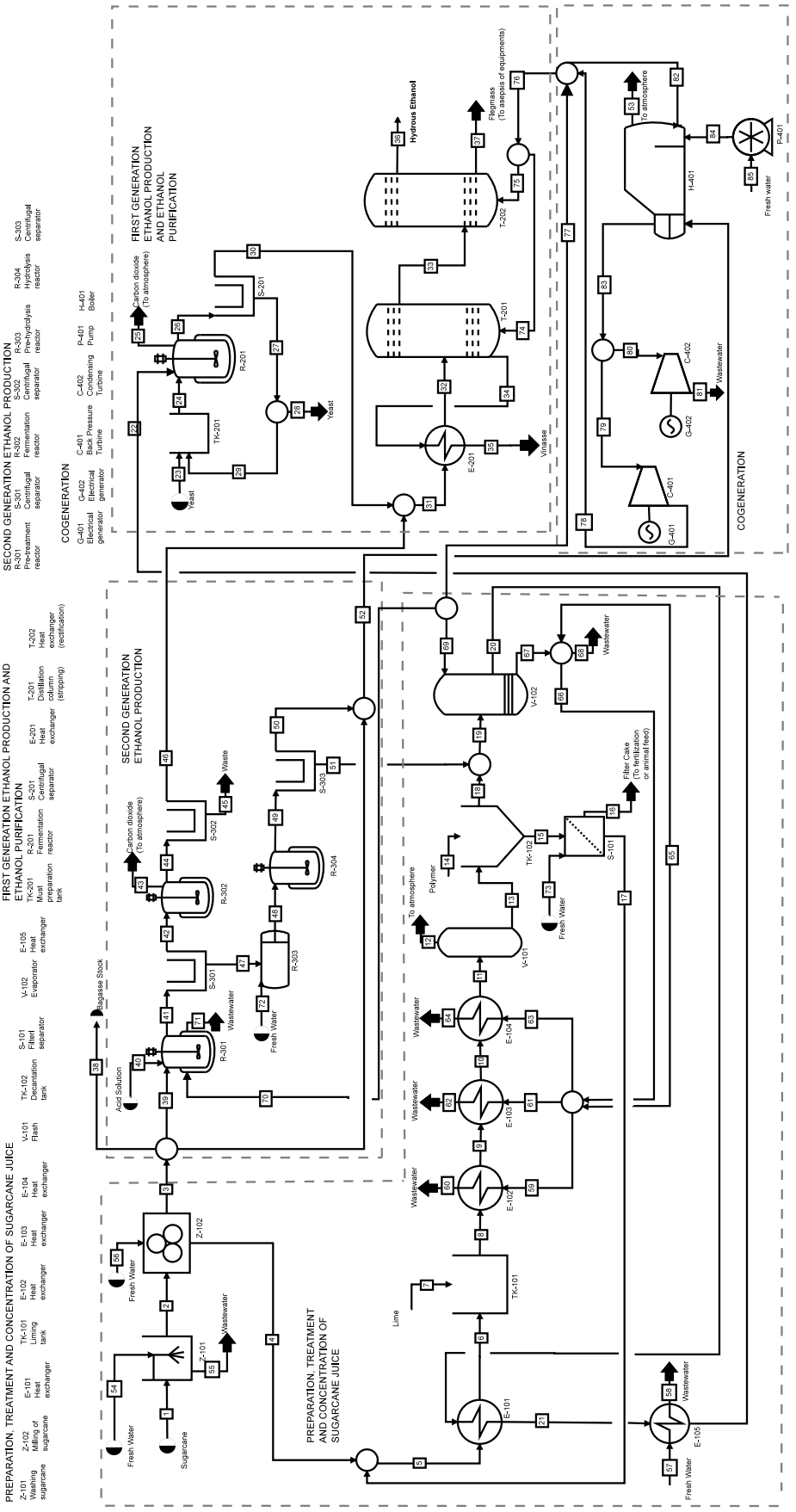

Figure 6.1: Process flowsheet of the sugarcane biorefinery. Adapted from Furlan et al. (2013).

According to Furlan et al. (2013) the biorefinery was modeled for a sugarcane input of 500 metric ton of cane per hour, and the composition of dry sugarcane bagasse is considered to be 39% in mass of cellulose, 37% of hemicelluloses, 21% of lignin and 3% of ash. The models involved in the biorefinery were mostly stoichiometric, except when a rigorous model was essential (Furlan et al., 2013).

In the first section, the sugarcane is cleaned (Z-101) with water to remove dirt carried during harvesting. Next, the sugars are extracted by mechanical pressure (Z-102). The solution containing the extracted sucrose (juice) follows to treatment to liming tank (TK-101), heating (E-102, E-103 and E-104) and pass by a flash tank to remove volatiles (V-101). Then, the juice goes to decanter (TK-102), the clarified juice follows to evaporators series (represented by V-102) in order to remove impurities which could decrease fermentation yields. The solution is concentrated and fermented by *Saccharomyces cerevisiae* (R-201), producing an alcoholic solution which is purified in distillation columns (T-201 and T-202), producing hydrous ethanol.

Second generation (2G) ethanol was produced via the biochemical route, using weak acid pretreatment and enzymatic hydrolysis. First, bagasse is pretreated (R-301) with a solution of H_2SO_4 (3 wt% at 120°Cand 2 bar of pressure). At this point, most hemicellulose is hydrolyzed, increasing cellulose accessibility. A filter (S-301) is used to separate the solid fraction from the liquid. The solid fraction is pre-hydrolyzed in a horizontal reactor (R-303), in order to decrease mixing power demands and water usage. The second hydrolysis is carried out in a stirred reactor (R-304) without any further addition of water or enzymes. The solid fraction (non-hydrolyzed cellulose + lignin) is separated from the glucose solution in a filter (S-303) and sent to the boiler to increase steam production. On the other hand, the liquid fraction is directed to the concentration step, being mixed to the 1G juice. The liquid fraction from S-301 is sent to a reactor (R-302), where the xylose in the solution is transformed to xylulose and fermented by *Saccharomices cerevisiae*. The resulting alcoholic solution is sent to the distillation columns (T-201 and T-202) with the wine from hexose fermentation.

The cogeneration system uses sugarcane bagasse, sugarcane trash, and alternatively, non-hydrolyzed cellulose and lignin, as fuel and produces steam and electric energy to supply process demands using a Rankine cicle. The cogeneration system includes a boiler (H-401), a back-pressure turbine (C-401), a condensing turbine (C-402) and a pump (P-401).

The process simulated adopted in this work (from Furlan et al. (2013)) contain some simplifications compared to a real process operation: (i) the water cycle is not completely included, then the water consumption per cane tonne processed is larger than values practiced in industries nowadays[1]; (ii) the models were most stoichiometric and (iii) the cogeneration plant does not simulates the generation of gases from combustion process.

[1] According to the process simulated by Furlan et al. (2013), the water consumption is 4.21 m^3_{water}/t_{cane}. This value correspond to the water captation practiced around the year 1995. Nowadays the water captation is less than 1.85 m^3_{water}/t_{cane}. The evolution of water captation and use in sugarcane industries are detailed in Elia Neto (2013).

6.2.1 Targeting and generation of alternatives

In this case study, the water, the carbon dioxide produced in the fermentation and combustion and the vinasse are the targets for process integration. The process was described as a source-interception-sink, where the interception device was discretized, as proposed by Gabriel and El-Halwagi (2005). According to the process description and Figure 6.1, the process units, process streams, fresh resources and interception devices of interest for this case study are summarized as follows. Figure 6.2 shows the summary of targets and alternatives chosen in this study case.

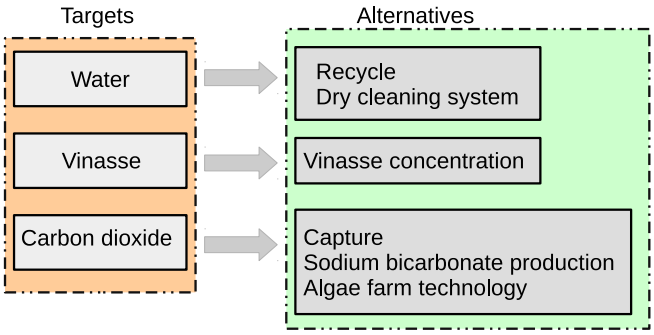

Figure 6.2: Summary of targets and alternatives for mass integration of sugarcane biorefinery.

1. Water

   - Process sources:
     - Stream 12 from V-101
     - Stream 55 from Z-101
     - Stream 58 from E-105
     - Stream 60 from E-102
     - Stream 62 from E-103
     - Stream 64 from E-104
     - Stream 68 from V-102
     - Stream 71 from R-301
     - Water from vinasse concentration plant

   - Process sinks:
     - Z-101 (Washing sugarcane)
     - Z-102 (Milling of sugarcane)
     - S-101 (Filter separator)
     - E-105 (Heat exchanger)
     - R-303 (Pre-hydrolysis reactor)
     - P-401 (Pump)

  - Wastewater treatment

2. Vinasse

   - Process sources:
     - Stream 35 from E-201
   - Interception process:
     - Evaporation plant with 5 effects
   - Process sinks:
     - Vinasse *in natura* for fertirrigation
     - Vinasse concentrated for fertirrigation
     - Water (return to water sinks)

3. Carbon dioxide (CO_2)

   - Process sources:
     - Stream 25 from R-201
     - Stream 43 from R-302
     - Stream 52 from H-401
   - Interception process:
     - CO_2 capture and compression
     - Sodium bicarbonate ($NaHCO_3$) production through soda method
     - Biodiesel and algae protein production through algae farm
     - Ethanol production through algae farm
   - Process sinks:
     - Compressed CO_2
     - $NaHCO_3$
     - Biodiesel and algae protein
     - Ethanol

The process and interception devices listed above are described in the sequence. The objective in this case study is minimize the costs associated with freshwater, wastewater treatment, fertirrigation using vinasse, interception device of vinasse, interception device for carbon dioxide recovery and maximize the profit with the products obtained from process of carbon dioxide recovery.

Two cases were evaluated for the sugarcane biorefinery. The first case (Case I) include as targets conventional sugarcane cleaning, CO_2 from fermentation process and vinasse concentration with evaporation. The second case (Case II) include as targets dry clean system for sugarcane, CO_2 from fermentation process and bagasse/residues from second generation processing combustion, and vinasse concentration with evaporation. These two cases were optimized using MFTMS and the hybrid algorithm FTMS-PSO.

6.2.2 Water recycle

The water network is composed by direct recycle, since the streams considered in the analysis is composed by water without impurities. The source-sink superstructure developed for water reuse is similar to the superstructure shown in the Figure 2.10. Additionally the unrecycled process sources are fed to the waste treatment system. The possibilities of water recycle to an equipment was determined based in the temperatures generally employed in sugarcane factories, as shown in Table 6.1.

For Case I, the problem has eight sources (including the water available from vinasse concentration) and six process sinks.

For Case II, the cleaning system of sugarcane adopted was a dry clean system. Then, the problem has seven sources and five sinks, since was eliminated the source and sink related to conventional clean system of sugarcane. The dry clean system has many advantages comparing with conventional system that employ water for the cleaning task. Regardless of rising in transportation costs, some of these advantages are: use of straw as fuel added to bagasse for electricity generation, reduced maintenance cost, increased efficiency of sugar recovery, increased milling capacity, increased potential for electricity generation, etc. The system used for economic estimation in this study case is based on data report by the companies Empral[1] and Embratec Zanini[2], reported in Empral (2010b) and Empral (2010a).

Most of industries that process sugarcane in Brazil do not are charged by water captation from hydrographic basins in its respective states. However, since 2011, some industries in São Paulo state started to be charged by water captation from three of the five hydrographic basins of the state. The tendency is apply this program in other regions. Then, the objective is diminishing the water captation as much as possible through technology improve, reuse and integration of water cycle.

[1] http://www.empral.com.br/jaboticabal/
[2] http://www.sermatec.com.br/

Table 6.1: Description of sinks and sources for water recycle.

	Sink	Sources possibles
Wastewater Treatment	It receives water from process at various temperatures and with impurities and perform the treatment. After the treatment the water return to process.	S-12, S-55, S-58, S-60, S-62, S-64, S-68, S-71, S-81
Z-101	Washing sugarcane - It operates around 30 °Cin the current process, however higher temperatures (up to 50 °C) can be employed.	Fresh water, Water from vinasse
E-105	Heat exchanger - It decreases the temperature of juice come from treatment to enter the fermentation process. Due temperature requirements, the sources available can not be used.	Fresh water
R-303	Pre-hydrolysis reactor - Water input for hydrolysis process, the temperature can vary from 30 to 50 °C.	Fresh water, Water from vinasse, S-58, S-81
Z-102	Milling of sugarcane - Water input in milling help to extract the juice from sugarcane, at current process the water temperature is 50 °C, but can vary from 30 to 50 °C	Fresh water, Water from vinasse, S-58, S-81
S-101	Filter separator - In the current process operates around 60 °C, but can be feed with water at other temperatures, from 40°Cup to approximately 100°C.	Fresh water, S-58, S-81, S-60, S-62
P-401	Pump - The water is pumped to boiler (H-401), the temperatures can be up to 110 °C.	Fresh water, S-12, S-60, S-62, S-64, S-68, S-71

6.2.3 Vinasse network

The vinasse is a liquid derived from wine distillation, that is result from juice sugarcane fermentation. For each liter of ethanol produced is generated from 7 to 14 liters of vinasse, a residue highly polluting. In the past (40 and 50 years) the quantity of vinasse produced were low and its disposition was done at water bodies and areas of sacrifice, but there were concerns about it in environmental agencies and in the scientific community (Corazza, 2001 *apud* Carvalho, 2010).

There are many alternatives for vinasse treatment and reuse, as stabilization ponds, biological filters (aerobic and anaerobic digestion), physical-chemical treatment, protein production, fertirrigation with *in natura* vinasse, recycling, use as animal feed supplement, cellular protein

production, concentration and combustion, methane production, and energy production.

According to Paoliello (2006), the experiments with physical-chemical treatment have been shown little success. The sedimentation even with the addition of coagulants and other additives such as alum, lime, ferric chloride, has been shown to be unsatisfactory. Furthermore, the sediment enters in anaerobic fermentation and produces odors. Studies using reverse osmosis, electrofloculation, electrodialysis, electroosmosis, were also performed, but with costs extremely high and degree of treatment limited.

The use of vinasse in powder to complement animal fed were also evaluated, in proportions of 10% for ruminants diet and in minor proportion for poultry and pigs. Some studies demonstrates the increase in milk production, although it has, in contrast, laxative effect in cattle. The vinasse has also been used in studies for the production of biomass of high protein level for human and animal consumption (food). The cell protein is obtained in an aerobic fermenter for propagation of microorganism (*Torulopsis utilis* or *Candida utilis*) in the substrate, that is vinasse. However, the process needs improvements, especially in design of fermenters, where the mass transfer of oxygen is essential to have success (Paoliello, 2006).

The anaerobic digestion can reduces the pollution potential of vinasse and simultaneously producing a biogas (composed basically by CH_4, CO_2, O_2, N_2, H_2O and H_2S) and a fertilizer as waste (Salomon (2007), Pompermayer and Paula Junior (2000)). The biogas is produced through an anaerobic fermentation, involving several stages (Paoliello, 2006). According to Granato and Silva (2002), the vinasse biodigestion reduces its organic pollutant load and produces a fuel competitive with fossil fuel, beyond be an economically viable alternative and beneficial to the environment. Despite efforts, there are technological, economic and political barriers related to use of biogas, and this alternative may become interested in Brazil in the coming years.

The vinasse combustion is a technology that allows final disposal and elimination of pollution potential of vinasse. The incineration of vinasse concentrated between 60 and 70°brix must be held in special burners, it is produced potassic ashes for fertilizer use, and vapor to the process or for electricity generation (Rocha, 2009). Actually there is no vinasse combustion plant in operation.

The vinasse is largely employed as fertilized due its constitution of salts (mainly potassium, calcium and magnesium) and organic matter, presenting also high values of BOD (biochemical oxygen demand) and COD (chemical oxygen demand).

In this study case was considered send vinasse to fertirrigation, that is a common practice in sugarcane factories in Brazil. The vinasse concentration is usually made using evaporation with multiple effects. The falling film evaporator have been shown the best results for vinasse concentration (Rocha, 2009). The number of effects may vary from 4 to 7, but generally is used 4 or 5 effects (Freire and Cortez, 2000 *apud* Rocha, 2009).

According to Rocha (2007 *apud* Carvalho, 2010) there are a economic radius in function of vinasse brix where the vinasse application has lower costs comparing to fertilizer application.

The author observed that from 25-30% of brix, the economic radius does not increase because from this value the volume of concentrated vinasse does not decrease significantly. This means that concentrate the vinasse beyond 25-30% of brix does not result in a growing economy transportation through trucks.

In this study was adopted an evaporation plant with 5 effects and the falling film evaporator for all effects. The vinasse concentration was fixed at 25% of brix and the total pressure drop was 1.2 bar. The initial vinasse brix was 4.5%, and the mass flow was 554,460.00 kg/h (stream 35 from E-201, Figure 6.1). The Figure 6.3 shows the flowsheet of the evaporation system adopted.

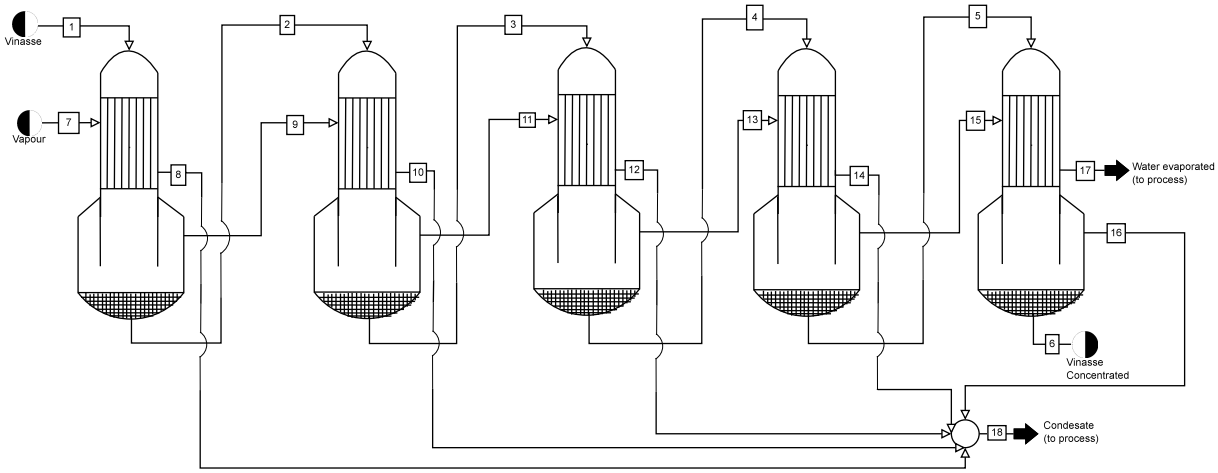

Figure 6.3: Process flowsheet of vinasse concentration with multiple effect evaporation.

The outlet pressure (P_n) of each effect was determined as indicated in the eq. 6.1 as reported by Castro and Andrade, 2007, where N is the total number of effects, P_0 and P_f is the initial and final pressure.

$$P_n = P_{n-1} - (P_0 - P_f)\frac{11 - (n-1).\frac{11-9}{N-1}}{10.N} \tag{6.1}$$

The boiling point elevation (BPE) in °C was calculated according eq. 6.2, where $x_{brix,out}$ is the mass fraction of brix at outlet of the evaporation effect, Araujo (2007).

$$BPE = \frac{2.x_{brix,out}}{1 - x_{brix,out}} \tag{6.2}$$

The overall heat transfer coefficient (U) in kJ/hm^2K was determined as shows eq. 6.3 (Rein, 2007), where T_s is temperature in °C of the heating steam in the calandria, H_{P_n} the steam enthalpy at evaporator pressure and k the Dessin coefficient. The evaporator area (A) of each effect was evaluated according to eq. 6.4, where $T_{s,n}$ is the heating steam temperature feed in the effect n and $T_{0,n}$ is the feed temperature of vinasse in the effect n.

$$U = k.(100 - x_{brix,out}).(T_s - 54).H_{P_n} \tag{6.3}$$

$$Q = U.A.(T_{s,in} - T_{0,n}) \tag{6.4}$$

The mass and temperatures along the effects of evaporation was determined with mass and energy balance, and the vapor properties was evaluated using steam tables. In order to minimize the costs with fertirrigation was analyzed different fractions of total vinasse mass send to concentration. These fractions ranged from 18%[1] to 100%, and for each vinasse mass was calculated the area of each effect. The costs of evaporation system was evaluated using the Capcost software (Turton, 1998) and other calculations was performed using electronic spreadsheets.

6.2.4 Carbon dioxide recovery

According to recent report of the Intergovernmental Panel on Climate Change (IPCC) titled "Climate Change 2014: Mitigation of Climate Change" (Edenhofer et al., 2014) the industry is responsible for 30% of greenhouse gas (GHG) emissions[2]. These emissions were dominated by CO_2 (85.1%), followed by methane (CH_4) (8.6%), hydrofluorocarbons (HFC) (3.5%), nitrous oxide (N_2O) (2.0%), perfluorocarbons (PFC) (0.5%) and sulphur hexafluoride (SF_6) (0.4%) emissions. The climate change mitigation[3] options in industry cited in the report include: energy efficiency (e.g., through furnace insulation, process coupling, or increased material recycling), emissions efficiency (e.g., from switching to non-fossil fuel electricity supply, or applying CCS (carbon dioxide capture and storage)to cement kilns), material efficiency in manufacturing (e.g., through reducing yield losses in blanking and stamping sheet metal or re-using old structural steel without melting) and product design (e.g., through extended product life, light-weight design, or de-materialization), product-service efficiency (e.g., through car sharing, or higher building occupancy); and service demand reduction (e.g., switching from private to public transport).

Inside the scenario of mitigation of GHG emissions, climate change, sustainable development and clean development mechanism (CDM[4]) the CO_2 emissions resulting of ethanol production from sugarcane need be avoided.

The carbon dioxide is generated during fermentation through the chemical reaction (eq. 6.5) and during combustion of bagasse and the residues from second generation processing, mainly formed by lignin and non hydrolyzed fibers , (eq. 6.6):

[1] This value was set due the minimum area allowed for falling film evaporators according to Turton (1998).

[2] These data refer to direct and indirect GHG emissions by source and gas in 2010.

[3] Mitigation is the effort to control the human sources of climate change and their cumulative impacts, notably the emission of greenhouse gases (GHGs) and other pollutants, such as black carbon particles, that also affect the planet's energy balance (Edenhofer et al., 2014).

[4] The Clean Development Mechanism (CDM) is one of the flexibility mechanisms defined in the Kyoto Protocol (IPCC, 2007) that provides for emissions reduction projects which generate Certified Emission Reduction units which may be traded in emissions trading schemes (Solomon et al., 2007).

$$C_6H_{12}O_6 \xrightarrow{Yeast} 2C_2H_5OH + 2CO_2 \tag{6.5}$$

$$C + O_2 \rightarrow CO_2 \tag{6.6}$$

The combustion gases were not evaluated in the simulated process used (Furlan et al. (2013)). Then, the CO_2 generation was evaluted based on composition of combustible stream (S-52) in the inlet of boiler (H-401) and in chemical reaction of carbon combustion (eq. 6.6).

Actually in Brazil, in most of ethanol sugarcane factories the carbon dioxide generated during the fermentation process is released directly to the atmosphere. According to results of an LCA (life cycle analysis) study of ethanol production reported by Muñoz et al. (2014), the GHG emissions of per kilogram bio-based ethanol in Brazil is about 1.5 kgCO_2eq, including emissions from degradation of ethanol at the end-of-life phase (ethanol emitted to air). Although the impact be less than fossil based ethanol, is necessary mitigate whenever possible the environmental impact.

In this study case was evaluated four alternatives to recover carbon dioxide produced during fermentation, that include biofuel from algae, that is known as third generation (3G) of fuel. These alternatives include: (i) carbon dioxide capture, (ii) sodium bicarbonate production, (iii) algae farm to ethanol production and (iv) algae farm to biodiesel and algae protein production. The carbon credits[1] resulting of CO_2 emissions avoid was also counted in the economic evaluation.

6.2.4.1 Dioxide carbon capture

CO_2 capture refers to the separation and entrapment of CO_2 from large stationary sources, and there are many capture technologies as solvent absorption, gas membrane separation, cryogenic methods, and pressure swing adsorption (Xu et al., 2010).

Compared to other CO_2 streams, the capture process from ethanol fermentation CO_2 is relatively simple and cost-effective, since CO_2 from an ethanol plant is highly-concentrated and nearly pure(Xu et al., 2010). Therefore, the only required purification processes are dehydration and compression, as shown in Figure 6.7. During dehydration (T-601), the residual moisture is removed from the gas in order to prevent corrosion in CO_2 pipelines. This is followed with compression (C-601) of the CO_2 gas to typical pipeline pressures. This process consist in one of the options analyzed in this study case.

[1] A carbon credit is a generic term for any tradable certificate or permit representing the right to emit one tonne of carbon dioxide or the mass of another greenhouse gas with a carbon dioxide equivalent (tCO_2eq) equivalent to one tonne of carbon dioxide.

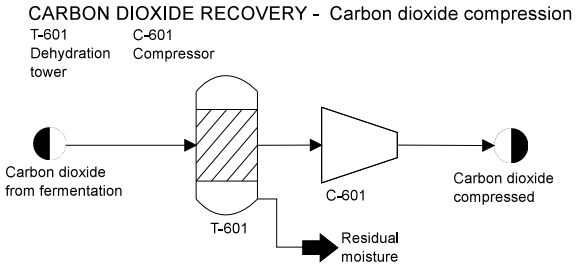

Figure 6.4: Process flowsheet of carbon dioxide compression.

Compressed CO_2 can be commercialized for several types of applications and uses, as beverage and food industries, plastic and rubber processing, water treatment, metal fabrication, chemical industry, among other. Some factories in Brazil are beginning invest in CO_2 recovery, as Grupo Toledo[1] from Alagoas state that are compressing and liquefying the CO_2 using the technology of Pentair[2] (Furtado, 2014).

6.2.4.2 Sodium bicarbonate production

Sodium bicarbonate ($NaHCO_3$) has a wide range of applications, among which may be cited: fire extinguisher (e. g., in chemical fire extinguishers), cooking (e. g., as a leavening agent), neutralization of acids and bases, medical uses (e. g., as an antacid), personal hygiene (e. g., teeth whitening), sports (e. g., as a supplement for athletes), cleaning agent (e. g., a solution in warm water will remove the tarnish from silver when the silver is in contact with a piece of aluminium foil), biopesticide (e. g., controlling fungus growth), and others. $NaHCO_3$ can be produced by many process, however in this study case will be considered the processes that use CO_2 as raw material. According to Cunha et al. (2009), two processes that use CO_2 as raw material can be highlighted, (i) "Soda method", that uses caustic soda as reagent (eq. 6.7) and (ii) "Carbonate method", that uses sodium carbonate as reagent (eq. 6.8). The impurities content in sodium carbonate (Na_2CO_3) is larger than impurities present in sodium hydroxide ($NaOH$), then sodium bicarbonate crystals from Carbonate process have lower quality, requiring larger operations for product purification (Cunha et al., 2009).

$$NaOH + CO_2 \rightarrow NaHCO_3 \tag{6.7}$$

$$Na_2CO_3 + CO_2 + H_2O \rightarrow 2NaHCO_3 \tag{6.8}$$

In this study case was used the Soda method and the simplified flowsheet[3] of the process is

[1] `http://www.grupotoledo.com.br/industrias/`

[2] `http://www.pentair.com.br/`

[3] This process flowsheet was built based on Cunha et al. (2009) description. Then some assumptions were done to obtain a PFD more intelligible, as the adoption of cooling water at 30 °C(*cw* at diagram) and reactor type.Cunha et al. (2009) analyzed three types of reactor: spherical reactor with magnetic mixing, pneumatic reactor with internal circulation type air-lift and PARR reactor. The PARR obtained the best result, with high purity of product

shown in Figure 6.5. The first step of the process is the dilution (TK-601) of *NaOH* until desired concentration to feed the reactor (R-601). The reaction step occur in batch mode, the process is exothermic than reactor refrigeration is necessary. The remainder of the process occur in continuous mode.Then, at the end of reaction when crystals were formed, the solution is sent to an intermediary storage tank (TK-603) to ensure uninterrupted feed in the centrifuge (S-601). The liquid from centrifuge is recycled to dilution tank (TK-601) and the solid with moisture is sent to dryer (T-601). The drying use atmospheric air previously heated. The outlet of dryer is sent to a cyclone separator (S-602) where the air is separated and sent to sleeve filter (S-603), where the fine particle is retained, and the clean air is emitted to atmosphere.

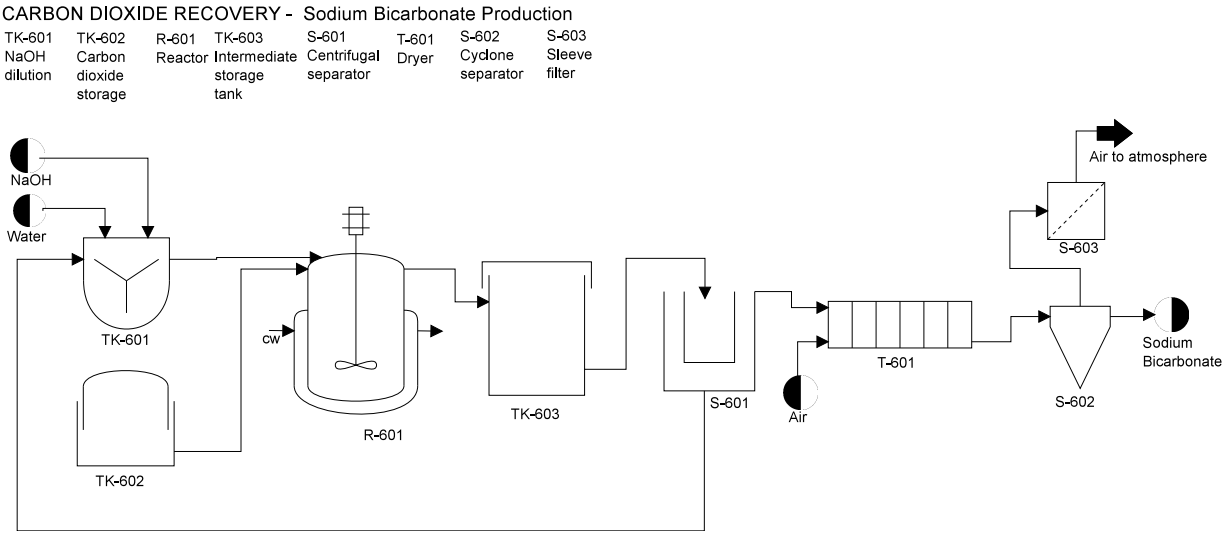

Figure 6.5: Process flowsheet of sodium bicarbonate production through soda method. Adapted from Cunha et al., 2009.

The process (Soda method) adopted in this study as one of the options to CO_2 recovery case was technical and economically evaluated by Cunha et al. (2009), and the findings will be used to economic estimation. In Brazil the production of sodium bicarbonate, and other inorganic salts using CO_2 from fermentation process is done by RAUDI Industry and Commerce Limited, using a process patented by the company (Pacheco and Silva, 2008; BeefPoint, 2009; JornalCana, 2007).

6.2.4.3 3G - Algae farm technology

The advantages of using microalgae CO_2 fixation includes rapid growth rates and high CO_2 fixation capabilities compared to conventional plants and high oil/carbohydrate production (Xu et al., 2010). Despite the benefits of algae productivity the problem was in scale-up the process at viable costs. Recently, the SEE ALGAE Technology (SAT)[1], an Austrian firm, presented a

and short reaction time for complete conversion.

[1] `http://www.seealgae.com/`

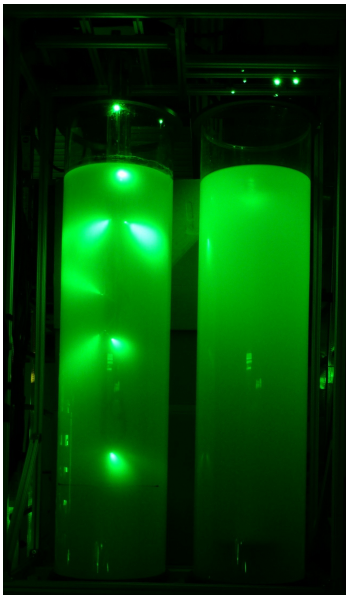

Figure 6.6: Prototype of photobioreactors (PBR) used by SAT. Source: See Algae Technology (SAT, 2012).

technology capable of produce ethanol, biodiesel and algae protein using algae, carbon dioxide (that can be captured from ethanol fermentation in the conventional process or from bagasse combustion, for example) and solar energy. The first algae-based biofuel industrial plant is currently under construction in Brazil, in the northeastern state of Pernambuco (Tyner, 2012). In SAT technology, a solar prism transfers sunlight to the reactors through optical fibers, and the algae growth is done in vertical reactors instead uncovered ponds (Figure 6.6).

For Case I, the mass fraction of CO_2 send to these processes need be larger than 25% of the total mass, because according to SAT (2012) the plant layout of 10 or more hectares is necessary to be economically attractive. The pre-synthesis of this work indicates that CO_2 fraction need be larger than 25% of the total mass available to obtain a algae farm with 10 hectares or more.

For Case II, since CO_2 mass available is large, the fraction of CO_2 send to these processes need be between 10% and 43%. The lower bound guarantee an algae farm with 10 hectare, and the upper bound guarantee an algae farm until 40 hectares. The upper bound was defined according to SAT (2012), since the algae SAT farm are available in easily scalable sizes up to 40 hectares.

The simplified process flowsheet for production of ethanol and biodiesel using algae farm technology from SAT are illustrated in Figures 6.7 and 6.8, respectively.

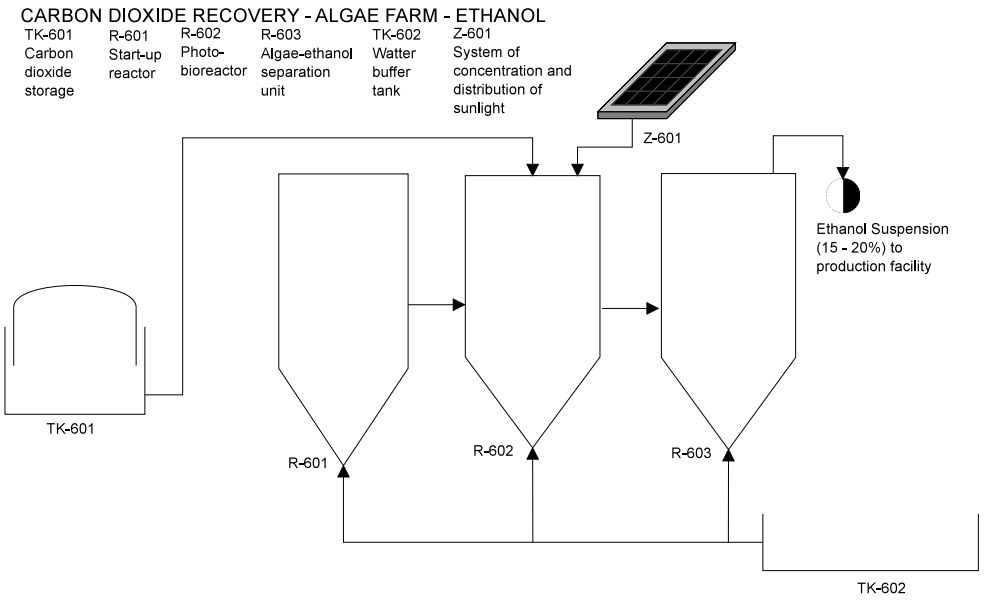

Figure 6.7: Process flowsheet of ethanol production using algae farm technology from SAT. Adapted from SAT (2012).

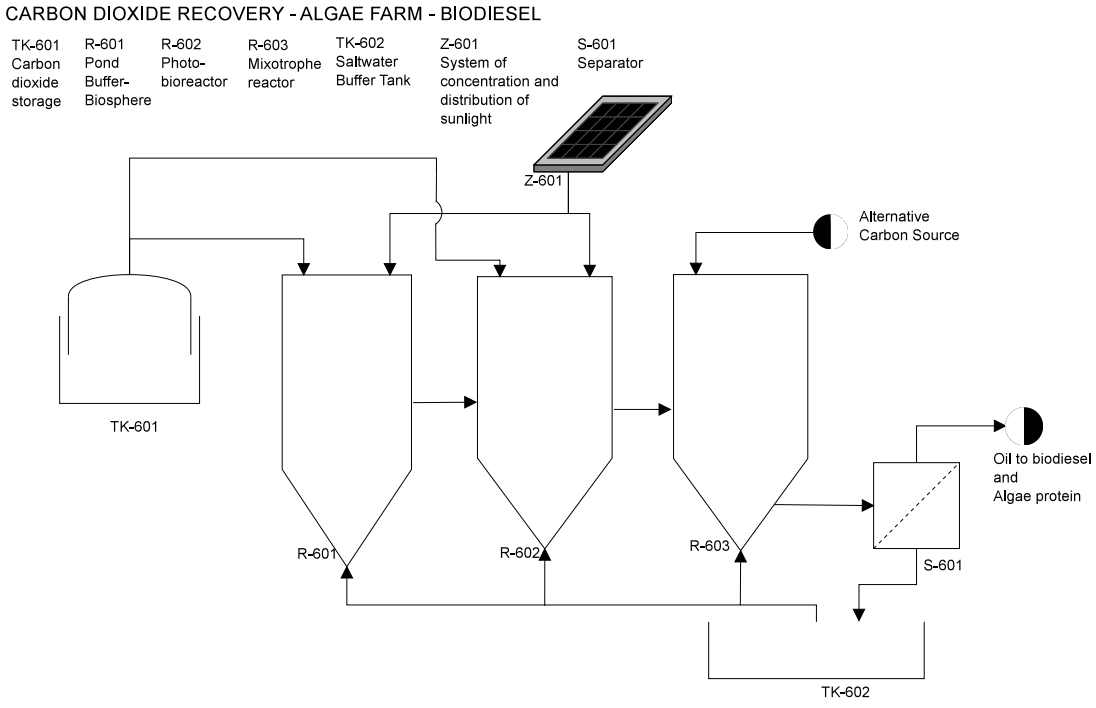

Figure 6.8: Process flowsheet of biodiesel and algae protein production using algae farm technology from SAT. Adapted from SAT (2012).

6.2.5 Economic estimation

The fixed capital investment (FCI) include cost of processing equipment, auxiliary units, acquiring and preparing land, civil structures, facilities, control system, piping, among others.

The fixed capital investment (FCI) for the CO_2 recovery process and dry cleaning of sugarcane was estimated using the six-tenths rule (eq. 6.9) to correct the production scale, based on FCI available at literature described above. The FCI was updated using the CEPCI (Chemical Engineering Plant Cost Index) cost index for the year 2012, according to eq. 6.10.

$$FCI_B = FCI_A \left(\frac{Capacity_B}{Capacity_A} \right)^{0.6} \tag{6.9}$$

$$FCI_B = FCI_A \left(\frac{CEPCI_B}{CEPCI_A} \right) \tag{6.10}$$

Where B refers to desired process, and A refers to known process.

The FCI of the vinasse concentration plant was calculated with the Capcost software based on the area of the evaporators, the operating pressure and the construction material (stainless steel).

The working capital investment (WCI) was set to 15% of FCI. The annualized fixed cost ($AFC = WCI + FCI$) was annualized according eq. 6.11, where N is the service life of the process in years and i the interest rate.

$$AFC = FCI \left(\frac{i(1+i)^N}{(i+1)^N - 1} \right) \tag{6.11}$$

The annualized operational cost (AOC) was estimated using the empirical correlations described in Silla (2003) and Coulson et al. (1999) and are described in Table 6.2. All estimates were made for the year 2012, considering the interest rate of 10 %, a life service of 10 years and 210 days of operation annually.

Table 6.2: Description of annualized operational cost (AOC).

Variable Cost	
Raw materials + Utilities	25% of AOC
Fixed Cost	
Maintenance	5% of AFC
Operating labor	$L \times Quantity_{Product} \times Price_{Product}$
Laboratory	2% of Operating labor
Supervision	2% of Operating labor
Plant overheads	5% of Operating labor
Capital charges	15% of AFC
Insurance	1% of AFC
Local taxes	2% of AFC

The factor L in the operating labor costs can be estimated using eq. 6.12, Silla (2003). L is given in $h/kg_{product}$. The process-productivity factor, K, is given in Table 6.3 , which lists three

process types: batch, continuous (normally automated), and continuous (highly automated). The improvement in operating efficiency is the yearly fractional increase in productivity, p. The base year for computing the operating labor is 1952. Thus, n is the number of years since 1952. By assuming that the fractional increase in labor productivity is 0.02. Operating labor also depends on the the plant capacity, m, in kg/h. The complexity of a process, as determined by the number of process units, N, also affects the operating labor required.

$$L = \frac{K.N}{(1+p)^n.m^b} \tag{6.12}$$

Table 6.3: Process productivity factor K and Capacity exponents for eq. 6.12. Source: adapted from Silla (2003).

	Capacity factor, b		Process productivity factor, K	
Process type	< 5670 kg/h	> 5670 kg/h	$b = 0.76$	$b = 0.84$
Batch	0.76	0.84	0.401	0.536
Continuous (normally automated)	0.76	0.84	0.296	0.396
Continuous (highly automated)	0.76	0.84	0.174	0.233

The total annualized cost ($TAC = AFC + AOC$) was normalized on a per kg basis by dividing the TAC by the annual load of mass to be processed El-Halwagi (2012).

6.2.6 Optimization

The optimization of the source-interception-sink superstructure was performed using the Modified Flexible Tolerance Method (MFTMS) , a direct method of optimization, implemented in Python, described in the previous chapter (see Chapter 5) and the hybrid optimization method proposed previously (see Chapter 4) FTMS-PSO.

Two independent problems of optimization were solved: (i) water and vinasse network and (ii) CO_2 recovery network. The functions defined for these problems are described in the papers that are part of development of this chapter and are available in the sequence. For a given source and a removal efficiency, detailed simulation and costing was carried out ahead of synthesis, thereby eliminating a significant source of nonconvexity and enhancing the computation efficiency. Additionally, the modeling and costing of the interceptor was taken outside the optimization formulation and transformed into a pre-synthesis task.

Futhermore, the solution of these problems with a NLP optimization method, the MFTMS and FTMS-PSO, was possible with a low computational cost due the aplication of the explicit substitution method (see Section 5.2.1).

6.3 Results and Discussions

The results of vinasse network evaluation (design and economics) are described detailed in Appendix B. The CO_2 recovery costs evaluations are showed in Appendix C.

The superstructure and simplified process flowsheet integrated for Case I are shown in Figure 6.9 and 6.11, respectively.

The superstructure and simplified process flowsheet integrated for Case II are shown in Figure 6.10 and 6.12, respectively.

Tables 6.4 and 6.5 summarizes the results obtained with MFTMS and FTMS-PSO solving the problems described above.

In water and vinasse network, the water captation decreases from 4.21 m^3_{water}/t_{cane} at current process to 2.92 m^3_{water}/t_{cane} and 1.91 m^3_{water}/t_{cane} in integrated process for Case I and Case II, respectively. The vinasse volume was reduced in 14% in both cases. The CO_2 recovery allowed to increase biofuel production and additional income in both cases.

MFTMS and FTMS-PSO were able to find the solution in both cases analyzed, even in Case II that present additional complexity with the number of possibilities of recovery and constraints. In both cases can be observed that the hybrid method FTMS-PSO (best solution) was able to achieve the optimum in a lower number of iterations and objective functions evaluations than MFTMS. In all runs and cases, the solution of FTMS-PSO converged to the same point encountered by the MFTMS. These results can corroborate that the optimum reported here is the global optimum.

The economic results are shown in the papers enclosed in the sequence.

It is important to highlight that the strategy of use of explicit substitution method together with the presynthesis (modeling and costing of interceptors) performed outside the optimization formulation were crucial in the success obtained with MFTMS and FTMS-PSO optimization methods.

The results of the Case I using MFTMS of this chapter were presented in the paper titled *"Mass integration applied to sugarcane biorefinery using the modified flexible tolerance method"* presented in the XX Congresso Brasileiro de Engenharia Química (COBEQ). The results of Case II using MFTMS were presented in the paper titled *"Sugarcane Biorefinery Mass Integration Using a Modified Flexible Tolerance Method"* presented in the XXVII Congreso Interamericano y Colombiano de Ingenieria Química. Theses papers are presented in the sequence.

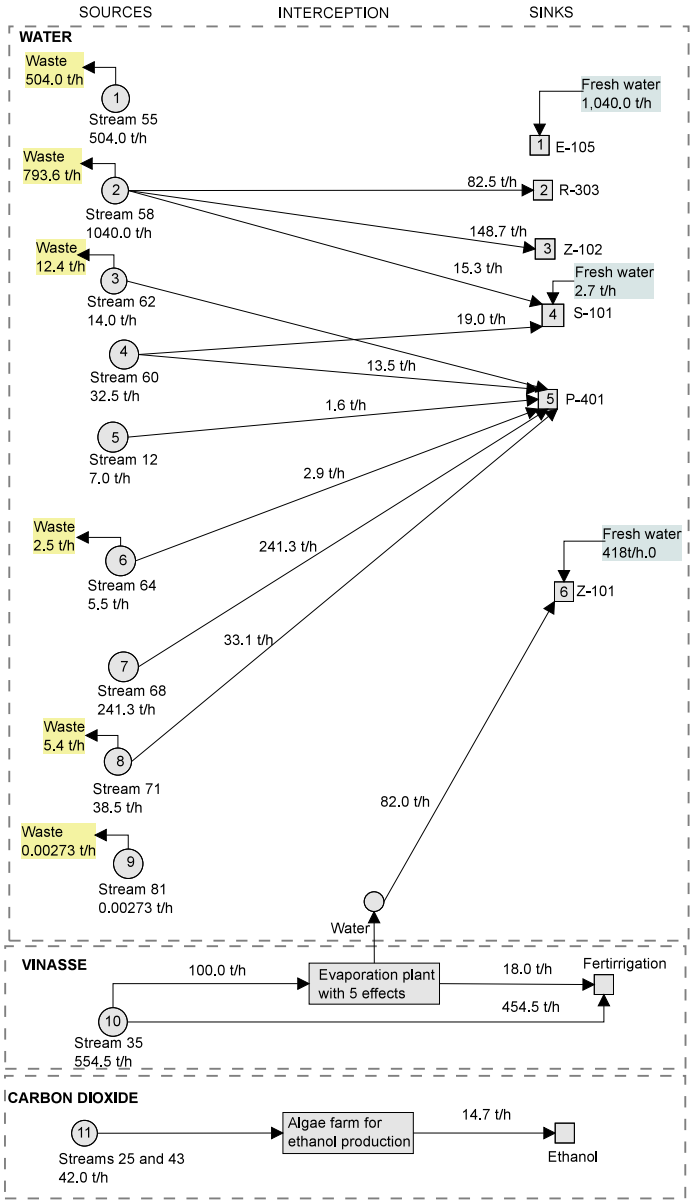

Figure 6.9: Superstructure integrated of the sugarcane biorefinery (Case I).

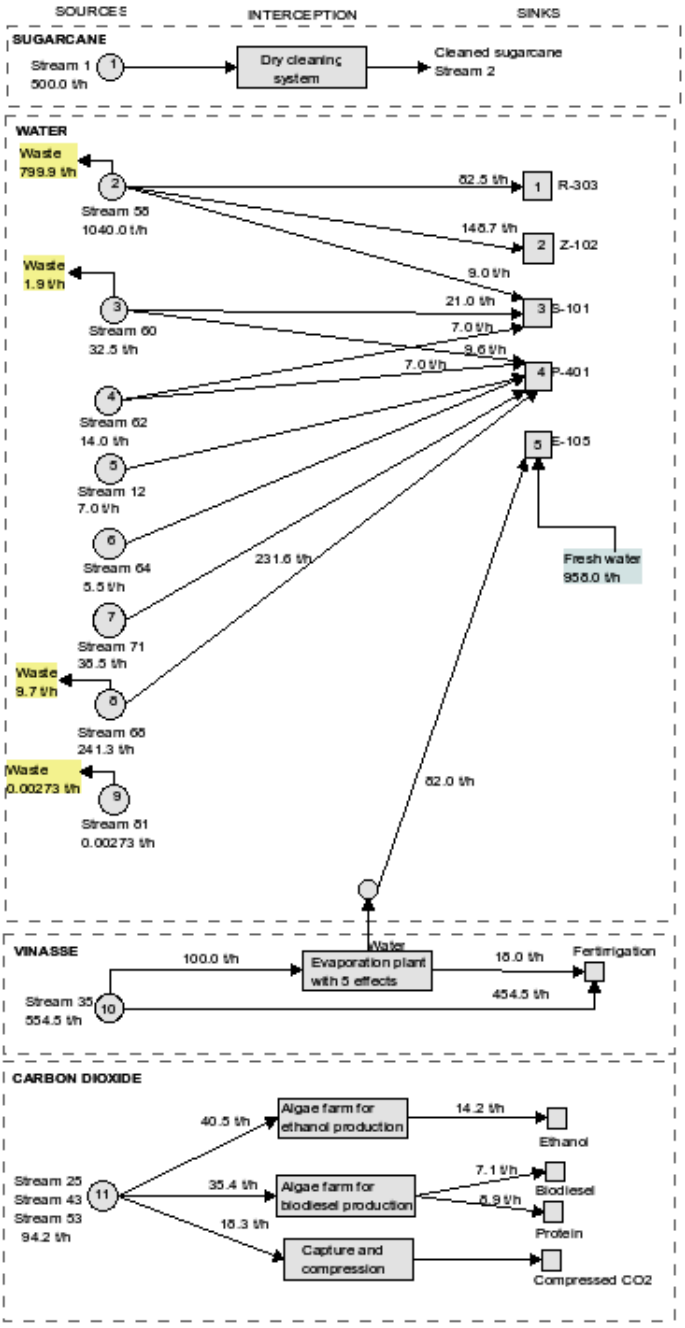

Figure 6.10: Superstructure integrated of the sugarcane biorefinery (Case II).

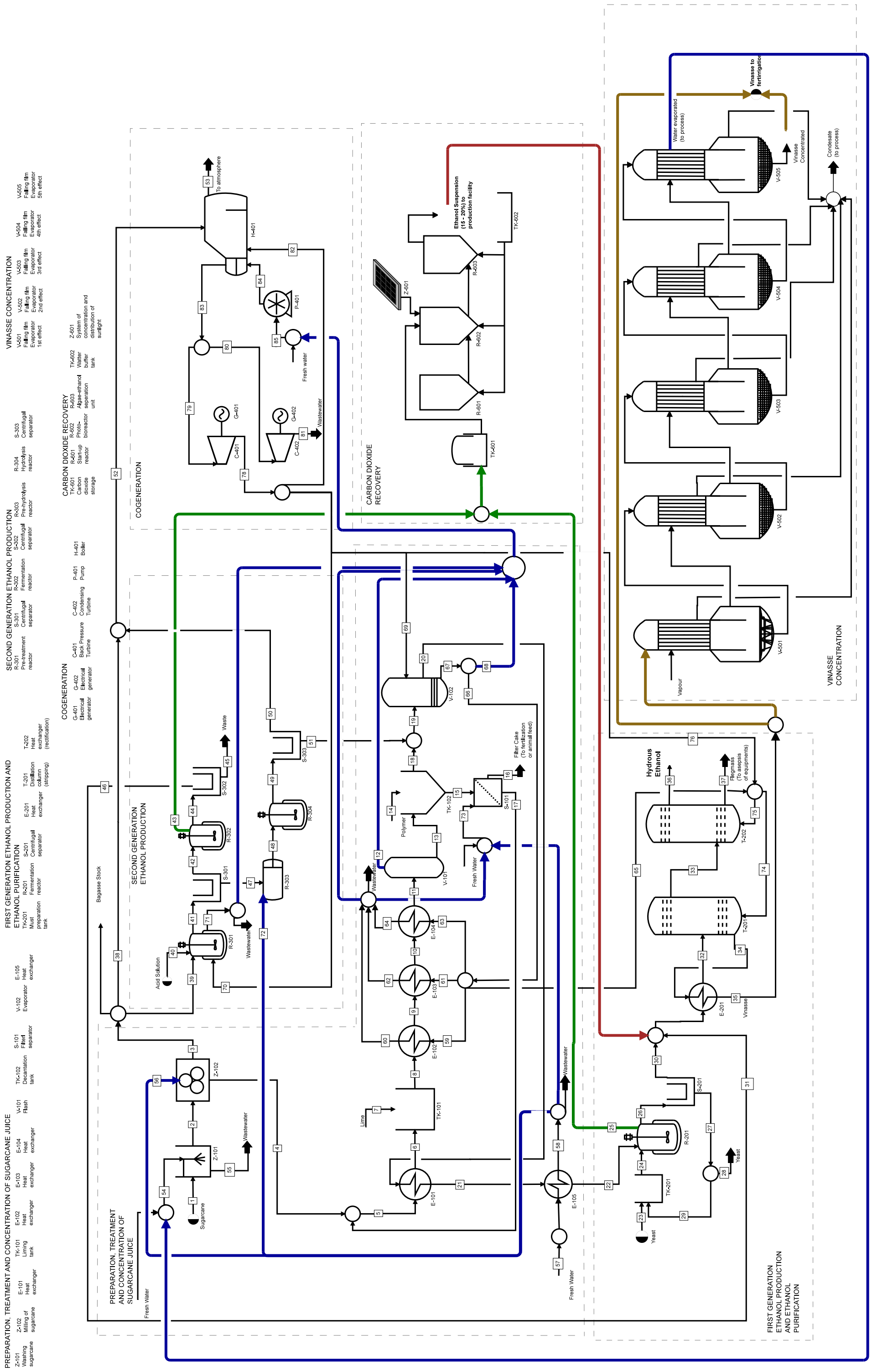

Figure 6.11: Process flowsheet integrated of the sugarcane biorefinery (Case I).

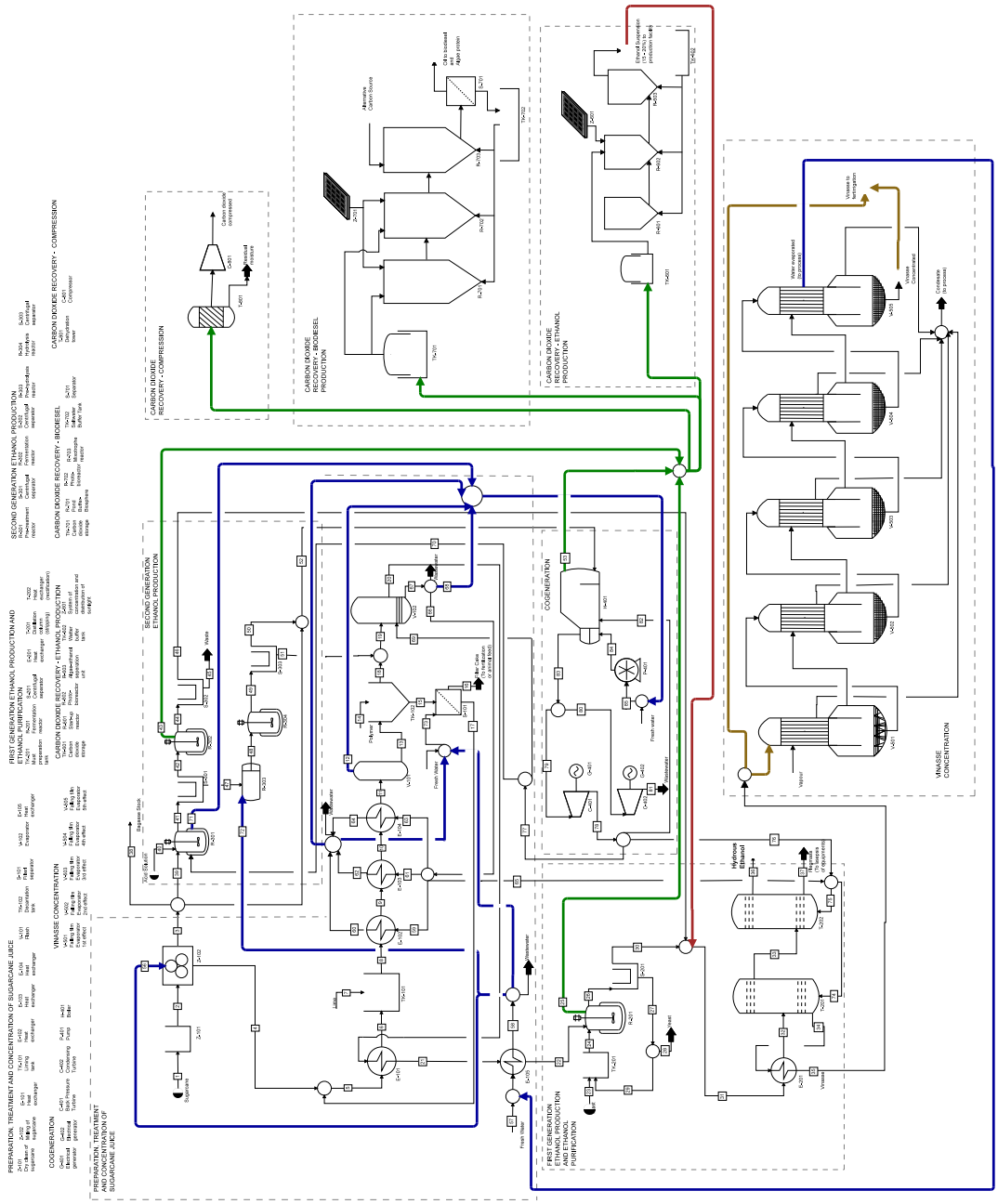

Figure 6.12: Process flowsheet integrated of the sugarcane biorefinery (Case II).

Table 6.4: Summary of MFTMS and FTMS-PSO solution for Cases I and II - Water and Vinasse Network. N_{it}: number of iterations, N_{eval}: number of objective function evaluations.

	Case I	Case II
Original Problem Formulation		
Number of variables	56	54
Number of equality constraints	40	36
Number of inequality constraints	54	49
Problem Reformulation		
Number of explicit variables	40	36
Number of variables	16	18
Number of equality constraints	0	0
Number of inequality constraints	51	49
MFTMS		
N_{eval}	1981	2398
N_{it}	1312	1652
FTMS-PSO		
N_{eval} (Best/Worst)	1600 / 2616	2245 / 2475
N_{it} (Best/Worst)	1012 / 1877	1277 / 1652

Table 6.5: Summary of MFTMS and FTMS-PSO solution for Cases I and II - CO_2 recovery network. N_{it}: number of iterations, N_{eval}: number of objective function evaluations.

	Case I	Case II
Original Problem Formulation		
Number of variables	16	16
Number of equality constraints	13	13
Number of inequality constraints	8	8
Problem Reformulation		
Number of explicit variables	13	13
Number of variables	3	3
Number of inequality constraints	8	8
MFTMS		
N_{eval}	20	4415
N_{it}	10	1532
FTMS-PSO		
N_{eval} (Best/Worst)	171 / 256	230 / 409
N_{it} (Best/Worst)	100 / 154	128 / 238

MASS INTEGRATION APPLIED TO SUGARCANE BIOREFINERY USING THE MODIFIED FLEXIBLE TOLERANCE METHOD

A. M. LIMA[1], F. F. FURLAN[1], A. J. G. CRUZ[1,2] and W. H. KWONG[1,2]

[1]PPGEQ-UFSCar, Federal University of São Carlos, Department of Chemical Engineering
[2]Federal University of São Carlos, Department of Chemical Engineering
Contact e-mail: alice.medeirosdelima@gmail.com

ABSTRACT – This paper presents the application of mass integration methodology to a sugarcane biorefinery, using a modified flexible tolerance method (MFTM) for optimization. For environmental reasons, the targets for mass integration were water, emissions of carbon dioxide from the fermentation process, and vinasse. The MFTM presented good performance in optimization of the process configuration, with reductions of 29, 28, and 33% in the costs of fresh water supply, wastewater treatment, and vinasse fertirrigation (including the costs associated with vinasse concentration), respectively. In addition, emissions of CO_2 were avoided using algae farm technology for ethanol production, resulting in benefits to the environment as well as economic advantages including carbon credits and additional ethanol production.

1. INTRODUCTION

The production of ethanol from lignocellulosic materials has been extensively studied because it increases the amount of ethanol that can be produced from the same crop area, hence helping to meet the growing demand for biofuel. Environmental issues and the rise in petroleum costs have also stimulated research into the production of alternative fuels from renewable raw materials. Two options have been evaluated for fuel production from lignocellulosic raw materials, namely the use of dedicated crops, such as willow and elephant grass, and full utilization of the biomass derived from other processes, such as wastes from agricultural (wheat straw, sugarcane bagasse, and corn stover) and forestry sources.

Due to the large-scale production of ethanol from sugarcane in Brazil, sugarcane bagasse is one of the most suitable materials available for second-generation ethanol production, despite competition with the use of this material for energy production. However, the processes (biochemical and/or thermochemical) are not yet available for large-scale production, due to the high costs of enzymes and catalysts, low productivity, low profit margins, and difficulty in scaling up the hydrolysis step.

Mass integration methodology can be used to determine the minimum consumption of materials and utilities (solvents, water, etc.), minimum discharge of wastes, minimum purchase of fresh raw materials, minimum production of undesirable by-products, and maximum outputs of desirable products. The mass targets that need to be considered in the case of a sugarcane biorefinery include the minimum purchase of fresh water, the minimum expense with wastewater treatment, the minimum expense with vinasse fertirrigation, and recovery of carbon dioxide at the lowest cost and with the highest profit in terms of products.

The aim of the present work was to apply mass integration methodology to a sugarcane biorefinery, using a modified flexible tolerance method for the optimization task.

2. METHODOLOGY

The process adopted in this case study was developed by Furlan *et al.* (2013), who used EMSO software (Environment for Modeling, Simulation and Optimization) to perform the simulations. Simulation of the first-generation plant included the processes of cleaning, milling, physical and chemical treatment, concentration, fermentation, distillation, and cogeneration. The processes considered in the second-generation plant included the weak acid pretreatment, enzymatic hydrolysis, and fermentation of the resulting sugars. Figure 1(a) shows the process flowsheet for the sugarcane biorefinery. A complete process description can be found in Furlan *et al.* (2013).

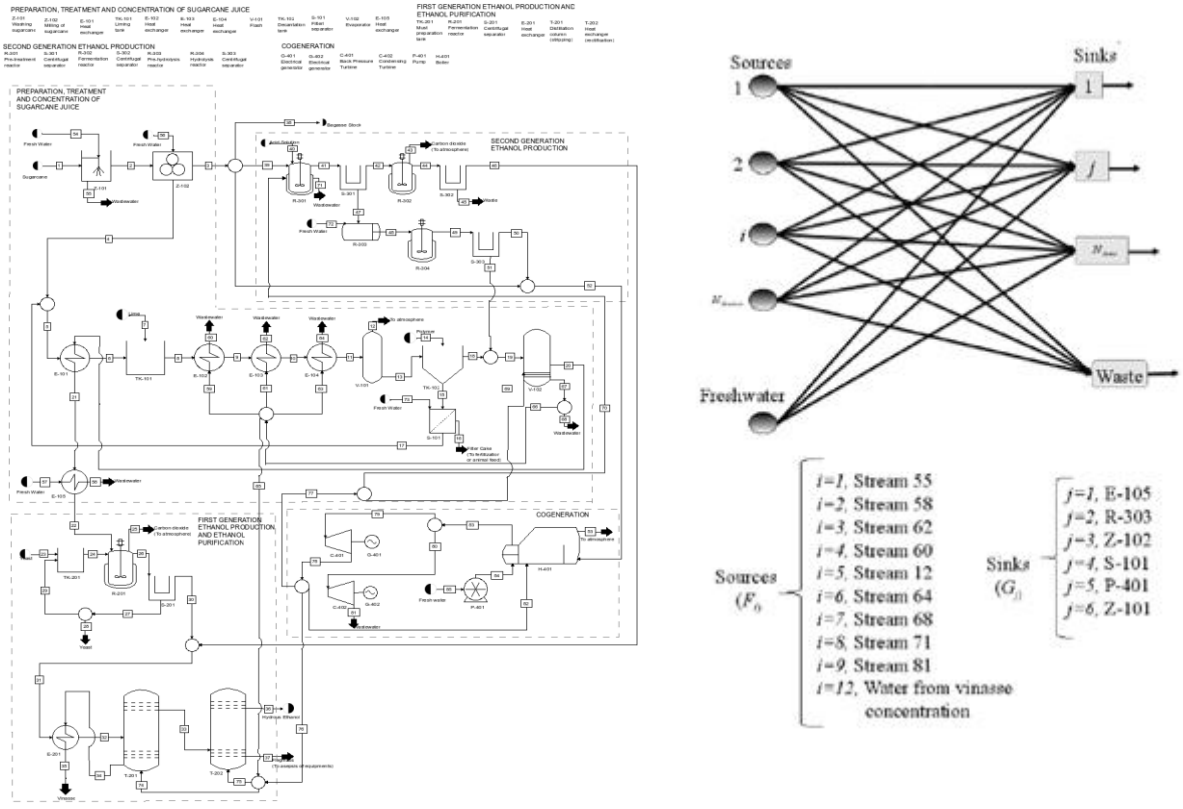

(a) (b)

Figure 1: (a) Process flowsheet for the sugarcane biorefinery (adapted from Furlan *et al.*, 2013); (b) Source-sink superstructure of the water network (adapted from El-Halwagi, 2012), and list of sources and sinks for the sugarcane biorefinery.

In this case study, the targets for process integration included water, the carbon dioxide produced during fermentation, and the vinasse. The process was described by a source-interception-sink configuration, where the interception device was discretized, as proposed by El-Halwagi (2012). The objective was to minimize the costs associated with fresh water, wastewater treatment, fertirrigation using vinasse, the vinasse interception device, and the CO_2 recovery interception device, and to maximize the profits associated with the products obtained from the CO_2 recovery process.

2.1. Water network

The water network included direct recycle of streams containing water free from impurities. The source-sink superstructure developed for water reuse is illustrated in Figure 1(b). The configuration included eight direct recycle sources (including the water available from vinasse concentration) and six process sinks. The unrecycled water streams were fed into the wastewater treatment system. The sources and sinks of water are listed in Figure 1(b), in accordance with the flow diagram shown in Figure 1(a).

2.2. Vinasse network

Vinasse is widely employed as a fertilizer due its high contents of salts (mainly of potassium, calcium, and magnesium) and organic matter. Concentration of vinasse is usually performed using a multiple-effect evaporator, and the best results have been obtained using the falling film evaporator (Rocha, 2009). The number of effects can vary from 4 to 7, but 4 or 5 effects are generally used (Freire and Cortez, 2000, *apud* Rocha, 2009). The application of vinasse can have substantial economic benefits, compared to the use of traditional fertilizers (Rocha, 2009; Carvalho, 2010). However, the financial gain varies as a function of vinasse Brix; at Brix levels greater than 25-30%, the volume of concentrated vinasse does not decrease significantly, which means that the concentration of vinasse beyond 25-30% Brix does not result in further economic gains when vinasse is transported by road.

In this study, an evaporation plant with five effects was adopted, with the falling film evaporator for all effects. The vinasse concentration was fixed at 25% Brix, the total pressure drop was 1.2 bar, and the initial vinasse Brix was 4.5%. The outlet pressure (P_n) of each effect was determined as indicated in Equation 1 (Castro and Andrade, 2007), where N is the total number of effects, and P_0 and P_f are the initial and final pressures. The boiling point elevation (BPE, in °C) was calculated according to Equation 2, where $x_{brix,out}$ is the Brix mass fraction at the exit of the evaporation effect (Araujo, 2007).

$$P_n = P_{n-1} - (P_0 - P_f)\frac{11-(n-1)\frac{11-9}{N-1}}{10\,N} \quad (1)$$

$$BPE = \frac{2\,x_{brix,out}}{1-x_{brix,out}} \quad (2)$$

The overall heat transfer coefficient (U, in kJ/h.m².K) was determined as shown in Equation 3 (Rein, 2007), where T_s is the temperature (in °C) of the heating steam in the calandria, H_{P_n} is the steam enthalpy at evaporator pressure, and k is the Dessin coefficient. The area (A) of each evaporator effect was determined according to Equation 4, where $T_{s,n}$ is the heating steam temperature of the feed in effect n, and $T_{0,n}$ is the feed temperature of vinasse in effect n.

$$U = k\,(100 - x_{brix,out})(T_s - 54)\,H_{P_n} \quad (3)$$

$$Q = UA\,(T_{s,n} - T_{0,n}) \quad (4)$$

The mass flowrates and temperatures in the evaporator effects were determined using mass and energy balances, and the vapor properties were evaluated using steam tables. In order to minimize the costs associated with fertirrigation, analysis was made of the degree of concentration using different proportions of the total vinasse mass flow. These fractions ranged from 18% to 100%, and the area of each effect was calculated for each mass flow of vinasse. The costs of the evaporation system were evaluated using Capcost software (Turton, 1998) and other calculations were performed using electronic spreadsheets.

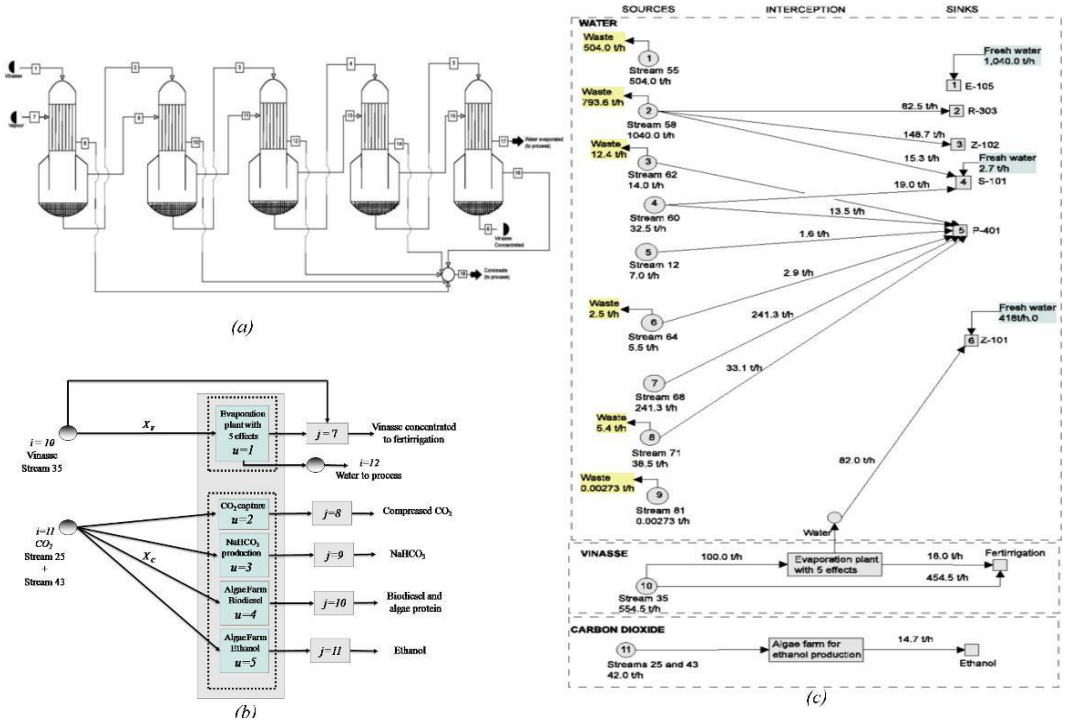

Figure 2: (a) Evaporation system with 5 effects; (b) Source-interceptor-sink superstructure for vinasse concentration and CO_2 recovery; (c) Optimized superstructure for the sugarcane biorefinery.

2.3. Carbon dioxide recovery

The capture of CO_2 from ethanol fermentation is simple, and due to the high purity, the only processes required are dehydration and compression. The cost of capture (including dehydration and compression) from ethanol facilities was reported to be in the range 6-12 USD/t_{CO2} (Xu *et al*., 2010). The CO_2 obtained from capture can be marketed for use by the CO_2 industry.

The production of $NaHCO_3$ was evaluated using the soda method, where caustic soda is used as the reagent ($NaOH + CO_2 \rightarrow NaHCO_3$). The purity of $NaHCO_3$ obtained from this process is greater than obtained using the carbonate method. An analysis of the economics of this system was provided by Cunha *et al*. (2009), considering the reactor, centrifugation of the product, drying, and fine particle separation in a cyclone.

The production of biodiesel and ethanol from algae analyzed in this work employed the SAT process developed by SEE ALGAE Technology (SAT, 2012). This process can produce biodiesel and algal protein from algae, or ethanol from genetically modified algae. The photobioreactor uses CO_2 and solar energy to activate the photosynthesis of the microalgae. Algae farms do not compete for arable land with crops intended for human consumption. Furthermore, algae are the most efficient plants in the world, with growth rates that far outstrip those of traditional crops. Evaluation of the productivity and economic performance of the process was based on data reported by SAT (2012), and the mass fraction of CO_2 delivered to this system needed to be greater than 25% of the total mass. The profit derived from carbon credits was also included, since emissions to the atmosphere were avoided using the proposed procedure. The objective of carbon dioxide recovery was to maximize the profit margin, since a variety of products can be obtained from the different processes analyzed.

Table 1 - Summary of costs, prices of products, and specific production of CO_2 recovery processes.

Process	Cost (USD/t)		Reference
Fresh water inputs	$C_{Fr} = 0.018$		JornalCana (2011)
Wastewater treatment	$C_{waste} = 0.0025$		PECEGE (2012)
Vinasse evaporation	$C_V = 1.509 X_V^3 + 0.501 X_V^2 - 3.125 X_V + 5.008 \text{, } 0.18 \leq X_V \leq 0.8$ $C_V = 8.034 X_V^2 - 15.91 X_V + 11.20 \text{, } 0.8 < X_V \leq 1.0$		This work
Vinasse fertirrigation	$C_{Fert} = 3.06$		CERES (2013)
CO_2 capture	$C_2 = 9.14$		Xu et al. (2010)
$NaHCO_3$ soda method	$C_3 = -17.75 X_{3,C}^2 + 37.67 X_{3,C} + 124.5 \text{, } 0.1 \leq X_{3,C} \leq 1.0 \text{ or } X_{3,C} = 0.0$		This work
Algae farm - biodiesel	$C_4 = -43.70 X_{4,C}^2 + 152.3 X_{4,C} + 18.0 \text{, } 0.25 \leq X_{4,C} \leq 1.0 \text{ or } X_{4,C} = 0.0$		This work
Algae farm - ethanol	$C_5 = -43.06 X_{5,C}^2 + 155.5 X_{5,C} + 17.92 \text{, } 0.25 \leq X_{5,C} \leq 1.0 \text{ or } X_{5,C} = 0.0$		This work
Products	**Price** (USD/t)	**SP** ($t_{product}/t_{CO2}$)	**Reference**
Carbon credits	$P_{creditC} = 7.73$	-	Investing.com (2012)
CO_2	$P_2 = 315.79$	$SP_2 = 1.0$	Santos et al. (2012)
$NaHCO_3$	$P_3 = 200.00$	$SP_3 = 1.91$	Qingdao (2014)
Biodiesel	$P_4^{biodiesel} = 1{,}513.22$	$SP_4^{biodiesel} = 0.22$	ANP (2012)
Algal protein	$P_4^{protein} = 473.08$	$SP_4^{protein} = 0.25$	SAT (2012)
Ethanol	$P_5 = 1{,}603.64$	$SP_5 = 0.35$	PECEGE (2012)

C_u: cost of process u; X_V: vinasse fraction sent to concentration; $X_{3,C}$: fraction of CO_2 in NaHCO3 production; $X_{4,C}$: fraction of CO_2 in algae farm for biodiesel production; $X_{5,C}$: fraction of CO_2 in algae farm for ethanol production; P_u: price of product from process u; SP_u: specific production of process u

2.4. Economic estimation

The fixed capital investment (*FCI*) for the CO_2 recovery process was estimated using the six-tenths rule to correct for the production scale. The *FCI* of the vinasse concentration plant was calculated using the Capcost software, based on the area of the evaporators, the operating pressure, and the construction material (stainless steel). The working capital investment (*WCI*) was set to 15% of the *FCI* (Silla, 2003). The annualized fixed cost (*AFC* = *WCI* + *FCI*) was corrected using the CEPCI cost index for the year 2012. The annualized operational cost (*AOC*) was estimated using the empirical correlations described by Silla (2003). All estimates were made for the year 2012, considering an interest rate of 10%, a service life of

10 years, and 210 days of operation annually. The total annualized cost (*TAC* = *AFC* + *AOC*) was normalized on a per kg basis by dividing the *TAC* by the annual quantity of mass to be processed (El-Halwagi, 2012).

2.5. Optimization

The optimization of the source-interception-sink superstructure was performed using the modified flexible tolerance method (MFTM) implemented in Python, as described by Lima *et al*. (2014). Since CO_2 recovery was independent of water and vinasse, two optimization problems were immediately resolved. The optimization functions are described in Equations 5 and 6. The equality constraints were composed of mass balances around each source, interception device, and sink, together with cost functions; the inequality constraints were the limits and bounds of each variable.

$$\text{Minimize} \quad TAC = C_{Fr} F_{Fr} + C_{waste} G_{waste} + C_V(X_V) W_V X_V + C_{Fert} G_{Fert} \tag{5}$$

$$\text{Minimize} \quad TAC = \sum_{u=2}^{5} C_u(X_{u,C}) W_C X_{u,C} - \sum_{u=2}^{5} W_C X_{u,C} P_u SP_u - W_C P_{creditC} \tag{6}$$

where: C_{Fr} = cost of fresh water, F_{Fr} = flow rate of fresh water inputs, C_{waste} = cost of wastewater treatment, G_{waste} = flow rate of wastewater sent for treatment, $C_V(X_V)$ = cost of vinasse concentration, W_V = vinasse flow rate, X_V = vinasse fraction sent to concentration, C_{Fert} = cost of fertirrigation, G_{Fert} = flow rate of vinasse for fertirrigation, $C_u(X_{u,C})$ = cost of CO_2 recovery in process u, W_C = flow rate of CO_2, $X_{u,C}$ = fraction of CO_2 in process u, P_u = price of product obtained from process u, SP_u = specific production ($t_{product}/t_{CO2}$), $P_{creditC}$ = price of carbon credits.

3. RESULTS AND DISCUSSION

The costs, production rates, and prices adopted and calculated in this work are shown in Table 1. The solution of this problem using a nonlinear optimization method was possible because the modeling and costing of the interceptors was performed outside the optimization formulation and transformed into a presynthesis task, with discretization of the interceptors. After transformation of the equality constraints using the explicit substitution method, the water and vinasse problem (Equation 5) had 16 variables and 51 inequality constraints. The solution obtained using the MFTM was reached after 1981 function evaluations and 1312 iterations. After transformation of the equality constraints (using the explicit substitution method), the CO_2 recovery problem (Equation 6) had 3 variables and 8 inequality constraints, and the solution using the MFTM was reached after 20 function evaluations and 10 iterations. The optimized diagram is shown in Figure 2(c).

The results obtained using mass integration are summarized in Table 2. The main features were reductions of 29, 28, and 33% in the costs of fresh water inputs, wastewater treatment, and vinasse fertirrigation (including the costs associated with vinasse concentration),

respectively. Moreover, CO_2 emissions were avoided using the algae farm technology for ethanol production, which provided both environmental benefits and economic advantages including carbon credits and a 32% increase in ethanol production.

Table 2 - Optimization results for the sugarcane biorefinery.

	Current process	**Optimized process**
Cost of fresh water (USD/y)	187,436.01	132,536.05
Cost of wastewater treatment (USD/y)	23,260.81	16,609.74
Fresh water inputs (t/y)	10,621,374.02	7,363,113.92
Wastewater generation (t/y)	9,456,025.51	6,643,895.34
Cost of fertirrigation with vinasse (USD/y)	14,257,542.86	9,537,666.334
Vinasse for fertirrigation (t/y)	2,794,478.4	2,382,013.388
CO_2 emissions (t/y)	212,452.52	0
Carbon credits (USD/y)	-	1,642,255.51
Cost of CO_2 interception (USD/y)	-	27,695,268.79
Profit due to ethanol from algae (USD/y)	-	119,243,896.10
Ethanol production from algae (t/y)	-	74,358.27

4. CONCLUSIONS

The results of this work indicate that environmental and economic benefits can be obtained by applying mass integration methodology to a biorefinery concept. The inclusion of a presynthesis task involving the modeling, costing, and discretization of the interceptors was essential in order to be able to apply the modified flexible tolerance method, because this avoided both nonconvexity of the objective function and bilinearity of several constraints present in the mixed-integer nonlinear program formulation. The use of mass integration enabled a reduction of more than 30% in the costs associated with fresh water inputs and wastewater treatment, compared with the current process, and 14% of the vinasse volume was used for fertirrigation (with the same composition in terms of nutrients). In addition, the CO_2 could be recovered using algae farm technology for ethanol production.

These findings are not intended to be definitive or exhaustive, since the simulated process adopted for integration contained a number of simplifications, compared to a real process, and some of the technologies analyzed are protected by patents, so process information was limited to that provided by the manufacturers. Nonetheless, the results provide an indication of an economically viable way of achieving substantial advances in terms of water consumption and pollution reduction.

5. ACKNOWLEDGMENTS

The authors thank CNPq and CAPES for financial support.

6. REFERENCES

ANP, Agência Nacional do Petróleo, Gás Natural e Biocombustíveis . Resumo dos leilões na fase da mistura obrigatória - 2012, 2012.

ARAUJO, E. C. C. *Evaporadores*. EdUFSCar, SP, Brazil, 2007.

CARVALHO, T. C. *Redução do volume de vinhaça através do processo de evaporação*. Master's thesis (in Portuguese), State University of São Paulo (UNESP), Faculty of Mechanical Engineering, 2010.

CASTRO, S. B.; ANDRADE, S. A. C. *Tecnologia do Açúcar* . Editora Universitária UFPE, PE, Brazil, 2007.

CERES, Inteligência Financeira. *Estudo de viabilidade técnica e econômica de um grupo selecionado de tecnologias inovadoras relacionadas à cadeia sucroenergética*. Relatório técnico, MDIC, 2013.

CUNHA, L. C.; POIANI, L. M.; GUBULIN, J. C. Análise das viabilidades técnica e econômica para produção de bicarbonato de sódio a partir de dióxido de carbono residual de processos fermentativos. In: VI Congresso de Meio Ambiente da AUGM , São Carlos, 2009.

EL-HALWAGI, M. M. *Sustainable Design Through Process Integration*. Butterworth-Heinemann, 2012.

FURLAN, F. F.; FILHO, R. T.; PINTO, F. H. P. B.; COSTA, C. B. B.; CRUZ, A. J. G.; GIORDANO, R. L. C.; GIORDANO, R. C. Bioelectricity versus bioethanol from sugarcane bagasse: is it worth being flexible? *Biotechnol. Biofuels*, 6(1), 1-12, 2013.

Investing.com. *Crédito carbono*, 2012.

JornalCana. *Cobrança pelo uso da água ganha impulso em regiões de usinas*, 2011.

LIMA, A. M.; CRUZ, A. J. G.; KWONG, W. H. Constrained nonlinear optimization using modified flexible tolerance method: Application in mass integration. *Braz. J. Chem. Eng.* (submitted), 2014.

PECEGE. Custos de produção de cana-de-açúcar, açúcar e etanol no Brasil: Fechamento da safra 2011/2012. Relatório técnico, ESALQ, Piracicaba, 2012.

QINGDAO Sonef Chemical Company Limited. Sodium bicarbonate. 2014.

REIN, P. *Cane Sugar Engineering.* Verlag Dr. Albert Bartens KG, Berlin, Germany, 2007.

ROCHA, M. H. *Uso da análise do ciclo de vida para comparação do desempenho ambiental de quatro alternativas para tratamento da vinhaça*. Master's thesis (in Portuguese), Federal University of Itajubá, Institute of Mechanical Engineering, 2009.

SANTOS, D.; REBELATO, M.; RODRIGUES, A. Análise da viabilidade econômica de uma planta para captura de CO_2 na indústria alcooleira. *Revista Gestão e Tecnologia*, 12, 64-88, 2012.

SAT, SEE ALGAE Technology GmbH. *Commercial infrastructure for production of algae-based compounds*. 2012.

SILLA, H. *Chemical Process Engineering: Design and Economics*. Taylor & Francis, 2003.

TURTON, R. Capcost software. 1998.

XU, Y.; ISOM, L.; HANNA, M. A. Adding value to carbon dioxide from ethanol fermentations. *Bioresour. Technol*., 101, 3311-3319, 2010.

XXVII Congreso Interamericano y Colombiano de Ingenieria Química
Cartagena, Colombia, Octubre 6 a 8 de 2014

Sugarcane Biorefinery Mass Integration Using a Modified Flexible Tolerance Method

Alice Medeiros Lima[a]*, Felipe Fernando Furlan[a], Antonio José Gonçalves Cruz[a,b], Wu Hong Kwong[a,b]

[a]*Programa de Pós-Graduação em Engenharia Química, Universidade Federal de São Carlos, Rodovia Washington Luís (SP 310), km 235,CEP 13565-905,São Carlos, Brazil*
[b]*Departamento de Engenharia Química, Universidade Federal de São Carlos, Rodovia Washington Luís (SP 310), km 235, CEP 13565-905, São Carlos, Brazil*
**E-mail:alice.medeirosdelima@gmail.com*

Resumen

The aim of this paper is to apply the mass integration methodology to sugarcane biorefinery using for the optimization task a modified flexible tolerance method. The targets for mass integration were water, carbon dioxide emissions from fermentation process and bagasse combustion, and vinasse. The results showed a reduction of 53% in the costs of fresh water captation, 56% in the costs of wastewater treatment and 33% in the costs of vinasse fertirrigation. Moreover, emissions of CO_2 were avoided using the algae farm technology for biofuels production, which brings great benefits to the environment, beyond economic advantages as the carbon credit and production of bioethanol, biodiesel and algae protein.

Palabras clave: mass integration, optimization, sugarcane biorefinery, modified flexible tolerance method

1. Introduction

The production of ethanol from lignocellulosic materials has been extensively studied because it increases the amount of ethanol that can be produced from the same crop area, hence helping to meet the growing demand for biofuel. Environmental issues and the rise in petroleum costs have also stimulated research into the production of alternative fuels from renewable raw materials. Due to the large scale production of ethanol from sugarcane in Brazil, the sugarcane bagasse is one of the most suitable feedstock studied for the second-generation production of ethanol, despite competition with the use of this material for energy production. Mass integration methodology can be used to determine the minimum consumption of material utilities, minimum discharge of wastes, minimum purchase of fresh raw materials, minimum production of undesirable by-products, and maximum outputs of desirable products. The mass targets chosen for the sugarcane biorefinery include the minimum purchase of fresh water, the minimum expense with wastewater treatment, the minimum expense with vinasse fertirrigation and the process with lower cost and recovery of CO_2 at the lowest cost and with the highest profit in terms of products. Therefore, the aim of this work is to apply the mass integration methodology to sugarcane biorefinery using for the optimization task the modified flexible tolerance method (Lima *et al.*, 2014).

2. Methodology

The process adopted in this case study was developed by Furlan *et al.* (2013), who used EMSO software to perform the simulations. Simulation of the first generation plant

included cleaning, milling, physical and chemical treatment, concentration, fermentation, distillation and cogeneration. The process considered in the second generation plant included the weak acid pretreatment, enzymatic hydrolysis and fermentation of the resulting sugars. A complete process description can be found in Furlan *et al.* (2013). Figure 1(a) shows the process flowsheet for the sugarcane biorefinery.

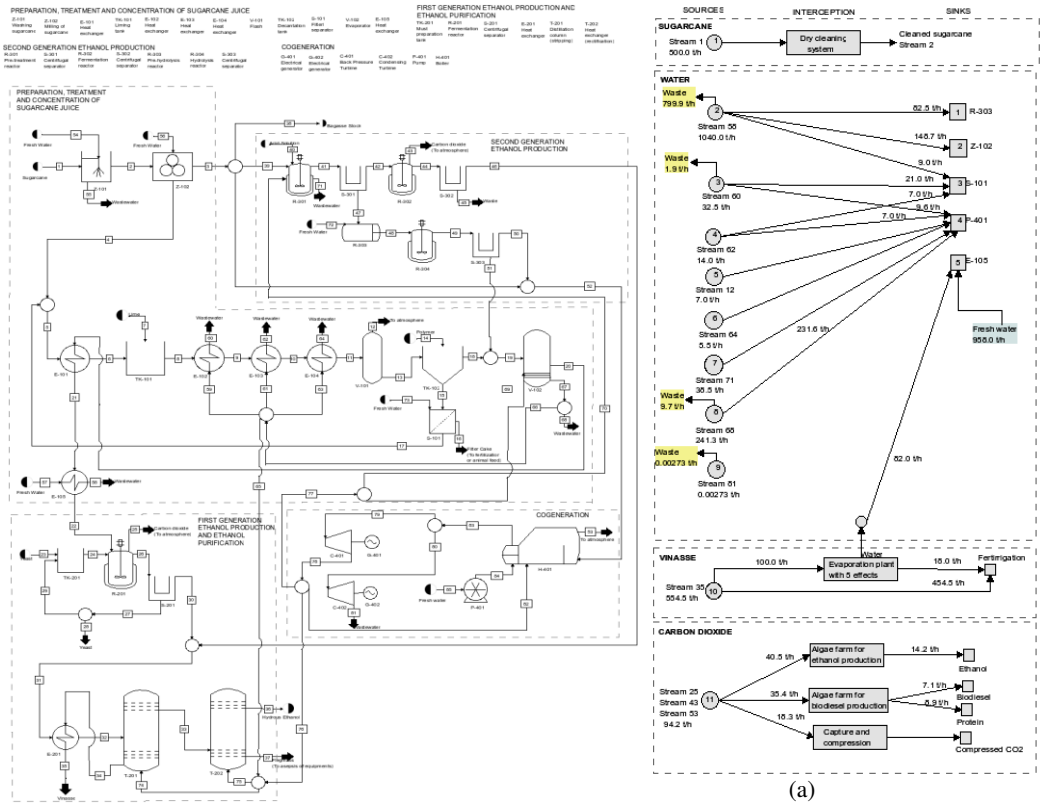

(a)

(b)

Figure 1: (a) Process flowsheet of the sugarcane biorefinery (adapted from Furlan *et al*., 2013). (b) Optimized superstructure for the sugarcane biorefinery.

The process was described as a source-interception-sink, where the interception device was discretized, as proposed by El-Halwagi (2012). The objective is minimize the costs associated with freshwater, wastewater treatment, fertirrigation using vinasse, interception device of vinasse, interception device for CO_2 recovery and maximize the profit with the products obtained from process of CO_2 recovery.

2.1 Water network

The water network is a case of direct recycle (source-sink superstructure), since the streams considered in the analysis is composed by water without impurities. The problem has seven sources (including the water available from vinasse concentration) and five processes sinks. The unrecycled process sources are fed to the wastewater treatment system.The use of dry cleaning system for sugarcane was also evaluated, and then a large amount of water use in conventional system is avoided.

2.2 Vinasse network

Vinasse is widely employed as a fertilizer due its high contents of salts (mainly of potassium, calcium and magnesium) and organic matter. In this study an evaporation plant with 5 effects (falling film evaporator for all effects) was adopted. The vinasse concentration was fixed at 25% of brix, the total pressure drop was 1.2 bar and the initial vinasse brix was 4.5%. The outlet pressure (P_n) of each effect was determined as indicated in the Equation 1 (Castro and Andrade, 2007), where N is the total number of effects, P_0 and P_f is the initial and final pressures The boiling point elevation (*BPE*), in Celsius degree, was calculated according to Equation 2, where $x_{brix;out}$ is the brix mass fraction at the exit of the evaporation effect (Araujo, 2007). The overall heat transfer coefficient (U) in kJ/hm^2K was determined as shown in Equation 3 (Rein, 2007), where T_s is the temperature of the heating steam in the calandria, in Celsius degree, H_{Pn} the steam enthalpy at evaporator pressure and k the Dessin coefficient. The area (A) of each evaporator effect was determined according to Equation 4, where $T_{s,n}$ is the heating steam temperature of the feed in the effect n and $T_{0,n}$ is the feed temperature of vinasse in the effect n.

$$P_n = P_{n-1} - (P_0 - P_f)\frac{11-(n-1)\cdot\left(\frac{11-9}{N-1}\right)}{10N} \quad (1)$$

$$BPE = \frac{2x_{brix,out}}{1-x_{brix,out}} \quad 2)$$

$$U = k \cdot (100 - x_{brix,out}) \cdot (T_s - 54)H_{P_n} \quad (3)$$

$$Q = U \cdot A \cdot (T_{s,n} - T_{0,n}) \quad (4)$$

The mass flowrate and temperatures along the effects of evaporation were determined with mass and energy balances. The vapor properties were evaluated using steam tables. In order to minimize the costs associated with fertirrigation, analysis was made of the degree of concentration using different proportions of the total vinasse mass flow. These fractions ranged from 18% to 100%, and the area of each effect was calculated for each mass flow of vinasse. The costs of evaporation system were evaluated using the Capcost software (Turton, 1998) and other calculations were performed using electronic spreadsheets.

2.3 Carbon dioxide*(CO_2)* recovery

The CO_2 capture from ethanol fermentation and bagasse combustion is simple, and the cost of capture (including dehydration and compression) from ethanol facilities was reported to be in the range of 6-12 USD/t_{CO2} (Xu *et al*., 2010). The CO_2 obtained from capture can be sold for use by the CO_2 industry.

The $NaHCO_3$ production was evaluated using the soda method, where caustic soda is used as reagent ($NaOH + CO_2 \rightarrow NaHCO_3$). The economic analysis reported by Cunha *et al*. (2009) including reactor, centrifugation of product, drying and fine particle separation in a cyclone, was used for process economic estimation.

The biodiesel and bioethanol production from algae analyzed in this work employed the SAT process developed by SEE ALGAE Technology (SAT, 2012). The SAT process can produce biodiesel and algae protein from algae, or bioethanol from genetically modified algae. The photobioreactor uses CO_2 and solar energy to activate the process of photosynthesis of microalgae. Evaluation of productivity and economic performance was based on data reported by SAT (2012), and the mass fraction of CO_2 sent to these processes need be between 10% and 43% of the total mass.

2.4 Economic estimation

The fixed capital investment (*FCI*) for the CO_2 recovery process and dry cleaning of sugarcane was estimated using the six-tenths rule to correct the production scale. The *FCI* of the vinasse concentration plant was calculated with the Capcost software based on the area of the evaporators, the operating pressure and the construction material (stainless steel).

Table 1: Summary of costs, prices of products and specific production of CO_2 recovery processes

Process	**Costs** (USD/t)	**Reference**
Fresh water captation	0.018	JornalCana, 2011
Wastewater treatment	0.0025	PECEGE, 2012
Vinasse evaporation	$C_V = 1.509X_V^3 + 0.501X_V^2 - 3.125X_V + 5.008, 0.18 \le X_V \le 0.8$ $C_V = 8.034X_V^2 - 15.91X_V + 11.20, 0.8 < X_V \le 1.0$	This work.
Fertirrigation	$C_{Fert} = 3.06$	CERES, 2013
CO_2 capture	$C_2 = 9.14$	Xu *et al*., 2010
$NaHCO_3$ production	$C_3 = -17.75X_{3,C}^2 + 37.67X_{3,C} + 124.5$, $0.1 \le X_{3,C} \le 1.0$ or $X_{3,C} = 0.0$	This work.
Algae farm (biodiesel)	$C_4 = -43.70X_{4,C}^2 + 152.3X_{4,C} + 18.0$, $0.1 \le X_{4,C} \le 0.43$ or $X_{4,C} = 0.0$	This work.
Algae farm (bioethanol)	$C_5 = -29.78X_{5,C}^2 + 114.4X_{5,C} + 13.25$, $0.1 \le X_{5,C} \le 0.43$ or $X_{5,C} = 0.0$	This work.
Products	**Price** (USD/t)	**SP** ($t_{product}/t_{CO2}$)	**Reference**
Carbon credit	$P_{creditC} = 7.73$	-	Investing , 2012
CO_2	$P_2 = 315.79$	$SP_2 = 1.0$	Santos *et al*,2012.
$NaHCO_3$	$P_3 = 200.00$	$SP_3 = 1.91$	Qingdao, 2014
Biodiesel	$P_4^{biodiesel} = 1,513.22$	$SP_4^{biodiesel} = 0.22$	ANP, 2012
Algae protein	$P_4^{protein} = 473.08$	$SP_4^{protein} = 0.25$	SAT, 2012
Ethanol	$P_5 = 1,603.64$	$SP_5 = 0.35$	PECEGE, 2012

Table 2: Optimization results of sugarcane biorefinery

	Current process	**Optimized Process**
Cost of fresh water (USD/y)	187,436.010	86,934.207
Cost of wastewater treatment (USD/y)	23,260.810	10,225.528
Fresh water inputs (t/y)	10,621,374.020	4,829,678.140
Wastewater generation (t/y)	9,456,025.510	4,090,211.239
Cost dry cleaning of sugarcane (USD/y)	.000	195,984.872
Cost of fertirrigation with vinasse (USD/y)	14,257,542.860	9,537,666.34
Vinasse for fertirrigation (t/y)	2,794,478.400	2,382,013.38
CO_2 emissions (t/y)	474,498.441	.000
Carbon credits (USD/y)	-	3,669,956.640
Cost of CO_2(Algae farm - Bioethanol) (USD/y)	-	11,623,432.328
Cost of CO_2(Algae farm - Biodiesel) (USD/y)	-	12,414,321.728
Cost of CO_2(Capture) (USD/y)	-	835,317.094
Profit due to Ethanol from algae (USD/y)	-	114,584,221.806
Ethanol production from algae (t/y)	-	71,452.584
Profit due to Biodiesel from algae (USD/y)	-	54,241,792.483
Biodiesel production from algae (t/y)	-	35,845.279
Profit due to Protein from algae (USD/y)	-	21,197,105.500
Protein production from algae (t/y)	-	44,806.598

The working capital investment (*WCI*) was set to 15% of *FCI*. The annualized fixed cost ($AFC = WCI + FCI$) was corrected using the CEPCI cost index for the year 2012. The annualized operational cost (*AOC*) was estimated using the empirical correlations described in Silla (2003). All estimates were made for the year 2012, considering the interest rate of 10%, a life service of 10 years and 210 days of operation annually. The total annualized cost ($TAC = AFC + AOC$) was normalized on a per kg basis by dividing the *TAC* by the annual load of mass to be processed (El-Halwagi, 2012).

2.5 Optimization

The optimization of the source-interception-sink superstructure was performed using the modified flexible tolerance method (MFTM), a direct method of optimization, implemented in Python (Lima *et al.*, 2014). Since the CO_2 recovery was independent of water and vinasse, two optimization problems were solved. The optimization functions are described in Equations 5 and 6, where C_{Fr} is the cost of fresh water, F_{Fr} the flowrate of fresh water captation, C_{waste} the cost of wastewater treatment, G_{waste} the flowrate of wastewater send to treatment, $C_V(X_V)$ the cost of vinasse concentration, W_V the vinasse flowrate, X_V the vinasse fraction send to concentration, C_{Fert} the cost of fertirrigation, G_{Fert} the flowrate of vinasse for fertirrigation, $C_u(X_{u,C})$ the cost of CO_2 recovery through process u, W_C the flowrate of CO_2, $X_{u,C}$ the fraction of CO_2 process u, P_u the price of product obtained from process u, SP_u the specific production ($t_{product}/t_{CO2}$) and $P_{creditC}$ the price of carbon credit. The equality constraints are composed by mass balances around each source, interception devices and sinks, and cost functions; the inequality constraints are the limits and bounds of each variable.

$$\text{Minimize } TAC = C_{Fr}F_{Fr} + C_{waste}G_{waste} + C_V(X_V)W_V X_V + C_{Fert}G_{Fert} \tag{5}$$

$$\text{Minimize } TAC = \sum_{u=2}^{5} C_u(X_{u,C})W_C X_{u,C} - \sum_{u=2}^{5} W_C X_{u,C} P_u SP_u - W_C P_{creditC} \tag{6}$$

3. Results and Discussion

The costs, production rates and prices adopted and calculated in this work are shown in Table 1. The solution of this problem using a NLP optimization method was possible because the modeling and costing of the interceptors were taken outside the optimization formulation and transformed into a presynthesis task, with discretization of the interceptors. After transformation of equality constraints using the explicit substitution method, the water and vinasse problem (Equation 5), had 18 variables and 49 inequality constraints. The solution obtained using the MFTM was reached in 2398 function evaluations and 1652 iterations. After transformation of equality constraints using the explicit substitution method, the CO_2 recovery problem (Equation 6) had 3 variables and 8 inequality constraints, and the solution using the MFTM was reached after 4415 function evaluations and 1532 iterations. The superstructure optimized is shown in the Figure 1(b). The results obtained using mass integration are summarized in Table 2. The main features were reductions of 53%, 56% and 33% in the costs of fresh water captation, wastewater treatment and vinasse fertirrigation (including the costs associated with vinasse concentration), respectively. Moreover, the CO_2 emissions were avoided using the algae farm technology for biofuels production, which brings great benefits to the environment. Beyond economic advantages as the carbon credits and a increase of 31% in ethanol production, it was also possible produce biodiesel, algae protein and compressed CO_2 for utilization by CO_2 industry.

4. Conclusions

The results of this work indicate that environmental and economic benefits can be obtained by applying mass integration methodology to a biorefinery concept. The use of mass integration enabled a reduction of more than 52% of the costs with water captation and treatment compared with current process and 14% of vinasse volume used for fertirrigation (with the same nutrients composition). In addition to this, the CO_2 can be recovery using algae farm technology to bioethanol and biodiesel production.These findings do not intend to be ultimate or exhaustive, since the process simulation adopted for integration contained a number of simplifications, compared to a real process, and some of the technologies analyzed are protected by patents, so process information are limited to that provided by manufacturers. Nonetheless, the results provide an indication of an economically viable way of achieving substantial advances in terms of water consumption and pollution reduction.

Acknowledgments

The authors thank to CAPES, FAPESP and CNPq for financial support.

References

ANP. (2012). Resumo dos leilões na fase da mistura obrigatória.

ARAUJO, E.C.C. (2007) *Evaporadores*. São Carlos: EdUFSCar.

CARVALHO, T.C. (2010) Redução do volume de vinhaça através do processo de evaporação. Master's thesis (in Portuguese), UNESP, Faculty of Mechanical Engineering.

CASTRO,S.B.&ANDRADE, S.A.C.(2007) *Tecnologia do Açúcar*. Brasil: UFPE.

CERES. (2013) Estudo de viabilidade técnica e econômica de um grupo selecionado de tecnologias inovadoras relacionadas à cadeia sucroenergética. MDIC.

CUNHA, L.C.,POIANI, L.M.& GUBULIN, J.C.(2009) Análise das viabilidades técnica e econômica para produção de bicarbonato de sódio a partir de dióxido de carbono residual de processos fermentativos. *Proceedings of VI Congresso de Meio Ambiente da AUGM*, *São Carlos.*

EL-HALWAGI, M.M. (2012) *Sustainable Design through Process Integration*.Elsevier.

FURLAN, F.F., FILHO, R.T., PINTO, F.H.P.B., COSTA, C.B.B., CRUZ, A.J.G., GIORDANO, R.L.C. &GIORDANO, R.C.(2013) Bioelectricity versus bioethanol from sugarcane bagasse: is it worth being flexible? *Biotechnol. Biofuels* 6.p.1-12.

Investing.com. (2012) Crédito carbono. Available in: http://br.investing.com/commodities/ carbon-emissions. Acessed in 3fev 2014

JornalCana.(2011) Cobrança pelo uso da água ganha impulso em regiões de usinas.

LIMA, A.M., CRUZ, A.J.G. & KWONG, W.H.(2014) Constrained nonlinear optimization using modified flexible tolerance method: Application in mass integration. *Braz. J. Chem. Eng* (submitted).

PECEGE. (2012) Custos de produção de cana-de-açúcar, açúcar e etanol no Brasil: Fechamento da safra 2011/2012. Relatório técnico, ESALQ, Piracicaba.

QINGDAO Sonef Chemical Company Limited .(2014) Bicarbonato de sódio.

REIN, P. (2007) *Cane Sugar Engineering.* Berlin: Verlag Dr. Albert Bartens KG.

ROCHA, M.H. (2009) Uso da análise do ciclo de vida para comparação do desempenho ambiental de quatro alternativas para tratamento da vinhaça. Master's thesis (in Portuguese, Federal University of Itajubá, Institute of Mechanical Engineering.

SANTOS, D., REBELATO, M.&RODRIGUES, A. (2012) Análise da viabilidade

econômica de uma planta para captura de CO_2 na indústria alcooleira. *Revista Gestão e Tecnologia.*12.p.64-88.

SAT, SEE ALGAE Technology GmbH. (2012) *Commercial infrastructure for production of algae-based compounds*.

SILLA, H. (2003) *Chemical Process Engineering*. USA: Marcel Dekker, Inc.

TURTON, R. (1998) Capcost software.

XU, Y., ISOM, L. & HANNA, M.A. (2010) Adding value to carbon dioxide from ethanol fermentations. *Bioresour. Technol.*101.p.3311-3319.

6.4 Conclusions

The results obtained applying mass integration methodology in this simplified process of sugarcane biorefinery with MFTMS and FTMS-PSO indicates many opportunities to improve the process.

For Case I, the integration indicates reductions of 29, 28, and 33% in the costs of fresh water inputs, wastewater treatment, and vinasse fertirrigation (including the costs associated with vinasse concentration), respectively. Moreover, CO_2 emissions were avoided using the algae farm technology for ethanol production, which provided both environmental benefits and economic advantages including carbon credits and a 32% increase in ethanol production.

For Case II, the optimization indicates reductions of 53%, 56% and 33% in the costs of fresh water captation, wastewater treatment and vinasse fertirrigation (including the costs associated with vinasse concentration), respectively. The CO_2 emissions were also avoided using the algae farm technology for biofuels production. Beyond economic advantages as the carbon credits and a increase of 31% in ethanol production (as in Case I), it was also possible produce biodiesel, algae protein and compressed CO_2 for utilization by CO_2 industry.

These findings do not intend to be ultimate or exhaustive, since the process simulation adopted for integration contained a number of simplifications, compared to a real process, and some of the technologies analyzed are protected by patents, so process information are limited to that provided by manufacturers. Nonetheless, the results provide an indication of an economically viable way of achieving substantial advances in terms of water consumption and pollution reduction.

CHAPTER 7

Conclusions and Final Remarks

Optimization of process is an important key to make chemical industry process sustainable, efficient and economically viable. One optimization problem very significant is the process synthesis, that involves putting together separate elements into a connected or a coherent whole. Inside the category of process synthesis problems, there are a subcategory of problems, which is of interest in this work, i. e. the mass integration system synthesis.

Mass integration problems solution involve the targeting and generation/selection of alternatives. The targeting include among others, minimum consumption of material utilities, minimum discharge of wastes, minimum purchase of fresh raw materials, minimum production of undesirable by products, and maximum sales of desirable products. The generation of alternatives involves the development of a framework that embeds all potential configurations of interest. The selection involves find the optimum configuration among the proposed alternatives generated, that means the solution of an optimization problem using an appropriate optimization method.

In this scope, the objective of this work was to develop an optimization method based in the Flexible Tolerance Method (FTM) and to apply it in mass integration problems. The purpose of use the Flexible Tolerance Method lies in the fact of its simplicity, free derivative use and good performance. Thus, the method improvement can bring advantages to allow its applicability in complex problems, as system synthesis of mass integration.

The modifications of Flexible Tolerance Method included: (i) hybridization with different unconstrained method to perform the inner search using free derivative algorithms, (ii) hybridization with the stochastic method Particle Swarm Optimization (PSO) during initialization to find initial points, (iii) scaling of variables, (iv) using adaptive parameters in FTM and (v) use of a barrier when the search exceeds the variables limits.

Of the approaches tested the adaptive parameters do not brought improvements in the FTM.

The scaling of variables brought greats improvements as comparing with the original form of FTM, reducing number of functions evaluations, the number of iterations and the processing time.

The hybridization also brought good results. In the first case, with the hybridization with unconstrained methods to perform the inner search, could be seen that FTMS-Powell presented similar performance of FTMS, but do not outperforms the FTMS as could be seen in the Chapter 4. The FTMS-BFGS presented a lower success rate and generally lower number of iterations and objective functions evaluations. Despite the FTMS-PSO had presented a lower success rate compared with the other codes (FTMS and FTMS-Powell), this method can be useful since no starting point is required, and different starting points is generated in each run, what can help in find the global optimum point in nonlinear constrained optimization problems.

The insertion of a barrier in the FMTS code, called MFTMS, also brings greats benefits to initial implementation. This barrier acted imposing the permanence of the polyhedron vertices inside the range of variables variability. The MFTMS was also hybridized with PSO, however this strategy do not outperforms the results obtained by FTMS-PSO, as indicated in Chapter 5. This modification (barrier) was proposed after the observation that sometimes the upper and lower limits of variables were exceeded during the search process. As exposed in Chapter 5, the MFTMS could in most study cases (the benchmark problems and the mass integration problems) improve the performance of FTMS, with lower number of iterations, objective functions evaluations and processing time, mainly in problems with large number of variables.

The study case proposed in this work, the integration of a sugarcane biorefinery include first, second and third ethanol generation of processing, also brought great results. The solution can be achieved with MFTMS and FTMS-PSO, economic and environmental advantages can be reach with the optimum solution encountered. The CO_2 emission was avoided incorporating the algae farm technology (3G), the vinasse concentration reduced the costs associated with fertirrigation and water captation was reduced using recycling and change of technology for sugarcane cleaning (with dry cleaning system). In the first case studied, that includes vinasse concentration, use of CO_2 from fermentation and just recycle of water, the costs reduction were around 30%, and a increase of 31% in ethanol production. In the second case studied, that includes vinasse concentration, use of CO_2 from fermentation and bagasse burn, recycle of water and dry cleaning system for sugarcane, the costs were reduced around 50% in water system (captation and treatment) and 30% in vinasse fertirrigation. In this case, also was possible increase the ethanol production in 32% and biodiesel from algae.

Among the contributions from this thesis, are highlighted:

- The performance assessment of the flexible tolerance method in chemical processes synthesis problems, specifically mass integration;
- The assessment of several improvement proposals for flexible tolerance method: variables scaling, hybridization with other optimization methods, the use of variable parameters and

the barrier;

- The acquisition of a modified algorithm from the flexible tolerance method that has better performance than the original algorithm;
- The proposal of several improvement opportunities for the sugarcane biorefinery reflecting economic and environmental gains through mass integration by using the optimization algorithm obtained in this work.

7.1 Suggestions for future works

As suggestions for future works based in the results found in this thesis, can be highlighted:

- To perform the evaluation performance for the best codes generated in this work in problems with a larger number of variables than the ones tested here (until $n = 40$);
- To analyze the controllability of mass integrated network generated;
- To analyze the operability of the mass exchange network generated;
- To evaluate the performance of the best algorithms proposed in this work in problems of combined energy and mass integration;
- To hybridize MFTMS with different methods. One of the approach can include use of different method to perform the unconstrained search, maybe using gradient based methods. Other approach consist of use of stochastic methods during initialization of MFTMS method to generation of initial conditions.
- To combine a stochastic method (as PSO for example) with the deterministic method MFTMS, using the stochastic method to control the structural changes and the deterministic method to control the changes in the continuous variables, which can be useful if the problem involves a large number of integer variables;
- To incorporate a more complete model for sugarcane biorefinery to analyze the strategies of mass integration proposed and optimized in this work;
- To solve the mass integration problem of the sugarcane biorefinery adding heat and power integration;
- To apply optimization codes proposed in this work in other types of nonlinear constrained optimization problems.

Bibliography

Al-Otaibi, M. and M. El-Halwagi (2006). "Targeting Techniques for Enhancing Process Yield". In: *Chemical Engineering Research and Design* 84.10, pp. 943 –951. ISSN: 0263-8762. DOI: http://dx.doi.org/10.1205/cherd.05056.

Araujo, E. C. C. (2007). *Evaporadores*. SP, Brasil: EdUFSCar.

Becceneri, J. C., S. Sthephany, H. F. C. Velho, and A. J. Silva Neto (2010). *Otimização por Colônia de Formigas (Ant Colony Optimization)*. URL: http://mtc-m19.sid.inpe.br/col/sid.inpe.br/mtc-m19@80/2010/01.20.19.27/doc/cap7.pdf.

BeefPoint (2009). *M.Cassab e Raudi firmam parceria para produção e distribuição do único bicarbonato de sódio verde do mundo, obtido a partir de fontes renováveis*. [Online; accessed 4-June-2014]. URL: http://www.beefpoint.com.br/parceiros/novidades/m-cassab-e-raudi-firmam-parceria-para-producao-e-distribuicao-do-unico-bicarbonato-de-sodio-verde-do-mundo-obtido-a-partir-de-fontes-renovaveis-52468/.

Carvalho, T. C. (2010). "Redução do volume de vinhaça através do processo de evaporação". MA thesis. SP - Brasil: Universidade Estadual Paulista - Faculdade de Engenharia Mecânica.

Castro, S. B. and S. A. C. Andrade (2007). *Tecnologia do Açúcar*. PE, Brasil: Editora Universitária UFPE.

Chen, L., Z. Gao, J. Du, and P. Yao (2007). "A Simultaneous Optimization Method for the Structure and Composition Differences of a Mass Exchange Network". In: *Chinese Journal of Chemical Engineering* 15.2, pp. 254 –261. ISSN: 1004-9541. DOI: http://dx.doi.org/10.1016/S1004-9541(07)60067-6. URL: http://www.sciencedirect.com/science/article/pii/S1004954107600676.

Chen, X. and Y. Yin (2006). "The Flexible Tolerance Method for Estimating Hydrologic Parameters in the Root Zone". In: *JAWRA Journal of the American Water Resources Association* 42.2, pp. 495–512. ISSN: 1752-1688. DOI: 10.1111/j.1752-1688.2006.tb03853.x.

Chew, I. M. L., R. R. Tan, D. C. Y. Foo, and A. S. F. Chiu (2009). "Game theory approach to the analysis of inter-plant water integration in an eco-industrial park". In: *Journal of Cleaner Production* 17.18, pp. 1611 –1619. ISSN: 0959-6526. DOI: http://dx.doi.org/10.1016/j.jclepro.2009.08.005.

Constantinescu, D. (2000). "Smooth and Time-Optimal Trajectory Planning for Industrial Manipulators along Specified Paths". In: *J. Rob. Syst* 17, pp. 223–249.

Coulson, J. M., R. K. Sinnott, J. F. Richardson, J. R. Backhurst, and J. H. Harker (1999). *Coulson & Richardson's Chemical Engineering: Chemical Engineering Design. 3rd ed*. Coulson & Richardson's Chemical Engineering. Butterworth-Heinemann. ISBN: 9780750641425.

Cunha, L. C., L. M. Poiani, and J. C. Gubulin (2009). "Análise das viabilidades técnica e econômica para produção de bicarbonato de sódio a partir de dióxido de carbono residual de processos fermentativos." In: *VI congresso de meio ambiente da AUGM*. Universidade Federal de São Carlos. São Carlos.

Deb, K. and S. Srivastava (2012). "A genetic algorithm based augmented Lagrangian method for constrained optimization". In: *Computational Optimization and Applications* 53.3, pp. 869–902. ISSN: 0926-6003. DOI: 10.1007/s10589-012-9468-9.

Edenhofer, O., R. Pichs-Madruga, Y. Sokona, E. Farahani, S. Kadner, K. Seyboth, A. Adler, I. Baum, S. Brunner, P. Eickemeier, B. Kriemann, J. Savolainen, S. Schlömer, C. von Stechow, T. Zwickel, and J.C. (eds.) Minx (2014). *IPCC, 2014: Climate Change 2014: Mitigation of Climate Change. Contribution of Working Group III to the Fifth Assessment Report of the Intergovernmental Panel on Climate Change*. Tech. rep. Cambridge University Press.

Edgar, T.F., D.M. Himmelblau, and L.S. Lasdon (2001). *Optimization of Chemical Processes*. McGraw-Hill Chemical Engineering Series. McGraw-Hill Education. ISBN: 9780071189774.

El-Halwagi, M., L. Williams, J. Hall, H. Aglan, D. Mortley, and A. Trotman (2003). "Mass Integration and Scheduling Strategies for Resource Recovery in Planetary Habitation". In: *Chemical Engineering Research and Design* 81.2, pp. 243 –250. ISSN: 0263-8762. DOI: http://dx.doi.org/10.1205/026387603762878700.

El-Halwagi, M.M. (1997). *Pollution Prevention through Process Integration: Systematic Design Tools*. Elsevier Science. ISBN: 9780080514185.

El-Halwagi, M.M. (2006). *Process Integration*. Process Systems Engineering. Elsevier Science. ISBN: 9780080454290.

El-Halwagi, M.M. (2012). *Sustainable Design Through Process Integration: Fundamentals and Applications to Industrial Pollution Prevention, Resource Conservation, and Profitability Enhancement*. Butterworth Heinemann. Butterworth-Heinemann. ISBN: 9781856177443.

El-Halwagi, M.M. and V. Manousiouthakis (1989). "Synthesis of mass exchange networks". In: *AIChE Journal* 35.8, pp. 1233–1244. ISSN: 1547-5905. DOI: 10.1002/aic.690350802.

Elia Neto, A. (2013). *Gestão dos Recursos Hídricos na Agroindústria Canavieira*. URL: www.unica.com.br/download.php?idSecao=17&id=12610505.

Empral (2010a). *Como reduzir as perdas industriais atuando sobre a limpeza de cana*. [Online; accessed 1-June-2014]. URL: http://www.empral.com.br/jaboticabal/downloads/05.pdf.

— (2010b). *Limpeza de cana a seco - Tecnologia Empral*. [Online; accessed 1-June-2014]. URL: http://www.stab.org.br/12sba/4.JOAOKASPUTES.SERMATEC.26.10.10.45hs.pdf.

Faria, D. C. (2004). "Reuso das Correntes de Efluentes Aquosos em Refinarias de Petróleo". MA thesis. Departamento de Engenharia Química e Engenharia de Alimentos - Universidade Federal de Santa Catarina.

Fenton, R. G., W. L. Cleghorn, and J. Fu (1989). "A Modified Flexible Tolerance Method for Nonlinear Programming". In: *Engineering Optimization* 15.2, pp. 141–152. DOI: 10.1080/03052158908941148.

Fontana, D. (2002). "Recuperação de Águas de Processos - Desenvolvimento de um Problema Padrão." MA thesis. Departamento de Engenharia Química - Universidade Federal do Rio Grande do Sul.

Fortin, Félix-Antoine, François-Michel De Rainville, Marc-André Gardner, Marc Parizeau, and Christian Gagné (2012). "DEAP: Evolutionary Algorithms Made Easy". In: *Journal of Machine Learning Research* 13, pp. 2171–2175.

Furlan, F. F., C. B. B. Costa, G. C. Fonseca, R. P. Soares, A. R. Secchi, A. J. G. Cruz, and R. C. Giordano (2012). "Assessing the production of first and second generation bioethanol from sugarcane through the integration of global optimization and process detailed modeling". In: *Computers & Chemical Engineering* 43.0, pp. 1 –9. ISSN: 0098-1354. DOI: http://dx.doi.org/10.1016/j.compchemeng.2012.04.002.

Furlan, F. F., R. T. Filho, F. H. P. B. Pinto, C. B. B. Costa, A. J. G. Cruz, R. L. C. Giordano, and R. C. Giordano (2013). "Bioelectricity versus bioethanol from sugarcane bagasse: is it worth being flexible?" In: *Biotechnology for Biofuels* 6.1, pp. 1–12. DOI: 10.1186/1754-6834-6-142. URL: http://dx.doi.org/10.1186/1754-6834-6-142.

Furtado, M. (2014). *Tecnologia ambiental: Usinas recuperam CO2*. [Online; accessed 3-June-2014]. URL: http://www.quimica.com.br/pquimica/tecnologia-ambiental/tecnologia-ambiental-usinas-recuperam-co2/.

Gabriel, F. B. and M.M. El-Halwagi (2005). "Simultaneous synthesis of waste interception and material reuse networks: Problem reformulation for global optimization". In: *Environmental Progress* 24.2, pp. 171–180. ISSN: 1547-5921. DOI: 10.1002/ep.10081. URL: http://dx.doi.org/10.1002/ep.10081.

Gao, F. and L. Han (2012). "Implementing the Nelder-Mead simplex algorithm with adaptive parameters". In: *Computational Optimization and Applications* 51.1, pp. 259–277. ISSN: 0926-6003. DOI: 10.1007/s10589-010-9329-3. URL: http://dx.doi.org/10.1007/s10589-010-9329-3.

Gill, P.E., W. Murray, and M.H. Wright (1981). *Practical optimization*. Academic Press. ISBN: 9780122839504.

Granato, E. F. and C. L. Silva (2002). "Geração de energia elétrica a partir do resísuo vinhaça". In: *Procedings of the 4th Encontro de Energia no Meio Rural*.

Gutterres, M., P. M. Aquim, J. B. Passos, and J. O. Trierweiler (2010). "Water reuse in tannery beamhouse process". In: *Journal of Cleaner Production* 18.15, pp. 1545 –1552. ISSN: 0959-6526. DOI: http://dx.doi.org/10.1016/j.jclepro.2010.06.017. URL: http://www.sciencedirect.com/science/article/pii/S0959652610002295.

Himmelblau, D.M. (1972). *Applied nonlinear programming*. McGraw-Hill.

Hortua, A. C. (2007). "Chemical Process Optimization and pollution prevention via mass and property integration". MA thesis. Texas A&M University.

Hou, Y., J. Wang, Z. Chen, X. Li, and J. Zhang (2014). "Simultaneous integration of water and energy on conceptual methodology for both single- and multi-contaminant problems". In: *Chemical Engineering Science* 117.0, pp. 436 –444. ISSN: 0009-2509. DOI: http://dx.doi.org/10.1016/j.ces.2014.07.004.

Hu, X. and R. Eberhart (2002). "Solving Constrained Nonlinear Optimization Problems with Particle Swarm Optimization". In: *6th World Multiconference on Systemics, Cybernetics and Informatics (SCI) 2002*, pp. 203–206.

Jiménez-Gutiérrez, A., J. Lona-Ramírez, J. M. Ponce-Ortega, and M. El-Halwagi (2014). "An {MINLP} model for the simultaneous integration of energy, mass and properties in water networks". In: *Computers & Chemical Engineering* 71.0, pp. 52 –66. ISSN: 0098-1354. DOI: http://dx.doi.org/10.1016/j.compchemeng.2014.07.008.

Jones, Eric, Travis Oliphant, Pearu Peterson, et al. (2001). *SciPy: Open source scientific tools for Python*. URL: http://www.scipy.org/.

JornalCana (2007). *Até gás carbônico tem novas rotas de produção*. [Online; accessed 4-June-2014]. URL: http://www.jornalcana.com.br/ate-gas-carbonico-tem-novas-rotas-de-producao/.

Kennedy, J. and R. Eberhart (1995). "Particle swarm optimization". In: *Neural Networks, 1995. Proceedings., IEEE International Conference on*. Vol. 4, 1942–1948 vol.4. DOI: 10.1109/ICNN.1995.488968.

Koziel, S. and Z. Michalewicz (1999). "Evolutionary Algorithms, Homomorphous Mappings, and Constrained Parameter Optimization". In: *Evol. Comput.* 7.1, pp. 19–44. ISSN: 1063-6560. DOI: 10.1162/evco.1999.7.1.19.

Liang, J. J. and P. N. Suganthan (2006). *Comparison of Results on the 2006 CEC Benchmark Function Set*. URL: http://web.mysites.ntu.edu.sg/epnsugan/PublicSite/Shared%20Documents/CEC-2006/Comparison-of-Results.pdf.

Liang, J. J., T. P. Runarsson, E. Mezura-Montes, M. Clerc, P. N. Suganthan, C. A. Coello, and K. Deb (2006). "Problem definitions and evaluation criteria for the CEC 2006 special ses-

sion on constrained real-parameter optimization". In: *Nangyang Technological University, Singapore, Tech. Rep*.

Lima, A. M., W. H. Kwong, and A. J. G. Cruz (2013). "Comparative Study and Application of the Flexible Tolerance Method in Synthesis and Analysis of Processes with Mass Integration." In: *Journal of Chemistry and Chemical Engineering* 7.3, pp. 228 –238. URL: http://www.davidpublishing.com/DownLoad/?id=12068.

Martinez-Hernandez, E., J. Sadhukhan, and G. M. Campbell (2013). "Integration of bioethanol as an in-process material in biorefineries using mass pinch analysis". In: *Applied Energy* 104.0, pp. 517 –526. ISSN: 0306-2619. DOI: http://dx.doi.org/10.1016/j.apenergy.2012.11.054.

Menon, R., M. A. S. S. Ravagnani, and A. N. Módenes (2001). "Minimização da emissão de poluentes utilizando a análise pinch em conjunto com técnicas de programação matemática." In: *Acta Scientiarum* 23.6, pp. 1341 –1349. URL: http://periodicos.uem.br/ojs/index.php/ActaSciTechnol/article/download/2760/1825.

Mitchell, M. (1998). *An Introduction to Genetic Algorithms*. A Bradford book. Bradford Books. ISBN: 9780262631853.

Moncada, J., J. A. Tamayo, and C. A. Cardona (2014). "Integrating first, second, and third generation biorefineries: Incorporating microalgae into the sugarcane biorefinery". In: *Chemical Engineering Science* 118.0, pp. 126 –140. ISSN: 0009-2509. DOI: http://dx.doi.org/10.1016/j.ces.2014.07.035.

Muñoz, I., K. Flury, N. Jungbluth, G. Rigarlsford, L. Canals, and H. King (2014). "Life cycle assessment of bio-based ethanol produced from different agricultural feedstocks". In: *The International Journal of Life Cycle Assessment* 19.1, pp. 109–119.

Naish, M. D. (2004). "Sensing-system planning for the surveillance of moving objects". PhD thesis. Department of Mechanical and Industrial Engineering, University of Toronto.

Nápoles-Rivera, F., J. M. Ponce-Ortega, M. M. El-Halwagi, and A. Jiménez-Gutiérrez (2010). "Global optimization of mass and property integration networks with in-plant property interceptors". In: *Chemical Engineering Science* 65.15, pp. 4363 –4377. ISSN: 0009-2509. DOI: http://dx.doi.org/10.1016/j.ces.2010.03.051. URL: http://www.sciencedirect.com/science/article/pii/S0009250910002125.

Nelles, O. (2001). *Nonlinear System Identification: From Classical Approaches to Neural Networks and Fuzzy Models*. Engineering online library. Springer. ISBN: 9783540673699.

Nocedal, J. and S.J. Wright (1999). *Numerical Optimization*. Springer series in operations research and financial engineering. Springer. ISBN: 9780387987934.

Omowunmi, S. and A. Susu (2011). "Application of Tikhonov Regularization Technique to the Kinetic Data of an Autocatalytic Reaction: Pyrolysis of N-Eicosane". In: *Engineering* 3, pp. 1161–1170. DOI: 10.4236/eng.2011.312145.

Pacheco, G. and F.F. Silva (2008). "Utilização de Resíduos Gerados por Indústria do Setor Sucroalcoleiro, Pela RAUDI Indústria e Comércio LTDA, na Produção de Bicarbonato de Sódio". In: *Agro@mbiente On-line* 2.1, pp. 92–94. ISSN: 1982-8470.

Paoliello, J. M. M. (2006). "Aspectos ambientais e potencial energético no aproveitamento de res'ıduos da industria sucroalcooleira". PhD thesis. Universidade Estadual Paulista.

Paviani, D. A. and D. M. Himmelblau (1969). "Constrained nonlinear optimization by heuristic programming". In: *Operations Research*.

Pompermayer, R. S. and D. R. Paula Junior (2000). "Estimativa do potencial brasileiro de produção de biogás através da biodigestão da vinhaça e comparação com outros energéticos". In: *Proceedings of the 3. Encontro de Energia no Meio Rural*. SciELO Brasil.

Powell, M. J. D. (1964). "An efficient method for finding the minimum of a function of several variables without calculating derivatives". In: *The Computer Journal* 7.2, pp. 155–162. DOI: 10.1093/comjnl/7.2.155.

Rein, P. (2007). *Cane Sugar Engineering*. Berlin, Germany: Verlag Dr. Albert Bartens KG.

Rocha, M. H. (2009). "Uso da análise do ciclo de vida para comparação do desempenho ambiental de quatro alternativas para tratamento da vinhaça". MA thesis. MG - Brasil: Universidade Federal de Itajubá - Instituto de Engenharia Mecânica.

Rubio-Castro, E., J. M. Ponce-Ortega, M. Serna-González, A. Jiménez-Gutiérrez, and M. M. El-Halwagi (2011). "A global optimal formulation for the water integration in eco-industrial parks considering multiple pollutants". In: *Computers & Chemical Engineering* 35.8, pp. 1558 –1574. ISSN: 0098-1354. DOI: http://dx.doi.org/10.1016/j.compchemeng.2011.03.010.

Salomon, K. R. (2007). "Avaliação técnico-econômica e ambiental da utilização do biogás proveniente da biodigestão da vinhaça em tecnologias para geração de eletricidade". In: *Itajubá - MG: Universidade Federal de Itajubá*.

SAT, SEE ALGAE Technology GmbH (2012). *Commercial Infrastructure for Production of Algae-Based Compounds*. URL: http://www.seealgae.com/documents/SAT_Company_Eng.pdf.

Savelski, M. J. and M. J. Bagajewicz (2000). "On the optimality conditions of water utilization systems in process plants with single contaminants". In: *Chemical Engineering Science* 55.21, pp. 5035 –5048. ISSN: 0009-2509. DOI: http://dx.doi.org/10.1016/S0009-2509(00)00127-5. URL: http://www.sciencedirect.com/science/article/pii/S0009250900001275.

Shang, W., S. Zhao, and Y. Shen (2009). "A flexible tolerance genetic algorithm for optimal problems with nonlinear equality constraints". In: *Advanced Engineering Informatics* 23.3, pp. 253 –264. ISSN: 1474-0346. DOI: http://dx.doi.org/10.1016/j.aei.2008.09.001. URL: http://www.sciencedirect.com/science/article/pii/S1474034608000773.

Silla, H. (2003). *Chemical Process Engineering: Design And Economics*. Chemical Industries. Taylor & Francis. ISBN: 9780824742744.

Silva, A. P. (2009). "Projeto ótimo de redes de trocadores de calor utilizando técnicas não-determinísticas." PhD thesis. COPPE, Universidade Federal do Rio de Janeiro.

Smith, R.M. (2005). *Chemical Process: Design and Integration*. Wiley. ISBN: 9780470011911.

Soeiro, F. J. C. P., J. C. Becceneri, and A. J. Silva Neto (2010). *Recozimento Simulado (Simulated Annealing)*. URL: http://mtc-m19.sid.inpe.br/col/sid.inpe.br/mtc-m19\%4080/2010/01.20.19.25/doc/cap5.pdf.

Solomon, Susan, Dahe Qin, Martin Manning, Zhenlin Chen, Melinda Marquis, KB Averyt, M Tignor, and Henry L Miller (2007). "IPCC, 2007: Climate change 2007: The physical science basis. Contribution of Working Group I to the fourth assessment report of the Intergovernmental Panel on Climate Change". In: *SD Solomon (Ed.)*

Sujo-Nava, D., L. A. Scodari, C. S. Slater, K. Dahm, and M. J. Savelski (2009). "Retrofit of sour water networks in oil refineries: A case study". In: *Chemical Engineering and Processing: Process Intensification* 48.4, pp. 892 –901. ISSN: 0255-2701. DOI: http://dx.doi.org/10.1016/j.cep.2008.12.002. URL: http://www.sciencedirect.com/science/article/pii/S0255270108002869.

Teles M. L. ; Gomes, H. M. (2010). "Comparação de algoritmos genéticos e programação quadrática sequencial para otimização de problemas em engenharia". In: *Teoria e Prática na Engenharia Civil*.

Turton, R. (1998). *CAPCOST software to accompany: Analysis, synthesis, and design of chemical processes / Richard Turton ... [et al.]. [electronic resource] /*. English. Accompanying book catalogued separately.

Tyner, W. E. (2012). "The Great Green Fleet makes its operational debut". In: 3.5, 515–517.

Wagialla, K. M. (2012). "Synthesis of mass integration networks: Integrated approach to optimization of stream matching for a metal pickling process". In: *Computers & Chemical Engineering* 44.0, pp. 11 –19. ISSN: 0098-1354. DOI: http://dx.doi.org/10.1016/j.compchemeng.2012.04.012. URL: http://www.sciencedirect.com/science/article/pii/S0098135412001251.

Wagialla, K. M., M. M. El-Halwagi, and J. M. Ponce-Ortega (2012). "An integrated approach to the optimization of in-plant wastewater interception with mass and property constraints". In: *Clean Technologies and Environmental Policy* 14.2, pp. 257–265. ISSN: 1618-954X. DOI: 10.1007/s10098-011-0395-8. URL: http://dx.doi.org/10.1007/s10098-011-0395-8.

Wikipedia (2014). *Carbon credit— Wikipedia, The Free Encyclopedia*. [Online; accessed 2-June-2014]. URL: http://en.wikipedia.org/wiki/Carbon_credit.

Xu, Y., L. Isom, and M. A. Hanna (2010). "Adding value to carbon dioxide from ethanol fermentations". In: *Bioresource Technology* 101.10, pp. 3311 –3319. ISSN: 0960-8524. DOI: http://dx.doi.org/10.1016/j.biortech.2010.01.006.

Zhang, P. and Y. Ren (1989). “Flexible tolerance simplex method and its application to multi-component spectrophotometric determinations”. In: *Analytica Chimica Acta* 222.1, pp. 323 –333. ISSN: 0003-2670. DOI: http://dx.doi.org/10.1016/S0003-2670(00)81907-8. URL: http://www.sciencedirect.com/science/article/pii/S0003267000819078.

APPENDIX A

Problems formulation

A.1 G Suite - problems definition

These problems was taken from Liang et al. (2006), except the problem g20 that was taken from Paviani and Himmelblau (1969).

g01.

Standard randomly generated test problem of non-convex quadratic programming.

Minimize:

$$f(x) = 5\sum_{i=1}^{4} x_i - 5\sum_{i=1}^{4} x_i^2 - \sum_{i=5}^{13} x_i \tag{A.1}$$

Subject to:

$$g_1(x) = 2x_1 + 2x_2 + x_{10} + x_{11} - 10 \leq 0$$

$$g_2(x) = 2x_1 + 2x_2 + x_{10} + x_{12} - 10 \leq 0$$

$$g_3(x) = 2x_2 + 2x_3 + x_{11} + x_{12} - 10 \leq 0$$

$$g_4(x) = -8x_1 + x_{10} \leq 0$$

$$g_5(x) = -8x_2 + x_{11} \leq 0$$

$$g_6(x) = -8x_3 + x_{12} \leq 0$$

$$g_7(x) = -2x_4 - x_5 + x_{10} \leq 0$$

$$g_8(x) = -2x_6 - x_7 + x_{11} \leq 0$$

$$g_9(x) = -2x_8 - x_9 + x_{12} \leq 0$$

g02.

Nonlinear problem with global maximum unknown.

Minimize:

$$f(x) = -\left| \frac{\sum_{i=1}^{n} \cos^4(x_i) - 2\prod_{i=1}^{n} \cos^2(x_i)}{\sqrt{\sum_{i=1}^{n} i x_i^2}} \right| \tag{A.2}$$

Subject to:

$$g_1(x) = 0.75 - \prod_{i=1}^{n} x_i \leq 0$$

$$g_2(x) = \sum_{i=1}^{n} x_i - 7.5n \leq 0$$

g03.

Problem with polynomial objective function and quadratic equality constraint.
Minimize:

$$f(x) = -\left(\sqrt{n}\right)^n \prod_{i=1}^{n} x_i \tag{A.3}$$

Subject to:

$$h_1(x) = \sum_{i=1}^{n} x_i^2 - 1 = 0$$

g04.

Standard randomly generated test problem of non-convex quadratic objective function and constraints.

Minimize:

$$f(x) = 5.3578547x_3^2 + 0.8356891x_1x_5 + 37.293239x_1 - 40792.141 \tag{A.4}$$

Subject to:

$$g_1(x) = 85.334407 + 0.0056858x_2x_5 + 0.0006262x_1x_4 - 0.0022053x_3x_5 - 92 \leq 0$$

$$g_2(x) = -85.334407 - 0.0056858x_2x_5 - 0.0006262x_1x_4 + 0.0022053x_3x_5 \leq 0$$

$$g_3(x) = 80.51249 + 0.0071317x_2x_5 + 0.0029955x_1x_2 + 0.0021813x_3^2 - 110 \leq 0$$

$$g_4(x) = -80.51249 - 0.0071317x_2x_5 - 0.0029955x_1x_2 - 0.0021813x_3^2 + 90 \leq 0$$

$$g_5(x) = 9.300961 + 0.0047026x_3x_5 + 0.0012547x_1x_3 + 0.0019085x_3x_4 - 25 \leq 0$$

$$g_6(x) = -9.300961 - 0.0047026x_3x_5 - 0.0012547x_1x_3 - 0.0019085x_3x_4 + 20 \leq 0$$

g05.

Problem with cubic objective function and nonlinear constraints.

Minimize:

$$f(x) = 3x_1 + 0.000001x_1^3 + 2x_2 + (0.000002/3)x_2^3 \tag{A.5}$$

Subject to:

$$g_1(x) = -x_4 + x_3 - 0.55 \leq 0$$

$$g_2(x) = -x_3 + x_4 - 0.55 \leq 0$$

$$h_3(x) = 1000\sin(-x_3 - 0.25) + 1000\sin(-x_4 - 0.25) + 894.8 - x_1 = 0$$

$$h_4(x) = 1000\sin(x_3 - 0.25) + 1000\sin(x_3 - x_4 - 0.25) + 894.8 - x_2 = 0$$

$$h_5(x) = 1000\sin(x_4 - 0.25) + 1000\sin(x_4 - x_4 - 0.25) + 1294.8 = 0$$

g06.

Problem with cubic objective function and quadratic constraints.

Minimize:

$$f(x) = (x_1 - 10)^3 + (x_2 - 20)^3 \tag{A.6}$$

Subject to:

$$g_1(x) = -(x_1 - 5)^2 - (x_2 - 5)^2 + 100 \leq 0$$

$$g_2(x) = (x_1 - 6)^2 - (x_2 - 5)^2 - 82.81 \leq 0$$

g07.

Problem with quadratic objective function and linear and nonlinear constraints.

Minimize:

$$f(x) = x_1^2 + x_2^2 + x_1x_2 - 14x_1 - 16x_2 + (x_3 - 10)^2 + 4(x_4 - 5)^2 + (x_5 - 3)^2 \\ +2(x_6 - 1)^2 + 5x_7^2 + 7(x_8 - 11)^2 + 2(x_9 - 10)^2 + (x_{10} - 7)^2 + 45 \tag{A.7}$$

Subject to:

$$g_1(x) = -105 + 4x_1 + 5x_2 - 3x_7 + 9x_8 \leq 0$$

$$g_2(x) = 10x_1 - 8x_2 - 17x_7 + 2x_8 \leq 0$$

$$g_3(x) = -8x_1 + 2x_2 + 5x_9 - 2x_{10} - 12 \leq 0$$

$$g_4(x) = 3(x_1 - 2)^2 + 4(x_2 - 3)^2 + 2x_3^2 - 7x_4 - 120 \leq 0$$

$$g_5(x) = -5x_1^2 + 8x_2 + (x_3 - 6)^2 - 2x_4 - 40 \leq 0$$

$$g_6(x) = x_1^2 + 2(x_2 - 2)^2 + 2x_1x_2 + 14x_5 - 6x_6 \leq 0$$

$$g_7(x) = 0.5(x_1 - 8)^2 + 2(x_2 - 4)^2 + 3x_5^2 - x_6 - 30 \leq 0$$

$$g_8(x) = -3x_1 + 6x_2 + 12(x_9 - 8)^2 - 7x_{10} \leq 0$$

g08.

Nonlinear problem with many local optima, the highest peaks are located along x axis. In the feasible region, the problem presents two maximum of almost equal fitness of value of 0.1.

Minimize:

$$f(x) = -\frac{\sin^3(2\pi x_1)\sin(2\pi x_2)}{x_1^3(x_1 + x_2)} \tag{A.8}$$

Subject to:

$$g_1(x) = x_1^2 - x_2 + 1 \leq 0$$

$$g_2(x) = 1 - x_1 + (x_2 - 4)^2 \leq 0$$

g09.

Nonlinear problem with nonlinear constraints.

Minimize:

$$f(x) = (x_1 - 10)^2 + 5(x_2 - 12)^2 + x_3^4 + 3(x_4 - 11)^2 + 10x_5^6 + 7x_6^2 + x_7^4 - 4x_6x_7 - 10x_6 - 8x_7 \tag{A.9}$$

Subject to:

$$g_1(x) = -127 + 2x_1^2 + 3x_2^4 + x_3 + 4x_4^2 + 5x_5 \leq 0$$

$$g_2(x) = -282 + 7x_1 + 3x_2 + 10x_3^2 + x_4 - x_5 \leq 0$$

$$g_3(x) = -196 + 23x_1 + x_2^2 + 6x_6^2 - 8x_7 \leq 0$$

$$g_4(x) = 4x_1^2 + x_2^2 - 3x_1x_2 + 2x_3^2 + 5x_6 - 11x_7 \leq 0$$

g10.

Heat exchanger design.
Minimize:

$$f(x) = x_1 + x_2 + x_3 \tag{A.10}$$

Subject to:

$$g_1(x) = -1 + 0.0025(x_4 + x_6) \leq 0$$

$$g_2(x) = -1 + 0.0025(x_5 + x_7 - x_4) \leq 0$$

$$g_3(x) = -1 + 0.001(x_8 - x_5) \leq 0$$

$$g_4(x) = -x_1x_6 + 833.3325x_4 + 100x_1 - 83333.333 \leq 0$$

$$g_5(x) = -x_2x_7 + 1250x_5 + x_2x_4 - 1250x_4 \leq 0$$

$$g_6(x) = -x_3x_8 + 1250000 + x_3x_5 - 2500x_5 \leq 0$$

g11.

Problem with quadratic objective function and quadratic constraint.

Minimize:

$$f(x) = x_1^2 + (x_2 - 1)^2 \tag{A.11}$$

Subject to:

$$h(x) = x_2 - x_1^2 = 0$$

g12.

Problem with disjointed components, the feasible region of the search space consists of 9^3 disjointed spheres.

Minimize:

$$f(x) = -(100 - (x_1 - 5)^2 - (x_2 - 5)^2 - (x_3 - 5)^2)/100 \tag{A.12}$$

Subject to:

$$g(x) = (x_1 - p)^2 + (x_2 - q)^2 + (x_3 - r)^2 - 0.0625 \leq 0$$

Where$p, q, r = 1.\ 2.\ \cdots .\ 9$. The feasible region of the search space consists of 9^3 disjointed spheres. A point (x_1, x_2, x_3) is feasible only if there exist p, q, r such that the above inequality holds.

g13.

Problem with nonlinear objective function and constraints.

Minimize:

$$f(x) = \exp(x_1 x_2 x_3 x_4 x_5) \tag{A.13}$$

Subject to:

$$h_1(x) = x_1^2 + x_2^2 + x_3^2 + x_4^2 + x_5^2 - 10.0 = 0$$

$$h_2(x) = x_2 x_3 - 5x_4 x_5 = 0$$

$$h_3(x) = x_1^3 + x_2^3 + 1 = 0$$

g14.

Problem of chemical equilibrium at constant temperature and pressure.

Minimize: $f(x) = \sum_{i=1}^{10} x_i \left(c_i + \ln \frac{x_i}{\sum_{j=1}^{10} x_j} \right)$

Subject to:

$$h_1(x) = x_1 + 2x_2 + 2x_3 + x_6 + x_{10} - 2 = 0$$

$$h_2(x) = x_4 + 2x_5 + x_6 + x_7 - 1 = 0$$

$$h_3(x) = x_3 + x_7 + x_8 + 2x_9 + x_{10} - 1 = 0$$

Where: $\vec{c} = \begin{bmatrix} -6.089 & -17.164 & -34.054 & -5.914 & -24.721 & -14.986 & -24.1 & -10.708 & -26.662 & -22.179 \end{bmatrix}$

g15.

Nonlinear problem with nonlinear equality constraints.

Minimize:

$$f(x) = 1000 - x_1^2 - 2x_2^2 - x_3^2 - x_1x_2 - x_1x_3 \tag{A.14}$$

Subject to:

$$h_1(x) = x_1^2 + x_2^2 + x_3^2 - 25 = 0$$

$$h_2(x) = 8x_1 + 14x_2 + 7x_3 - 56 = 0$$

g16.

The objective function is the net profit of a hypothetical wood-pulp plant. The constraints include the usual material and energy balances as well as several empirical equations.

Minimize:

$$\begin{aligned} f(x) = {} & 0.000117y_{14} + 0.1365 + 0.00002358y_{13} + 0.000001502y_{16} + 0.0321y_{12} \\ & + 0.004324y_5 + 0.0001\frac{c_{15}}{c_{16}} + 37.48\frac{y_2}{c_{12}} - 0.0000005843y_{17} \end{aligned} \tag{A.15}$$

Subject to:

$$g_1(x) = \frac{0.28}{0.72}y_5 - y_4 \leq 0$$

$$g_2(x) = x_3 - 1.5x_2 \leq 0$$

$$g_3(x) = 3496\frac{y_2}{c_{12}} - 21 \leq 0$$

$$g_4(x) = 110.6 + y_1 - {}^{62212}/_{c_{17}} \leq 0$$

$$g_5(x) = 213.1 - y_1 \leq 0$$

$$g_6(x) = y_1 - 405.23 \leq 0$$

$$g_7(x) = 17.505 - y_2 \leq 0$$

$$g_8(x) = y_2 - 1053.6667 \leq 0$$

$$g_9(x) = 11.275 - y_3 \leq 0$$

$$g_{10}(x) = y_3 - 35.03 \leq 0$$

$$g_{11}(x) = 214.228 - y_4 \leq 0$$

$$g_{12}(x) = y_4 - 665.585 \leq 0$$

$$g_{13}(x) = 7.458 - y_5 \leq 0$$

$$g_{14}(x) = y_5 - 584.463 \leq 0$$

$$g_{15}(x) = 0.961 - y_6 \leq 0$$

$$g_{16}(x) = y_6 - 265.916 \leq 0$$

$$g_{17}(x) = 1.612 - y_7 \leq 0$$

$$g_{18}(x) = y_7 - 7.046 \leq 0$$

$$g_{19}(x) = 0.146 - y_8 \leq 0$$

$$g_{20}(x) = y_8 - 0.222 \leq 0$$

$$g_{21}(x) = 107.99 - y_9 \leq 0$$

$$g_{22}(x) = y_9 - 273.366 \leq 0$$

$$g_{23}(x) = 922.693 - y_{10} \leq 0$$

$$g_{24}(x) = y_{10} - 1286.105 \leq 0$$

$$g_{25}(x) = 926.832 - y_{11} \leq 0$$

$$g_{26}(x) = y_{11} - 1444.046 \leq 0$$

$$g_{27}(x) = 18.766 - y_{12} \leq 0$$

$$g_{28}(x) = y_{12} - 537.141 \leq 0$$

$$g_{29}(x) = 1072.163 - y_{13} \leq 0$$

$$g_{30}(x) = y_{13} - 3247.039 \leq 0$$

$$g_{31}(x) = 8961.448 - y_{14} \leq 0$$

$$g_{32}(x) = y_{14} - 26844.086 \leq 0$$

$$g_{33}(x) = 0.063 - y_{15} \leq 0$$

$$g_{34}(x) = y_{15} - 0.386 \leq 0$$

$$g_{35}(x) = 71084.33 - y_{16} \leq 0$$

$$g_{36}(x) = -140000 + y_{16} \leq 0$$

$$g_{37}(x) = 2802713 - y_{17} \leq 0$$

$$g_{38}(x) = y_{17} - 12146108 \leq 0$$

Where:

$$y_1 = x_2 + x_3 + 41.6$$

$$c_1 = 0.024x_4 - 4.62$$

$$y_2 = {}^{12.5}/_{c_1} + 12$$

$$c_2 = 0.0003535x_1^2 + 0.5311x_1 + 0.08705y_2x_1$$

$$c_3 = 0.052x_1 + 78 + 0.002377y_2x_1$$

$$y_3 = c_2/c_3$$

$$y_4 = 19y_3$$

$$c_4 = 0.04782(x_1 - y_3) + \frac{0.1956(x_1 - y_3)^2}{x_2} + 0.6376y_4 + 1.584y_3$$

$$c_5 = 100x_2$$

$$c_6 = x_1 - y_3 - y_4$$

$$c_7 = 0.950 - c_4/c_5$$

$$y_5 = c_6c_7$$

$$y_6 = x_1 - y_5 - y_4 - y_3$$

$$c_8 = (y_5 + y_4)0.995$$

$$y_7 = c_8/y_1$$

$$y_8 = c_8/3798$$

$$c_9 = y_7 - 0.0663y_7/y_8 - 0.3153$$

$$y_9 = 96.82/c_9 + 0.321y_1$$

$$y_{10} = 1.29y_5 + 1.258y_4 + 2.29y_3 + 1.71y_6$$

$$y_{11} = 1.71x_1 - 0.452y_4 + 0.580y_3$$

$$c_{10} = 12.3/752.3$$

$$c_{11} = (1.75y_2)(0.995x_1)$$

$$c_{12} = 0.995y_{10} + 1998$$

$$y_{12} = c_{10}x_1 + c_{11}/c_{12}$$

$$y_{13} = c_{12} - 1.75y_2$$

$$y_{14} = 3623 + 64.44x_2 + 58.4x_3 + {}^{146312}/_{(y_9 + x_5)}$$

$$c_{13} = 0.995y_{10} + 60.8x_2 + 48x_4 - 0.1121y_{14} - 5095$$

$$y_{15} = y_{13}/c_{13}$$

$$y_{16} = 148000 - 331000y_{15} + 40y_{13} - 61y_{15}y_{13}$$

$$c_{14} = 2324y_{10} - 28740000y_2$$

$$y_{17} = 14130000 - 1328y_{10} - 531y_{11} + c_{14}/c_{12}$$

$$c_{15} = y_{13}/y_{15} - y_{13}/0.52$$

$$c_{16} = 1.104 - 0.72y_{15}$$

$$c_{17} = y_9 + x_5$$

g17.

Optimization of an electrical network.

Minimize:

$$f(x) = f(x_1) + f(x_2) \tag{A.16}$$

$$f(x_1) = \begin{cases} 30x_1 & 0 \le x_1 \le 300 \\ 31x_1 & 300 \le x_1 \le 400 \end{cases}$$

$$f(x_2) = \begin{cases} 28x_2 & 0 \le x_2 \le 100 \\ 29x_2 & 100 \le x_2 \le 200 \\ 30x_2 & 200 \le x_2 \le 1000 \end{cases}$$

Subject to:

$$h_1(x) = -x_1 + 300 - \frac{x_3 x_4}{131.078}\cos(1.48477 - x_6) + \frac{0.90798x_3^2}{131.078}\cos(1.47588)$$

$$h_2(x) = -x_2 - \frac{x_3 x_4}{131.078}\cos(1.48477 + x_6) + \frac{0.90798x_4^2}{131.078}\cos(1.47588)$$

$$h_3(x) = -x_5 - \frac{x_3 x_4}{131.078}\sin(1.48477 + x_6) + \frac{0.90798x_4^2}{131.078}\sin(1.47588)$$

$$h_4(x) = 200 - \frac{x_3 x_4}{131.078}\sin(1.48477 - x_6) + \frac{0.90798x_3^2}{131.078}\sin(1.47588)$$

g18.

Maximization the area of a hexagon in which the maximum diameter was unity.

Minimize:

$$f(x) = -0.5(x_1 x_4 - x_2 x_3 + x_3 x_9 - x_5 x_9 + x_5 x_8 - x_6 x_7) \tag{A.17}$$

Subject to:

$$g_1(x) = x_3^2 + x_4^2 - 1 \le 0$$

$$g_2(x) = x_9^2 - 1 \le 0$$

$$g_4(x) = x_1^2 + (x_2 - x_9)^2 - 1 \leq 0$$

$$g_5(x) = (x_1 - x_5)^2 + (x_2 - x_6)^2 - 1 \leq 0$$

$$g_6(x) = (x_1 - x_7)^2 + (x_2 - x_8)^2 - 1 \leq 0$$

$$g_7(x) = (x_3 - x_5)^2 + (x_4 - x_6)^2 - 1 \leq 0$$

$$g_8(x) = (x_3 - x_7)^2 + (x_4 - x_8)^2 - 1 \leq 0$$

$$g_9(x) = x_7^2 + (x_8 - x_9)^2 - 1 \leq 0$$

$$g_{10}(x) = x_2 x_3 - x_1 x_4 \leq 0$$

$$g_{11}(x) = -x_3 x_9 \leq 0$$

$$g_{12}(x) = x_5 x_9 \leq 0$$

$$g_{13}(x) = x_6 x_7 - x_5 x_8 \leq 0$$

g19.

Problem formulated by the Shell Development Company for the original Colville study.

Minimize:

$$f(x) = \sum_{j=1}^{5} \sum_{i=1}^{5} c_{ij} x_{(10+i)} x_{(10+j)} + 2 \sum_{j=1}^{5} d_j x_{(10+j)}^3 - \sum_{i=1}^{10} b_i x_i \tag{A.18}$$

Subject to:

$$g_j(x) = -2 \sum_{i=1}^{5} c_{ij} x_{(10+i)} - 3 d_j x_{(10+j)}^2 - e_j + \sum_{i=1}^{10} a_{ij} x_i \leq 0 \quad j = 1. \cdots . 5$$

Where:

$$\vec{b} = [-40. \ -2. \ -0.25. \ -4. \ -4. \ -1. \ -40. \ -60. \ 5. \ 1]$$

$$\vec{e} = [-15. \ -27. \ -36. \ -18. \ -12]$$

$$\vec{d} = [4. \ 8. \ 10. \ 6. \ 2]$$

$$\vec{c} = \begin{bmatrix} 30 & -20 & -10 & 32 & -10 \\ -20 & 39 & -6 & -31 & 32 \\ -10 & -6 & 10 & -6 & -10 \\ 32 & -31 & -6 & 39 & -20 \\ -10 & 32 & -10 & -20 & 30 \end{bmatrix}$$

$$\vec{a} = \begin{bmatrix} -16 & 2 & 0 & 1 & 0 \\ 0 & -2 & 0 & 0.4 & 2 \\ -3.5 & 0 & 2 & 0 & 0 \\ 0 & -2 & 0 & -4 & -1 \\ 0 & -9 & -2 & 1 & -2.8 \\ 2 & 0 & -4 & 0 & 0 \\ -1 & -1 & -1 & -1 & -1 \\ -1 & -2 & -3 & -2 & -1 \\ 1 & 2 & 3 & 4 & 5 \\ 1 & 1 & 1 & 1 & 1 \end{bmatrix}$$

g20.

[1] Minimization of the cost of blending multicomponent mixtures.

Minimize:

$$f(x) = \sum_{i=1}^{24} a_i x_i \tag{A.19}$$

Subject to:

$$g_i(x) = \frac{x_i + x_{(i+12)}}{\sum_{j=1}^{24} x_j} - e_i \leq 0 \quad i = 1.\,2.\,3$$

$$g_i(x) = \frac{x_{(i+3)} + x_{(i+15)}}{\sum_{j=1}^{24} x_j} - e_i \leq 0 \quad i = 4.\,5.\,6$$

$$h_i(x) = \frac{x_{(i+12)}}{b_{(i+12)} \sum_{j=13}^{24} \frac{x_j}{b_j}} - \frac{c_i x_i}{40 b_i \sum_{j=1}^{12} \frac{x_j}{b_j}} = 0 \quad i = 1. \cdots . 12$$

$$h_{13}(x) = \sum_{i=1}^{24} x_i - 1 = 0$$

$$h_{14}(x) = \sum_{i=1}^{12} \frac{x_i}{d_i} + k \sum_{i=13}^{24} \frac{x_i}{b_i} - 1.671 = 0$$

Where $k = (0.7302)(530)\frac{14.7}{40}$, and the other parameters are described in the Table A.1.

[1] Problem g20 used in this work was taken from Paviani and Himmelblau (1969) although the same problem is reported in Liang et al. (2006). However, in Liang et al. (2006) there are some differences in the constraint equations, and a different optimum point is shown. Here, the equations follow those presented in Paviani and Himmelblau (1969).

Table A.1: Parameters values for the problem g20.

i	a_i	b_i	c_i	d_i	e_i
1	0.0693	44.094	123.7	31.244	0.1
2	0.0577	58.12	31.7	36.12	0.3
3	0.05	58.12	45.7	34.784	0.4
4	0.2	137.4	14.7	92.7	0.3
5	0.26	120.9	84.7	82.7	0.6
6	0.55	170.9	27.7	91.6	0.3
7	0.06	62.501	49.7	56.708	
8	0.1	84.94	7.1	82.7	
9	0.12	133.425	2.1	80.8	
10	0.18	82.507	17.7	64.517	
11	0.1	46.07	0.85	49.4	
12	0.09	60.097	0.64	49.1	
13	0.0693	44.094			
14	0.0577	58.12			
15	0.05	58.12			
16	0.2	137.4			
17	0.26	120.9			
18	0.55	170.9			
19	0.06	62.501			
20	0.1	84.94			
21	0.12	133.425			
22	0.18	82.507			
23	0.1	46.07			
24	0.09	60.097			

A.2 Mass integration problems

Problem 1.

Maximize the overall process yield.

Maximize:

$$f(x) = {}^{A14}/_{x_1} \tag{A.20}$$

Subject to:

$$g_1(x) = x_3 - x_6 \geq 0$$

$$g_2(x) = x_5 - 300.0 \geq 0$$

$$g_3(x) = 860.0 - x_5 \geq 0$$

$$g_4(x) = x_{26} - 380.0 \geq 0$$

$$g_5(x) = 384.0 - x_{26} \geq 0$$

$$g_6(x) = x_{28} - 2.5 \geq 0$$

$$g_7(x) = 5.0 - x_{28} \geq 0$$

$$g_8(x) = 0.76 - x_{29} \geq 0$$

$$g_9(x) = x_{29} + 0.55 \geq 0$$

$$g_{i+9}(x) = x_i - LB_i \geq 0. \quad i = 1.....31 \text{ except for } i = 5, 26, 28 \text{ and } 29$$

$$h_1(x) = x_2 x_3 - x_4 = 0$$

$$h_2(x) = x_2 - 0.33 + 0.0000042.(x_5 - 580)^2 = 0$$

$$h_3(x) = x_6 - {}^{46}/_{44}.x_4 = 0$$

$$h_4(x) = x_1 + E4 + E6 + E12 - (x_6 + x_7 + x_8 + E14 + x_9 + E16 + x_{10}) = 0$$

$$h_5(x) = A1 + A4 + A6 + A12 + x_4 - (x_{11} + x_{12} + A14 + A2 + x_{13} + x_{14}) = 0$$

$$h_6(x) = x_{15} - x_{16} - x_8 = 0$$

$$h_7(x) = A15 - x_{17} - x_{12} = 0$$

$$h_8(x) = x_{18} - x_3 + x_6 - E4 = 0$$

$$h_9(x) = x_{19} - x_{20} - x_1 = 0$$

$$h_{10}(x) = x_{19} - x_9 - x_3 = 0$$

$$h_{11}(x) = x_{21} - E14 - E16 - x_{15} = 0$$

$$h_{12}(x) = x_{16} - x_{20} - x_{10} = 0$$

$$h_{13}(x) = x_{17} - x_{22} - x_{14} = 0$$

$$h_{14}(x) = x_{23} + A4 + x_4 - x_{24} - A2 = 0$$

$$h_{15}(x) = x_{24} + A6 + A12 - (x_{11} + x_{12} + x_{13} + A14 + x_{17}) = 0$$

$$h_{16}(x) = x_9 - x_{25}.x_{19} = 0$$

$$h_{17}(x) = x_{25} + 0.0274.x_{26} - 10.5122 = 0$$

$$h_{18}(x) = x_{27} - 0.653.\exp(0.085.x_{28}) = 0$$

$$h_{19}(x) = x_{16} - x_{27}.x_{15} = 0$$

$$h_{20}(x) = x_{29} - 0.14x_{30} - 0.89 = 0$$

$$h_{21}(x) = A14 - x_{29}x_{31} = 0$$

$$h_{22}(x) = x_{31} - (x_{24} + A6 + A12 - x_{11}) = 0$$

$$h_{23}(x) = x_{31} - (A14 + A15 + x_{13}) = 0$$

Where A14=100.000; E6=400;E4=E14=E16=E12=A1=A2=A4=A6=A12=A15=0

The LB_i(lower bound) e UB_i(upper bound) are described in Al-Otaibi and El-Halwagi (2006).

Problem 2.

Minimization of the total load of a toxic pollutant discharged into terminal plant wastewater.

Minimize:

$$f(x) = x_1.x_2 + x_3.x_4 + x_5.x_6 \tag{A.21}$$

Subject to:

$$g_1(x) = 65.0 - x_{22} \geq 0$$

$$g_2(x) = 8.0 - x_{23} \geq 0$$

$$g_3(x) = 0.15 - x_7 \geq 0$$

$$g_4(x) = x_7 - 0.09 \geq 0$$

$$g_5(x) = 0.09 - x_{12} \geq 0$$

$$g_6(x) = x_{12} - 0.075 \geq 0$$

$$g_7(x) = 0.085 - x_{17} \geq 0$$

$$g_8(x) = x_{17} - 0.075 \geq 0$$

$$g_{i+8}(x) = x_i - LB_i \geq 0. \quad i = 1, ..., 30 \text{ except for } i = 7, 12, 17, 22 \text{ and } 23$$

$$h_1(x) = x_7 - x_8 - x_9 - x_{10} - x_{11} = 0$$

$$h_2(x) = x_{12} - x_{13} - x_{14} - x_{15} - x_{16} = 0$$

$$h_3(x) = x_{17} - x_{18} - x_{19} - x_{20} - x_{21} = 0$$

$$h_4(x) = x_7 x_{22} - x_8 x_4 - x_9 . x_6 - x_{10} x_2 = 0$$

$$h_5(x) = x_{12} x_{23} - x_{13} x_4 - x_{14} x_6 - x_{15} x_2 = 0$$

$$h_6(x) = x_{17} x_{24} - x_{18} x_4 - x_{19} x_6 - x_{20} x_2 = 0$$

$$h_7(x) = x_7 - x_{25} = 0$$

$$h_8(x) = x_{12} - x_{26} = 0$$

$$h_9(x) = x_{17} - x_{27} = 0$$

$$h_{10}(x) = x_{25} - x_1 - x_{10} - x_{15} - x_{20} = 0$$

$$h_{11}(x) = x_{26} - x_3 - x_8 - x_{13} - x_{18} = 0$$

$$h_{12}(x) = x_{27} - x_5 - x_9 - x_{14} - x_{19} = 0$$

$$h_{13}(x) = (0.15 + 0.2x_7) x_{28} - (x_7 - 0.09) x_{22} - 6.030 = 0$$

$$h_{14}(x) = 0.15. (x_{28} - x_{29}) - x_{12}. (x_4 - x_{23}) = 0$$

$$h_{15}(x) = \left(\frac{x_{12}}{0.015}\right)^{1.3} - \frac{\left(1 - \frac{0.015}{x_{12}}\right). (x_{28} - 0.1.x_{23})}{(x_{29} - 0.1x_{23})} - \frac{0.015}{x_{12}} = 0$$

$$h_{16}(x) = 0.15. (x_{29} - x_{30}) - x_{17}. (x_6 - x_{24}) = 0$$

$$h_{17}(x) = \left(\frac{x_{17}}{0.015}\right)^{1.3} - \frac{\left(1 - \frac{0.015}{x_{17}}\right). (x_{29} - 0.1.x_{24})}{(x_{30} - 0.1x_{24})} - \frac{0.015}{x_{17}} = 0$$

$$h_{18}(x) = x_{28} - 5.x_2 = 0$$

$$h_{19}(x) = x_{24} = 0$$

The LB_i(lower bound) e UB_i(upper bound) are described in El-Halwagi (1997).

Problem 3.

Production of phenol from cumene hydroperoxide.

Minimize:

$$f(x) = x_1 + x_2 \tag{A.22}$$

Subject to:

$$g_0(x) = -x_3 + 0.015$$

$$g_1(x) = -x_4 + 0.1$$

$$g_2(x) = -x_5 + 0.015$$

$$g_{2+i}(x) = x_i - LB_i \geq 0. \quad i = 1, ..., 27 \text{ except for } i = 3, 4 \text{ and } 5$$

$$h_1(x) = x_1 - (0.0006.x_6 + 0.0004.x_7).8000.0 + 0.0011999999987892807$$

$$h_2(x) = x_6 - (x_8 + x_9 + x_{10})$$

$$h_3(x) = x_7 - (x_{11} + x_{12} + x_{13})$$

$$h_4(x) = Wwash101 - (x_{14} + x_{15} + x_{16} + x_{17})$$

$$h_5(x) = WD101 - (x_{18} + x_{19} + x_{20} + x_{21})$$

$$h_6(x) = Wwash102 - (x_{22} + x_{23} + x_{24} + x_{25})$$

$$h_7(x) = Gwash101 - (x_{14} + x_{18} + x_{22} + x_8 + x_{11})$$

$$h_8(x) = GR104 - (x_{15} + x_{19} + x_{23} + x_9 + x_{12})$$

$$h_9(x) = Gwash102 - (x_{16} + x_{20} + x_{24} + x_{10} + x_{13})$$

$$h_{10}(x) = Gwash101.x_3 - (x_{14}.0.016 + x_{18}.0.024 + x_{22}.0.22 + x_{11}.0.012)$$

$$h_{11}(x) = GR104.x_4 - (x_{15}.0.016 + x_{19}.0.024 + x_{23}.0.22 + x_{12}.0.012)$$

$$h_{12}(x) = Gwash102.x_5 - (x_{16}.0.016 + x_{20}.0.024 + x_{24}.0.22 + x_{13}.0.012)$$

$$h_{13}(x) = x_{26} - (x_{17} + x_{21} + x_{25})$$

$$h_{14}(x) = x_2 - (x_{14}.5.0 + x_{15}.3.5 + x_{16}.2.0 + x_{18}.2.0 + x_{19}.1.0 +$$

$$x_{20}.4.0 + x_{22}.3.0 + x_{23}.5.0 + x_{24}.2.0 + x_8.4.5 + x_9.3.0 + x_{10}.3.5$$

$$+x_{11}.2.5 + x_{12}.1.0 + x_{13}.1.5) - 0.0039999999935389496$$

Where: Wwash101 = 8083.169; WD101 = 3900.383; Wwash102 = 3279.965; Gwash101 = 6000.0; GR104 = 2490.0; Gwash102 = 4400.0.

The LB_i(lower bound) e UB_i(upper bound) are described in Hortua (2007).

APPENDIX B

Vinasse concentration

B.1 Design resume

This appendix describes the streams of the plant of vinasse concentration, composed by 5 effects of falling film evaporator. The streams number are according to the Figure B.1.

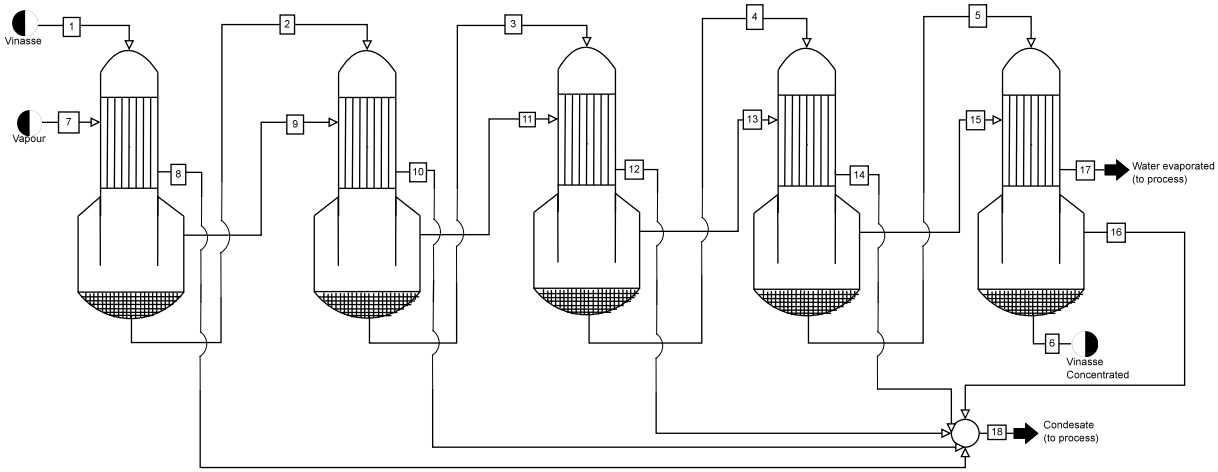

Figure B.1: Flowsheet of vinasse concentration with 5 effects of falling film evaporator.

The table B.1 shows the parameters adopted and calculated for the evaporators design. The Tables B.2 to B.11 in the sequence show the area calculated for different fractions of vinasse *in natura* send to concentration. These fractions range from 100% to 18%.

Table B.1: Parameters for the set of evaporators.

General parameters		
Total pressure drop ΔP (bar)		1.2
Number of evaporators		5
Pressure drop between the effects		0.5
Factors of pressure drop by effect		
f1	1	0.22
f2	2	0.21
f3	3	0.2
f4	4	0.19
f5	5	0.18

Table B.2: Streams information for vinasse concentration flowsheet. 100% of vinasse *in natura* send to concentration.

Parameters		**1st effect**	**2nd effect**	**3rd effect**	**4th effect**	**5th effect**			
Evaporator area [m^2]		286	466	446	471	454			
U, Global Heat Transfer coefficient [kJ/m^2.h.°C]		7.23E+04	6.02E+04	5.02E+04	3.78E+04	2.08E+04			
Qe(kJ/h)		3.00E+08	2.08E+08	2.04E+08	2.19E+08	1.99E+08			
BPE		0.11	0.14	0.20	0.30	0.67			
Stream	**1**	**2**	**3**	**4**	**5**	**6**	**7**	**8**	**9**
Mass flow rate (kg/h)	554,460.00	462,050.00	372,398.51	277,230.00	191,928.46	99,802.80	133,944.63	133,944.63	92,410.00
Temperature (°C)	61.00	101.52	94.10	84.99	72.71	51.70	116.00	110.95	101.52
Pressure (bar)	1.33	1.07	0.81	0.57	0.35	0.13	1.48	1.48	1.07
Cp, Calorific capacity (kJ/kg.°C)	4.07	4.04	4.01	3.95	3.85	3.55	1.85		1.85
Latent heat (kJ/kg)	-	-	-	-	-	-	2,227.13	2,227.13	2,252.76
Components mass fraction (%)									
Water	95.50	94.60	93.30	91.00	87.00	75.00	100.00	100.00	100.00
Brix	4.50	5.40	6.70	9.00	13.00	25.00	0.00	0.00	0.00
Stream	**10**	**11**	**12**	**13**	**14**	**15**	**16**	**17**	**18**
Mass flow rate (kg/h)	92,410.00	89,651.49	89,651.49	95,168.51	95,168.51	85,301.54	85,301.54	92,125.66	496,476.17
Temperature (°C)	101.40	94.10	93.95	84.99	84.79	72.71	72.41	51.70	95.31670471
Pressure (bar)	1.07	0.81	0.81	0.57	0.57	0.35	0.35	0.13	0.86
Cp, Calorific capacity (kJ/kg.°C)		1.85		1.85		1.86		1.86	1.85
Latent heat (kJ/kg)	2,252.76	2,272.32	2,272.32	2,295.91	2,295.91	2,327.09	2,327.09	2,379.47	2,268.77
Components mass fraction (%)									
Water	100.00	100.00	100.00	100.00	100.00	100.00	100.00	100.00	100.00
Brix	0.00	0.00	0.00	0.00	0.00	0.00	0.00	0.00	0.00

Table B.3: Streams information for vinasse concentration flowsheet. 90% of vinasse *in natura* send to concentration.

Parameters	**1st effect**	**2nd effect**	**3rd effect**	**4th effect**	**5th effect**
Evaporator area [m^2]	257	420	401	424	409
U, Global Heat Transfer coefficient [kJ/m^2.h.°C]	7.23E+04	6.02E+04	5.02E+04	3.78E+04	2.08E+04
Qe(kJ/h)	2.70E+08	1.87E+08	1.83E+08	1.97E+08	1.79E+08
BPE	0.11	0.14	0.20	0.30	0.67

Stream	**1**	**2**	**3**	**4**	**5**	**6**	**7**	**8**	**9**
Mass flow rate (kg/h)	499,014.00	415,845.00	335,158.66	249,507.00	172,735.62	89,822.52	120,550.17	120,550.17	83,169.00
Temperature (°C)	61.00	101.52	94.10	84.99	72.71	51.70	116.00	110.95	101.52
Pressure (bar)	1.33	1.07	0.81	0.57	0.35	0.13	1.48	1.48	1.07
Cp, Calorific capacity (kJ/kg.°C)	4.07	4.04	4.01	3.95	3.85	3.55	1.85		1.85
Latent heat (kJ/kg)	-	-	-	-	-	-	2,227.13	2,227.13	2,252.76
Components mass fraction (%)									
Water	95.50	94.60	93.30	91.00	87.00	75.00	100.00	100.00	100.00
Brix	4.50	5.40	6.70	9.00	13.00	25.00	0.00	0.00	0.00

Stream	**10**	**11**	**12**	**13**	**14**	**15**	**16**	**17**	**18**
Mass flow rate (kg/h)	83,169.00	80,686.34	80,686.34	85,651.66	85,651.66	76,771.38	76,771.38	82,913.10	446,828.56
Temperature (°C)	101.40	94.10	93.95	84.99	84.79	72.71	72.41	51.70	95.31670471
Pressure (bar)	1.07	0.81	0.81	0.57	0.57	0.35	0.35	0.13	0.86
Cp, Calorific capacity (kJ/kg.°C)		1.85		1.85		1.86		1.86	1.85
Latent heat (kJ/kg)	2,252.76	2,272.32	2,272.32	2,295.91	2,295.91	2,327.09	2,327.09	2,379.47	2,268.77
Components mass fraction (%)									
Water	100.00	100.00	100.00	100.00	100.00	100.00	100.00	100.00	100.00
Brix	0.00	0.00	0.00	0.00	0.00	0.00	0.00	0.00	0.00

Table B.4: Streams information for vinasse concentration flowsheet. 80% of vinasse *in natura* send to concentration.

Parameters	**1st effect**	**2nd effect**	**3rd effect**	**4th effect**	**5th effect**
Evaporator area [m^2]	229	373	357	377	363
U, Global Heat Transfer coefficient [kJ/m^2.h.C]	7.23E+04	6.02E+04	5.02E+04	3.78E+04	2.08E+04
Qe(kJ/h)	2.40E+08	1.67E+08	1.63E+08	1.75E+08	1.59E+08
BPE	0.11	0.14	0.20	0.30	0.67

Stream	**1**	**2**	**3**	**4**	**5**	**6**	**7**	**8**	**9**
Mass flow rate (kg/h)	443,568.00	369,640.00	297,918.81	221,784.00	153,542.77	79,842.24	107,155.71	107,155.71	73,928.00
Temperature (C)	61.00	101.52	94.10	84.99	72.71	51.70	116.00	110.95	101.52
Pressure (bar)	1.33	1.07	0.81	0.57	0.35	0.13	1.48	1.48	1.07
Cp, Calorific capacity (kJ/kg.C)	4.07	4.04	4.01	3.95	3.85	3.55	1.85		1.85
Latent heat (kJ/kg)	-	-	-	-	-	-	2,227.13	2,227.13	2,252.76
Components mass fraction (%)									
Water	95.50	94.60	93.30	91.00	87.00	75.00	100.00	100.00	100.00
Brix	4.50	5.40	6.70	9.00	13.00	25.00	0.00	0.00	0.00

Stream	**10**	**11**	**12**	**13**	**14**	**15**	**16**	**17**	**18**
Mass flow rate (kg/h)	73,928.00	71,721.19	71,721.19	76,134.81	76,134.81	68,241.23	68,241.23	73,700.53	397,180.94
Temperature (C)	101.40	94.10	93.95	84.99	84.79	72.71	72.41	51.70	95.31670471
Pressure (bar)	1.07	0.81	0.81	0.57	0.57	0.35	0.35	0.13	0.86
Cp, Calorific capacity (kJ/kg.C)		1.85		1.85		1.86		1.86	1.85
Latent heat (kJ/kg)	2,252.76	2,272.32	2,272.32	2,295.91	2,295.91	2,327.09	2,327.09	2,379.47	2,268.77
Components mass fraction (%)									
Water	100.00	100.00	100.00	100.00	100.00	100.00	100.00	100.00	100.00
Brix	0.00	0.00	0.00	0.00	0.00	0.00	0.00	0.00	0.00

Table B.5: Streams information for vinasse concentration flowsheet. 70% of vinasse *in natura* send to concentration.

Parameters	**1st effect**	**2nd effect**	**3rd effect**	**4th effect**	**5th effect**
Evaporator area [m^2]	200	326	312	330	318
U, Global Heat Transfer coefficient [kJ/m^2.h.°C]	7.23E+04	6.02E+04	5.02E+04	3.78E+04	2.08E+04
Qe(kJ/h)	2.10E+08	1.46E+08	1.43E+08	1.53E+08	1.39E+08
EPE	0.11	0.14	0.20	0.30	0.67

Stream	**1**	**2**	**3**	**4**	**5**	**6**	**7**	**8**	**9**
Mass flow rate (kg/h)	388,122.00	323,435.00	260,678.96	194,061.00	134,349.92	69,861.96	93,761.24	93,761.24	64,687.00
Temperature (°C)	61.00	101.52	94.10	84.99	72.71	51.70	116.00	110.95	101.52
Pressure (bar)	1.33	1.07	0.81	0.57	0.35	0.13	1.48	1.48	1.07
Cp, Calorific capacity (kJ/kg.°C)	4.07	4.04	4.01	3.95	3.85	3.55	1.85		1.85
Latent heat (kJ/kg)	-	-	-	-	-	-	2,227.13	2,227.13	2,252.76
Components mass fraction (%)									
Water	95.50	94.60	93.30	91.00	87.00	75.00	100.00	100.00	100.00
Brix	4.50	5.40	6.70	9.00	13.00	25.00	0.00	0.00	0.00

Stream	**10**	**11**	**12**	**13**	**14**	**15**	**16**	**17**	**18**
Mass flow rate (kg/h)	64,687.00	62,756.04	62,756.04	66,617.96	66,617.96	59,711.08	59,711.08	64,487.96	347,533.32
Temperature (°C)	101.40	94.10	93.95	84.99	84.79	72.71	72.41	51.70	95.31670471
Pressure (bar)	1.07	0.81	0.81	0.57	0.57	0.35	0.35	0.13	0.86
Cp, Calorific capacity (kJ/kg.°C)		1.85		1.85		1.86		1.86	1.85
Latent heat (kJ/kg)	2,252.76	2,272.32	2,272.32	2,295.91	2,295.91	2,327.09	2,327.09	2,379.47	2,268.77
Components mass fraction (%)									
Water	100.00	100.00	100.00	100.00	100.00	100.00	100.00	100.00	100.00
Brix	0.00	0.00	0.00	0.00	0.00	0.00	0.00	0.00	0.00

Table B.6: Streams information for vinasse concentration flowsheet. 60% of vinasse *in natura* send to concentration.

Parameters	**1st effect**	**2nd effect**	**3rd effect**	**4th effect**	**5th effect**
Evaporator area [m^2]	172	280	267	283	272
U, Global Heat Transfer coefficient [kJ/m^2.h.°C]	7.23E+04	6.02E+04	5.02E+04	3.78E+04	2.08E+04
Qe(kJ/h)	1.80E+08	1.25E+08	1.22E+08	1.31E+08	1.19E+08
BPE	0.11	0.14	0.20	0.30	0.67

Stream	**1**	**2**	**3**	**4**	**5**	**6**	**7**	**8**	**9**
Mass flow rate (kg/h)	332,676.00	277,230.00	223,439.10	166,338.00	115,157.08	59,881.68	80,366.78	80,366.78	55,446.00
Temperature (°C)	61.00	101.52	94.10	84.99	72.71	51.70	116.00	110.95	101.52
Pressure (bar)	1.33	1.07	0.81	0.57	0.35	0.13	1.48	1.48	1.07
Cp, Calorific capacity (kJ/kg.C)	4.07	4.04	4.01	3.95	3.85	3.55	1.85		1.85
Latent heat (kJ/kg)	-	-	-	-	-	-	2,227.13	2,227.13	2,252.76
Components mass fraction (%)									
Water	95.50	94.60	93.30	91.00	87.00	75.00	100.00	100.00	100.00
Brix	4.50	5.40	6.70	9.00	13.00	25.00	0.00	0.00	0.00

Stream	**10**	**11**	**12**	**13**	**14**	**15**	**16**	**17**	**18**
Mass flow rate (kg/h)	55,446.00	53,790.90	53,790.90	57,101.10	57,101.10	51,180.92	51,180.92	55,275.40	297,885.70
Temperature (°C)	101.40	94.10	93.95	84.99	84.79	72.71	72.41	51.70	95.31670471
Pressure (bar)	1.07	0.81	0.81	0.57	0.57	0.35	0.35	0.13	0.86
Cp, Calorific capacity (kJ/kg.°C)		1.85		1.85		1.86		1.86	1.85
Latent heat (kJ/kg)	2,252.76	2,272.32	2,272.32	2,295.91	2,295.91	2,327.09	2,327.09	2,379.47	2,268.77
Components mass fraction (%)									
Water	100.00	100.00	100.00	100.00	100.00	100.00	100.00	100.00	100.00
Brix	0.00	0.00	0.00	0.00	0.00	0.00	0.00	0.00	0.00

Table B.7: Streams information for vinasse concentration flowsheet. 50% of vinasse *in natura* send to concentration.

Parameters	**1st effect**	**2nd effect**	**3rd effect**	**4th effect**	**5th effect**
Evaporator area [m^2]	143	233	223	236	227
U, Global Heat Transfer coefficient [kJ/m^2.h.°C]	7.23E+04	6.02E+04	5.02E+04	3.78E+04	2.08E+04
Qe(kJ/h)	1.50E+08	1.04E+08	1.02E+08	1.09E+08	9.93E+07
BPE	0.11	0.14	0.20	0.30	0.67

Stream	**1**	**2**	**3**	**4**	**5**	**6**	**7**	**8**	**9**
Mass flow rate (kg/h)	277,230.00	231,025.00	186,199.25	138,615.00	95,964.23	49,901.40	66,972.32	66,972.32	46,205.00
Temperature (°C)	61.00	101.52	94.10	84.99	72.71	51.70	116.00	110.95	101.52
Pressure (bar)	1.33	1.07	0.81	0.57	0.35	0.13	1.48	1.48	1.07
Cp, Calorific capacity (kJ/kg.°C)	4.07	4.04	4.01	3.95	3.85	3.55	1.85		1.85
Latent heat (kJ/kg)	-	-	-	-	-	-	2,227.13	2,227.13	2,252.76
Components mass fraction (%)									
Water	95.50	94.60	93.30	91.00	87.00	75.00	100.00	100.00	100.00
Brix	4.50	5.40	6.70	9.00	13.00	25.00	0.00	0.00	0.00

Stream	**10**	**11**	**12**	**13**	**14**	**15**	**16**	**17**	**18**
Mass flow rate (kg/h)	46,205.00	44,825.75	44,825.75	47,584.25	47,584.25	42,650.77	42,650.77	46,062.83	248,238.09
Temperature (°C)	101.40	94.10	93.95	84.99	84.79	72.71	72.41	51.70	95.31670471
Pressure (bar)	1.07	0.81	0.81	0.57	0.57	0.35	0.35	0.13	0.86
Cp, Calorific capacity (kJ/kg.°C)		1.85		1.85		1.86		1.86	1.85
Latent heat (kJ/kg)	2,252.76	2,272.32	2,272.32	2,295.91	2,295.91	2,327.09	2,327.09	2,379.47	2,268.77
Components mass fraction (%)									
Water	100.00	100.00	100.00	100.00	100.00	100.00	100.00	100.00	100.00
Brix	0.00	0.00	0.00	0.00	0.00	0.00	0.00	0.00	0.00

Table B.8: Streams information for vinasse concentration flowsheet. 40% of vinasse *in natura* send to concentration.

Parameters	**1st effect**	**2nd effect**	**3rd effect**	**4th effect**	**5th effect**
Evaporator area [m^2]	114	186	178	189	182
U, Global Heat Transfer coefficient [kJ/m^2.h.°C]	7.23E+04	6.02E+04	5.02E+04	3.78E+04	2.08E+04
Qe(kJ/h)	1.20E+08	8.33E+07	8.15E+07	8.74E+07	7.94E+07
BPE	0.11	0.14	0.20	0.30	0.67

Stream	**1**	**2**	**3**	**4**	**5**	**6**	**7**	**8**	**9**
Mass flow rate (kg/h)	221,784.00	184,820.00	148,959.40	110,892.00	76,771.38	39,921.12	53,577.85	53,577.85	36,964.00
Temperature (°C)	61.00	101.52	94.10	84.99	72.71	51.70	116.00	110.95	101.52
Pressure (bar)	1.33	1.07	0.81	0.57	0.35	0.13	1.48	1.48	1.07
Cp, Calorific capacity (kJ/kg.°C)	4.07	4.04	4.01	3.95	3.85	3.55	1.85		1.85
Latent heat (kJ/kg)	-	-	-	-	-	-	2,227.13	2,227.13	2,252.76
Components mass fraction (%)									
Water	95.50	94.60	93.30	91.00	87.00	75.00	100.00	100.00	100.00
Brix	4.50	5.40	6.70	9.00	13.00	25.00	0.00	0.00	0.00

Stream	**10**	**11**	**12**	**13**	**14**	**15**	**16**	**17**	**18**
Mass flow rate (kg/h)	36,964.00	35,860.60	35,860.60	38,067.40	38,067.40	34,120.62	34,120.62	36,850.26	198,590.47
Temperature (C)	101.40	94.10	93.95	84.99	84.79	72.71	72.41	51.70	95.31670471
Pressure (bar)	1.07	0.81	0.81	0.57	0.57	0.35	0.35	0.13	0.86
Cp, Calorific capacity (kJ/kg.C)		1.85		1.85		1.86		1.86	1.85
Latent heat (kJ/kg)	2,252.76	2,272.32	2,272.32	2,295.91	2,295.91	2,327.09	2,327.09	2,379.47	2,268.77
Components mass fraction (%)									
Water	100.00	100.00	100.00	100.00	100.00	100.00	100.00	100.00	100.00
Brix	0.00	0.00	0.00	0.00	0.00	0.00	0.00	0.00	0.00

Table B.9: Streams information for vinasse concentration flowsheet. 30% of vinasse *in natura* send to concentration.

Parameters		**1st effect**	**2nd effect**	**3rd effect**	**4th effect**	**5th effect**			
Evaporator area [m^2]		86	140	134	141	136			
U, Global Heat Transfer coefficient [kJ/m^2.h.°C]		7.23E+04	6.02E+04	5.02E+04	3.78E+04	2.08E+04			
Qe(kJ/h)		8.99E+07	6.25E+07	6.11E+07	6.56E+07	5.96E+07			
BPE		0.11	0.14	0.20	0.30	0.67			
Stream	**1**	**2**	**3**	**4**	**5**	**6**	**7**	**8**	**9**
Mass flow rate (kg/h)	166,338.00	138,615.00	111,719.55	83,169.00	57,578.54	29,940.84	40,183.39	40,183.39	27,723.00
Temperature (C)	61.00	101.52	94.10	84.99	72.71	51.70	116.00	110.95	101.52
Pressure (bar)	1.33	1.07	0.81	0.57	0.35	0.13	1.48	1.48	1.07
Enthalpy (kJ/kg)	-	-	-	-	-	-			
Cp, Calorific capacity (kJ/kg.°C)	4.07	4.04	4.01	3.95	3.85	3.55	1.85		1.85
Components mass fraction (%)									
Water	95.50	94.60	93.30	91.00	87.00	75.00	100.00	100.00	100.00
Brix	4.50	5.40	6.70	9.00	13.00	25.00	0.00	0.00	0.00
Stream	**10**	**11**	**12**	**13**	**14**	**15**	**16**	**17**	**18**
Mass flow rate (kg/h)	27,723.00	26,895.45	26,895.45	28,550.55	28,550.55	25,590.46	25,590.46	27,637.70	148,942.85
Temperature (°C)	101.40	94.10	93.95	84.99	84.79	72.71	72.41	51.70	95.31670471
Pressure (bar)	1.07	0.81	0.81	0.57	0.57	0.35	0.35	0.13	0.86
Enthalpy (kJ/kg)									
Cp, Calorific capacity (kJ/kg.°C)		1.85		1.85		1.86		1.86	1.85
Latent heat (kJ/kg)	2,252.76	2,272.32	2,272.32	2,295.91	2,295.91	2,327.09	2,327.09	2,379.47	2,268.77
Components mass fraction (%)									
Water	100.00	100.00	100.00	100.00	100.00	100.00	100.00	100.00	100.00
Brix	0.00	0.00	0.00	0.00	0.00	0.00	0.00	0.00	0.00

Table B.10: Streams information for vinasse concentration flowsheet. 20% of vinasse *in natura* send to concentration.

Parameters	**1st effect**	**2nd effect**	**3rd effect**	**4th effect**	**5th effect**
Evaporator area [m^2]	57	93	89	94	91
U, Global Heat Transfer coefficient [kJ/m^2.h.°C]	7.23E+04	6.02E+04	5.02E+04	3.78E+04	2.08E+04
Qe(kJ/h)	5.99E+07	41639458.8	4.07E+07	4.37E+07	3.97E+07
BPE	0.11	0.14	0.20	0.30	0.67

Stream	**1**	**2**	**3**	**4**	**5**	**6**	**7**	**8**	**9**
Mass flow rate (kg/h)	110,892.00	92,410.00	74,479.70	55,446.00	38,385.69	19,960.56	26,788.93	26,788.93	18,482.00
Temperature (°C)	61.00	101.52	94.10	84.99	72.71	51.70	116.00	110.95	101.52
Pressure (bar)	1.33	1.066	0.81	0.57	0.35	0.13	1.48	1.48	1.07
Enthalpy (kJ/kg)	-	-	-	-	-	-			
Cp, Calorific capacity (kJ/kg.°C)	4.07	4.04	4.01	3.95	3.85	3.55	1.85		1.85
Latent heat (kJ/kg)	-	-	-	-	-	-	2,227.13	2,227.13	2,252.76
Components mass fraction (%)									
Water	95.50	94.60	93.30	91.00	87.00	75.00	100.00	100.00	100.00
Brix	4.50	5.40	6.70	9.00	13.00	25.00	0.00	0.00	0.00

Stream	**10**	**11**	**12**	**13**	**14**	**15**	**16**	**17**	**18**
Mass flow rate (kg/h)	18,482.00	17,930.30	17,930.30	19,033.70	19,033.70	17,060.31	17,060.31	18,425.13	99,295.23
Temperature (°C)	101.40	94.10	93.95	84.99	84.79	72.71	72.41	51.70	95.31670471
Pressure (bar)	1.07	0.81	0.81	0.57	0.57	0.35	0.35	0.13	0.86
Enthalpy (kJ/kg)									
Cp, Calorific capacity (kJ/kg.°C)		1.85		1.85		1.86		1.86	1.85
Latent heat (kJ/kg)	2,252.76	2,272.32	2,272.32	2,295.91	2,295.91	2,327.09	2,327.09	2,379.47	2,268.77
Components mass fraction (%)									
Water	100.00	100.00	100.00	100.00	100.00	100.00	100.00	100.00	100.00
Brix	0.00	0.00	0.00	0.00	0.00	0.00	0.00	0.00	0.00

Table B.11: Streams information for vinasse concentration flowsheet. 18% of vinasse *in natura* send to concentration.

Parameters	**1st effect**	**2nd effect**	**3rd effect**	**4th effect**	**5th effect**
Evaporator area [m^2]	51	84	80	85	82
U, Global Heat Transfer coefficient [kJ/m^2.h.°C]	7.23E+04	6.02E+04	5.02E+04	3.78E+04	2.08E+04
Qe(kJ/h)	5.39E+07	3.75E+07	3.67E+07	3.93E+07	3.57E+07
BPE	0.11	0.14	0.20	0.30	0.67

Stream	**1**	**2**	**3**	**4**	**5**	**6**	**7**	**8**	**9**
Mass flow rate (kg/h)	99,802.80	83,169.00	67,031.73	49,901.40	34,547.12	17,964.50	24,110.03	24,110.03	16,633.80
Temperature (°C)	61.00	101.52	94.10	84.99	72.71	51.70	116.00	110.95	101.52
Pressure (bar)	1.33	1.07	0.81	0.57	0.35	0.13	1.48	1.48	1.07
Cp, Calorific capacity (kJ/kg.C)	4.07	4.04	4.01	3.95	3.85	3.55	1.85		1.85
Latent heat (kJ/kg)	-	-	-	-	-	-	2,227.13	2,227.13	2,252.76
Components mass fraction (%)									
Water	95.50	94.60	93.30	91.00	87.00	75.00	100.00	100.00	100.00
Brix	4.50	5.40	6.70	9.00	13.00	25.00	0.00	0.00	0.00

Stream	**10**	**11**	**12**	**13**	**14**	**15**	**16**	**17**	**18**
Mass flow rate (kg/h)	16,633.80	16,137.27	16,137.27	17,130.33	17,130.33	15,354.28	15,354.28	16,582.62	89,365.71
Temperature (°C)	101.40	94.10	93.95	84.99	84.79	72.71	72.41	51.70	95.31670471
Pressure (bar)	1.07	0.81	0.81	0.57	0.57	0.35	0.35	0.13	0.86
Cp, Calorific capacity (kJ/kg.°C)		1.85		1.85		1.86		1.86	1.85
Latent heat (kJ/kg)	2,252.76	2,272.32	2,272.32	2,295.91	2,295.91	2,327.09	2,327.09	2,379.47	2,268.77
Components mass fraction (%)									
Water	100.00	100.00	100.00	100.00	100.00	100.00	100.00	100.00	100.00
Brix	0.00	0.00	0.00	0.00	0.00	0.00	0.00	0.00	0.00

B.2 Economic estimation resume

Table B.12: Purchased cost of evaporator.

Case	Area of evaporator (m^2)					Purchased Cost (2012)
	1st effect	2nd effect	3rd effect	4th effect	5th effect	
#1 (100%)	286	466	446	471	454	$ 38,000,000.00
#2 (90%)	257	420	401	424	409	$ 34,870,000.00
#3 (80%)	229	373	357	377	363	$ 33,060,000.00
#4 (70%)	200	326	312	330	318	$ 28,380,000.00
#5 (60%)	172	280	267	283	272	$ 25,020,000.00
#6 (50%)	143	233	223	236	227	$ 21,550,000.00
#7 (40%)	114	186	178	189	182	$ 18,090,000.00
#8 (30%)	86	140	134	141	136	$ 14,140,000.00
#9 (20%)	57	93	89	94	91	$ 10,020,000.00
#10 (10%)	51	84	80	85	82	$ 9,270,000.00

The costs functions related to mass fraction of vinasse ($X_{Vinasse}$) send to evaporation unity of multiple effects are indicated in B.1-B.2.The Figures B.2 and B.3 show the costs varitions. In both cases evaluated, the cost associated with vinasse network were the same, since vinasse production does not change.

$$C_{Vinasse} = 1.509X_{Vinasse}^3 + 0.501X_{Vinasse}^2 - 3.125X_{Vinasse} + 5.008, 0.18 \leq X_{Vinasse} \leq 0.8 \quad \text{(B.1)}$$

$$C_{Vinasse} = 8.034X_{Vinasse}^2 - 15.91X_{Vinasse} + 11.20, 0.8 \leq X_{Vinasse} \leq 1.0 \quad \text{(B.2)}$$

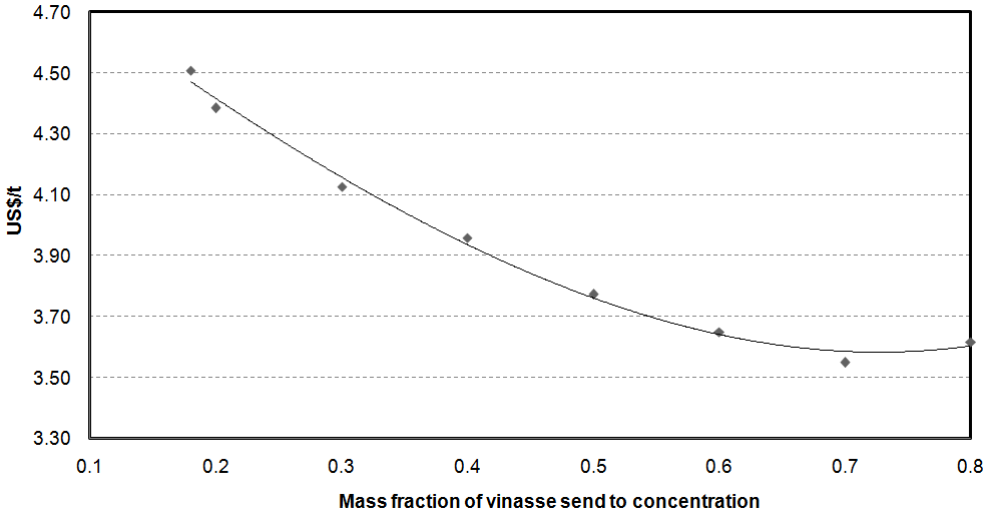

Figure B.2: TAC of vinasse concentration (US$/t) in function of mass fraction send to evaporation unity varying from 18% to 80%.

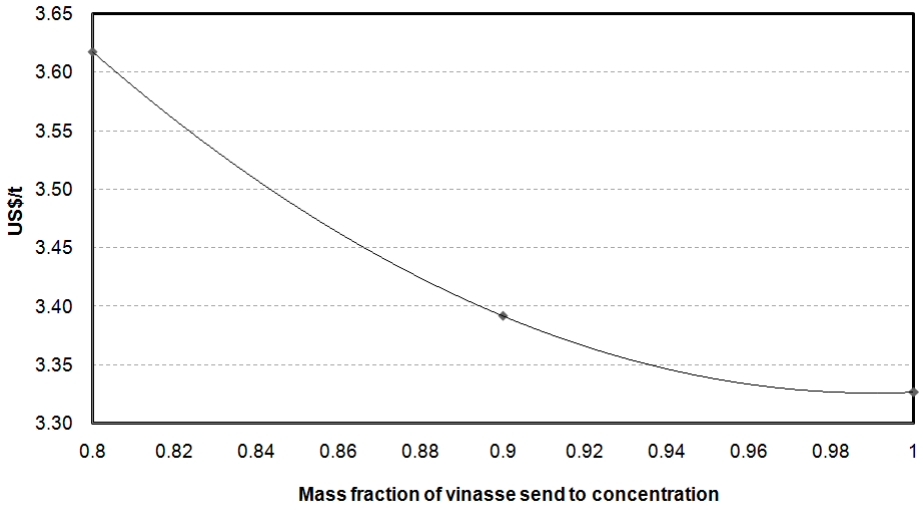

Figure B.3: TAC of vinasse concentration (US$/t) in function of mass fraction send to evaporation unity varying from 80% to 100%.

APPENDIX C

Summary of costs evaluations for sugarcane biorefinery

C.1 Case I

In Case I, the CO_2 network was formed by CO_2 produced during fermentation process. The costs functions related to mass fraction of CO_2 send to recovery are indicated in C.1-C.3 for bicarbonate production, biodiesel from algae farm and ethanol from algae farm, respectivelly.The Figures C.1 - C.3 show the costs varitions.

$$C_{NaHCO_3} = -17.75X^2_{NaHCO_3,C} + 37.67X_{NaHCO_3,C} + 124.5 \quad \text{(C.1)}$$

$$X_{NaHCO_3,C} = 0.0 \text{ or } 0.0 \leq X_{NaHCO_3,C} \leq 1.0$$

$$C_{Biodiesel} = -43.70X^2_{Biodiesel,C} + 152.3X_{Biodiesel,C} + 18.0 \quad \text{(C.2)}$$

$$X_{Biodiesel,C} = 0.0 \text{ or } 0.25 \leq X_{Biodiesel,C} \leq 1.0$$

$$C_{Ethanol} = -43.06X^2_{Ethanol,C} + 155.5X_{Ethanol,C} + 17.92 \quad \text{(C.3)}$$

$$X_{Ethanol,C} = 0.0 \text{ or } 0.25 \leq X_{Ethanol,C} \leq 1.0$$

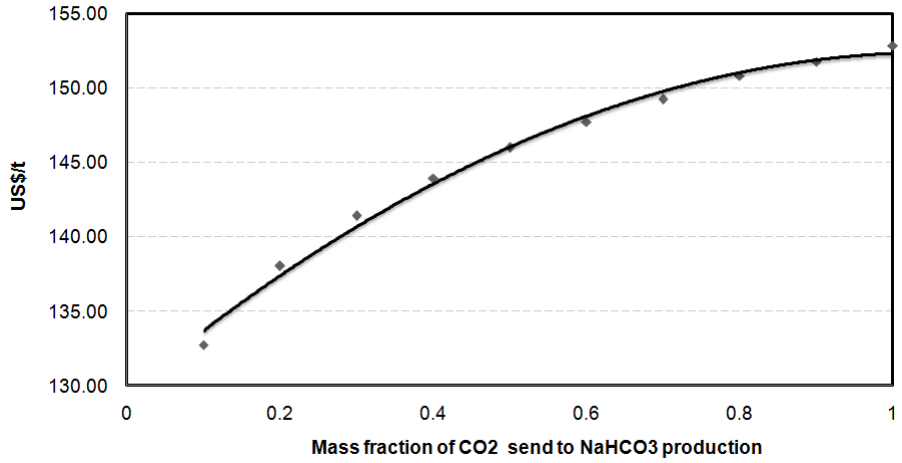

Figure C.1: TAC of CO_2 recovery (US$/t) throught $NaHCO_3$ production in function of mass fraction, Case I.

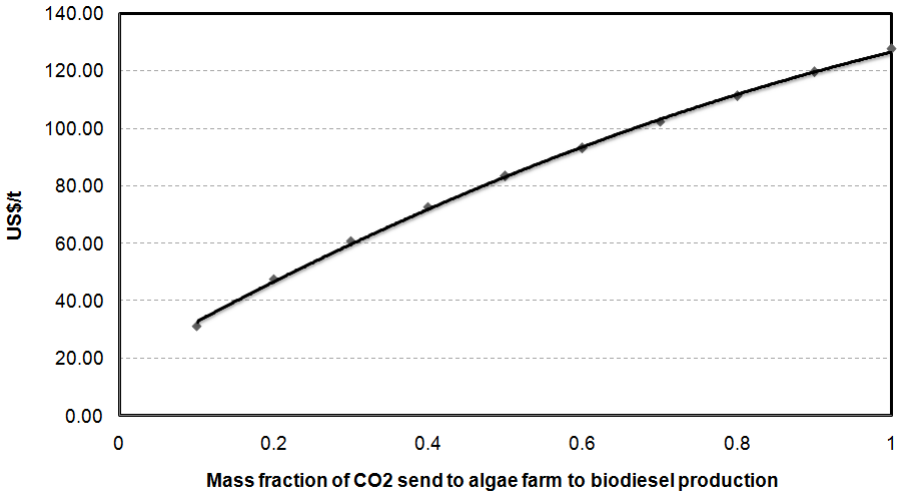

Figure C.2: TAC of CO_2 recovery (US$/t) throught algae farm for biodiesel production in function of mass fraction, Case I.

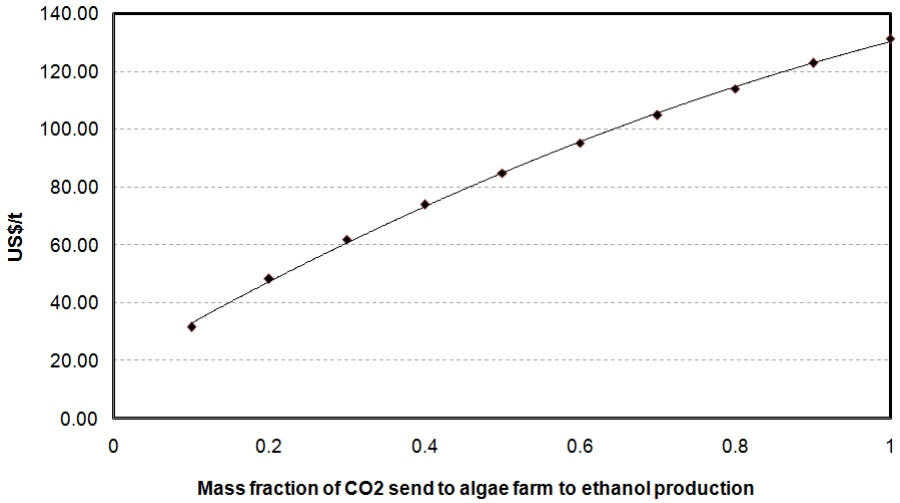

Figure C.3: TAC of CO_2 recovery (US$/t) throught algae farm for ethanol production in function of mass fraction, Case I.

C.2 Case II

In Case II, the CO_2 network was formed by CO_2 produced during fermentation process and during combustion. The costs functions related to mass fraction of CO_2 send to recovery are indicated in C.4-C.6 for bicarbonate production, biodiesel from algae farm and ethanol from algae farm, respectivelly.The Figures C.4 - C.6 show the costs varitions.

$$C_{NaHCO_3} = -20.29X^2_{NaHCO_3,C} + 43.03X_{NaHCO_3,C} + 129.5 \quad \text{(C.4)}$$

$$X_{NaHCO_3,C} = 0.0 \text{ or } 0.1 \leq X_{NaHCO_3,C} \leq 1.0$$

$$C_{Biodiesel} = -30.05X^2_{Biodiesel,C} + 110.8X_{Biodiesel,C} + 13.35 \quad \text{(C.5)}$$

$$X_{Biodiesel,C} = 0.0 \text{ or } 0.10 \leq X_{Biodiesel,C} \leq 0.43$$

$$C_{Ethanol} = -29.78X^2_{Ethanol,C} + 114.8X_{Ethanol,C} + 13.25 \quad \text{(C.6)}$$

$$X_{Ethanol,C} = 0.0 \text{ or } 0.10 \leq X_{Ethanol,C} \leq 0.43$$

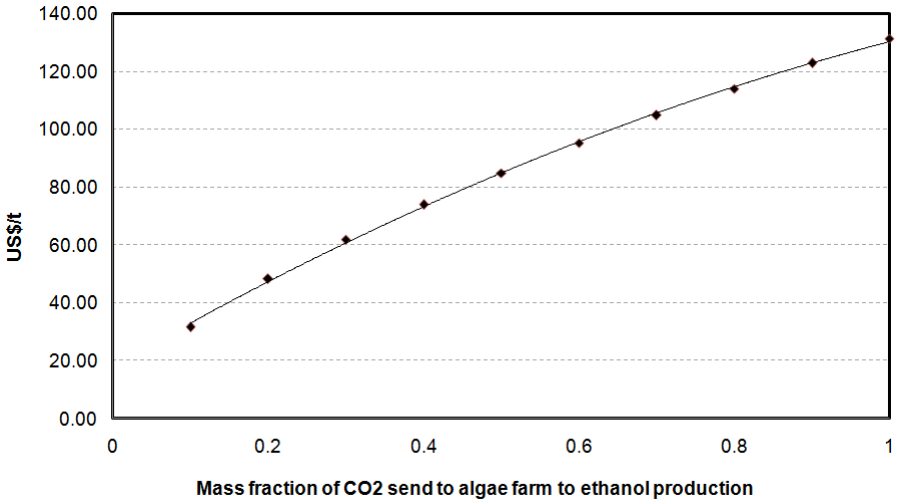

Figure C.4: TAC of CO_2 recovery (US$/t) throught $NaHCO_3$ production in function of mass fraction, Case II.

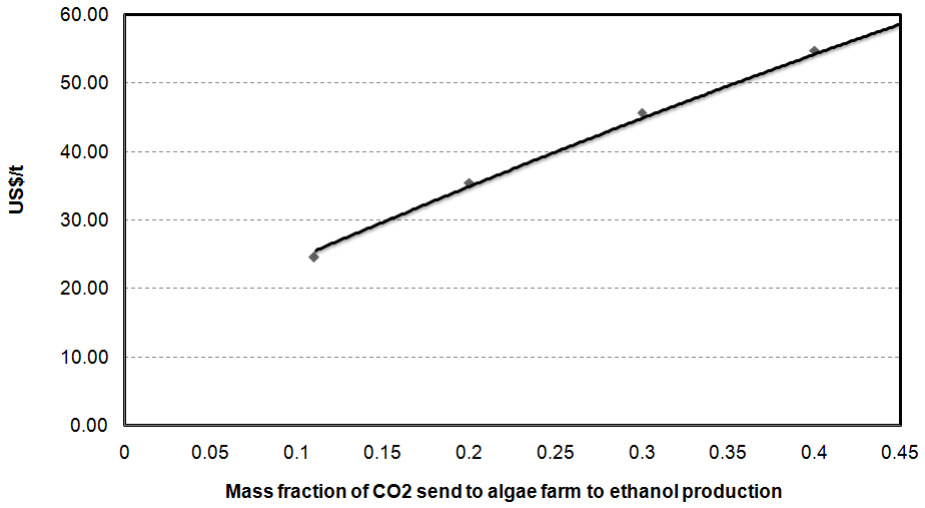

Figure C.5: TAC of CO_2 recovery (US$/t) throught algae farm for biodiesel production in function of mass fraction, Case II.

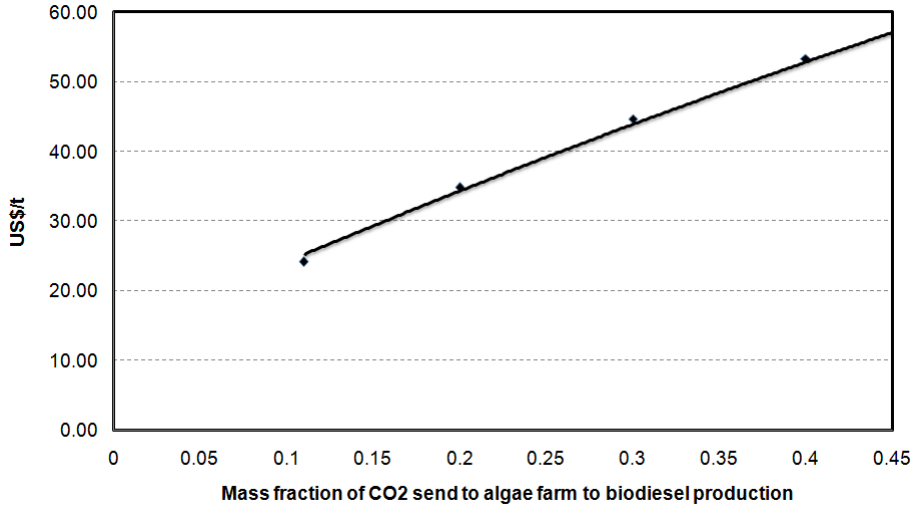

Figure C.6: TAC of CO_2 recovery (US$/t) throught algae farm for ethanol production in function of mass fraction, Case II.